

# DNA checkpoint override and redox signaling in *Schizosaccharomyces pombe*

Johanna Johansson Sjölander



UNIVERSITY OF GOTHENBURG

Thesis for the degree of doctor of philosophy  
University of Gothenburg  
Faculty of Science  
Department of Chemistry and Molecular Biology  
2019

Cover illustration by Karl Persson

DNA checkpoint override and redox signaling  
in *Schizosaccharomyces pombe*

© 2019 Johanna Johansson Sjölander

ISBN: 978-91-7833-686-9 (PRINT)

ISBN: 978-91-7833-687-6 (PDF)

<http://hdl.handle.net/2077/60786>

Printed in Källered, Sweden 2019

Printed by BrandFactory AB



*Dedicated to my family*



# DNA checkpoint override and redox signaling in *Schizosaccharomyces pombe*

## Abstract

This thesis covers intracellular stress signaling through genotoxic stress, overriding of checkpoint control, as well as cellular redox status in hypoxic and oxidative stress

**Papers I and II:** Caffeine has been shown to override cell cycle checkpoints in humans as well as in the fission yeast *Schizosaccharomyces pombe*. Understanding of the mechanism may aid in the development of compounds with similar overriding mechanisms for sensitization in cancer therapy. We show that caffeine induces accumulation of the mitotic inducer protein Cdc25, which removes inhibitory phosphorylation from the CDK Cdc2. Deletion of genes encoding the fission yeast checkpoint proteins Rad3 or Cds1 resulted in a higher constitutive level of Cdc25, suggesting a constitutive role in regulation of the Cdc25 level. Importantly, however, caffeine-induced Cdc25 accumulation is Rad3 independent. Mechanistically our results indicate that caffeine stabilizes and induces nuclear accumulation of Cdc25 as well as preventing Wee1, the kinase phosphorylating the same residue that Cdc25 dephosphorylates, from increasing in response to DNA damage, thereby enforcing progression into mitosis. Our results are in agreement with the known caffeine inhibition of TORC1 contributing to checkpoint override.

**Paper III:** FHIT, a human tumor suppressor, modulates DNA damage sensing, checkpoint control, proliferation and apoptosis. We investigated Aph1, the fission yeast homolog of FHIT, and found that deletion of the *aph1*<sup>+</sup> gene led to enhanced proliferation in sublethal concentrations of genotoxins. This phenotype was accompanied by elevated chromosome fragmentation and/or missegregation. Moreover, we show that an *aph1* deletion leads to knock-down of the checkpoint protein Rad1 in the 9-1-1 complex, and that Aph1 as well as all 9-1-1 proteins are downregulated in hypoxia.

**Paper IV:** H<sub>2</sub>O<sub>2</sub> induces oxidative stress, but is also a signaling molecule that exerts its function through reaction with selected thiols of protein cysteines. MAP kinase (MAPK) pathways are induced by H<sub>2</sub>O<sub>2</sub> in both human and fission yeast. We observed that an active site cysteine, shown to be involved in negative regulation of a human MAP kinase kinase (MAPKK), is evolutionarily conserved in all MAPKKs of budding yeast, fission yeast and humans, indicating that regulation of kinase activity through this cysteine may be a conserved feature of MAPK signaling in these organisms. The active site cysteine C458 in fission yeast MAPKK has no plausible cysteine partner for intramolecular disulfide bond formation. However, Wis1 kinase activity was still inactivated by reversible thiol oxidation in a C458 dependent way. The synthetic allosteric MAPKK modulator molecule INR119, predicted to bind in a site next to C458, protected against negative oxidative regulation *in vitro* targeting C458, resulting in enhanced MAPK signaling *in vivo*.

**Keywords:** Caffeine, Cell cycle, Checkpoint, Cdc25, Wee1, TORC1, FHIT, Proliferation, Aph1, Redox, Hypoxia, H<sub>2</sub>O<sub>2</sub>, Cysteine, Thiol, Allosteric, MAPK, Sty1, MAPKK, Wis1

## Svensk sammanfattning

Alla celler, både i encelliga och flercelliga organismer, svarar på stimuli genom att reglera olika signalvägar. Dessa signalvägar är ofta högradigt bevarade i evolutionen, och kan därmed studeras i modellorganismer mer lämpade för experimentella studier. Många sjukdomar, exempelvis cancer, är resultatet av störd signalering. Denna avhandling bygger på studier i den encelliga jästsvampen- och tillika modellorganismen *Schizosaccharomyces pombe*, och fördjupar sig i intracellulära signalvägar, som alla har cancerrelevans.

Koffein har visat sig kunna sätta de kontrollmekanismer som vid behov stoppar celldelningen ur funktion. Det viktigaste regleringsproteinerna i cellcykeln är Cdc2. En viktig regleringsmekanism av Cdc2 utgörs av inhiberande fosforylering av Y15, där kinaserna Wee1/Mik1 fosforylerar och fosfatet Cdc25 avlägsnar fosfatet. Vi visar att Cdc25 ackumuleras i cellkärnan om man tillsätter koffein, medan Wee1 istället ej ackumuleras som det ska vid DNA-skada om koffein finns närvarande. Detta leder till att cellcykeln inte stoppas trots DNA-skador. Ackumuleringen av Cdc25 är oberoende av Rad3, ett viktigt kontrollprotein som föreslagits vara målproteinerna för koffein. Våra resultat stödjer snarare TORC1, som också inhiberas av koffein, som det viktigaste målet avseende denna effekt.

Aph1 är motsvarigheten hos *S. pombe* till Fragile histidine triad protein (FHIT), en human tumörsuppressör. Vi visar att förlust av Aph1, i likhet med förlust av FHIT, leder till oreglerad celldelning såväl i normala förhållanden som i närvaro av DNA-skadande ämnen. Kombinerar man dessutom förlust av Aph1 med partiell funktionsförlust i ett annat viktigt kontrollprotein, Cds1, blir resultatet ojämn kromosomfördelning och/eller kromosomfragmentering. Förlust av Aph1 orsakar också nedreglering av Rad1, ett protein som är inblandat i DNA-skade responsen. Vi visar vidare att Aph1 är starkt reglerad av aktiviteten i mitokondriens elektrontransportkedja. Sammanfattningsvis finns flera likheter mellan FHIT och Aph1, och *S. pombe* bör därför vara en attraktiv modell med lägre komplexitet för att studera FHITs funktioner.

Väteperoxid är en oxidant som kan skada cellens strukturer, men också reglera signaleringen inuti cellen via oxidering av utvalda cysteiner i proteiner. Vi har identifierat en bromsmekanism hos signalproteinerna Wis1, ett MAPkinasernas, via ett specifikt cystein, som hindrar att signaleringen slås på i alltför låga koncentrationer av väteperoxid. Förlust av bromsfunktionen leder till stark känslighet mot just väteperoxid. En syntetisk molekyl, kallad INR119, binder vidare Wis1, förmodligen i en strukturell ficka bredvid cysteinet, och blockerar aktivitetens nedregleringen via det närliggande cysteinet. Detta leder till en uttalad förstärkning av signalvägen. Vi hoppas att vidare studier kan leda till kunskap om hur man kan förstärka signalering från MAPkinaserna hos människa för att därigenom sänka tröskeln till programmerad celledöd i vissa typer av cancer.

**Nyckelord:** DNA-skada, kontrollprotein, koffein, Cdc2, Cdc25, Wee1, Rad3, TORC1, FHIT, Aph1, Cds1, Rad1, hypoxi, elektrontransportkedja, Wis1, MAPKinasernas, väteperoxid, cystein.

## List of papers

**I:** Caffeine stabilizes Cdc25 independently of Rad3 in *Schizosaccharomyces pombe* contributing to checkpoint override.

John Patrick Alao, **Johanna J. Sjölander**, Juliane Baar, Nejla Özbaki-Yagan, Bianca Kakoschky, Per Sunnerhagen. 2014.

**Mol. Microbiol. 92:777-96.**

**II:** Caffeine stabilises fission yeast Wee1 in a Rad24-dependent manner but attenuates its expression in response to DNA damage contributing to checkpoint override.

John P. Alao, **Johanna J. Sjölander**, Charalampos Rallis, Per Sunnerhagen. 2019.

**Manuscript.**

**III:** The fission yeast FHIT homolog affects checkpoint control of proliferation and is regulated by mitochondrial electron transport.

**Johanna J. Sjölander**, Per Sunnerhagen. 2019.

**Cell Biol. Int., doi: 10.1002/cbin.11241. [Epub ahead of print]**

**IV:** A redox-sensitive thiol in Wis1 modulates the fission yeast MAPK response to H<sub>2</sub>O<sub>2</sub> and is the target of a small molecule.

**Johanna J. Sjölander**, Agata Tarczykowska, Cecilia Picazo Campos, Itziar Cossio, Itedale Redwan, Chunxia Gao, Carlos Solano, Michel Toledano, Morten Grötli, Mikael Molin, Per Sunnerhagen. 2019.

**Submitted.**



# TABLE OF CONTENTS

<b>Introduction</b> .....	7
<b>The use of model organisms in the understanding of cell biology</b> .....	7
<i>Schizosaccharomyces pombe</i> as a model organism .....	9
<b>Cell cycle regulation</b> .....	10
Cyclin dependent kinases (CDKs) drive the cell cycle .....	12
Regulation of CDK activity by the Cdc25 dual phosphatase and Wee1-like kinases .....	13
<b>Cellular stress responses and checkpoint control</b> .....	16
What is cellular stress?.....	16
DNA damage response and checkpoint control in mammals and <i>S. pombe</i> .....	16
Caffeine leads to checkpoint override in human and fission yeast cells .....	20
Hypoxia is a common feature in tumors, complicates cancer therapy, and is associated with worse prognosis.....	21
Aph1, the fission yeast homolog of the puzzling human tumor suppressor FHIT .....	22
Oxidative stress and H <sub>2</sub> O <sub>2</sub> induced signaling .....	26
Stress-activated MAPK pathways .....	30
The <i>S. pombe</i> Sty1 MAPK pathway .....	30
Human MAPKK MEK1, and the story behind INR119, the small molecule used in <b>Paper IV</b> .....	36

<b>Present study</b> .....	40
<b>Paper I</b>	
<b>Caffeine stabilizes Cdc25 independently of Rad3 in <i>Schizosaccharomyces pombe</i> contributing to checkpoint override</b> .....	40
<b>Paper II</b>	
<b>Caffeine stabilises fission yeast Wee1 in a Rad24-dependent manner but attenuates its expression in response to DNA damage contributing to checkpoint override</b> .....	42
<b>Paper III</b>	
<b>The fission yeast FHIT homolog affects checkpoint control of proliferation and is regulated by mitochondrial electron transport</b> .....	43
<b>Paper IV</b>	
<b>A redox-sensitive thiol in Wis1 modulates the fission yeast MAPK response to H<sub>2</sub>O<sub>2</sub> and is the target of a small molecule</b> .....	45
<b>Concluding remarks</b> .....	51
<b>Acknowledgements</b> .....	54
<b>References</b> .....	55
<b>Appendix</b> .....	68
<b>1:Sulfenylation protocol</b> .....	68



# Introduction

## The use of model organisms in the understanding of our own cells

The interest of humans in cell and molecular biology is first and foremost directed to knowledge important for survival and quality of our own lives. We are interested in understanding pathogens infecting humans or livestock, in different medical conditions and the development in treatment of these. Even so, some research relevant for understanding human health and quality of life on the cellular and molecular level is not performed on human cells, but in various eukaryotic model organisms, organisms for which systems of genetic manipulations have been developed, and which similar to our cells belong to the domain of eukaryotes, *i.e.* whose cells carry a nucleus. Examples of common eukaryotic multicellular models are mouse, rat, zebrafish, the nematode *Caenorhabditis elegans* as well as the fruit fly *Drosophila melanogaster* and the plant *Arabidopsis thaliana*. In addition, unicellular eukaryotic organisms such as yeasts are used. The wide range of models in use reflects that different model organisms are suitable for the understanding of different processes.

The simplest reason for using unicellular eukaryotic organisms for the understanding of processes in human cells is the complexity of our own cells and the interplay between them. It is sometimes hard to see the basal regulation in a system because of the complexity built upon it, “hard to see the forest because of all the trees...” It may be beneficial to first study intracellular processes in a simpler system, and then look for similarities with our own cells. When doing so it is however important to understand that the results can not be directly extrapolated to humans, but should be seen as a starting point for studies in more complex systems.

Using yeasts as models has many advantages when it comes to the everyday laboratory work. They are easily genetically manipulated, and they are easily grown with low-cost measures. The generation time is short, making it easy to scale up laboratory procedures when needed and many experiments can be repeated in a relatively short timeframe. The availability of haploid cells is also a clear advantage, as it is easier to study a genetic function without a second copy of the gene interfering with the result. Last but not most importantly, even

though less complex than our cells, many important pathways are conserved to a high degree, giving us the chance to study these in a simpler context.

This thesis contains four distinct pieces of basic research of intracellular signaling, covering oxidative, hypoxic, and genotoxic stress as well as overriding of checkpoint control. The main part of the data is obtained from studies carried out in the unicellular yeast *Schizosaccharomyces pombe* with minor complementing work in **Paper IV** performed in a human breast cancer cell line. The signaling pathways studied are quite diverse in nature but all have in common that the human counterparts are deregulated in cancer. A brief overview of the studied pathways is presented in **Fig. 1**.

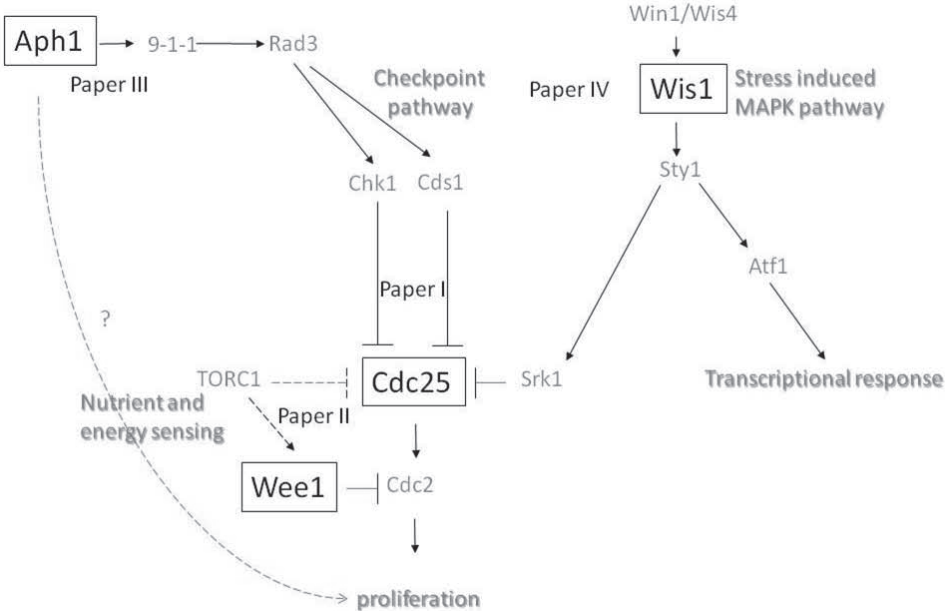


**Figure 1:** Schematic overview of the pathways studied in this thesis

## ***Schizosaccharomyces pombe* as a model organism**

Yeasts are fungi, but the word yeast is not the name of a monophyletic group of fungi, but a descriptive word given to a fungus with a unicellular way of life. The yeast *Schizosaccharomyces pombe* is a model organism used to study *e.g.* various principles of intracellular regulation and responses in the eukaryotic cell. It is a fungus belonging to the group *Ascomycetes* which also contains the more commonly used model organism *Saccharomyces cerevisiae* (baker's yeast). This is one of the budding yeasts, which divide asymmetrically by budding of smaller daughter cells from the mother cell. It appears that budding yeasts have evolved faster and accumulated more specialized features than most other eukaryotes including *S. pombe*. The fission yeast *S. pombe* has not passed through major genome duplications [1] in contrast to budding yeast, which has gone through at least one full genome duplication, with following reduction of gene number to approx. 5500 [2]. In addition, budding yeast has lost many genes that are conserved between fission yeast and mammals [3]. Therefore *S. pombe* keeps more of its basal ascomycete characteristics and is genetically closer to the point of evolutionary split between fungi and animal cells [4].

In contrast to the ovoid-shaped budding yeast cells, the cells of *S. pombe* are rod shaped, and grow by tip elongation [5]. *S. pombe* is commonly called fission yeast as it divides symmetrically by binary fission. Fission yeast has approximately 5000 open reading frames divided on 3 chromosomes, and the open reading frames have a higher frequency of introns (within 43 % of genes) [6] compared to budding yeast (within 5 % of genes), and the pre-mRNA splicing machinery is more closely related to human than is the budding yeast counterpart [7]. The commonly used laboratory strains all come from a single isolate that is close to isogenic, however containing different mating types. The mating types of fission yeast are called  $h^-$  and  $h^+$ , as well as  $h^{90}$ .  $h^-$  and  $h^+$  are opposite mating types whereas  $h^{90}$  can switch between the mating types and thereby mates with both  $h^-$ ,  $h^+$ , as well as with  $h^{90}$  [4]. Mating between haploid cells only takes place when compatible mating types are in close proximity during nitrogen limitation, forming a zygote that directly undergoes meiosis leading to formation of an ascus containing 4 ascospores [8].

Whereas budding yeast has been widely used for many different research areas, studies using fission yeast have historically been especially important in elucidating cell cycle regulation and cell cycle checkpoints. Budding yeast has also contributed significantly in the understanding of the eukaryotic cell cycle and checkpoint control. However, in these areas of

research fission yeast complements this knowledge as some aspects of this regulation, such as the regulation of inhibitory phosphorylation on Y15 of CDK1, the key regulator of the cell cycle [9], is more typical for other eukaryotic cells. Fission yeast also complements budding yeast studies in the field of eukaryotic chromosomes, as some budding yeast chromosome features such as centromeres [10], replication origins [11] and heterochromatin [12] are less typical of eukaryotes. Other common areas of research are intracellular signaling pathways such as stress responses as well as transcriptional and post-transcriptional regulation. The conserved signaling pathways studied in fission yeast often have counterparts of the mammalian proteins, however with fewer versions/isoforms. One illustrative example of this are the members of the Cdc25 family, the phosphatases that removes inhibitory phosphate groups on CDKs. In mammalian cells there are three isoforms of CDC25, called CDC25A, CDC25B, and CDC25C [13], whereas in fission yeast only one form of Cdc25 exists [14]. Other examples are CDKs involved in regulation of mitotic and meiotic cell cycles, where fission yeast uses the same CDK, called Cdc2, in all regulation steps of both cycles [15, 16], whereas human cells have multiple CDKs with more specialized functions [17]. Another example is mitogen-activated protein kinase (MAPK) pathways, where human have multiple pathways [18], whereas fission yeast has only three [19].

## **Cell cycle regulation**

### The eukaryotic cell cycle

A typical eukaryotic mitotic cell division cycle contains four distinct phases: a DNA synthesis phase (S phase), a mitotic phase (M phase), and two intervening growth phases ( $G_1$  and  $G_2$ ). Newly separated cells grow in  $G_1$  before entering S phase, where genome duplication takes place. S phase is further separated from mitosis, where the replicated sister chromatids are separated from each other, by the second growth phase,  $G_2$ . After a certain point in  $G_1$ , called START in yeasts, roughly equivalent to the restriction point in mammalian cells, cells are committed to entering replication [20, 21]. At specific points in the cell cycle, named checkpoints, certain criteria must be fulfilled before entering the next stage of the cycle. These criteria can for example be to have reached a certain size of the cell, non-damaged DNA, undamaged, fully replicated, DNA, or proper alignment of the sister chromosomes in the metaphase-to-anaphase transition. The checkpoints of the cell cycle ensure that the events

of the cell cycle are coordinated, executed in the right order as well as making sure problems are settled before entering the next stage. [22].

### The fission yeast mitotic cell cycle

The mitotic cell cycle in fission yeast is dominated by a long G<sub>2</sub> phase, whereas G<sub>1</sub> is much shorter. The major checkpoint of the fission yeast cell cycle is also at the boundary between G<sub>2</sub> and M phase [23, 24]. A peculiarity of fission yeast is the fact that cytokinesis, the separation of the cytoplasm into two cells, is separated in time from closure of M-phase, and therefore a second round of DNA replication is often initiated before completion of the cytokinesis of the ongoing cell cycle [25]. In most eukaryotic cells the end of mitotic phase instead normally coincides with cytokinesis even though cytokinesis regulation is distinct from mitosis [26],

### The cell cycle is regulated by oscillating build-up and degradation of key proteins

A major selective proteolytic machinery within the cell is the proteasome. The eukaryotic 26S proteasomes are highly selective multiprotein barrel-shaped complexes that degrade proteins within their internal proteolytic cavity. Generally proteins covalently labeled with chains of a certain small protein unit, called ubiquitin (Ub), are let into the chamber and a chain of at least four Ub units are needed for proteasome dependent hydrolysis [27]. As the cell cycle is driven by oscillating events of build-up and degradation of key factors, the ubiquitination labeling system, targeting substrates for degradations by the proteasome, plays a vital role in cell cycle regulation where the degradation of selected proteins can either inactivate or activate a process depending on the function of the protein. Deregulation of the proteolytic system can result in cellular proliferation, genomic instability as well as cancer [28].

The E1 enzymes, E2 ubiquitin-conjugating enzymes, and E3 ligases together target selected proteins with polyubiquitin chains. Both ubiquitin ligases and the proteasome itself localize to the cytoplasm as well as the nucleus of eukaryotic cells [27] Two important eukaryotic E3 complexes are constituted by the anaphase-promoting complex or cyclosome (APC/C), and the SCF (Skp1-Cullin1-F-box E3 ubiquitin ligase). At the border of the anaphase-to-metaphase transition, the activity of APC/C is needed for ubiquitination of

securins [28], in *S. pombe* called Cut2 [29], inhibitors of the transition, whose degradation is essential for sister chromosome separation. The activity of APC/C is highest at the anaphase-to-mitosis transition and later ceases in G<sub>1</sub>. The SCF complex is instead active throughout the cell cycle but mainly regulates the progression of G<sub>1</sub> to S phase [28].

## **Cyclin dependent kinases (CDKs) drive the cell cycle**

CDKs are serine/threonine kinases that are not themselves catalytically active unless bound to a regulatory subunit, a cyclin. The cyclins are so termed as their levels build up, having their maximum concentration at the point where they are needed, and thereafter are destroyed in proteasomes. Humans have 20 different CDKs named CDK 1-20 [17], whereas the fission yeast has 7 CDKs [30]. CDKs are further traditionally separated into either cell-cycle or transcriptional CDKs, even though this division is somewhat confusing as the transcriptional regulation itself effect cell cycle transition, and as at least human and fission yeast CDK7 has dual roles as part of the transcription factor IIIH as well as being a CDK-activating kinase (CAK) of CDK1/Cdc2, and in humans also CDK2, CDK4 and CDK6 [31, 32].

Conserved CDKs of the cell cycle type catalyze the progression through the eukaryotic cell cycle by phosphorylation of key regulatory substrates [33]. These CDKs are tightly regulated by their association with cyclins as well as through inhibitory phosphorylation and physical interactions with CDK inhibitors (CKI) and for full activity activating phosphorylation by CDK activating kinases (CAKs) are necessary [34].

A CDK without its cyclin is not only inactive, but the same CDK has different substrate specificity depending on its bound cyclin [35]. Therefore the association with the proper cyclin is regulated through build-up and breakdown, during the course of the cell cycle, hence the term cyclin [36]. The master mitotic regulator in metazoans is called CDK1. The CDKs 1, 2, and 3 as well as CDK4 and 6 together constitute the mitotic cell cycle CDKs in mammals [37]. CDK1 in mammals is normally mainly responsible for initiation of mitosis through phosphorylating proteins involved in nuclear envelope breakdown, chromosome condensation and spindle assembly, whereas CDKs 3 as well as 4/6 have roles during G<sub>1</sub> [37]. CDK2 is involved in the transition between G<sub>1</sub> and S-phase as well as from S-phase to G<sub>2</sub> [38] and is essential in meiosis [39, 40]. In mouse, CDK1 is the only cell cycle type CDK

absolutely essential for the mitotic cell cycle [40], whereas CDK2 and CDK4 as well as CDK4 and CDK6 have overlapping functions and can substitute for each other except for in certain tissues [39]. Conditional CDK1 knock-out mice arrest in the blastocyst stage [41]. The only cell cycle type CDK of fission yeast is called Cdc2, carrying out all the classical cell cycle CDK functions in all transitions of the cell cycle both in the mitotic [42, 43] as and meiotic cell cycles [16]. Cdc2 is also the homolog of human CDK1, and human CDK1 was itself first identified through complementation studies in fission yeast [44]. Cdc2 binds different cyclins, Cdc13 (G<sub>2</sub>/M) [45], Cig1 [46] and Puc1 (G<sub>1</sub>) [47], and Cig2 (G<sub>1</sub>/S) [48] depending on the stage of the cell cycle. However it is fully possible to drive the cell cycle with only Cdc2 and Cdc13 if they are fused to form a chimeric protein making CDK activity independent of cyclic build up and degradation of cyclins. Further, when regulating the activation level of the fused Cdc2-Cdc13 module, different thresholds were shown to be responsible for the different cell cycle transitions. This suggests that the major regulation by the different cyclins is to confer different activation levels of the CDK and that the substrate specificity may be regulated by the activation level [49].

## **Regulation of CDK activity by the Cdc25 dual phosphatase and Wee1-like kinases**

One of the determining factors of the CDK1/Cdc2 activity of in the cell is the level of conserved inhibitory phosphorylation on Y15 and to a lesser extent also on T14 [9]. This regulation is regulated through the Wee1/Mik1/MYT1 family of kinases [50] and the counteracting activities of Cdc25 phosphatases [51]. Both cell cycle checkpoints and stress response pathways target cell-cycle progression through the regulation of Y15 phosphorylation by both decreasing the activities of Cdc25 and increasing the activities of Wee1/Mik1/MYT1 [52, 53, 54, 55].

The importance of Cdc25 as a regulator in the cell cycle was first identified in fission yeast [56] In mammals the CDC25 dual phosphatase exists in three isoforms, CDC25A, CDC25B, and CDC25C [57]. CDC25A was first identified through its sequence homology to the single version of fission yeast CDC25 [58]. The catalytic domains of the mammalian isoforms are well conserved whereas their regulatory domains are more diverse [59]. While CDC25B and CDC25C promote G<sub>2</sub>/M progression by primarily

dephosphorylating CDK1, CDC25A also removes inhibitory phosphate groups on CDK4, CDK6, and CDK2 as well as CDK1. This makes CDC25A involved in all transitions of the mammalian mitotic cell cycle and CDC25A inhibition is important in checkpoint control [60]. The levels of mammalian CDC25 isoforms as well as the fission yeast Cdc25 is periodically built up as well as ceasing, during the cell cycle, for efficient transition between the different phases. In fission yeast the Cdc25 protein level is at its maximum shortly at the end of mitosis but never goes down to zero [61]. Different patterns of slower migrating forms of Cdc25 on SDS-PAGE are prominent depending on the stage of the cell cycle [61, 62]. These constitute differently phosphorylated forms of Cdc25, as phosphatase treatment eliminates the slow migrating forms [62]. The slowest migrating forms are found peaking at the maximum of Cdc25 activity. Stalling the cell cycle at a certain point, results in stockpiling of Cdc25 with the same pattern of slow migrating forms. The function of this counterintuitive stockpiling during a time where progression is stopped is presumably for prompt induction of progression when it again becomes possible. Although the Cdc25 activity peaks at mitosis, Cdc25 is partly active also during the rest of the cell cycle and has functions in the other phase transitions as well [62].

Cdc25 phosphatases are in many ways themselves regulated by phosphorylation. Hyperphosphorylated forms are as already mentioned found at the highest degree of activity. Localisation is regulated through its interaction with 14-3-3 proteins [63], in fission yeast mainly Rad24 [64] and to a lesser degree Rad25 [65]. This interaction can be induced by phosphorylation on certain residues performed by multiple kinases. The checkpoint kinases CHK1/Chk1, CHK2/Cds1 are able to phosphorylate CDC25/Cdc25 on these residues [52, 66], and additionally cellular stress also regulates cell cycle progression via phosphorylation of the same residues. This phosphorylation leading to stress-induced checkpoint arrest is induced through induction of MAPK signaling in mammals through p38-mediated activation of MAPKAP2 [66, 67] and in fission yeast through the Sty1-activated Srk1 kinase [68], where MAPKAP2 and Srk1 both directly phosphorylate Cdc25/CDC25. When in complex with the 14-3-3/Rad24 proteins, Cdc25/CDC25 is excluded from the nucleus and thereby not in contact with its target CDK [69]. Dephosphorylation performed by the mammalian CDC14-related fission yeast protein phosphatase Clp1 targets Cdc25 for polyubiquitination, in fission yeast by the E3 ligase Pub1, leading to its subsequent degradation by the proteasome [70, 71].



Wee1, a CDK inactivating kinase was also first identified in fission yeast [72], where deficiency of the protein resulted in premature mitotic entry as well as entry of smaller cells into S phase. In fission yeast smaller-sized cells are commonly termed the wee1 phenotype (“wee” means small in Scottish). Fission yeast Wee1 and Mik1 both phosphorylate Cdc2 Y15, and in the case of Wee1 also T14 [53, 73], even though phosphorylation on T14 is rather unusual in *S. pombe* [74]. Fission yeast Wee1 as well as Mik1 are responsible for regulation the cell cycle transitions, however Wee1 is more crucial in regulation of normal cell cycle progression whereas Mik1 is mainly responsible for inactivation of Cdc2 in the DNA damage and replication checkpoint controls [53]. Mammalian WEE1 also plays a critical role in proper timing of cell division, through the modulation of CDK1 and CDK2 activity by inhibitory phosphorylation of conserved Y15 residues on both kinases, thereby controlling entry into mitosis and DNA replication during S phase [75,76]. The human MYT1 kinase is required for T14 phosphorylation [77].

14-3-3 proteins in humans have been shown to regulate cell cycle progression also through their binding to WEE1, which positively regulates its enzymatic activity [78]. For Wee1 or Mik1 in fission yeast this was not previously shown. In **Paper II** we demonstrate that in the absence of DNA damaging agents, caffeine treatment leads to an increase of Wee1 in a way dependent of the 14-3-3 protein Rad24, in support of a conserved interaction between this 14-3-3 protein and Wee1 in fission yeast.

TORC1, Target of rapamycin complex 1, is a conserved major regulator of translation responding to the nutrient and energy status of the cell, regulating global translation accordingly [79]. TORC1 impacts growth, proliferation and survival and some inhibitors including rapamycin are used as anti-cancer agents [80]. Inhibition of TORC1 have additionally been shown to increase the lifespan in various organisms from yeast to mammals [81, 82]. The mammalian complex mTORC1 contains the PIKK related kinase mTOR, also found in the mTORC2 complex [83], whereas the corresponding kinase in fission yeast TORC1 is called Tor2 [84]. Fission yeast TORC1 regulates both Wee1 and Cdc25 where inhibition of TORC1 leads to higher Cdc25 activity and a decrease in the Wee1 level of the cell, thereby enforcing cell cycle progression into mitosis [85].

## **Cellular stress responses and checkpoint control**

### **What is cellular stress?**

From a cell's point of view, a stressful condition is a condition leading to energy deficiency or adverse effects/damage of any of the macromolecules of the cell such as proteins, RNA, DNA, or lipids. The response of the cell will depend on the type of stress, the level and duration of the insult, through the changes the stress confers on the molecular level [86], and there will be a redirection of the transcriptional and translational expression machinery in favor of genes important for handling of the stress. The result can be antioxidant production upon oxidative stress or the upregulation of heat shock proteins handling a formed burden of unfolded proteins. In the case of DNA damage, induction of intracellular signaling will result in the cell division cycle being stopped, as well as repair pathways being induced. In multicellular higher organisms, unresolved stressful issues can ultimately lead to induction of programmed cell death [87].

### **DNA damage response and checkpoint control in mammals and *S. pombe***

DNA damage is a result from for example chemical agents either resulting in strand breaks (bleomycin, phleomycin) [88], or modifications of DNA bases, for example through covalent binding of the chemical to the base [89] forming an adduct and thereby interfering with proper readout during replication. Examples of physical DNA damaging agents are ultraviolet (UV) light and ionizing radiation (IR). DNA damage can also form during normal metabolism through hydrolysis as well as oxidation and alkylation of DNA [90]. For the integrity of the genome and ultimately for the survival of the cell, lesions have to be dealt with in a proper way. If not corrected the error may lead to a mutation, a permanent change of the sequence through the next round of replication and thereafter be passed on to the following daughter cells. The protection of genetic integrity is coordinated by the DNA damage response.

The components of the DNA damage response pathway in eukaryotes were originally identified as involved in checkpoint control, the concept addressed as ensuring the events of the cell cycle being processed in the right order and each phase completed before the next phase was entered [22]. The identified DNA damage and replication checkpoint

pathways were seen as protecting the genome through detection of damage or stalled replication forks, and stopping of the cell cycle progression until damage was repaired or the block resolved [22]. Later it became clear that protection of the genome by the same network of proteins that stops cell cycle progression through checkpoint signaling is also directly involved in actual repair processes by regulation on multiple levels including physical interaction with repair proteins, transcriptional translocation of repair proteins and activation of deoxynucleotide synthesis [91].

As in the field of basal cell cycle regulation, much of the early work and understanding of the checkpoint signaling in eukaryotes was carried out in the fission yeast *S. pombe* and the budding yeast *S. cerevisiae*. Studies within higher organisms showed that these responses protecting genetic integrity are extensively conserved among eukaryotes, including between these yeast species and mammals [92], though the mammalian pathways are as expected more elaborate [91]. Human, fission yeast as well as budding yeast versions of proteins in the DNA damage response of importance for understanding this thesis are summarized in **Table 1**.

<i>S. pombe</i>	<i>H. sapiens</i>	<i>S. cerevisiae</i>	Function
Rad26	ATRIP	Lcd1/Ddc2	Rad3 (ATR) regulator
Rad3	ATR	Mec1	Sensor kinase
Rad17	RAD17	Rad24	9-1-1 clamp loader
Rad4/cut5	TOPBP1	DPB11	Adaptor
Rad1	RAD1	Rad17	Sensor (part of 9-1-1 complex)
Hus1	HUS1, HUS1B	Mec3	Sensor (part of 9-1-1 complex)
Rad9	RAD9A, RAD9B	Ddc1	Sensor (part of 9-1-1 complex)
Crb2/Rhp9	TP53BP1	Rad9	Mediator
Chk1	CHK1	Chk1	Effector kinase
Cds1	CHK2	Mek1	Effector kinase
Tel1	ATM	Tel1	Sensor kinase
Cdc25	CDC25A, CDC25B, CDC25C	Mih1	Phosphatase of inhibitory CDK phosphorylation
Wee1/Mik1	WEE1, WEE2, MYT1	Swe1	CDK inhibitory Kinase

**Table 1.** DNA damage response proteins

## The DNA damage response (DDR)

Processing of DNA damage, as well as replication stress, will result in intermediates containing stretches of single stranded DNA (ssDNA). In replication stress this is caused by helicase activities becoming uncoupled from polymerase activities upon stalled replication forks [93]. Also resection of double strands breaks can result in ssDNA. The ssDNA induces coating of this DNA with replication protein A (RPA) [94]. To the DNA damage, in *S. pombe* two distinct DNA damage sensor complexes are further recruited, called Rad3/Rad26 (ATR/ATRIP in vertebrates) and the 9-1-1 complex respectively [95]. The 9-1-1 complex is a heterotrimeric ring structure built up of Rad1/RAD1, Hus1/HUS1, and Rad9/RAD9 – all closely related to the homotrimers of the processivity clamp for DNA polymerase, the proliferating cell nuclear antigen (PCNA) [96], and this specialized clamp is loaded onto damaged DNA by a replication clamp loader replication factor C (RFC) with one of the subunits exchanged for Rad17/RAD17 [97]. The RAD17-containing complex loads the checkpoint specific clamp, onto 5' recessed DNA ends whereas the normal RFC instead prefers 3' recessed end DNA substrates [98]. Studies in *Xenopus* cell extracts suggest that formation of the extended ssDNA covered with RPA is enough for recruitment of the ATR/ATRIP complex, whereas recruitment of the complex containing RAD17 and the 9-1-1 heterotrimer requires also an adjacent double stranded stretch as in the case of primed DNA [99]. Even though Rad3/Rad26 (ATR/ATRIP) and the 9-1-1 complex are independently recruited to damaged DNA, both complexes are needed for a full checkpoint response [100], and their interdependency is largely coordinated by Topoisomerase II $\beta$ -binding protein 1 (TOPBP1, in fission yeast called Rad4/Cut5). In *Xenopus* it has been shown that recruitment of the 9-1-1 complex is important for induction of ATR (Rad3) through recruitment of TOPBP1, which in turn binds ATR/ATRIP leading to ATR activation [100]. This is essentially conserved in fission yeast, as the interaction between Rad9 and Rad4 (TOPBP1) is required for activation of the Rad3 (ATR)-dependent Chk1-induced DNA damage checkpoint. Further, Rad3 (ATR) and Tel1 (ATM) phosphorylate Rad9 T412/S423, and Rad3 coprecipitates with Rad4 (TOPBP1) when these Rad9 residues are phosphorylated [101], again demonstrating the regulatory interdependency of the two complexes. In human HeLa cells TOPBP1 and RAD9 in the 9-1-1 complex are independently recruited to damaged DNA. Once they are recruited, a direct contact is established which leads to ATR activation as well as accumulating recruitment of TOPBP1 resulting in amplification of ATR induced checkpoint signaling [102].

*S. pombe* Rad3 as well as human ATR and its closely related protein ATM and the catalytic subunit of the DNA-PK complex are all PIKK related proteins and these PIKK related kinases orchestrate the DNA damage response by phosphorylation of multiple targets important in checkpoint signaling and DNA repair [103]. *S. pombe* Rad3 activates the checkpoint effector kinases Chk1 as well as Cds1, the ortholog of human CHK2. In fission yeast, Chk1 is the effector kinase of the DNA damage checkpoint pathway [104], whereas Cds1 is the effector kinase of the replication checkpoint pathway [105]. This contrasts to in human cells, where ATR (Rad3) activates CHK1 in response to stalled replication forks due to shortage of nucleotides or when DNA damage cause physical blocks for DNA synthesis [106], thus in this respect human CHK1 function closer resembles that of fission yeast Cds1 (CHK2). Human ATM (Tel1) activates CHK2 (Cds1) upon DNA damage in the form of double strand breaks [107]. ATR is additionally involved in the DNA damage response upon double strand breaks (DSB), however loading of ATR in response to DSB is ATM dependent [108]. In contrast, *S. pombe* Tel1 (ATM) does not have a major role in DNA damage response signaling, but Rad3 (ATR) is responsible for activation of both the Chk1 (CHK1) and Cds1 (CHK2) induced routes. Both Tel1 and Rad3 as well as the 9-1-1 complex, Rad26 and Rad17 are however involved in telomere genetic integrity maintenance and this function is independent of Chk1 and Cds1 [109]. The human DNA-PK activates DNA damage repair of DSB through non-homologous end-joining (NHEJ) [110]. Ku70, a protein corresponding to a subunit in the human DNA-PK complex, is essential for NHEJ also in fission yeast, however the catalytic subunit of DNA-PK is not conserved in fission yeast and the related proteins Rad3 and Tel1 are dispensable for induction of NHEJ [111]. *S. pombe* Chk1 and Cds1 phosphorylate a wide array of targets, and although activated by different types of DNA damage, both *S. pombe* effector kinases have several common downstream targets such as the MBF transcription factor [112], Wee1 [113], and Cdc25 [52, 114]. Interestingly Chk1 also binds the unphosphorylated Cdk1-Cyclin complex Cdc2-Cdc13. The Cdc2-Cdc13-Chk1 complex has additionally been proposed to be involved in the DNA damage response [74]. In similarity to fission yeast, human CHK1 and CHK2 also directly phosphorylate CDC25A, leading to checkpoint-induced cell cycle arrest [115, 116, 66]. Crosstalk and overlapping of substrates between ATM/CHK2 and ATR/CHK1 as well as DNA-PK exist in mammals [108, 117], and ATR, CHK1, and CHK2 [118] as well as DNA-PK [119, 120] are all able to phosphorylate p53, the most extensively studied tumor suppressor protein, a protein however not conserved in fission yeast.

The human 9-1-1 complex in turn, in addition to its role in induction of checkpoint signaling, is involved in base excision repair (BER) by interaction with BER enzymes such as MYH1 and MUTY [121, 122] and this function is conserved in fission yeast [123, 124]. The *S. pombe* 9-1-1 complex is also involved in the transcriptional regulation of BER enzymes and can additionally act as a nuclease processivity factor to promote chromosome resection [125].

## **Caffeine confers checkpoint override in human and fission yeast cells**

Caffeine has been shown to override cell cycle checkpoints in human cells [126] as well as in the fission yeast *Schizosaccharomyces pombe* [127, 128]. Therapeutic application of caffeine as a sensitizing agent in cancer therapy is however impractical because of the very high and physiologically irrelevant doses needed to accomplish this effect, as well as its obvious pleiotropic effects, but the understanding of the mechanism underlying caffeine-induced checkpoint override may aid in the development of other compounds with similar overriding mechanisms.

Caffeine has been shown to inhibit the central activators of checkpoint control ATM and ATR proteins as well as the fission yeast ATR homolog Rad3 *in vitro* [126, 128]. For this reason caffeine has been widely studied as an ATR/ATM inhibitor. Therefore the checkpoint overriding effect of caffeine has been proposed to be through inhibiting ATM/ATR or Rad3 [126]. It has however been shown that the checkpoint override effect of caffeine *in vivo* is not through inhibition of ATM and ATR [129]. One study indicated that one of the caffeine checkpoint override effects was to enhance CDK activity through interfering with 14-3-3 binding to CDC25C [130]. Additionally CHK1, the effector kinase of the replication checkpoint in mammalian cells, has also been shown to stabilize CDC25A [115, 131]. In **Paper I** we thus investigated the role of Cdc25 in the caffeine-induced checkpoint override in *S. pombe*, and whether the effect is Rad3-dependent.

Both mammalian and fission yeast TORC1, Target of rapamycin complex I, contain a PIKK related kinase. TORC1, like the PIKK related kinases ATM/ATR and Rad3, is also inhibited by caffeine [132, 133]. Fission yeast TORC1 in turn regulates both Cdc25 and Wee1 [85], clearly impacts cell cycle progression, and may therefore be important in the *in vivo* checkpoint overriding effect of caffeine. In **Paper II** we study how caffeine regulates

Wee1. The contribution of this regulation and its possible link to TORC1 inhibition to checkpoint override is investigated.

## **Hypoxia is a common feature in tumors, complicates cancer therapy, and is associated with worse prognosis**

Hypoxia is a state with a lower than normal oxygen availability. Because of poor perfusion of blood vessels in parts of a solid tumor, the interior of a tumor often contains areas with lower oxygen pressure than surrounding tissues, and the interior of a tumor may be close to anoxic [134]. Hypoxia can further be chronic or acute and the state may be complicated by alternating events of vessels forming and collapsing leading to variable blood flow. For various types of anticancer therapies including surgery, chemotherapy, as well as radiotherapy, it has been demonstrated that hypoxia interferes with the efficiency of the treatment [134]. Hypoxic tumors are also associated with higher frequency of metastases and the presence of hypoxic tumors are prognostic of poorer outcome [135].

The Hypoxia inducible factor 1 (HIF-1) is a master transcription factor in mammalian cells that regulates the response to hypoxia, and this transcription factor is also well known to be stabilized in hypoxic cancer cells [136], leading to transcriptional reprogramming of the cellular metabolism. HIF-1 induction also has a role in induction of metastasis and in stimulation of angiogenesis [137], thereby being involved in reoxygenation of hypoxic tissues. No homolog of HIF-1 exists in fission yeast, instead the transcription factor mainly responsible for induction of hypoxic responses is called Sterol regulatory element 1 (Sre1). This protein is a membrane-bound transcription factor that upon hypoxia is cleaved off from the endoplasmic reticulum and is thereby activated. Also in response to low sterol levels Sre1 is activated, and both oxygen depletion and depletion of sterols lead to upregulation of the same set of genes in a Sre1-dependent manner. It has been proposed that Sre1 together with its partner Scp1 indirectly monitor the oxygen supply by the extent of oxygen-dependent and highly oxygen-consuming sterol synthesis [138]. Sre1 belongs to a class of sterol regulatory element-binding proteins (SREBPs) also conserved in mammals, where they are involved in lipid homeostasis [139].

## Hypoxia impacts the DNA damage response

It is known that different levels and durations of hypoxia affect the DNA repair pathways differently. In human cells acute hypoxia initially induces a DNA damage response in the absence of DNA damage, induced by activated CHK2 through ATM [140], and in extreme hypoxia CHK1 is activated by ATR due to replication stress [141]. Under chronic hypoxia instead the DNA repair pathways are downregulated [142]. A concomitant reoxygenation process will lead to regeneration of reactive oxygen species (ROS) resulting in DNA damage as well as induction of a DNA damage response [141]. Thus both long term hypoxia and reoxygenation may lead to higher frequency of DNA damage, and /or unresolved DNA damage especially in those hypoxic cells where the checkpoint pathways are defective, thus leading to genetic instability [143]. In **Paper III** we investigate the regulation in hypoxia of Aph1, the fission yeast homolog of the human tumor suppressor FHIT.

## **Aph1, the fission yeast homolog of the puzzling human tumor suppressor FHIT**

Many tumor suppressor proteins are involved in checkpoint signaling, DNA damage repair and/or induction of apoptosis. In terms of being involved, the human tumor suppressor Frigile Histidine Triad protein (FHIT) is literally all over the place, impacting all these common tumor suppressor functions. We got interested in the FHIT homolog Aph1 in fission yeast as the suggested functions of FHIT are so diverse. In **Paper III**, we therefore used genetic methods to investigate basic cellular functions of the FHIT homolog in the less complicated context of fission yeast.

## FHIT and related proteins

The human gene of FHIT is located at locus FRA3B on chromosome 3 [144]. FRA3B constitutes a so called inducible fragile site – a heritable region in the genome that reveals chromosomal abnormalities distinguishable in the microscope such as gaps, weak staining, constrictions or even breaks when replication is partially inhibited, but not entirely stopped. This partial inhibition can in the lab be obtained by the use of certain reagents, or through specific culturing conditions. The abnormalities are cytologically visual in mitosis as



a region failing to condense properly, and may lead to breakage of the chromosome during mitosis. Inducible fragile sites are further divided in common or rare, depending on their frequency in the population, where common sites are cytogenetically apparent in all individuals however only visible in a fraction (up to 30 %) of cells [145]. Inducible fragile sites generally have a few characteristics in common. Their sequences are able to form secondary structures and/or contain sequences that perturb the progress of the replication fork. When extra replication stress further amplifies these characteristics it may result in non-replicated regions and defective chromatin organization leading to fragility of the chromosome in that region [146].

Among fragile regions, rearrangements such as deletions or translocations are more common because of higher frequencies of strand breaks. The locus FRA3B, where the gene of FHIT is located, is one of thirteen common fragile sites induced in humans by the replication inhibitor aphidicolin [146], and this region constitutes the most highly inducible common fragile site [147].

As the locus FRA3B is more prone to breaks and rearrangements, it may not be surprising that abnormalities in the FHIT gene located there are commonly seen in cancer. Importantly however, FHIT is itself a well established tumor suppressor, with FHIT<sup>-/-</sup> mice spontaneously developing tumors at a higher frequency than control mice, and both FHIT<sup>+/-</sup> and FHIT<sup>-/-</sup> mice were highly susceptible to induction of tumors by N-nitrosomethylbenzylamine [148]. Altogether it seems like the combination of the protein having tumor suppressing effects as well as the gene being prone to break, because of its location on an inducible fragile site, makes FHIT a very common factor in early tumor development [149]. The picture of FHIT as a tumor suppressor is currently very complex, and FHIT seems to have several anti-tumor molecular functions. FHIT depletion induces the formation of double strand breaks through elevated replication stress, due to downregulation of the available level of dTTP through lower levels of thymidine kinase 1 [150]. In FHIT<sup>-/-</sup> constitutive knock-out cells there is additionally a higher burden of single base substitutions in the total exome possibly because of an imbalance in the dNTP pool caused by the lower dTTP level [151]. FHIT also modulates the level and /or activity of proteins involved in sensing of DNA damage and checkpoint control, such as Hus1 in the 9-1-1 complex (Rad9-Rad1-Hus1), CHK1 [152], and CHK2 [153], through unknown mechanisms. FHIT also clearly affects the balance between survival and apoptosis, as reintroduction of FHIT in FHIT-negative human cancer cell lines induces apoptosis [154]. In mitochondria FHIT is in

direct physical interaction with ferredoxin reductase in the electron transport chain and this interaction results in higher production of ROS, which in turn favors apoptosis [155]. It has also been shown that loss of FHIT expression leads to superinduction of ROS-eliminating enzymes [156], changing the balance in the opposite direction. FHIT is further able to stabilize the tumor suppressor protein p53, by reducing the level of the p53 negative regulator Mdm2. This is mediated through a direct interaction between FHIT and Mdm2 as indicated by co-immunoprecipitation experiments in cells from human non-small cell lung cancer [157].

Fission yeast Aph1, human FHIT and the budding yeast Hnt2/Aph1 are all members of the FHIT branch of the Histidine Triad superfamily (HIT superfamily). The HIT superfamily members all have the common sequence motif, H $\phi$ H $\phi$ H $\phi$ , where  $\phi$  is a hydrophobic amino acid. The HIT superfamily is composed of nucleotide hydrolases and transferases. The FHIT branch in turn consists of diadenine polyphosphate (Ap<sub>n</sub>A) hydrolases, and unlike the Fission Yeast Aph1 which prefers AppppA as the substrate, the FHIT and Hnt2 proteins favor catalysis of ApppA over AppppA [158]. Importantly however, for FHIT it has been shown that it is not the actual hydrolysis of its substrates that is responsible for tumor suppression; because the mutant form FHIT<sup>H96N</sup>, which is unable to perform hydrolysis but is still able to bind substrate, keeps the tumor suppression capacity. Therefore it has even been proposed that binding of substrate to FHIT activates the protein in analogy to how the exchange of GDP to GTP activates G-proteins [159]. That the anti-tumor effect of FHIT is independent of actual ApppA catabolism opens the possibility that both ApppA and AppppA or even a distinct but related molecule is the second messenger for the anti-tumor activities of FHIT. It is also not clear if binding of Ap<sub>n</sub>A is related to tumor-suppressing activities at all [158]. A later study [160] actually indicates that it may be another closely related molecule that is important in the tumor suppressing activities of Fhit, the 5' cap structure m7GpppN, generated through the 5' – 3' RNA decay pathway of mRNA. The FHIT homologs in yeasts are strikingly understudied, however, the budding yeast homolog Hnt2/Aph1 was shown to be involved in scavenger decapping of 5'cap structures, and importantly this function was conserved for FHIT in HEK293 cells [160]. In eukaryotes the mRNA 5'cap structure is recognized by eIF4E in the 40S initiation complex of the ribosome, and the 5'- capped mRNA is additionally protected against 5'exonucleases [161]. Therefore the 5' cap structure is important for both mRNA stability as well as initiation of translation. FHIT has been shown to influence the mRNA turnover of multiple genes including a subset of mRNAs involved in cancer. Translation is also affected by FHIT [162], possibly through its 5'cap-binding

properties which may explain some of the complexity in how FHIT exerts its pleiotropic anti-tumor activities. FHIT re-introduction was additionally shown in this study to change the relative occupancy of ribosomes in the 5' untranslated region and the coding region, and the identified mRNAs all had either confirmed or putative upstream open reading frames. In the case of the positive regulation by FHIT on translation of TK1, the regulation was dependent on the presence of the TK1 5' untranslated region (5'-UTR), a region with a predicted extensive secondary structure [163]. The authors suggested that this effect may be indirect through hydrolysis of loose 5' cap structures otherwise competing for eIF4E binding instead of the 5' cap of TK1 mRNA. However that hydrolysis of the 5' cap structure is responsible for this effect is contradicted in the same study by the fact that the FHIT<sup>H96N</sup> mutant lacking catalytic activity, but retaining substrate binding of ApppA [159] as well as GpppG [160] is as efficient in promoting TK1 translation as the wt version. This strongly indicates the regulation through the 5'-UTR is not through elimination of loose 5' cap structures, but rather through binding of either loose 5' caps, thus thereby competing with eIF4E binding, or more likely, to 5' cap structures when still attached to intact mRNA. The only argument so far against FHIT being an mRNA binding protein is that it has not been found in common screens directed against mRNA binding proteins [163]. In our experience human FHIT is however a weakly expressed protein which may impact such a result. If FHIT does bind 5' cap structures on intact mRNA or only loose 5' cap structures, and how this actually leads to regulation of certain key mRNAs is an open question hopefully answered in the future, and studies in the less complex yeast systems of both budding and fission yeasts should be useful in this context.

### Fission yeast Aph1

The fission yeast Aph1 protein shares 52% identical sequence with the human FHIT protein [164]. Aph1 itself, a bis(5'-nucleosidyl)-tetrphosphatase, is a largely unstudied non-essential protein in fission yeast, and most information available is therefore currently from high throughput studies. In the BioGRID database only one physical interaction, with itself, is recorded [165], which makes it plausible that it forms a homodimer as does human FHIT [159]. For the Aph1 gene only three positive genetic interactions are so far observed, the mitochondrial import receptor subunit Tom70, the cell division cycle-related protein Res1 (subunit of MBF transcription factor) and the checkpoint protein Hus1 in the 9-1-1 complex,

all from the same large-scale study [166]. The positive interaction between Hus1 and Aph1 correlates well with the human homolog FHIT modulating the human HUS1 protein level [152]. The only in depth article studying Aph1 function tested high level overexpression of Aph1, achieved by the use of the CMV promoter, which led to a longer generation time and a significant decrease in the in the AppppA level [164]. FHIT in human cells is localized in the cytoplasm, the nucleus and in the mitochondria [167]. The localization of Aph1 in fission yeast is according to the fission yeast genome database PomBase (<https://www.pombase.org/>) expected to be like in human cells, but for the mitochondrial localization this has not yet been experimentally proven.

## **Oxidative stress and H<sub>2</sub>O<sub>2</sub> induced signaling**

Aerobic metabolism will naturally cause production of ROS. Intracellular H<sub>2</sub>O<sub>2</sub> as well as other ROS is produced in metabolic pathways from oxidases, oxidoreductases, from peroxisome leakage as well as from the mitochondrial electron transport chain. The ROS superoxide, likewise produced intracellularly, is also a precursor of H<sub>2</sub>O<sub>2</sub> [168]. Oxidative stress refers to the situation when ROS are not sufficiently detoxified by the cell, leading to oxidative damage of its molecules and structures. This can be caused by imbalance in metabolic activities but also by external application of oxidative stressful agents. Many health issues such as neurodegenerative disorders as well as normal biological aging are strongly correlated with oxidative damage of cells and higher ROS levels [169, 170], and thus correlates with the so called “free radical hypothesis of aging”. Therefore produced H<sub>2</sub>O<sub>2</sub> was earlier seen as solely harmful for the cell, but with time this view have changed and it is now recognized that H<sub>2</sub>O<sub>2</sub> is not only a metabolic byproduct but also beneficial through induction of cellular signaling. As a signaling molecule, H<sub>2</sub>O<sub>2</sub> mainly transfers the signal through reacting with selected thiols of cysteine residues in proteins [168].

### H<sub>2</sub>O<sub>2</sub>-induced cysteine oxidations

Even though one generally talks about the thiol (SH group) of the cysteine as reacting with H<sub>2</sub>O<sub>2</sub>, it is generally rather the deprotonated thiolate (S<sup>-</sup>) that reacts. Hence, the first step for a direct reaction with H<sub>2</sub>O<sub>2</sub> is the deprotonation of the thiol, and stabilization of the thiolate form, which depends on pH as well as the local environment of surrounding

amino acids where specific hydrogen bond donors as well as a electropositive local environment stabilize the thiolate [171]. It is however still hard to predict which cysteines are reactive with  $H_2O_2$ , without empirically testing the reactivity. Additionally, the concentration of the protein and  $H_2O_2$  is very important for the reaction kinetics. Thus, even though all cysteines are able to react with  $H_2O_2$  given high enough  $H_2O_2$  concentration, most cysteine thiols will not react with  $H_2O_2$  under physiological conditions due to kinetic restraints [172]. Oxidation of the thiolate with one  $H_2O_2$  molecule will result in sulfenylation (SOH). SOH is a very unstable intermediate and will if possible quickly further react either with a nearby cysteine, resulting in a disulfide (-S-S) bond [173], or less commonly with a nitrogen resulting in a sulfenamide ring [174]. The sulfenylated cysteine, the disulfide and the sulfenamide can be reduced back to a thiol/thiolate either by a chemical reductant such as  $\beta$ -mercaptoethanol, DTT or TCEP, or in the cell by reduction mainly through the glutathione and thioredoxin antioxidant systems [172, 175], and are therefore considered to be reversible cysteine oxidations. Further oxidation with  $H_2O_2$  of a sulfenylated cysteine results in overoxidation into less reversible groups such as sulfinylated and sulfonylated cysteines. Sulfinylated cysteines can however in some proteins be converted back to thiolate form by the enzyme sulfiredoxin in an energy-requiring process [176].

#### The thioredoxin- and glutathione-based antioxidant systems

Antioxidants keep the cytoplasm of aerobically growing cells a reduced environment despite the highly oxidizing environment on earth. Many oxidoreductases, *i.e.* proteins able to undergo oxidations and reductions, such as thioredoxins (Trx), glutaredoxins (Grx), glutathione peroxidases (Gpx), and peroxiredoxins (Prx), all share a common fold called the thioredoxin fold. This fold is built up by four inner  $\beta$ -strands surrounded by three  $\alpha$ -helices and generally also contains the active site motif Cys-X-X-Cys. The different proteins in the thioredoxin fold family have additional folds giving their different individual specificities for redox processes [177]. Thioredoxin, the protein giving name to this common fold is able to reduce protein disulfides and is itself reduced by thioredoxin reductase (TrxR) receiving electrons from NADPH [178].

Glutathione, a highly abundant cellular antioxidant, is a thiol-containing tripeptide constituted by the amino acids glycine, cysteine and glutamic acid with an unusual peptide bond between the cysteine amino group and the side chain carboxy group of the glutamic acid residue [179]. The glutathione based antioxidant system contains glutathione as well as a number of proteins that all are able to undergo redox reactions, and thus can be

oxidized and reduced. Glutathione is able to cycle between a reduced (GSH) and oxidized (GSSG) state. Glutathione is oxidized to sulfenic acid, SOH, thereafter commonly forming a disulfide with another glutathione molecule giving glutathione disulfide, GSSG. Glutathione reductase (GR) is responsible for the reduction of GSSG back to two GSH molecules. Glutaredoxins (Grx), in turn, are enzymes that use GSH to resolve protein disulfides by using GSH as the reductant. Glutathione peroxidase (Gpx) instead scavenges peroxide by catalyzing the reaction of two GSH molecules into GSSG [180]. S-glutathionylation refers to the coupling of glutathione to the sulfur atom of the thiol in a cysteine residue in a protein through a disulfide bond. Glutathionylation can be a spontaneous or enzyme-catalyzed reaction [181].

In contrast to Trxs and Grxs, Prxs, in similarity to Gpxs, rather reduce peroxide directly instead of protein disulfides [172]. The budding yeast 2-Cys-Prx Tsa1 as well as the fission yeast 2-Cys-Prx Tpx1 use thioredoxin for their reduction of peroxide, in analogy to how Gpx uses GSH for reduction of peroxide. Therefore Tsa1 and Tpx1 are referred to as thioredoxin peroxidases (Tpxs) [182]. In the presence of higher concentrations of H<sub>2</sub>O<sub>2</sub> the peroxidoredoxins such as Tsa1 and Tpx1 peroxidative cysteine sulfenic acid can be “over-oxidized” to sulfenic acid and then further to sulfonic acid. This over-oxidation shuts down the peroxidative activity of the protein and may instead activate a chaperone function forming ring-shaped high molecular weight stacked structures around client proteins [183, 184]. The peroxidative function of sulfenic acid-modified 2-Cys-Prxs can be recovered in an ATP-dependent process catalyzed by sulfiredoxin (Srx), thereby reactivating the peroxidative activity [185].

### H<sub>2</sub>O<sub>2</sub> as a signaling molecule

H<sub>2</sub>O<sub>2</sub> thus not only causes oxidative damage, but is especially in the low physiologically relevant concentration range, capable of regulating important cellular events, and may be seen as a second messenger [186]. H<sub>2</sub>O<sub>2</sub> mainly induces cellular signaling through induction of thiol oxidation of selected cysteines in signaling proteins such as kinases, transcription factors and phosphatases. The cysteine oxidation results in a redox switch leading either to activation or inhibition of a protein function, for example through disulfide formation or through S-thiolation with glutathione [187, 188]. The oxidation event may be direct in a few cases such as in the bacterial H<sub>2</sub>O<sub>2</sub> OxyR, where H<sub>2</sub>O<sub>2</sub>-induced oxidation results in an intramolecular disulfide resulting in recruitment of this activator/repressor of

transcription to promoters of selected genes resulting in upregulation of antioxidant levels [189]. In most cases though, the cysteines of the H<sub>2</sub>O<sub>2</sub>-scavenging Gpxs and Prxs, are the primary targets of H<sub>2</sub>O<sub>2</sub> [172]. As an example, mitochondrial Prx3 and Gpx1 together scavenge 99 % of the H<sub>2</sub>O<sub>2</sub> present in the mitochondrial matrix [190], reducing the capability of other thiols to react with H<sub>2</sub>O<sub>2</sub> directly in this cellular compartment. Proteins such as Prxs and Grxs are however not only capable of scavenging H<sub>2</sub>O<sub>2</sub>, but also to transfer the oxidation to selected cysteines of other proteins through direct protein-protein interactions in processes commonly referred to as redox relay [172].

In the process of redox relay from a 2-Cys-Prx to another protein, the peroxidative cysteine of the Prx is first sulfenylated directly by H<sub>2</sub>O<sub>2</sub>. The sulfenylated cysteine thereafter reacts with a cysteine in the target protein forming an intermolecular disulfide. This mixed disulfide is thereafter resolved either by Trx or by another cysteine of the target protein, resulting in an intramolecular disulfide. Within this protein further redox rearrangements can occur between the cysteines in the molecule, resulting in disulfide shuffling [172]. This is the mechanism by which the fission yeast thioredoxin peroxidase Tpx1 induces activation of the transcription factor Pap1 by transferring oxidation to Pap1 leading to an intramolecular disulfide inactivation of the Pap1 nuclear export signal (NES) [191]. A similar mechanism activates the *S. cerevisiae* Pap1 homolog Yap1 first through the glutaredoin Gpx3, which thereafter forms a mixed disulfide with Yap1 which is resolved by a second cysteine within Yap1 resulting in a Yap1 intramolecular disulfide inactivating the Yap1 NES [192]. In a certain strain background (W303) the budding yeast Tpx1 homolog Tsa1 is instead the sensor leading to inactivation of the Yap1 NES [193].

Glutathionylation affecting protein function has in turn been determined in different locations of multiple kinases, generally inhibiting enzymatic activity [194]. Local environment within a protein structure may stabilize either the thiol or thiolate form, and a low pKa value of a cysteine, *i.e.* the pH where half of the thiols are deprotonated, would indicate higher reactivity because of the higher proportion of the more reactive thiolate form at physiological pH. Interestingly a large scale study of human proteins found little correlation between confirmed S-glutathionylated cysteines and their predicted pKa value from structure. The same study further noted that surprisingly many of the affected cysteines were relatively buried within the protein structure [195]. These notions are definitely counterintuitive in the case of cysteines directly reacting with H<sub>2</sub>O<sub>2</sub>, and GSH only protecting the cysteine from further oxidation; however less surprising if the process is indirect through redox relay induced by another primary H<sub>2</sub>O<sub>2</sub> sensor.

## **Stress-activated MAPK pathways**

MAPK pathways are important signaling pathways conserved from yeasts to humans

MAPK pathways are a group of conserved pathways found in all eukaryotes from yeast to humans [196]. The name Mitogen Activated Protein Kinase refers to the fact that the first MAPK pathway identified, the mammalian ERK pathway, responds to growth factors (mitogens). Later it was found that a number of related MAPK pathways are induced by several other types of stimuli such as different cellular stress conditions [197]. Signals are transmitted from sensors in the membrane and further transduced through a phosphorylation cascade between the different intracellular compartments of the pathway. Different MAPK pathways are involved in important cellular events such as proliferation, differentiation, development, cell cycle regulation, survival and cell death [198]. MAPK pathways responding to extracellular stress are called SAPK (Stress Activated Protein Kinase) pathways. Examples of human SAPK pathways are the human Jun N-terminal Kinase (JNK) and p38 pathways [199].

The core of a MAPK pathway consists of a module of three kinases sequentially phosphorylating the next kinase in the module [200]. The central part in the MAPK cascade is the MAP kinase (MAPK), itself being activated by dual phosphorylation on two neighboring tyrosine and threonine residues [196]. The kinase activating the MAPK is called the MAP Kinase Kinase (MAPKK) whereas kinases activating the MAPKK are called MAP Kinase Kinase Kinases (MAPKKKs). MAPK pathways such as ERK and the SAPKs p38 and JNK are often deregulated in cancers and this deregulation is of importance in oncogenesis [201-203].

### **The *S. pombe* Sty1 MAPK pathway**

The Sty1 MAPK pathway is a stress-activated pathway consisting of orthologs of the human p38 and ERK1/2 pathways

In fission yeast only three different MAPK pathways exist; the stress-induced Sty1/Spc1/Phh1 pathway, the cell integrity Pmk1 pathway and the mating pheromone-responsive Spk1 pathway [204] [54] [205].

Of the three MAPK pathways in fission yeast, the Sty1 pathway is by far the most studied. Like the p38 and JNK pathways in humans, the Sty1 pathway is a SAPK and



the most important stress-induced pathway in fission yeast, required for adaptation to and survival in a wide array of cellular stresses. Loss of function of either Sty1 or Wis1, the MAPKK of Sty1, leads to partial sterility, loss of viability in stationary phase and hypersensitivity to hyperosmotic shock, as well as a delay in G<sub>2</sub> [54, 206]. Examples of stimuli that have been shown to induce the pathway include osmotic stress [207], oxidative stress [208], cold [209], nutrient deprivation [206, 207, 210], UV light [211], ionizing radiation, [212], heat [207, 213, 214], exposure to cadmium [210], arsenite [215] and arsenate ions [216]. Upon activation, Sty1 accumulates in the nucleus and induces transcriptional responses by phosphorylation of the transcription factor Atf1 leading to its activation. Most of the transcriptional response resulting from induction of the Sty1 pathway is actually attributed to this single transcription factor [217]. Atf1 forms a heterodimer with Pcr1 and this heterodimer is responsible for induction of transcription of a variety of stress response genes. However it has also been shown that the cellular transcriptional responses to specific stresses are not entirely overlapping in cells lacking Pcr1 or Atf1, but some transcripts require only Atf1 for induction. Furthermore, both Pcr1 and Atf1 are actually capable of downregulation of transcription of certain genes [218]. For a simple overview of the pathway see **Fig 2**.

Sty1 is itself a homolog of the budding yeast MAPK Hog1 and the human MAPK p38 [207]. Wis1, the MAPKK of the pathway and the subject of interest in **Paper IV**, is a homolog of budding yeast Pbs2 and is the structural homolog of human MEK1 [219], the MAPKK in the ERK pathway.

#### Initiation of Sty1 activation may be regulated within large complexes containing multiple constituents of the pathway

Generally multiple distinct MAPKKs may phosphorylate the same MAPK, and the same MAPK may phosphorylate more than one MAPK. In contrast, the interaction between a certain MAPK and MAPK is more specific and the same MAPK/MAPK only interacts with one, or in case of more than one, a closely related set of MAPK/MAPK partners [18]. Wis1 is the only MAPKK of Sty1, and Wis1 activates Sty1 through dual phosphorylation on T171 and Y173 [220]. Sty1 is also the only known target of Wis1. Conveniently, activated dually phosphorylated Sty1 can be detected using an antibody against phosphorylated p38, and the degree of activation of Sty1 can therefore be followed by western blotting.

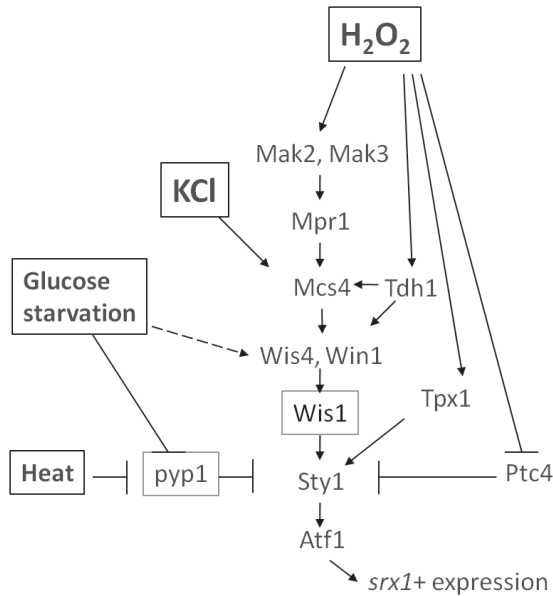


**Figure 2:** Overview of the *Sty1* pathway.

Two different MAPKKKs called Win1 [221] and Wis4/Wik1/Wak1 [222] in turn activate Wis1 by phosphorylation on S469 and T473. Interestingly, the MAPKKKs of the *Sty1* pathway are under some circumstances redundant whereas in other situations, both MAPKKKs are required. The paralogs Win1 and Wis4 are redundant in low peroxide stress [223], whereas in hyperosmotic shock and high peroxide stress both MAPKKKs are required [223, 224]. The underlying cause of the need for both MAPKKKs in osmotic stress is that osmotic stress signaling requires a complex containing both MAPKKKs forming a heteromer [224]. The same complex also contains the response regulator Mcs4. Further, only one of the MAPKKKs in the complex actually needs to be activated for efficient activation of Wis1. Importantly the same study showed that in the absence of stress, the Win1-Wis4-Mcs4 heteromer physically interacts with Wis1, and when the complex is stimulated by osmotic stress, Wis1 detaches from the complex. This detachment of Wis1 is not triggered by the phosphorylation of Wis1 by Win1 and/or Wis4, as the detachment also occurs when both Win1 and Wis4 have mutations making them defective in phosphorylation [224].

Also in oxidative stress the MAPKKK heteromer is involved in phosphotransfer to Sty1 [224], however presumably the heteromer is more important in H<sub>2</sub>O<sub>2</sub> concentrations where both Win1 and Wis4 are required. It is also not yet known if Win1 or Wis4 can form homodimers. Another study shows that also Sty1 is associated with Wis1 in the absence of stress, and that Sty1 dissociates from Wis1 in response to osmotic stress in the form of 0.6 M KCl [225]. Thus, all three levels of kinases of the Sty1 MAPK module, MAPKKK, MAPKK and MAPK, are likely forming a common complex in the absence of stress. This complex also contains Mcs4 which is associated with the MAPKKKs in the absence of stress [224], the GAPDH Tdh1, which co-precipitates with Win1 and Wis4 in the absence of stress [226], as well as the thioredoxin peroxidase Tpx1, which co-precipitates with Sty1 also in the absence of stress [227].

#### Indirect activation of the Sty1 pathway through inhibition of dephosphorylating activities

Attenuation of Sty1 activity is carried out by several different phosphatases such as the tyrosine phosphatases Pyp1, Pyp2, as well as PP2C serine/threonine phosphatases Ptc1, Ptc3 [207, 228] and Ptc4 [229].

Even though stimulation of the Sty1 pathway through Win1/Wis4 - Wis1 leads to induction of Sty1 phosphorylation, Wis1 also under non-stressed conditions phosphorylates Sty1 to some extent and therefore this must constantly be attenuated by dephosphorylating activities targeting Sty1. Pyp1 is the most important phosphatase under non-stressed conditions and it constitutively dephosphorylates Sty1. In the *pyp1Δ* mutant an increased basal level of Sty1 phosphorylation also under non-stressed conditions is seen showing the importance of Pyp1 in continuous inactivation [214]. Some stresses such as heat [213, 228, 214] and Cd<sup>2+</sup> exposure as well as low glucose stress [210], actually induce higher Sty1 activation not mainly through stimulation through the MAPKKK-MAPKK-MAPK module but rather through inhibition of Pyp1. The other phosphatases Pyp2 and Ptc 1-4 rather seem to quench the Sty1 phosphorylation upon stimulation by stress. Interestingly Ptc4 is specifically involved in attenuation of the oxidative stress activation of a mitochondrial Sty1 pool [229]. It is not yet known if also the MAPKKKs and MAPKK of the pathway also are to some extent located within the mitochondria. Further, it remains to be elucidated how dephosphorylation of the other kinases of the pathway is achieved.

Sensing of peroxide stress induces the Sty1 and Pap1 pathways, respectively, and these are activated in differential H<sub>2</sub>O<sub>2</sub> concentrations due to mechanisms involving redox relay

Peroxide is sensed in fission yeast by two different signaling pathways, the Sty1 and Pap1 pathways, and these are induced in different H<sub>2</sub>O<sub>2</sub> concentration [230]. In the Sty1 pathway, the two histidine kinases Mak2 and Mak3 constitute a "two-component system" [231], similar to those found in bacteria. The two-component system stimulates the MAPKKKs through transfer of a phosphoryl group from the sensor histidine kinases via the phosphotransferase Mpr1 to an aspartic acid in the response regulator Mcs4, which further transmits the phosphorylation to Win1/Wis4 [232]. How peroxide stress is sensed by the two-component system is not yet known.

The Pap1 pathway is activated in the low H<sub>2</sub>O<sub>2</sub> concentration range. Pap1 itself is activated through redox relay resulting in internal disulfide formation within Pap1, rendering its NES inactive, resulting in translocation of this transcription factor into the nucleus. The redox relay is coming directly from Tpx1, a typical 2-Cys peroxidase, and in the absence of Tpx1, the cysteines in Pap1 are not able to be oxidized [233].

Tpx1 is inactivated by higher H<sub>2</sub>O<sub>2</sub> concentrations by oxidation of its catalytic cysteine to sulfinic acid [191], and so Pap1 is also inactivated, and not localized in the nucleus. Tpx1 can be reactivated by the sulfiredoxin Srx1 [183]. The expression of *srx1*<sup>+</sup> is however dependent on active Sty1 [230], and so the action of Pap1 is limited to a window of H<sub>2</sub>O<sub>2</sub> concentrations where peroxide levels are either low, or Sty1 activation high enough to sustain the Srx1 level needed to reactivate Tpx1 [191]. Tpx1 is also involved in Sty1 signaling. In low H<sub>2</sub>O<sub>2</sub> levels, activation of Sty1 is Tpx1-dependent, whereas at higher concentrations Sty1 is gradually becoming Tpx1 independent [227]. This indicates that Tpx1 is involved in induction of Sty1 activation in lower but not higher H<sub>2</sub>O<sub>2</sub> concentrations. The cysteine of Tpx1 directly reacting with H<sub>2</sub>O<sub>2</sub> is called the peroxidative cysteine, and upon oxidation by H<sub>2</sub>O<sub>2</sub> this cysteine forms a mixed disulfide with Sty1 C35. Interestingly, mutating this cysteine in Sty1 to serine makes Sty1 phosphorylation entirely independent of Tpx1 [227], indicating that oxidation of this cysteine may also have inhibiting properties. Indeed, this study shows that in the *sty1-C35S* mutant, a *tpx1Δ* deletion actually results in stronger phosphorylation of Sty1, indicating that Tpx1 coordinates the Sty1 activation level and has both stimulating and inhibiting effects on Sty1 activation.

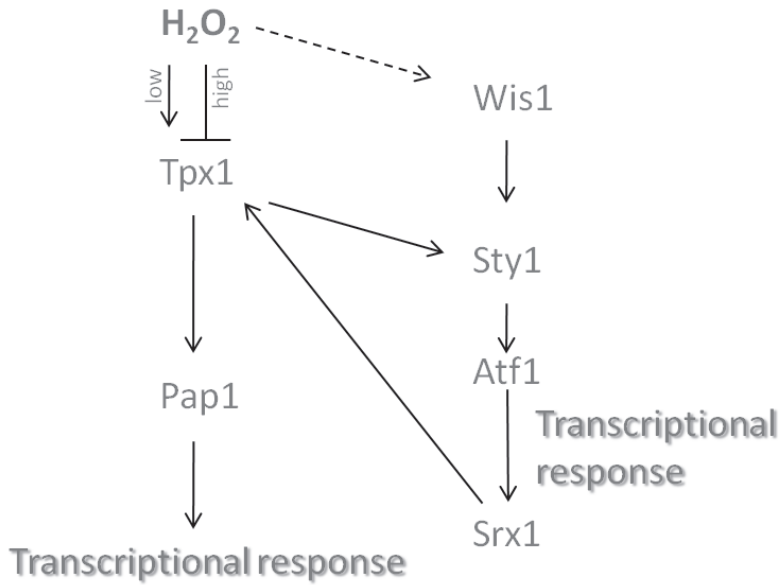


**Figure 3:** *Tpx1 regulates the differential concentration dependency of induction of the Pap1 and Sty1 pathways*

The glycolytic enzyme glyceraldehyde-3-phosphate dehydrogenase (GAPDH) Tdh1 is important for Sty1 activation in peroxide-induced oxidative stress. Tdh1 is constitutively physically associated with both Win1 and Wis4, also in the absence of H<sub>2</sub>O<sub>2</sub>. The same is true for the physical interaction of Tdh1 and Mcs4. The physical interaction between the MAPKKKs and Mcs4 is further not Tdh1-dependent, however Tdh1 is required for the interaction between Mpr1 and Mcs4 [226]. Interestingly, in response to H<sub>2</sub>O<sub>2</sub>, the catalytic cysteine residue Tdh1 C152 is S-thiolated and this in turn transiently strengthens a physical interaction of Tdh1 with Mcs4. Mutation of Tdh1 Cys152 to serine abrogated the enhanced transient association between Tdh1 and Mcs4 in response to H<sub>2</sub>O<sub>2</sub> while the same mutation did not affect the physical interaction between Tdh1 and Win1/Wis4 [226]. Tdh1 dissociates from Mcs4 upon osmostress, while oxidative stress promotes the association between Mcs4 and Tdh1. Thus, this interaction has been proposed to direct the Win1-Wis4-Mcs4 heteromer responsive to phosphorelay from the two-component system in oxidative stress [224].

## **The human MAPKK MEK1, and the story behind INR119, the small molecule used in Paper IV**

### Targeting MAPK pathways with small molecules

MEK1, a MAPKK of the ERK1/2 pathway, is the closest human structural homolog of the fission yeast MAPKK Wis1. As MAPK pathways including the ERK1/2 pathway are often deregulated in cancer, much effort has also been directed to develop chemical tools to understand these pathways and to target them in anti-cancer treatment. Selective small molecules such as the MEK1 inhibitors PD98059 and U0126 [234, 235] have provided useful information when studying the human ERK1/2 pathway, and in recent years interest in the potential of small molecules in cancer therapy have generated inhibitors targeting components in MAPK pathways that are approved for treatment of certain cancers. Examples are the MAPKK inhibitors trametinib [236], cobimetinib [237] as well as the MAPKKK B-RAF inhibitor dabrafenib [238]. Chemical inhibitors may directly bind to the catalytic site leading to direct competitive substrate inhibition by blocking access of the normal substrate(s), or they may bind allosterically, *i.e.* in a place that is not the actual catalytic site but that still affects activity of the enzymatic function. The repertoire of possible mechanisms of action of allosterically working effectors is far greater compared to compounds binding in a substrate-competitive way. Allosteric triggers may also increase as well as decrease a protein's enzymatic activity by for example altered access to the active site or changes of the conformation within the active site. Other possibilities are changes in dynamic properties of the protein or associations with other proteins. Indeed, potentially even a combination of these mechanisms may exist. [239, 240].

### Allosteric MEK1 inhibitors including INR119 bind a common allosteric pocket next to the catalytic site

Already in 1995, the small molecule compound PD98059 was identified as the first small molecule non-ATP competitive inhibitor of MEK1 and MEK2, two closely related MAPKKs of the ERK1/2 pathway. PD98059 was found to inhibit the dephosphorylated form of MEK1 as well as a mutant MEK1 with low levels of constitutive activity in a non-ATP competitive mode [234]. PD98059 was further found to prevent the activation of MEK1 by the MAPKKK RAF or MEK kinase but did not inhibit RAF-activated MEK1 [241],

suggesting that the effect of the compound is different depending on the activation state of MEK1, presumably because of conformational differences between phosphorylated and non-phosphorylated MEK1. In 1998, UO126, another allosteric inhibitor, with greater affinity, was identified and UO126 further appeared to have the same or at least an overlapping binding site as PD98059 as their binding was mutually exclusive [235]. In this study both PD98059 and UO126 showed seven to tenfold higher affinity for a constitutively active recombinant MEK1 compared to wild type activated MEK1 obtained by immunoprecipitation from stimulated cells, demonstrating that even subtle conformational changes such as between the recombinant constitutively active MEK1 and wild type activated MEK1 is enough to have a great impact on the binding affinity of both allosteric compounds.

Different studies [242, 243] have performed X-ray crystallography of non-phosphorylated MEK1 together with different ATP-noncompetitive inhibitors, revealing binding within a common allosteric pocket, in close proximity however not overlapping with, the ATP-binding site. The allosteric pocket is physically separated from the ATP-binding site by the side chains M143 and K97 [242]. The first study used an analog of a clinical candidate MEK1 inhibitor PD18435, called PD318088. The authors co-crystallized this compound with nonphosphorylated MEK1 and MEK2 showing that it binds in a non-ATP competitive way within the identified allosteric pocket very close to the MgATP-binding site. The authors concluded that inhibition of the kinase activity of MEK1 and MEK2 by PD18435-related inhibitors is likely performed through stabilization of a closed but catalytically inactive conformation [242]. Fischmann et al. [243] instead crystallized nonphosphorylated MEK1 together with and without allosteric inhibitors PD325901 and UO126, as well as together with  $Mg^{2+}$  and nucleotides. The allosteric inhibitors as expected also bound in a non-ATP competitive way within the previously described allosteric pocket. These authors also concluded that although the binding of allosteric inhibitors did lead to conformational changes, this was not within the active site, and therefore the inhibiting function is likely through stabilization of a naturally occurring inactive state. This explains the higher effect of the inhibitors seen on non-phosphorylated MEK1 as well as the need for the inhibitors to be incubated with MEK1 before pathway stimuli. An important difference in MEK1 bound to PD325901 compared to UO126, is that PD325901 structurally extends towards the nucleotide, and also interacts with it through several hydrogen bonds. UO126 however forms hydrogen bonds with the catalytic amino acid residues K97 and D208 (D in the DFG-motif) as well as with F209 (F in the DFG motif) and the V211 shortly C-terminal of the DFG motif [243].

INR119 is structurally closely related to the MEK1 inhibitor PD98059, and was designed to bind the allosteric site of MEK1.

As mentioned above, U0126 has the same or at least an overlapping binding site as PD98059 as their binding is mutually exclusive [235]. As U0126 binds the same allosteric pocket as PD318088, therefore PD98059 is expected to bind this allosteric pocket as well. Redwan et al [244] in turn used computational modeling of the known binding of PD318088 and U0126 to dock PD98059 within the allosteric pocket and used the computed information to design a range of PD98059-related compounds, thereby investigating the use of PD98059 as a starting point for designing new chromone-based MEK1/2 inhibitors. Docking of PD98059 in the model showed that PD98059 likely binds similar to what PD318088 does but without projection from the allosteric pocket towards the ATP binding site. Docking of PD98059 in the allosteric pocket predicted hydrogen bonding of the compound to F209 in the DFG motif as well as V211 and S212. INR119, the small molecule in focus in this thesis, is compound 15 in this publication. The only difference between INR119 and PD98059 is that INR119 has an ethoxy group in the 3-position where PD98059 has a methoxy group. This substitution was done as the authors observed that the area of the pocket would be utilized more efficiently. As seen in **Suppl Fig S3A of Paper IV** of this thesis, this small substitution resulted in a much stronger inhibition of the MEK1 activity, as measured by phosphorylation of ERK1/2 phosphorylation in human MCF7 cells.

### MEK1 Kinase activity and the DFG motif

As in all kinases, the kinase fold of MEK1 consists of one N-terminal and one C-terminal lobe, where the N-lobe largely consists of  $\beta$ -sheets as well as an  $\alpha$ -helix called helix C, whereas the C-lobe mainly consists of multiple helices. The catalytic site is placed in the interface cleft of the N- and C-lobes. During a catalytic cycle of MEK1 the active site in the cleft opens and closes. When open, this allows ADP to be released and ATP to enter, whereas the closed form enables alignment of the catalytic residues in the catalytically active positions (reviewed by Wu and Park [245]).

The activation segment of most kinases starts with the motif DFG. The MEK1 activation segment exists in different conformations depending on the activation of the protein, and the kinase is activated by dual phosphorylation on S218 and S222 in the



activation segment. The aspartate in the DFG motif is very close to the MEK1/2 allosteric site and plays a very important role in the catalytically active conformation. In the active “DFG-aspartate in” conformation, the aspartate side chain of D208 in the DFG motif faces into the ATP-binding pocket and coordinates  $Mg^{2+}$ , whereas in the inactive DFG-aspartate out conformation, the aspartate side chain is instead facing out from the pocket making catalysis impossible [246]. Another structural element that changes conformation relative to the rest of the protein between active and inactive state is the C-helix of the N-lobe. When MEK1 is active, a salt bridge is formed between G114 in the C-helix and L97 in the K/D/D catalytic triad, whereas in the inactive conformation instead L97 forms a hydrogen bond with S212 in the activation segment [246]. Gopalbhai et al. [247] showed that MEK1 is actually phosphorylated *in vivo* on S212, and that this phosphorylation is inhibitory. Interestingly, the equivalent residue is conserved among all MAPKK family members in yeasts and mammals including fission yeast Wis1, and when the authors mutated the corresponding residue in the *S. cerevisiae* MAPKKs Pbs2 or Ste7 to the phosphomimicking residue aspartate, similarly their biological function was abrogated. In *S. pombe* the result of such a phosphomimicking change of the equivalent residue has not yet been tested, nor has the corresponding site been found to be phosphorylated *in vivo* in Wis1 or in the budding yeast Pbs2 or Ste7. It is however intriguing that S212 is one of the residues that PD98059 and INR119 is calculated to form hydrogen bonds with when bound in the allosteric pocket of MEK1 [244], and the corresponding serine in *S. pombe* Wis1 (**Paper IV Suppl. Fig. S3D**), and possibly phosphorylation of S212 may stabilize the same inactive conformation as binding of allosteric inhibitors within the allosteric site.

## Present study

### Paper I:

#### **Caffeine stabilizes Cdc25 independently of Rad3 in *Schizosaccharomyces pombe* contributing to checkpoint override.**

##### Caffeine induces stockpiling of Cdc25 in a Rad3 independent way

We show that caffeine treatment results in elevated levels of Cdc25 in fission yeast. Caffeine also has a differential impact on cell cycle progression in *cdc2-3w* (a temperature sensitive mutant carrying a mutation in *cdc2* that makes it able to divide and sporulate normally independently of Cdc25 [72]), and *cdc2-3w cdc25Δ* mutants suggesting that Cdc25 is an important factor in mediating caffeine induced checkpoint override. Caffeine-induced Cdc25 accumulation was not associated with accelerated progression through mitosis, but rather with delayed progression through cytokinesis. We further show that deletion of the fission yeast ATR homolog Rad3 or the CHK2 homolog Cds1, the effector kinase in the fission yeast replication checkpoint indeed resulted in a higher constitutive level of Cdc25. In *cds1Δ*, the level of Cdc25 was also elevated compared to in *rad3Δ*, indicating that the effect seen in *rad3Δ* is through the resulting deregulation of Cds1. The stabilizing effect that the *rad3Δ* or the *cds1Δ* deletion had on Cdc25 level suggests a constitutive role in regulation of the Cdc25 level. This is not performed by regulating the mRNA level, as the *cdc25<sup>+</sup>* mRNA level was rather suppressed in *rad3Δ* and *cds1Δ*. Treatment with cycloheximide to follow protein degradation when translation is stopped, also rather indicated slower degradation of Cdc25 in these mutants. Importantly however, even in the absence of Rad3, caffeine stabilizes Cdc25, showing that caffeine is capable of doing this in a Rad3-independent manner. Further, in our hands caffeine did not abolish Chk1 phosphorylation when exposed to phleomycin, or inhibit Cds1 phosphorylation following exposure to hydroxyurea (HU). Thus, caffeine does not affect the Rad3-dependent phosphorylation of these kinases. Caffeine induces stockpiling of Cdc25, but this does not result in a higher *cdc25<sup>+</sup>* mRNA level, but in fact rather the opposite, excluding elevated mRNA synthesis, or reduced mRNA turnover, as the mechanism of Cdc25 protein

accumulation. This leaves the possibility of either elevated translation or suppression of protein degradation as likely mechanisms. Caffeine addition results in a longer half-life of Cdc25 degradation as seen in cycloheximide-treated cells, and caffeine-treated cells also fail to properly reduce the Cdc25 level when reaching stationary phase. Together this indicates caffeine stabilizes Cdc25 protein by suppressing the rate of its degradation.

#### Caffeine induces nuclear Cdc25 localisation in HU

We used two different strains with GFP-tagged versions of Cdc25; Cdc25-GFP<sup>int</sup> and Cdc25<sup>(9A)</sup>-GFP<sup>int</sup> [114], both in the endogenous chromosomal locus under the control of the endogenous promoter. The Cdc25<sup>(9A)</sup>-GFP<sup>int</sup> form of Cdc25 has all the Cds1 phosphorylation sites converted from serine/threonine to alanine, and thus cannot be phosphorylated on these sites by Cds1, Chk1, or Srk1, that all have been shown to phosphorylate these sites resulting in cell cycle arrest and nuclear exclusion of Cdc25 [52] [68]. On exposure to HU, Cdc25-GFP<sup>int</sup> becomes phosphorylated, is exported from the nucleus and stockpiles within the cytoplasm whereas Cdc25<sup>(9A)</sup>-GFP<sup>int</sup> is instead degraded within the nucleus [114, 248]. Interestingly, co-exposure to HU and caffeine suppressed the accumulation of Cdc25-GFP<sup>int</sup> whereas the same co-exposure instead resulted in accumulation of the Cdc25<sup>(9A)</sup>-GFP<sup>int</sup> version. When the GFP fluorescence was inspected under the microscope, the strains expressing Cdc25-GFP<sup>int</sup> or Cdc25<sup>(9A)</sup>-GFP<sup>int</sup> both demonstrated increased *nuclear* levels of Cdc25 in cells co-exposed to HU and caffeine relative to cells only exposed to HU. Thus, caffeine treatment results in Cdc25 being located in the same cellular compartment as its target Cdc2. As expected, caffeine confers lower Cdc2 phosphorylation and this is more pronounced in HU. The suppression of Cdc2 phosphorylation is performed in a Cdc25-dependent manner even in the *cdc2-3w* mutant. Altogether this indicates a caffeine checkpoint override mechanism depending on higher Cdc25 activity which presumably is the combined result of a higher total Cdc25 content as well as the nuclear localization of Cdc25.

## **Paper II:**

### **Caffeine stabilises fission yeast Wee1 in a Rad24-dependent manner but attenuates its expression in response to DNA damage contributing to checkpoint override**

Caffeine targets TORC1 [133, 249, 132]. TORC1 is further known to regulate both Cdc25 and Wee1, and contributes to cell cycle regulation. TORC1 inhibition suppresses Wee1 expression as well as resulting in an increase of Cdc25 activation, thereby driving cells into mitosis [85]. Caffeine is additionally known to target other pathways, and for example also the Sty1 stress response pathway is activated by caffeine in fission yeast [250]. The signaling of Rad3, Sty1 and TORC1 all coincides on Cdc25 and Wee1. In **paper I** we demonstrated that the checkpoint overriding effect of caffeine is not dependent on Rad3. Various studies indicate that a major cellular target of caffeine may be TORC1 *in vivo* [132, 249, 133], and the effects of caffeine treatment resemble those of TORC1 inhibition [85, 251]. In **Paper II** we further investigated the caffeine checkpoint overriding effect by studying the effect of caffeine on Wee1, as well as further inspecting its effect on Cdc25. We found that in response to DNA damage with caffeine present, the expected increase in Wee1 was completely missing, whereas caffeine treatment in the absence of DNA damage was instead resulting in a Rad24-dependent Wee1 increase. Caffeine-induced accumulation of Cdc25 was in contrast not dependent on Rad24. The stabilising effect of caffeine on Cdc25 is also independent of Sty1 signaling, as indicated by Cdc25<sup>12A</sup>-GFPint [248, 114], accumulating in caffeine to a even higher degree than the wt version, demonstrating that phosphorylating through the Sty1 and Rad3 pathways are rather counteracting the Cdc25 stabilization effect. Inhibition of TORC1 with the TORC1 inhibitor Torin1 resulted in elevated sensitivity to the genotoxin phleomycin, indicating that TORC1 inhibition does indeed cause checkpoint override. Our results support the view that caffeine-induced inhibition of TORC1 impacting at least Wee1 contributes to checkpoint override in fission yeast, but does not exclude other contributing pathways.

## Paper III

### **The fission yeast FHIT homolog affects checkpoint control of proliferation and is regulated by mitochondrial electron transport**

#### Aph1 is involved in proliferation control and regulates Rad1 in the 9-1-1 complex

The first step in the investigation of Aph1 to understand human FHIT is naturally to identify FHIT functions conserved between the fission yeast and human orthologs. In **Paper II**, we therefore performed experiments on proliferation of *aph1Δ* deletion mutants, and found that they proliferated to a much higher extent in sublethal concentrations of the genotoxins HU, doxorubicin or phleomycin, indicating malfunctioning checkpoint regulation upon loss of the *aph1*<sup>+</sup> gene. When proliferation experiments were performed in a strain background carrying a partially defective *cds1* allele, *aph1* deletion resulted in elevated chromosome loss and/or fragmentation. Together these results indicate conservation of functions in proliferation control and checkpoint signaling between Aph1 and FHIT. We found the FHIT connection with the 9-1-1 complex [152] suggestive as this complex and its functions are so well conserved between eukaryotes, and discovered that deletion of *aph1* leads to downregulation of the Rad1 protein level.

#### Aph1 level is regulated through activity of the mitochondrial electron transport chain

We experienced a position-dependent behavior of the *aph1Δ* deletion strains in the microtiter plate, which disappeared when we exchanged the commonly used lid for a membrane allowing the same oxygen availability to all wells. This differential behavior indicates oxygen dependency. As a subpool of FHIT had been shown to be located within mitochondria, and in contact with ferredoxin reductase, a component of the electron transport chain [155], we explored if Aph1 was regulated by oxygenation of the culture. We found that the Aph1 protein level is reversibly downregulated in hypoxia and that this regulation was dependent on the activity level of the mitochondrial electron transport chain.

Is mammalian FHIT also downregulated in hypoxia or by blocking of mitochondrial electron transport?

Recently FHIT was identified as a modifier of BMPR2 (bone morphogenetic protein receptor type 2), a protein frequently mutated or downregulated in pulmonary arterial hypertension (PAH). This condition is characterized by progressive narrowing of pulmonary arteries, and this serious condition may lead to right heart failure and ultimately death [252]. An emerging “metabolic theory of PAH” proposes that PAH may be caused by mitochondria-based metabolic abnormalities resulting in reduced oxidative phosphorylation [253]. Chronic hypoxia can also lead to pulmonary hypertension (PH), leading to chronic obstructive pulmonary disease (COPD) [254]. Rats carrying a deletion within exon 1 of *BMPR2* were shown to be more prone to develop hypoxia-induced pulmonary hypertension [255]. Both FHIT and BMPR2 are downregulated in patients with PAH on the mRNA and protein expression levels, and interestingly *FHIT*<sup>-/-</sup> mice experienced worse hypoxic PH and additionally failed to recover in normoxia [252]. Altogether, FHIT has been implicated as a modifier of a protein for which reduced signaling is a key event in development of medical conditions where hypoxia or suppression of oxidative phosphorylation is implicated. Thus, it would certainly be interesting to investigate hypoxic downregulation of the mammalian FHIT protein as hypothesized by our results for the fission yeast ortholog Aph1.

## Paper IV

### **A redox-sensitive thiol in Wis1 modulates the fission yeast MAPK response to H<sub>2</sub>O<sub>2</sub> and is the target of a small molecule.**

An inhibitory mechanism targets the cysteine in the CDFG motif of human MAPKKs as well as fission yeast MAPKK Wis1

The human p38 pathway is activated in H<sub>2</sub>O<sub>2</sub> [256]. Despite this fact, MKK6, a MAPKK in this pathway, is actually inactivated by a disulfide bond upon H<sub>2</sub>O<sub>2</sub> treatment *in vivo* and *in vitro* [257], thus H<sub>2</sub>O<sub>2</sub> regulates this pathway both through stimulation and inhibition. Also MEK1 and JNKK1 were inactivated by a mechanism reversible by DTT treatment, suggesting that the same mechanism of inhibition is present also in other MAPKKs of human cells. One of the cysteines of this H<sub>2</sub>O<sub>2</sub>-induced disulfide, MKK6 C196, directly precedes the DFG motif, thus forming an extended CDFG motif. Given the importance of the aspartate in the DFG motif for catalytic activity, this places C196 within the active site of the kinase. We observed that this active site cysteine is evolutionarily conserved in all MAPKKs, and in addition also in a number of MAPKs of budding yeast, fission yeast and humans, making us suspect that regulation of kinase activity through this cysteine within the CDFG motif may be a conserved feature of MAPK signaling in these organisms. Interestingly the cysteine in the fission yeast MAPK Sty1 is also regulated by intramolecular disulfide formation in response to high levels of H<sub>2</sub>O<sub>2</sub>, and this disulfide includes the cysteine in the CDFG motif of Sty1 [258]. Thus the CDFG cysteine may be involved in regulation also at the MAPK level.

We observed that although Wis1 C458 is conserved in the CDFG motif (**Paper IV Fig. 1 A**), there is no plausible cysteine partner for intramolecular disulfide bond formation. However, Wis1 kinase activity was evidently still inactivated by reversible thiol oxidation at low H<sub>2</sub>O<sub>2</sub> levels *in vitro* in a C458 dependent way. A higher Sty1 phosphorylation in H<sub>2</sub>O<sub>2</sub> concentrations lower than 1 mM was seen in a *wis1-C458S* mutant. This indicates that a H<sub>2</sub>O<sub>2</sub>-induced negative regulation targets Wis1 C458 in low H<sub>2</sub>O<sub>2</sub> concentrations.

The CDFG cysteine in Wis1 is oxidized in the absence of external H<sub>2</sub>O<sub>2</sub> but the nature of the oxidation may be changed upon H<sub>2</sub>O<sub>2</sub> treatment

Presently we do not know the nature of the oxidation event leading to inactivation of Wis1. This inactivation does however seem very important as the *wis1-C458S* mutant was unable to grow in oxidative stress on plates containing 0.5 mM H<sub>2</sub>O<sub>2</sub>; however it had no problem to grow in hyperosmosis (0.6 M KCl). Our unpublished results also indicate that this cysteine is important in aging (**Fig. 4**), as *wis1-C458S* mutant cells were unable to reinitiate growth after extended time spent in stationary phase. This defect in resumption of growth was presumably because a large fraction of cells were no longer viable as cells appeared shriveled when inspected in the microscope.

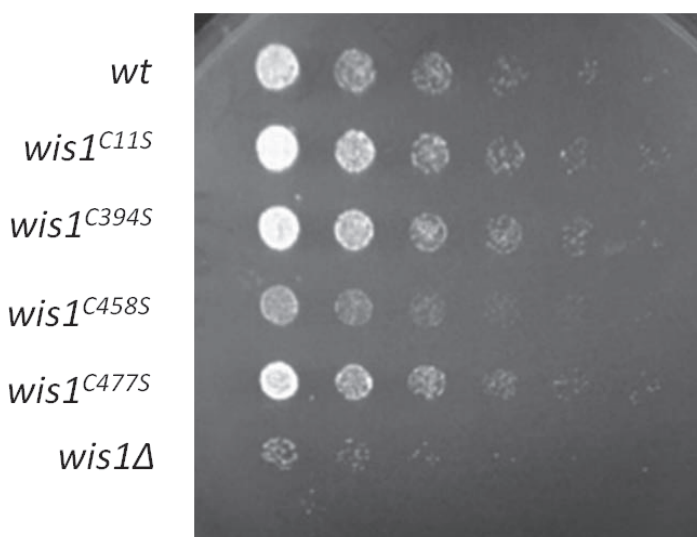


**Figure 4:** *Wis1<sup>C458S</sup>* mutants are sensitive to stationary phase. Cells were first grown to mid-log phase and thereafter incubated for additional 48 h within the same culture and culture conditions. Cells were thereafter serially diluted and spotted on a YES agar plate. The plate was thereafter incubated 48 h for visualization of reentering of growth. For corresponding control plate of log phase cells, see **Fig. 2F Paper IV**.

To confirm that cysteines within Wis1 are oxidized, we used the mPEG assay [259], to get information on the extent of total reversible oxidations of the cysteines in Wis1. This assay couples a molecule of approx. 5 kDa to each reversibly oxidized cysteine. The mPEG data we have indicate that more than one cysteine within Wis1 is oxidized already without externally applied H<sub>2</sub>O<sub>2</sub>, and C458 is one of these cysteines. According to the mPEG



results, this oxidation event does however not result in a net change of the total number of reversibly oxidized cysteines per Wis1 molecule. This indicates that either one already oxidized cysteine form is exchanged for another oxidated form, or that oxidation of one cysteine is exchanged to another cysteine. Sulfenylation is a reversible oxidation itself and additionally an intermediate of other reversible and irreversible thiol oxidations. We decided to perform a sulfenylation assay *in vivo* ([260], adjusted protocol kindly given to us by Michel Toledano) to capture changes in the level of this important intermediate upon H<sub>2</sub>O<sub>2</sub> treatment in Wis1. The sulfenylation in endogenously expressed HA-tagged wild type was evaluated. The result (**Fig. 5**) reveals that upon addition of H<sub>2</sub>O<sub>2</sub> the Wis1 sulfenylation increases. Thus, both mPEG and sulfenylation data suggest Wis1 is reversibly oxidized. The mPEG data do not show changes in the total level of reversibly oxidized cysteines upon H<sub>2</sub>O<sub>2</sub>, however the sulfenylation data clearly show that there are changes in the level of Wis1 sulfenylated thiols, supporting Wis1 is redox modified in H<sub>2</sub>O<sub>2</sub>.

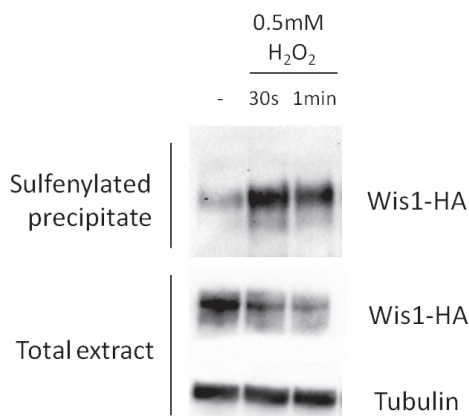


**Figure 5:** *Wis1 is sulfenylated upon H<sub>2</sub>O<sub>2</sub> treatment*

*Wt (JJS15) cells were first incubated with the sulfenylation probe DYn-2 and thereafter exposed to 0.5 mM H<sub>2</sub>O<sub>2</sub>. Cells were lysed and proteins precipitated by methanol/Chloroform. DYn-2 modified protein was further reacted with CuAAC click reagents (biotin azide, copper(II)TBTA complex, ascorbate), and labeled proteins were thereafter pulled down with streptavidin beads. Protein was subjected to SDS-PAGE and Wis1 detected by anti-HA antibodies. For detailed protocol, see Appendix 1.*

In **Paper IV** we excluded the formation of an intramolecular disulfide as the inactivating oxidation event, but several other alternatives still exist. It may be glutathionylation, a disulfide between Wis1 and another protein or even between two Wis1 molecules, or other less studied reversible oxidations such as the cyclic sulfenamide

formation. This modification has been shown to result in inhibition of tyrosine phosphatase 1B (PTP1B), where the thiol of the catalytic cysteine reacts with the amino group of the backbone of the amino acid residue directly C terminal of it, resulting in inactivation [174]. PTP1B can be reactivated, and this is preferentially performed by the thioredoxin system [175]. In the case of C458 reacting with the next amino acid, this would correspond to the aspartate in the DFG motif, thereby potentially destroying  $Mg^{2+}$  coordination for catalysis. The appeal of this kind of cysteine modification is that it does not require a neighboring cysteine partner. When it comes to the possibility of C458 forming a disulfide with another molecule such as GSH or another protein molecule, we constructed a structural homology model (**paper IV Suppl. Fig. 3A**), and this suggests that anything as big as a peptide/protein coupled to this cysteine should impair ATP binding in analogy to the intramolecular disulfide in MKK6 [257], thus resulting in inhibition. The homology model does however not suggest that sulfenylation, sulfinylation or sulfonylation should result in Wis1 inactivation based on spatial constraints alone. The natural next approach to obtain information about the nature of inactivating oxidation of C458 would be through mass spectrometry.

#### Negative regulation targeting C458 can be blocked by the use of the allosteric inhibitor INR119, predicted to bind adjacent to C458

As mentioned, next to the active site in the human Wis1 homolog MEK1, there is an allosteric site binding various non-ATP competitive inhibitors such as UO126 and PD98059. Our homology-based structural model of Wis1 indicated that there was indeed a pocket in Wis1 in the corresponding place, structurally very similar to the allosteric pocket in MEK1. As the allosteric pocket is in very close proximity to the CDFG motif, we explored the possibility that binding of inhibitors in this pocket may impact the negative regulation through the cysteine in the CDFG motif. We expected reinforcement of Wis1 inhibition, but instead we found that binding of the allosteric MEK1 inhibitor INR119 protected against negative regulation *in vitro* targeting C458 in the Wis1 CDFG motif, therefore resulting in higher Styl phosphorylation *in vivo*. In **paper IV** we focus on the Wis1 kinase stimulating activities of INR119. However this stimulation on Wis1 activity is only seen if INR119 binds before addition of  $H_2O_2$ . If added at the same time as  $H_2O_2$ , binding of INR119 instead results in partial inhibition of Wis1 (**Fig. 6**). Altogether it seems like Wis1 molecules binding INR119 before C458 are negatively modulated by  $H_2O_2$ , resulting in stronger Wis1 signaling,

whereas Wis1 molecules binding INR119 after H<sub>2</sub>O<sub>2</sub> have modulated C458 resulting in inhibition of Wis1.

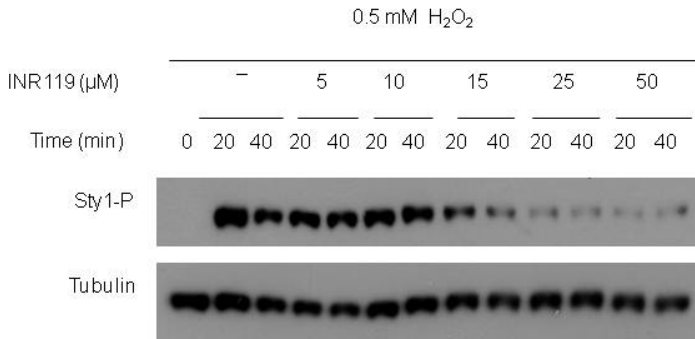


**Figure 6:** When added simultaneous with H<sub>2</sub>O<sub>2</sub>, omitting the INR119 pretreatment, INR119 instead inhibits Wis1 signaling suppressing Sty1 phosphorylation in a dose-responsive way. For experimental conditions see **Paper IV**

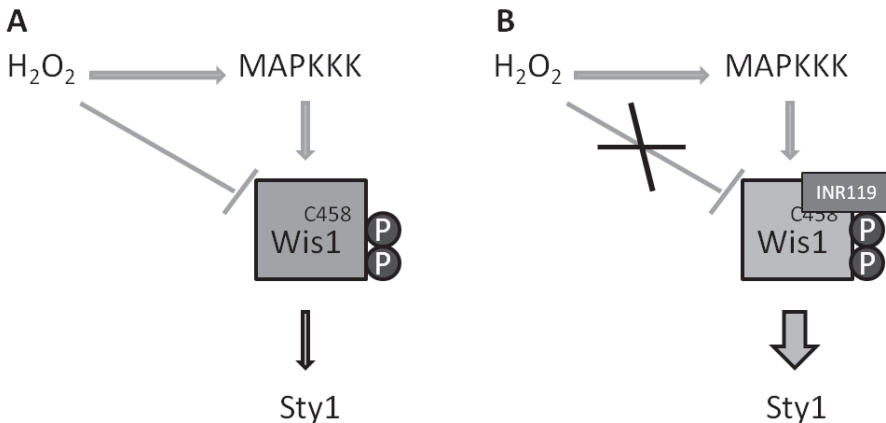


**Figure 7:** Proposed model of INR119 action as a Wis1 signaling enhancer

**A)** H<sub>2</sub>O<sub>2</sub> induces pathway activation through MAPKKK activation, however at low H<sub>2</sub>O<sub>2</sub> concentrations negative regulation targeting Wis1 C458 functions as a break holding the activity of Wis1 down, until H<sub>2</sub>O<sub>2</sub> reaches the appropriate level for Sty1 activation.

**B)** INR119 binds Wis1 in an allosteric site next to the active site and very close to C458. If bound before H<sub>2</sub>O<sub>2</sub> is added, INR119 protects against negative regulation targeting C458 through stabilization of a conformation unresponsive to negative regulation through C458, resulting in higher Wis1 activity in low H<sub>2</sub>O<sub>2</sub> levels.

## Proposed model of INR119 mechanism of action

Why then would binding of INR119 before and after C458 modulation result in so different outputs? This may be explained if INR119 simply stabilizes some part of the Wis1 conformation, a conformation that if INR119 is bound before C458 modulation would result in unresponsiveness to negative regulation through C458 (**Fig. 7**), while if C458 is already modulated by the inhibiting oxidation event, INR119 may instead stabilize an already inhibited conformation.

The protective effect against C458 targeting inactivation was dependent on Wis1, the presence of a MAPKKK (Win1 and/or Wis4), as well as on Tpx1 and Tdh1. However, even though deletion mutants of the two-component pathway did impact the Sty1 phosphorylation level, they were not necessary for the protection against C458-targeting Wis1 inactivation. The dependency on Tpx1 and Tdh1 (**Fig. 8 A,B**), but not on the two-component system (**Fig. 8 C,D**), does suggest some kind of redox relay involved in the negative regulation mechanism targeting C458.

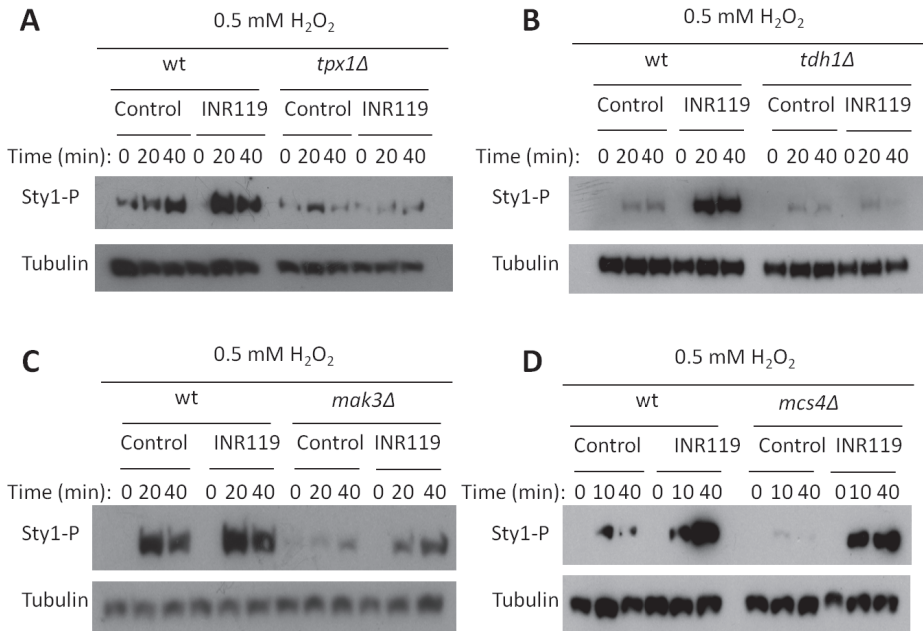


**Figure 8:** *INR119* induced enhancement of *Sty1*-phosphorylation is dependent on *Tpx1*(A) and *Tdh1*(B), but not on *Mak3*(C) or *Mcs4*(D). For experimental conditions see **Paper IV**.

## Concluding remarks

In this thesis the model organism *S. pombe* is used to study various aspects in stress signaling, where the focus has been on relevance to cancer. In **papers I and II** we investigate the caffeine checkpoint override mechanism in *S. pombe*. In principle, a compound making cancer cells evade checkpoint arrest upon cancer therapy, may be used as sensitizing treatment making therapy more efficient. Caffeine has been shown to cause checkpoint override in human and fission yeast, and even though the high doses needed as well as the pleiotropic effects of caffeine make it unsuitable as a sensitizing agent, the knowledge of the overriding mechanism may aid in development of more suitable agents. In **Paper I** we conclude the checkpoint override mechanism of caffeine is linked to the mitotic inducer protein Cdc25 which removes the inhibitory phosphorylation from the CDK Cdc2. Cdc25 accumulated in response to caffeine treatment, and is also located within the nucleus upon caffeine treatment in combination with the cytostatic HU, thus in the same cellular compartment as the CDK it activates. Caffeine has been proposed to exert its checkpoint overriding effects through inhibition of the checkpoint protein Rad3/ATR. We show that although Rad3 deletion in similarity to caffeine treatment does cause Cdc25 accumulation, and likely is involved in constitutive regulation of Cdc25 stability, the caffeine treatment induces Cdc25 accumulation and checkpoint override independently of Rad3. In **Paper II** we further investigated the caffeine effect on Wee1, the kinase inhibiting Cdc2 by Y15 phosphorylation. We demonstrate that although caffeine stabilizes Wee1 in a Rad24-dependent manner, caffeine has the opposite effect upon DNA damage with significantly lower Wee1 levels. Altogether our findings in **Paper I and II** demonstrate that caffeine overrides the DNA damage checkpoints by its positive regulation of the Cdc25 phosphatase and negative regulation of the Wee1 kinase thereby removing the Cdc2 double lock mechanism normally enforced by checkpoint control. Inhibition of TORC1 by caffeine is suggested to contribute to checkpoint override.

FHIT is a human tumor suppressor protein that has been assigned very diverse tumor suppressing functions. In **paper III** we take the first step towards establishing the fission yeast ortholog Aph1 as a model of FHIT molecular functions by demonstrating that some tumor suppressing functions are evolutionary conserved between FHIT and Aph1. Loss of Aph1 gives rise to a phenotype generally more prone to proliferate and therefore resulting in uncontrolled proliferation also in genotoxic compounds. *aph1* deletion additionally aggravates the phenotype of a partial defective allele of the checkpoint effector kinase Cds1.

This leads to chromosome mis-segregation and/or fragmentation upon growth in the cancer chemotherapy agent doxorubicin. We further discovered that the Aph1 protein level is regulated by the activity of the mitochondrial electron transport chain, and that Aph1 is strongly reduced in hypoxia in a manner reversible by reoxygenation. Deletion of *aph1* additionally leads to reduction of Rad1 in the 9-1-1 complex, a complex important in DNA damage sensing and checkpoint activation. All three components in the 9-1-1 complex are, in similarity to Aph1, downregulated in hypoxia. Recently, human FHIT has been implicated in regulation of BMPR2, a protein in turn important in development of PAH. Interestingly PAH is a condition proposed to be caused by mitochondrial malfunction. Given our results concerning Aph1, mitochondrial electron transport and oxygenation, the aspects of human FHIT in hypoxia and reoxygenation should be further investigated.

Human MAPK pathways are often deregulated in cancer. H<sub>2</sub>O<sub>2</sub> can induce oxidative damage, but is additionally involved in cellular signaling as a second messenger inducing its effects through oxidation of selected cysteines. **In paper IV** we investigate the impact of H<sub>2</sub>O<sub>2</sub> on a MAPK signaling pathway in fission yeast. MAPKKs of fission yeast, budding yeast and humans contain a cysteine directly downstream of the conserved DFG motif, placing it within the active site of the kinase. The human MAPK p38 pathway is induced by H<sub>2</sub>O<sub>2</sub>, even so MKK6, one of two MAPKKs in the pathway, is inhibited by H<sub>2</sub>O<sub>2</sub> by the formation of an intramolecular disulfide involving this active site cysteine. We demonstrate that the MAPKK Wis1 in the fission yeast MAPK Sty1 pathway is inhibited by H<sub>2</sub>O<sub>2</sub> by a mechanism involving the corresponding active site cysteine, despite lacking an intramolecular disulfide partner cysteine. *In vitro* it is possible to turn Wis1 kinase activity off with H<sub>2</sub>O<sub>2</sub> and then reactivate using a reductant, indicating that the mechanism depends on reversible oxidation. Mutating the active site cysteine leads to elevated kinase activity in low H<sub>2</sub>O<sub>2</sub> concentrations, indicating that inhibition through this cysteine works as a brake to hold activation of Wis1 down in low concentrations. *In vitro* the use of the synthetic small molecule INR119 blocks kinase inactivation upon low H<sub>2</sub>O<sub>2</sub>, *in vivo* this leads to elevated Wis1 signaling. Altogether our results indicate that Wis1, in analogy to human MKK6, is both stimulated and inhibited by H<sub>2</sub>O<sub>2</sub>. This balanced regulation is of most importance for the viability of the cell upon H<sub>2</sub>O<sub>2</sub> treatment as well as in aging, and *in vivo* inhibition of Wis1 is likely caused by redox relay from another protein. It is further possible to manipulate the redox-dependent regulation of Wis1 through the use of the small molecule INR119. This opens the possibility that the same can be done using similar compounds on other MAPKKs

including human ones, thus enforcing stronger signaling output. This effect would be desirable in sensitizing treatment in cancer therapy.

## Acknowledgements

To my supervisor Per, for your kind supervision, and for trusting my work without looking over my shoulder.

To my husband Per, for all love and support during hard times and for putting up with my strange working hours.

To my daughter Tora for all the joy you give me every day.

To my Parents and Parents in law for all support.

To Mikael for redox related scientific input- and supervision, and Michel Toledano for reforming the Wis1 manuscript.

To Morten for your chemical knowledge and for providing me with INR119.

To John Patrick for teaching me how to work with *S. pombe* as well as cell culture, and of course for making my PhD time much more interesting.

To Julie for moral support and scientific advice.

To Jeanette for being my mentor when working in the course lab and to both Jeanette and Marie for nice lunch times.

To Agata for all your hard work and your way of making everyone feel like a family.

To Itziar for being a great student.

To Elena, Elisa and Heejung for making our lab a pleasant place to be in.

To Åsa for letting me inherit the “high-tech” hypoxia apparatus.

To Chunxia for making the Wis1 structural model.

To Cecilia for volunteering to make experiments in the never ending Wis1 project.

To Parmida, Mozghan, Ali, Azadeh, Valida, Andreas, Sansan, Michelle, Hanna, Catarina, Karl, Nafiseh, Kiran, Xin, Nejla, Dennis, as well as all other lab-mates coming and going over the years for great times in the lab!

To Karl again for making the front page illustration.



## References

1. Hughes, A.L. and R. Friedman, *Parallel evolution by gene duplication in the genomes of two unicellular fungi*. *Genome Res*, 2003. **13**(6A): p. 1259-64.
2. Seoighe, C. and K.H. Wolfe, *Yeast genome evolution in the post-genome era*. *Curr Opin Microbiol*, 1999. **2**(5): p. 548-54.
3. Aravind, L., et al., *Lineage-specific loss and divergence of functionally linked genes in eukaryotes*. *Proc Natl Acad Sci U S A*, 2000. **97**(21): p. 11319-24.
4. Hoffman, C.S., V. Wood, and P.A. Fantes, *An Ancient Yeast for Young Geneticists: A Primer on the Schizosaccharomyces pombe Model System*. *Genetics*, 2015. **201**(2): p. 403-23.
5. Nurse, P., *Fission yeast morphogenesis--posing the problems*. *Mol Biol Cell*, 1994. **5**(6): p. 613-6.
6. Wood, V., et al., *The genome sequence of Schizosaccharomyces pombe*. *Nature*, 2002. **415**(6874): p. 871-80.
7. Kuhn, A.N. and N.F. Kaufer, *Pre-mRNA splicing in Schizosaccharomyces pombe: regulatory role of a kinase conserved from fission yeast to mammals*. *Curr Genet*, 2003. **42**(5): p. 241-51.
8. Merlini, L., O. Dudin, and S.G. Martin, *Mate and fuse: how yeast cells do it*. *Open Biol*, 2013. **3**(3): p. 130008.
9. Berry, L.D. and K.L. Gould, *Regulation of Cdc2 activity by phosphorylation at T14/Y15*. *Prog Cell Cycle Res*, 1996. **2**: p. 99-105.
10. Westhorpe, F.G. and A.F. Straight, *The centromere: epigenetic control of chromosome segregation during mitosis*. *Cold Spring Harb Perspect Biol*, 2014. **7**(1): p. a015818.
11. Sun, J. and D. Kong, *DNA replication origins, ORC/DNA interaction, and assembly of pre-replication complex in eukaryotes*. *Acta Biochim Biophys Sin (Shanghai)*, 2010. **42**(7): p. 433-9.
12. Cam, H.P. and S. Whitehall, *Analysis of Heterochromatin in Schizosaccharomyces pombe*. *Cold Spring Harb Protoc*, 2016. **2016**(11).
13. Nilsson, I. and I. Hoffmann, *Cell cycle regulation by the Cdc25 phosphatase family*. *Prog Cell Cycle Res*, 2000. **4**: p. 107-14.
14. Moreno, S., P. Nurse, and P. Russell, *Regulation of mitosis by cyclic accumulation of p80cdc25 mitotic inducer in fission yeast*. *Nature*, 1990. **344**(6266): p. 549-52.
15. Gutierrez-Escribano, P. and P. Nurse, *A single cyclin-CDK complex is sufficient for both mitotic and meiotic progression in fission yeast*. *Nat Commun*, 2015. **6**: p. 6871.
16. Iino, Y., Y. Hiramane, and M. Yamamoto, *The role of cdc2 and other genes in meiosis in Schizosaccharomyces pombe*. *Genetics*, 1995. **140**(4): p. 1235-45.
17. Malumbres, M., et al., *Cyclin-dependent kinases: a family portrait*. *Nat Cell Biol*, 2009. **11**(11): p. 1275-6.
18. Morrison, D.K., *MAP kinase pathways*. *Cold Spring Harb Perspect Biol*, 2012. **4**(11).
19. Perez, P. and J. Cansado, *Cell integrity signaling and response to stress in fission yeast*. *Curr Protein Pept Sci*, 2010. **11**(8): p. 680-92.
20. Hartwell, L.H., *Saccharomyces cerevisiae cell cycle*. *Bacteriol Rev*, 1974. **38**(2): p. 164-98.
21. Pardee, A.B., *A restriction point for control of normal animal cell proliferation*. *Proc Natl Acad Sci U S A*, 1974. **71**(4): p. 1286-90.
22. Hartwell, L.H. and T.A. Weinert, *Checkpoints: controls that ensure the order of cell cycle events*. *Science*, 1989. **246**(4930): p. 629-34.
23. Nurse, P., *Genetic control of cell size at cell division in yeast*. *Nature*, 1975. **256**(5518): p. 547-51.

24. Lee, M. and P. Nurse, *Cell cycle control genes in fission yeast and mammalian cells*. Trends Genet, 1988. **4**(10): p. 287-90.
25. Mitchison, J.M. and J. Creanor, *Induction synchrony in the fission yeast. Schizosaccharomyces pombe*. Exp Cell Res, 1971. **67**(2): p. 368-74.
26. McIntosh, J.R., *Mitosis*. Cold Spring Harb Perspect Biol, 2016. **8**(9).
27. Sorokin, A.V., E.R. Kim, and L.P. Ovchinnikov, *Proteasome system of protein degradation and processing*. Biochemistry (Mosc), 2009. **74**(13): p. 1411-42.
28. Bochis, O.V., et al., *The Importance of Ubiquitin E3 Ligases, SCF and APC/C, in Human Cancers*. Clujul Med, 2015. **88**(1): p. 9-14.
29. Yanagida, M., *Cell cycle mechanisms of sister chromatid separation; roles of Cut1/separin and Cut2/securin*. Genes Cells, 2000. **5**(1): p. 1-8.
30. Cao, L., et al., *Phylogenetic analysis of CDK and cyclin proteins in premetazoan lineages*. BMC Evol Biol, 2014. **14**: p. 10.
31. Devos, M., et al., *Fission yeast Cdk7 controls gene expression through both its CAK and C-terminal domain kinase activities*. Mol Cell Biol, 2015. **35**(9): p. 1480-90.
32. Fisher, R.P., *Secrets of a double agent: CDK7 in cell-cycle control and transcription*. J Cell Sci, 2005. **118**(Pt 22): p. 5171-80.
33. Suryadinata, R., M. Sadowski, and B. Sarcevic, *Control of cell cycle progression by phosphorylation of cyclin-dependent kinase (CDK) substrates*. Biosci Rep, 2010. **30**(4): p. 243-55.
34. Morgan, D.O., *Principles of CDK regulation*. Nature, 1995. **374**(6518): p. 131-4.
35. Peeper, D.S., et al., *A- and B-type cyclins differentially modulate substrate specificity of cyclin-cdk complexes*. EMBO J, 1993. **12**(5): p. 1947-54.
36. Evans, T., et al., *Cyclin: a protein specified by maternal mRNA in sea urchin eggs that is destroyed at each cleavage division*. Cell, 1983. **33**(2): p. 389-96.
37. Satyanarayana, A. and P. Kaldis, *Mammalian cell-cycle regulation: several Cdks, numerous cyclins and diverse compensatory mechanisms*. Oncogene, 2009. **28**(33): p. 2925-39.
38. Yasuda, H., M. Kamijo, and Y. Ohba, *[The characterization of human cdc2 kinase and CDK2]*. Yakugaku Zasshi, 1993. **113**(12): p. 829-46.
39. Hochegger, H., S. Takeda, and T. Hunt, *Cyclin-dependent kinases and cell-cycle transitions: does one fit all?* Nat Rev Mol Cell Biol, 2008. **9**(11): p. 910-6.
40. Ortega, S., et al., *Cyclin-dependent kinase 2 is essential for meiosis but not for mitotic cell division in mice*. Nat Genet, 2003. **35**(1): p. 25-31.
41. Diril, M.K., et al., *Cyclin-dependent kinase 1 (Cdk1) is essential for cell division and suppression of DNA re-replication but not for liver regeneration*. Proc Natl Acad Sci U S A, 2012. **109**(10): p. 3826-31.
42. Nurse, P. and Y. Bissett, *Gene required in G1 for commitment to cell cycle and in G2 for control of mitosis in fission yeast*. Nature, 1981. **292**(5823): p. 558-60.
43. Nurse, P., P. Thuriaux, and K. Nasmyth, *Genetic control of the cell division cycle in the fission yeast Schizosaccharomyces pombe*. Mol Gen Genet, 1976. **146**(2): p. 167-78.
44. Lee, M.G. and P. Nurse, *Complementation used to clone a human homologue of the fission yeast cell cycle control gene cdc2*. Nature, 1987. **327**(6117): p. 31-5.
45. Hagan, I., J. Hayles, and P. Nurse, *Cloning and sequencing of the cyclin-related cdc13+ gene and a cytological study of its role in fission yeast mitosis*. J Cell Sci, 1988. **91** ( Pt 4): p. 587-95.
46. Benito, J., C. Martin-Castellanos, and S. Moreno, *Regulation of the G1 phase of the cell cycle by periodic stabilization and degradation of the p25rum1 CDK inhibitor*. EMBO J, 1998. **17**(2): p. 482-97.

47. Martin-Castellanos, C., et al., *The *pu1* cyclin regulates the G1 phase of the fission yeast cell cycle in response to cell size*. Mol Biol Cell, 2000. **11**(2): p. 543-54.
48. Martin-Castellanos, C., K. Labib, and S. Moreno, *B-type cyclins regulate G1 progression in fission yeast in opposition to the *p25rum1* cdk inhibitor*. EMBO J, 1996. **15**(4): p. 839-49.
49. Coudreuse, D. and P. Nurse, *Driving the cell cycle with a minimal CDK control network*. Nature, 2010. **468**(7327): p. 1074-9.
50. Fattaey, A. and R.N. Booher, *Myt1: a Wee1-type kinase that phosphorylates Cdc2 on residue Thr14*. Prog Cell Cycle Res, 1997. **3**: p. 233-40.
51. Millar, J.B., et al., *Activation of MPF in fission yeast*. Ciba Found Symp, 1992. **170**: p. 50-8; discussion 58-71.
52. Furnari, B., et al., *Cdc25 inhibited in vivo and in vitro by checkpoint kinases Cds1 and Chk1*. Mol Biol Cell, 1999. **10**(4): p. 833-45.
53. Rhind, N. and P. Russell, *Roles of the mitotic inhibitors Wee1 and Mik1 in the G(2) DNA damage and replication checkpoints*. Mol Cell Biol, 2001. **21**(5): p. 1499-508.
54. Shiozaki, K. and P. Russell, *Cell-cycle control linked to extracellular environment by MAP kinase pathway in fission yeast*. Nature, 1995. **378**(6558): p. 739-43.
55. Lopez-Aviles, S., et al., *Inactivation of the Cdc25 phosphatase by the stress-activated *Srk1* kinase in fission yeast*. Mol Cell, 2005. **17**(1): p. 49-59.
56. Russell, P. and P. Nurse, **cdc25+* functions as an inducer in the mitotic control of fission yeast*. Cell, 1986. **45**(1): p. 145-53.
57. Karlsson-Rosenthal, C. and J.B. Millar, *Cdc25: mechanisms of checkpoint inhibition and recovery*. Trends Cell Biol, 2006. **16**(6): p. 285-92.
58. Sadhu, K., et al., *Human homolog of fission yeast *cdc25* mitotic inducer is predominantly expressed in G2*. Proc Natl Acad Sci U S A, 1990. **87**(13): p. 5139-43.
59. Boutros, R., V. Lobjois, and B. Ducommun, *CDC25 phosphatases in cancer cells: key players? Good targets?* Nat Rev Cancer, 2007. **7**(7): p. 495-507.
60. Shen, T. and S. Huang, *The role of Cdc25A in the regulation of cell proliferation and apoptosis*. Anticancer Agents Med Chem, 2012. **12**(6): p. 631-9.
61. Creanor, J. and J.M. Mitchison, *The kinetics of the B cyclin *p56cdc13* and the phosphatase *p80cdc25* during the cell cycle of the fission yeast *Schizosaccharomyces pombe**. J Cell Sci, 1996. **109** ( Pt 6): p. 1647-53.
62. Kovelman, R. and P. Russell, *Stockpiling of Cdc25 during a DNA replication checkpoint arrest in *Schizosaccharomyces pombe**. Mol Cell Biol, 1996. **16**(1): p. 86-93.
63. Kohama, Y., et al., *Regulation of the stability and activity of CDC25A and CDC25B by protein phosphatase PP2A and 14-3-3 binding*. Cell Signal, 2019. **54**: p. 10-16.
64. Lopez-Girona, A., et al., *Nuclear localization of Cdc25 is regulated by DNA damage and a 14-3-3 protein*. Nature, 1999. **397**(6715): p. 172-5.
65. Chen, L., T.H. Liu, and N.C. Walworth, *Association of Chk1 with 14-3-3 proteins is stimulated by DNA damage*. Genes Dev, 1999. **13**(6): p. 675-85.
66. Reinhardt, H.C. and M.B. Yaffe, *Kinases that control the cell cycle in response to DNA damage: Chk1, Chk2, and MK2*. Curr Opin Cell Biol, 2009. **21**(2): p. 245-55.
67. Mikhailov, A., M. Shinohara, and C.L. Rieder, *The p38-mediated stress-activated checkpoint. A rapid response system for delaying progression through antephase and entry into mitosis*. Cell Cycle, 2005. **4**(1): p. 57-62.
68. Lopez-Aviles, S., et al., *Activation of *Srk1* by the mitogen-activated protein kinase *Sty1/Spc1* precedes its dissociation from the kinase and signals its degradation*. Mol Biol Cell, 2008. **19**(4): p. 1670-9.

69. Zeng, Y. and H. Piwnica-Worms, *DNA damage and replication checkpoints in fission yeast require nuclear exclusion of the Cdc25 phosphatase via 14-3-3 binding*. Mol Cell Biol, 1999. **19**(11): p. 7410-9.
70. Wolfe, B.A. and K.L. Gould, *Fission yeast Clp1p phosphatase affects G2/M transition and mitotic exit through Cdc25p inactivation*. EMBO J, 2004. **23**(4): p. 919-29.
71. Nefsky, B. and D. Beach, *Pub1 acts as an E6-AP-like protein ubiquitin ligase in the degradation of cdc25*. EMBO J, 1996. **15**(6): p. 1301-12.
72. Russell, P. and P. Nurse, *Negative regulation of mitosis by wee1+, a gene encoding a protein kinase homolog*. Cell, 1987. **49**(4): p. 559-67.
73. Lee, M.S., T. Enoch, and H. Piwnica-Worms, *mik1+ encodes a tyrosine kinase that phosphorylates p34cdc2 on tyrosine 15*. J Biol Chem, 1994. **269**(48): p. 30530-7.
74. Caspari, T. and V. Hilditch, *Two Distinct Cdc2 Pools Regulate Cell Cycle Progression and the DNA Damage Response in the Fission Yeast S.pombe*. PLoS One, 2015. **10**(7): p. e0130748.
75. Schmidt, M., et al., *Regulation of G2/M Transition by Inhibition of WEE1 and PKMYT1 Kinases*. Molecules, 2017. **22**(12).
76. Hughes, B.T., et al., *Essential role for Cdk2 inhibitory phosphorylation during replication stress revealed by a human Cdk2 knockin mutation*. Proc Natl Acad Sci U S A, 2013. **110**(22): p. 8954-9.
77. Liu, F., et al., *The human Myt1 kinase preferentially phosphorylates Cdc2 on threonine 14 and localizes to the endoplasmic reticulum and Golgi complex*. Mol Cell Biol, 1997. **17**(2): p. 571-83.
78. Rothblum-Oviatt, C.J., C.E. Ryan, and H. Piwnica-Worms, *14-3-3 binding regulates catalytic activity of human Wee1 kinase*. Cell Growth Differ, 2001. **12**(12): p. 581-9.
79. Kimball, S.R. and L.S. Jefferson, *Control of translation initiation through integration of signals generated by hormones, nutrients, and exercise*. J Biol Chem, 2010. **285**(38): p. 29027-32.
80. Murugan, A.K., *mTOR: Role in cancer, metastasis and drug resistance*. Semin Cancer Biol, 2019.
81. Deprez, M.A., et al., *The TORC1-Sch9 pathway as a crucial mediator of chronological lifespan in the yeast Saccharomyces cerevisiae*. FEMS Yeast Res, 2018. **18**(5).
82. Hara, K., *Roles of mTOR in ageing and longevity*. Nihon Rinsho, 2016. **74**(9): p. 1479-1484.
83. Proud, C.G., *mTOR Signalling in Health and Disease*. Biochem Soc Trans, 2011. **39**(2): p. 431-6.
84. Nakashima, A., T. Sato, and F. Tamanoi, *Fission yeast TORC1 regulates phosphorylation of ribosomal S6 proteins in response to nutrients and its activity is inhibited by rapamycin*. J Cell Sci, 2010. **123**(Pt 5): p. 777-86.
85. Atkin, J., et al., *Torin1-mediated TOR kinase inhibition reduces Wee1 levels and advances mitotic commitment in fission yeast and HeLa cells*. J Cell Sci, 2014. **127**(Pt 6): p. 1346-56.
86. Kultz, D., *Molecular and evolutionary basis of the cellular stress response*. Annu Rev Physiol, 2005. **67**: p. 225-57.
87. Fulda, S., et al., *Cellular stress responses: cell survival and cell death*. Int J Cell Biol, 2010. **2010**: p. 214074.
88. Mazzei, T., *Chemistry and mechanism of action of bleomycin*. Chemioterapia, 1984. **3**(5): p. 316-9.
89. Poirier, M.C., *Chemical-induced DNA damage and human cancer risk*. Discov Med, 2012. **14**(77): p. 283-8.

90. Hakem, R., *DNA-damage repair; the good, the bad, and the ugly*. EMBO J, 2008. **27**(4): p. 589-605.
91. Harper, J.W. and S.J. Elledge, *The DNA damage response: ten years after*. Mol Cell, 2007. **28**(5): p. 739-45.
92. Melo, J. and D. Toczyski, *A unified view of the DNA-damage checkpoint*. Curr Opin Cell Biol, 2002. **14**(2): p. 237-45.
93. Chen, R. and M.S. Wold, *Replication protein A: single-stranded DNA's first responder: dynamic DNA-interactions allow replication protein A to direct single-strand DNA intermediates into different pathways for synthesis or repair*. Bioessays, 2014. **36**(12): p. 1156-61.
94. Tammaro, M., et al., *The N-terminus of RPA large subunit and its spatial position are important for the 5'→3' resection of DNA double-strand breaks*. Nucleic Acids Res, 2015. **43**(18): p. 8790-800.
95. Melo, J.A., J. Cohen, and D.P. Toczyski, *Two checkpoint complexes are independently recruited to sites of DNA damage in vivo*. Genes Dev, 2001. **15**(21): p. 2809-21.
96. Parrilla-Castellar, E.R., S.J. Arlander, and L. Karnitz, *Dial 9-1-1 for DNA damage: the Rad9-Hus1-Rad1 (9-1-1) clamp complex*. DNA Repair (Amst), 2004. **3**(8-9): p. 1009-14.
97. Zou, L., D. Cortez, and S.J. Elledge, *Regulation of ATR substrate selection by Rad17-dependent loading of Rad9 complexes onto chromatin*. Genes Dev, 2002. **16**(2): p. 198-208.
98. Ellison, V. and B. Stillman, *Biochemical characterization of DNA damage checkpoint complexes: clamp loader and clamp complexes with specificity for 5' recessed DNA*. PLoS Biol, 2003. **1**(2): p. E33.
99. MacDougall, C.A., et al., *The structural determinants of checkpoint activation*. Genes Dev, 2007. **21**(8): p. 898-903.
100. Lee, J., A. Kumagai, and W.G. Dunphy, *The Rad9-Hus1-Rad1 checkpoint clamp regulates interaction of TopBP1 with ATR*. J Biol Chem, 2007. **282**(38): p. 28036-44.
101. Furuya, K., et al., *Chk1 activation requires Rad9 S/TQ-site phosphorylation to promote association with C-terminal BRCT domains of Rad4TOPBP1*. Genes Dev, 2004. **18**(10): p. 1154-64.
102. Ohashi, E., et al., *Interaction between Rad9-Hus1-Rad1 and TopBP1 activates ATR-ATRIP and promotes TopBP1 recruitment to sites of UV-damage*. DNA Repair (Amst), 2014. **21**: p. 1-11.
103. Marechal, A. and L. Zou, *DNA damage sensing by the ATM and ATR kinases*. Cold Spring Harb Perspect Biol, 2013. **5**(9).
104. Walworth, N.C. and R. Bernards, *rad-dependent response of the chk1-encoded protein kinase at the DNA damage checkpoint*. Science, 1996. **271**(5247): p. 353-6.
105. Murakami, H. and H. Okayama, *A kinase from fission yeast responsible for blocking mitosis in S phase*. Nature, 1995. **374**(6525): p. 817-9.
106. Cimprich, K.A. and D. Cortez, *ATR: an essential regulator of genome integrity*. Nat Rev Mol Cell Biol, 2008. **9**(8): p. 616-27.
107. Lee, J.H. and T.T. Paull, *Direct activation of the ATM protein kinase by the Mre11/Rad50/Nbs1 complex*. Science, 2004. **304**(5667): p. 93-6.
108. Cuadrado, M., et al., *ATM regulates ATR chromatin loading in response to DNA double-strand breaks*. J Exp Med, 2006. **203**(2): p. 297-303.
109. Matsuura, A., T. Naito, and F. Ishikawa, *Genetic control of telomere integrity in Schizosaccharomyces pombe: rad3(+) and tell1(+) are parts of two regulatory networks independent of the downstream protein kinases chk1(+) and cds1(+)*. Genetics, 1999. **152**(4): p. 1501-12.

110. Hnizda, A. and T.L. Blundell, *Multicomponent assemblies in DNA-double-strand break repair by NHEJ*. *Curr Opin Struct Biol*, 2019. **55**: p. 154-160.
111. Manolis, K.G., et al., *Novel functional requirements for non-homologous DNA end joining in Schizosaccharomyces pombe*. *EMBO J*, 2001. **20**(1-2): p. 210-21.
112. Ivanova, T., et al., *The DNA damage and the DNA replication checkpoints converge at the MBF transcription factor*. *Mol Biol Cell*, 2013. **24**(21): p. 3350-7.
113. Boddy, M.N., et al., *Replication checkpoint enforced by kinases Cds1 and Chk1*. *Science*, 1998. **280**(5365): p. 909-12.
114. Frazer, C. and P.G. Young, *Carboxy-terminal phosphorylation sites in Cdc25 contribute to enforcement of the DNA damage and replication checkpoints in fission yeast*. *Curr Genet*, 2012. **58**(4): p. 217-34.
115. Sorensen, C.S., et al., *ATR, Claspin and the Rad9-Rad1-Hus1 complex regulate Chk1 and Cdc25A in the absence of DNA damage*. *Cell Cycle*, 2004. **3**(7): p. 941-5.
116. Falck, J., et al., *The ATM-Chk2-Cdc25A checkpoint pathway guards against radioresistant DNA synthesis*. *Nature*, 2001. **410**(6830): p. 842-7.
117. Serrano, M.A., et al., *DNA-PK, ATM and ATR collaboratively regulate p53-RPA interaction to facilitate homologous recombination DNA repair*. *Oncogene*, 2013. **32**(19): p. 2452-62.
118. Shieh, S.Y., et al., *The human homologs of checkpoint kinases Chk1 and Cds1 (Chk2) phosphorylate p53 at multiple DNA damage-inducible sites*. *Genes Dev*, 2000. **14**(3): p. 289-300.
119. Lees-Miller, S.P., Y.R. Chen, and C.W. Anderson, *Human cells contain a DNA-activated protein kinase that phosphorylates simian virus 40 T antigen, mouse p53, and the human Ku autoantigen*. *Mol Cell Biol*, 1990. **10**(12): p. 6472-81.
120. Lees-Miller, S.P., et al., *Human DNA-activated protein kinase phosphorylates serines 15 and 37 in the amino-terminal transactivation domain of human p53*. *Mol Cell Biol*, 1992. **12**(11): p. 5041-9.
121. Hwang, B.J., et al., *Association of the Rad9-Rad1-Hus1 checkpoint clamp with MYH DNA glycosylase and DNA*. *DNA Repair (Amst)*, 2015. **31**: p. 80-90.
122. Shi, G., et al., *Physical and functional interactions between MutY glycosylase homologue (MYH) and checkpoint proteins Rad9-Rad1-Hus1*. *Biochem J*, 2006. **400**(1): p. 53-62.
123. Jansson, K., et al., *The tumor suppressor homolog in fission yeast, myh1(+), displays a strong interaction with the checkpoint gene rad1(+)*. *Mutat Res*, 2008. **644**(1-2): p. 48-55.
124. Chang, D.Y. and A.L. Lu, *Interaction of checkpoint proteins Hus1/Rad1/Rad9 with DNA base excision repair enzyme MutY homolog in fission yeast, Schizosaccharomyces pombe*. *J Biol Chem*, 2005. **280**(1): p. 408-17.
125. Blaikley, E.J., et al., *The DNA damage checkpoint pathway promotes extensive resection and nucleotide synthesis to facilitate homologous recombination repair and genome stability in fission yeast*. *Nucleic Acids Res*, 2014. **42**(9): p. 5644-56.
126. Bode, A.M. and Z. Dong, *The enigmatic effects of caffeine in cell cycle and cancer*. *Cancer Lett*, 2007. **247**(1): p. 26-39.
127. Wang, S.W., et al., *Caffeine can override the S-M checkpoint in fission yeast*. *J Cell Sci*, 1999. **112 ( Pt 6)**: p. 927-37.
128. Moser, B.A., et al., *Mechanism of caffeine-induced checkpoint override in fission yeast*. *Mol Cell Biol*, 2000. **20**(12): p. 4288-94.
129. Cortez, D., *Caffeine inhibits checkpoint responses without inhibiting the ataxia-telangiectasia-mutated (ATM) and ATM- and Rad3-related (ATR) protein kinases*. *J Biol Chem*, 2003. **278**(39): p. 37139-45.

130. Qi, W., D. Qiao, and J.D. Martinez, *Caffeine induces TP53-independent G(1)-phase arrest and apoptosis in human lung tumor cells in a dose-dependent manner*. Radiat Res, 2002. **157**(2): p. 166-74.
131. Sorensen, C.S., et al., *Chk1 regulates the S phase checkpoint by coupling the physiological turnover and ionizing radiation-induced accelerated proteolysis of Cdc25A*. Cancer Cell, 2003. **3**(3): p. 247-58.
132. Reinke, A., et al., *Caffeine targets TOR complex I and provides evidence for a regulatory link between the FRB and kinase domains of Tor1p*. J Biol Chem, 2006. **281**(42): p. 31616-26.
133. Rallis, C., S. Codlin, and J. Bahler, *TORC1 signaling inhibition by rapamycin and caffeine affect lifespan, global gene expression, and cell proliferation of fission yeast*. Aging Cell, 2013. **12**(4): p. 563-73.
134. Ng, N., et al., *Challenges to DNA replication in hypoxic conditions*. FEBS J, 2018. **285**(9): p. 1563-1571.
135. Hiraga, T., *Hypoxic Microenvironment and Metastatic Bone Disease*. Int J Mol Sci, 2018. **19**(11).
136. Monti, E. and M.B. Gariboldi, *HIF-1 as a target for cancer chemotherapy, chemosensitization and chemoprevention*. Curr Mol Pharmacol, 2011. **4**(1): p. 62-77.
137. Simon, J.M., [*Hypoxia and angiogenesis*]. Bull Cancer, 2007. **94 Spec No**: p. S160-5.
138. Hughes, A.L., B.L. Todd, and P.J. Espenshade, *SREBP pathway responds to sterols and functions as an oxygen sensor in fission yeast*. Cell, 2005. **120**(6): p. 831-42.
139. Osborne, T.F. and P.J. Espenshade, *Evolutionary conservation and adaptation in the mechanism that regulates SREBP action: what a long, strange tRIP it's been*. Genes Dev, 2009. **23**(22): p. 2578-91.
140. Freiberg, R.A., et al., *Checking in on hypoxia/reoxygenation*. Cell Cycle, 2006. **5**(12): p. 1304-7.
141. Hammond, E.M., M.J. Dorie, and A.J. Giaccia, *ATR/ATM targets are phosphorylated by ATR in response to hypoxia and ATM in response to reoxygenation*. J Biol Chem, 2003. **278**(14): p. 12207-13.
142. Bindra, R.S., M.E. Crosby, and P.M. Glazer, *Regulation of DNA repair in hypoxic cancer cells*. Cancer Metastasis Rev, 2007. **26**(2): p. 249-60.
143. Bristow, R.G. and R.P. Hill, *Hypoxia and metabolism. Hypoxia, DNA repair and genetic instability*. Nat Rev Cancer, 2008. **8**(3): p. 180-92.
144. Ohta, M., et al., *The FHIT gene, spanning the chromosome 3p14.2 fragile site and renal carcinoma-associated t(3;8) breakpoint, is abnormal in digestive tract cancers*. Cell, 1996. **84**(4): p. 587-97.
145. Sutherland, G.R. and R.I. Richards, *The molecular basis of fragile sites in human chromosomes*. Curr Opin Genet Dev, 1995. **5**(3): p. 323-7.
146. Lukusa, T. and J.P. Fryns, *Human chromosome fragility*. Biochim Biophys Acta, 2008. **1779**(1): p. 3-16.
147. Smeets, D., J. Scheres, and T. Hustinx, *The most common fragile site in man is 3p14*. Hum Genet, 1986. **74**(3): p. 330.
148. Zanesi, N., et al., *The tumor spectrum in FHIT-deficient mice*. Proc Natl Acad Sci U S A, 2001. **98**(18): p. 10250-5.
149. Pichiorri, F., et al., *Fhit tumor suppressor: guardian of the preneoplastic genome*. Future Oncol, 2008. **4**(6): p. 815-24.
150. Saldivar, J.C., et al., *Initiation of genome instability and preneoplastic processes through loss of Fhit expression*. PLoS Genet, 2012. **8**(11): p. e1003077.
151. Paisie, C.A., et al., *Exome-wide single-base substitutions in tissues and derived cell lines of the constitutive Fhit knockout mouse*. Cancer Sci, 2016. **107**(4): p. 528-35.

152. Ishii, H., et al., *Fhit modulates the DNA damage checkpoint response*. *Cancer Res*, 2006. **66**(23): p. 11287-92.
153. Yutori, H., et al., *Restoration of fragile histidine triad expression restores Chk2 activity in response to ionizing radiation in oral squamous cell carcinoma cells*. *Cancer Sci*, 2008. **99**(3): p. 524-30.
154. Song, X., et al., *Restoration of fragile histidine triad (FHIT) expression inhibits cell growth and induces apoptosis in cutaneous T-cell lymphoma cell line*. *Cancer Invest*, 2010. **28**(10): p. 1019-23.
155. Druck, T., et al., *Fhit-Fdxr interaction in the mitochondria: modulation of reactive oxygen species generation and apoptosis in cancer cells*. *Cell Death Dis*, 2019. **10**(3): p. 147.
156. Boylston, J.A. and C. Brenner, *A knockdown with smoke model reveals FHIT as a repressor of Heme oxygenase 1*. *Cell Cycle*, 2014. **13**(18): p. 2913-30.
157. Nishizaki, M., et al., *Synergistic tumor suppression by coexpression of FHIT and p53 coincides with FHIT-mediated MDM2 inactivation and p53 stabilization in human non-small cell lung cancer cells*. *Cancer Res*, 2004. **64**(16): p. 5745-52.
158. Brenner, C., *Hint, Fhit, and GalT: function, structure, evolution, and mechanism of three branches of the histidine triad superfamily of nucleotide hydrolases and transferases*. *Biochemistry*, 2002. **41**(29): p. 9003-14.
159. Pace, H.C., et al., *Genetic, biochemical, and crystallographic characterization of Fhit-substrate complexes as the active signaling form of Fhit*. *Proc Natl Acad Sci U S A*, 1998. **95**(10): p. 5484-9.
160. Taverniti, V. and B. Seraphin, *Elimination of cap structures generated by mRNA decay involves the new scavenger mRNA decapping enzyme Aph1/FHIT together with Dcp5*. *Nucleic Acids Res*, 2015. **43**(1): p. 482-92.
161. Furuichi, Y., *Discovery of m(7)G-cap in eukaryotic mRNAs*. *Proc Jpn Acad Ser B Phys Biol Sci*, 2015. **91**(8): p. 394-409.
162. Kiss, D.L., et al., *Impact of FHIT loss on the translation of cancer-associated mRNAs*. *Mol Cancer*, 2017. **16**(1): p. 179.
163. Kiss, D.L., et al., *Identification of Fhit as a post-transcriptional effector of Thymidine Kinase 1 expression*. *Biochim Biophys Acta Gene Regul Mech*, 2017. **1860**(3): p. 374-382.
164. Ingram, S.W. and L.D. Barnes, *Disruption and overexpression of the Schizosaccharomyces pombe aph1 gene and the effects on intracellular diadenosine 5',5'''-P1, P4-tetraphosphate (Ap4A), ATP and ADP concentrations*. *Biochem J*, 2000. **350 Pt 3**: p. 663-9.
165. Vo, T.V., et al., *A Proteome-wide Fission Yeast Interactome Reveals Network Evolution Principles from Yeasts to Human*. *Cell*, 2016. **164**(1-2): p. 310-323.
166. Ryan, C.J., et al., *Hierarchical modularity and the evolution of genetic interactomes across species*. *Mol Cell*, 2012. **46**(5): p. 691-704.
167. Wali, A., *FHIT: doubts are clear now*. *ScientificWorldJournal*, 2010. **10**: p. 1142-51.
168. Reczek, C.R. and N.S. Chandel, *ROS-dependent signal transduction*. *Curr Opin Cell Biol*, 2015. **33**: p. 8-13.
169. Ku, H.H., U.T. Brunk, and R.S. Sohal, *Relationship between mitochondrial superoxide and hydrogen peroxide production and longevity of mammalian species*. *Free Radic Biol Med*, 1993. **15**(6): p. 621-7.
170. Squier, T.C., *Oxidative stress and protein aggregation during biological aging*. *Exp Gerontol*, 2001. **36**(9): p. 1539-50.
171. Poole, L.B., *The basics of thiols and cysteines in redox biology and chemistry*. *Free Radic Biol Med*, 2015. **80**: p. 148-57.



172. Randall, L.M., G. Ferrer-Sueta, and A. Denicola, *Peroxiredoxins as preferential targets in H<sub>2</sub>O<sub>2</sub>-induced signaling*. *Methods Enzymol*, 2013. **527**: p. 41-63.
173. Kettenhofen, N.J. and M.J. Wood, *Formation, reactivity, and detection of protein sulfenic acids*. *Chem Res Toxicol*, 2010. **23**(11): p. 1633-46.
174. Salmeen, A., et al., *Redox regulation of protein tyrosine phosphatase 1B involves a sulphenyl-amide intermediate*. *Nature*, 2003. **423**(6941): p. 769-73.
175. Schwertassek, U., et al., *Reactivation of oxidized PTP1B and PTEN by thioredoxin 1*. *FEBS J*, 2014. **281**(16): p. 3545-58.
176. Biteau, B., J. Labarre, and M.B. Toledano, *ATP-dependent reduction of cysteine-sulphinic acid by *S. cerevisiae* sulphiredoxin*. *Nature*, 2003. **425**(6961): p. 980-4.
177. Atkinson, H.J. and P.C. Babbitt, *An atlas of the thioredoxin fold class reveals the complexity of function-enabling adaptations*. *PLoS Comput Biol*, 2009. **5**(10): p. e1000541.
178. Hanschmann, E.M., et al., *Thioredoxins, glutaredoxins, and peroxiredoxins--molecular mechanisms and health significance: from cofactors to antioxidants to redox signaling*. *Antioxid Redox Signal*, 2013. **19**(13): p. 1539-605.
179. Forman, H.J., H. Zhang, and A. Rinna, *Glutathione: overview of its protective roles, measurement, and biosynthesis*. *Mol Aspects Med*, 2009. **30**(1-2): p. 1-12.
180. Ferguson, G.D. and W.J. Bridge, *The glutathione system and the related thiol network in *Caenorhabditis elegans**. *Redox Biol*, 2019. **24**: p. 101171.
181. Mailloux, R.J., X. Jin, and W.G. Willmore, *Redox regulation of mitochondrial function with emphasis on cysteine oxidation reactions*. *Redox Biol*, 2014. **2**: p. 123-39.
182. Demasi, A.P., G.A. Pereira, and L.E. Netto, *Cytosolic thioredoxin peroxidase I is essential for the antioxidant defense of yeast with dysfunctional mitochondria*. *FEBS Lett*, 2001. **509**(3): p. 430-4.
183. Bozonet, S.M., et al., *Oxidation of a eukaryotic 2-Cys peroxiredoxin is a molecular switch controlling the transcriptional response to increasing levels of hydrogen peroxide*. *J Biol Chem*, 2005. **280**(24): p. 23319-27.
184. Noichri, Y., et al., *In vivo parameters influencing 2-Cys Prx oligomerization: The role of enzyme sulfinylation*. *Redox Biol*, 2015. **6**: p. 326-333.
185. Woo, H.A., et al., *Reduction of cysteine sulfenic acid by sulfiredoxin is specific to 2-cys peroxiredoxins*. *J Biol Chem*, 2005. **280**(5): p. 3125-8.
186. Sies, H., *Role of metabolic H<sub>2</sub>O<sub>2</sub> generation: redox signaling and oxidative stress*. *J Biol Chem*, 2014. **289**(13): p. 8735-41.
187. Messens, J. and J.F. Collet, *Thiol-disulfide exchange in signaling: disulfide bonds as a switch*. *Antioxid Redox Signal*, 2013. **18**(13): p. 1594-6.
188. Mieyal, J.J. and P.B. Chock, *Posttranslational modification of cysteine in redox signaling and oxidative stress: Focus on s-glutathionylation*. *Antioxid Redox Signal*, 2012. **16**(6): p. 471-5.
189. Aslund, F., et al., *Regulation of the OxyR transcription factor by hydrogen peroxide and the cellular thiol-disulfide status*. *Proc Natl Acad Sci U S A*, 1999. **96**(11): p. 6161-5.
190. Cox, A.G., C.C. Winterbourn, and M.B. Hampton, *Mitochondrial peroxiredoxin involvement in antioxidant defence and redox signalling*. *Biochem J*, 2009. **425**(2): p. 313-25.
191. Vivancos, A.P., et al., *A cysteine-sulfenic acid in peroxiredoxin regulates H<sub>2</sub>O<sub>2</sub>-sensing by the antioxidant Pap1 pathway*. *Proc Natl Acad Sci U S A*, 2005. **102**(25): p. 8875-80.

192. Delaunay, A., et al., *A thiol peroxidase is an H<sub>2</sub>O<sub>2</sub> receptor and redox-transducer in gene activation*. Cell, 2002. **111**(4): p. 471-81.
193. Okazaki, S., A. Naganuma, and S. Kuge, *Peroxiredoxin-mediated redox regulation of the nuclear localization of Yap1, a transcription factor in budding yeast*. Antioxid Redox Signal, 2005. **7**(3-4): p. 327-34.
194. Moffett, A.S., et al., *Allosteric Control of a Plant Receptor Kinase through S-Glutathionylation*. Biophys J, 2017. **113**(11): p. 2354-2363.
195. Fowler, N.J., et al., *Features of reactive cysteines discovered through computation: from kinase inhibition to enrichment around protein degrons*. Sci Rep, 2017. **7**(1): p. 16338.
196. Widmann, C., et al., *Mitogen-activated protein kinase: conservation of a three-kinase module from yeast to human*. Physiol Rev, 1999. **79**(1): p. 143-80.
197. Seger, R. and E.G. Krebs, *The MAPK signaling cascade*. FASEB J, 1995. **9**(9): p. 726-35.
198. Robinson, M.J. and M.H. Cobb, *Mitogen-activated protein kinase pathways*. Curr Opin Cell Biol, 1997. **9**(2): p. 180-6.
199. Ichijo, H., *From receptors to stress-activated MAP kinases*. Oncogene, 1999. **18**(45): p. 6087-93.
200. Cobb, M.H. and E.J. Goldsmith, *How MAP kinases are regulated*. J Biol Chem, 1995. **270**(25): p. 14843-6.
201. De Luca, A., et al., *The RAS/RAF/MEK/ERK and the PI3K/AKT signalling pathways: role in cancer pathogenesis and implications for therapeutic approaches*. Expert Opin Ther Targets, 2012. **16 Suppl 2**: p. S17-27.
202. del Barco Barrantes, I. and A.R. Nebreda, *Roles of p38 MAPKs in invasion and metastasis*. Biochem Soc Trans, 2012. **40**(1): p. 79-84.
203. Heasley, L.E. and S.Y. Han, *JNK regulation of oncogenesis*. Mol Cells, 2006. **21**(2): p. 167-73.
204. Gotoh, Y., et al., *Schizosaccharomyces pombe Spk1 is a tyrosine-phosphorylated protein functionally related to Xenopus mitogen-activated protein kinase*. Mol Cell Biol, 1993. **13**(10): p. 6427-34.
205. Toda, T., et al., *The fission yeast pmk1+ gene encodes a novel mitogen-activated protein kinase homolog which regulates cell integrity and functions coordinately with the protein kinase C pathway*. Mol Cell Biol, 1996. **16**(12): p. 6752-64.
206. Stettler, S., et al., *The wis1 signal transduction pathway is required for expression of cAMP-repressed genes in fission yeast*. J Cell Sci, 1996. **109 ( Pt 7)**: p. 1927-35.
207. Degols, G., K. Shiozaki, and P. Russell, *Activation and regulation of the Spc1 stress-activated protein kinase in Schizosaccharomyces pombe*. Mol Cell Biol, 1996. **16**(6): p. 2870-7.
208. Nakagawa, C.W., K. Yamada, and N. Mutoh, *Two distinct upstream regions are involved in expression of the catalase gene in Schizosaccharomyces pombe in response to oxidative stress*. J Biochem, 1998. **123**(6): p. 1048-54.
209. Soto, T., et al., *Cold induces stress-activated protein kinase-mediated response in the fission yeast Schizosaccharomyces pombe*. Eur J Biochem, 2002. **269**(20): p. 5056-65.
210. Zhou, X., et al., *MAP kinase kinase kinase (MAPKKK)-dependent and -independent activation of Sty1 stress MAPK in fission yeast*. J Biol Chem, 2010. **285**(43): p. 32818-23.
211. Degols, G. and P. Russell, *Discrete roles of the Spc1 kinase and the Atf1 transcription factor in the UV response of Schizosaccharomyces pombe*. Mol Cell Biol, 1997. **17**(6): p. 3356-63.

212. Watson, A., et al., *Global gene expression responses of fission yeast to ionizing radiation*. Mol Biol Cell, 2004. **15**(2): p. 851-60.
213. Samejima, I., S. Mackie, and P.A. Fantes, *Multiple modes of activation of the stress-responsive MAP kinase pathway in fission yeast*. EMBO J, 1997. **16**(20): p. 6162-70.
214. Shiozaki, K., M. Shiozaki, and P. Russell, *Heat stress activates fission yeast Spc1/Sty1 MAPK by a MEKK-independent mechanism*. Mol Biol Cell, 1998. **9**(6): p. 1339-49.
215. Rodriguez-Gabriel, M.A. and P. Russell, *Distinct signaling pathways respond to arsenite and reactive oxygen species in Schizosaccharomyces pombe*. Eukaryot Cell, 2005. **4**(8): p. 1396-402.
216. Salgado, A., et al., *Response to arsenate treatment in Schizosaccharomyces pombe and the role of its arsenate reductase activity*. PLoS One, 2012. **7**(8): p. e43208.
217. Wilkinson, M.G., et al., *The Atf1 transcription factor is a target for the Sty1 stress-activated MAP kinase pathway in fission yeast*. Genes Dev, 1996. **10**(18): p. 2289-301.
218. Sanso, M., et al., *Transcription factors Pcr1 and Atf1 have distinct roles in stress- and Sty1-dependent gene regulation*. Eukaryot Cell, 2008. **7**(5): p. 826-35.
219. Ashworth, A., et al., *The amino acid sequence of a mammalian MAP kinase kinase*. Oncogene, 1992. **7**(12): p. 2555-6.
220. Millar, J.B., V. Buck, and M.G. Wilkinson, *Pyp1 and Pyp2 PTPases dephosphorylate an osmosensing MAP kinase controlling cell size at division in fission yeast*. Genes Dev, 1995. **9**(17): p. 2117-30.
221. Samejima, I., et al., *The fission yeast mitotic regulator win1+ encodes an MAP kinase kinase kinase that phosphorylates and activates Wis1 MAP kinase kinase in response to high osmolarity*. Mol Biol Cell, 1998. **9**(8): p. 2325-35.
222. Shieh, J.C., et al., *The Mcs4 response regulator coordinately controls the stress-activated Wak1-Wis1-Sty1 MAP kinase pathway and fission yeast cell cycle*. Genes Dev, 1997. **11**(8): p. 1008-22.
223. Quinn, J., et al., *Distinct regulatory proteins control the graded transcriptional response to increasing H(2)O(2) levels in fission yeast Schizosaccharomyces pombe*. Mol Biol Cell, 2002. **13**(3): p. 805-16.
224. Morigasaki, S., et al., *Response regulator-mediated MAPKKK heteromer promotes stress signaling to the Spc1 MAPK in fission yeast*. Mol Biol Cell, 2013. **24**(7): p. 1083-92.
225. Gaits, F., et al., *Phosphorylation and association with the transcription factor Atf1 regulate localization of Spc1/Sty1 stress-activated kinase in fission yeast*. Genes Dev, 1998. **12**(10): p. 1464-73.
226. Morigasaki, S., et al., *Glycolytic enzyme GAPDH promotes peroxide stress signaling through multistep phosphorelay to a MAPK cascade*. Mol Cell, 2008. **30**(1): p. 108-13.
227. Veal, E.A., et al., *A 2-Cys peroxiredoxin regulates peroxide-induced oxidation and activation of a stress-activated MAP kinase*. Mol Cell, 2004. **15**(1): p. 129-39.
228. Nguyen, A.N. and K. Shiozaki, *Heat-shock-induced activation of stress MAP kinase is regulated by threonine- and tyrosine-specific phosphatases*. Genes Dev, 1999. **13**(13): p. 1653-63.
229. Di, Y., et al., *H(2)O(2) stress-specific regulation of S. pombe MAPK Sty1 by mitochondrial protein phosphatase Ptc4*. EMBO J, 2012. **31**(3): p. 563-75.
230. Vivancos, A.P., et al., *Oxidative stress in Schizosaccharomyces pombe: different H2O2 levels, different response pathways*. Mol Genet Genomics, 2006. **276**(6): p. 495-502.
231. Buck, V., et al., *Peroxide sensors for the fission yeast stress-activated mitogen-activated protein kinase pathway*. Mol Biol Cell, 2001. **12**(2): p. 407-19.

232. Nguyen, A.N., et al., *Multistep phosphorelay proteins transmit oxidative stress signals to the fission yeast stress-activated protein kinase*. Mol Biol Cell, 2000. **11**(4): p. 1169-81.
233. Calvo, I.A., et al., *Dissection of a redox relay: H2O2-dependent activation of the transcription factor Pap1 through the peroxidatic Tpx1-thioredoxin cycle*. Cell Rep, 2013. **5**(5): p. 1413-24.
234. Dudley, D.T., et al., *A synthetic inhibitor of the mitogen-activated protein kinase cascade*. Proc Natl Acad Sci U S A, 1995. **92**(17): p. 7686-9.
235. Favata, M.F., et al., *Identification of a novel inhibitor of mitogen-activated protein kinase kinase*. J Biol Chem, 1998. **273**(29): p. 18623-32.
236. Salama, A.K. and K.B. Kim, *Trametinib (GSK1120212) in the treatment of melanoma*. Expert Opin Pharmacother, 2013. **14**(5): p. 619-27.
237. Signorelli, J. and A. Shah Gandhi, *Cobimetinib*. Ann Pharmacother, 2017. **51**(2): p. 146-153.
238. Ballantyne, A.D. and K.P. Garnock-Jones, *Dabrafenib: first global approval*. Drugs, 2013. **73**(12): p. 1367-76.
239. Laskowski, R.A., F. Gerick, and J.M. Thornton, *The structural basis of allosteric regulation in proteins*. FEBS Lett, 2009. **583**(11): p. 1692-8.
240. Dar, A.C. and K.M. Shokat, *The evolution of protein kinase inhibitors from antagonists to agonists of cellular signaling*. Annu Rev Biochem, 2011. **80**: p. 769-95.
241. Alessi, D.R., et al., *PD 098059 is a specific inhibitor of the activation of mitogen-activated protein kinase kinase in vitro and in vivo*. J Biol Chem, 1995. **270**(46): p. 27489-94.
242. Ohren, J.F., et al., *Structures of human MAP kinase kinase 1 (MEK1) and MEK2 describe novel noncompetitive kinase inhibition*. Nat Struct Mol Biol, 2004. **11**(12): p. 1192-7.
243. Fischmann, T.O., et al., *Crystal structures of MEK1 binary and ternary complexes with nucleotides and inhibitors*. Biochemistry, 2009. **48**(12): p. 2661-74.
244. Redwan, I.N., et al., *Towards the development of chromone-based MEK1/2 modulators*. Eur J Med Chem, 2014. **85**: p. 127-38.
245. Wu, P.K. and J.I. Park, *MEK1/2 Inhibitors: Molecular Activity and Resistance Mechanisms*. Semin Oncol, 2015. **42**(6): p. 849-62.
246. Roskoski, R., Jr., *MEK1/2 dual-specificity protein kinases: structure and regulation*. Biochem Biophys Res Commun, 2012. **417**(1): p. 5-10.
247. Gopalbhai, K., et al., *Negative regulation of MAPKK by phosphorylation of a conserved serine residue equivalent to Ser212 of MEK1*. J Biol Chem, 2003. **278**(10): p. 8118-25.
248. Frazer, C. and P.G. Young, *Redundant mechanisms prevent mitotic entry following replication arrest in the absence of Cdc25 hyper-phosphorylation in fission yeast*. PLoS One, 2011. **6**(6): p. e21348.
249. Wanke, V., et al., *Caffeine extends yeast lifespan by targeting TORC1*. Mol Microbiol, 2008. **69**(1): p. 277-85.
250. Calvo, I.A., et al., *Genome-wide screen of genes required for caffeine tolerance in fission yeast*. PLoS One, 2009. **4**(8): p. e6619.
251. Alao, J.P., et al., *Caffeine stabilizes Cdc25 independently of Rad3 in Schizosaccharomyces pombe contributing to checkpoint override*. Mol Microbiol, 2014. **92**(4): p. 777-96.
252. Dannewitz Prosseda, S., et al., *FHIT, a Novel Modifier Gene in Pulmonary Arterial Hypertension*. Am J Respir Crit Care Med, 2019. **199**(1): p. 83-98.

253. Paulin, R. and E.D. Michelakis, *The metabolic theory of pulmonary arterial hypertension*. *Circ Res*, 2014. **115**(1): p. 148-64.
254. Connolly, M.J. and P.I. Aaronson, *Key role of the RhoA/Rho kinase system in pulmonary hypertension*. *Pulm Pharmacol Ther*, 2011. **24**(1): p. 1-14.
255. Hautefort, A., et al., *Bmpr2 Mutant Rats Develop Pulmonary and Cardiac Characteristics of Pulmonary Arterial Hypertension*. *Circulation*, 2019. **139**(7): p. 932-948.
256. McCubrey, J.A., M.M. Lahair, and R.A. Franklin, *Reactive oxygen species-induced activation of the MAP kinase signaling pathways*. *Antioxid Redox Signal*, 2006. **8**(9-10): p. 1775-89.
257. Diao, Y., et al., *Oxidation-induced intramolecular disulfide bond inactivates mitogen-activated protein kinase kinase 6 by inhibiting ATP binding*. *Proc Natl Acad Sci U S A*, 2010. **107**(49): p. 20974-9.
258. Day, A.M. and E.A. Veal, *Hydrogen peroxide-sensitive cysteines in the Sty1 MAPK regulate the transcriptional response to oxidative stress*. *J Biol Chem*, 2010. **285**(10): p. 7505-16.
259. Burgoyne, J.R., O. Oviolu, and P. Eaton, *The PEG-switch assay: a fast semi-quantitative method to determine protein reversible cysteine oxidation*. *J Pharmacol Toxicol Methods*, 2013. **68**(3): p. 297-301.
260. H., T.T. and C. K., *Bioorthogonal chemical reporters for analyzing protein sulfenylation in cells*. *Curr. Protoc. Chem. Biol.*, 2012. **4**: p. 101-122.

## Appendix 1

### Sulfenic Acid Labeling - DYn-2 Protocol (Toledano's Lab) June 2019:

#### Reagents:

DYn-2 (Cayman Chemical, cat. no. 11220)

Biotin azide (Interchim cat. no. FP-PQI331)

Sodium ascorbate

Copper(II)-TBTA complex : Lumiprobe #21050 or Interchim #FY2780)

#### Protocol:

- Yeast cell culture grown to an  $OD_{600nm} = 0.5$  (for a total of 5-6  $OD_{600nm}$ )
- Pellet cells by centrifugation at 4000 rpm, 5 min at 4°C. Remove the supernatant and resuspend cells in 0.5 mL medium (SD complete for example).
- Add to each sample 0.5 mM of **the labeling reagent DYn-2**
- Incubate the cell suspension at 30 °C for 30 min with mixing (10 min) by gently pipetting up and down.
- Centrifuge the cell suspension at 4000 rpm, 5 min at 4°C.
- Wash the cell pellets with cold PBS (or 100 mM Hepes pH7.4) twice.
- **To lyse the cells**, add the equivalent of 100  $\mu$ L glass beads (5 cycles of 1 min vortex) and 200  $\mu$ L of PBS (or Hepes) followed by cooling in wet ice.
- Transfer the supernatant to a new tube (wash the beads with extra 200  $\mu$ L of PBS (or Hepes)) and centrifuge at 14000 x g for 15 min at 4°C. Recover the supernatant and discard the pellets. Check the proteins concentration, it should be adjusted to the same concentration between the different samples (usually 2.5-3mg/ml)
- The **proteins lysate are precipitated** using cold methanol and chloroform using the following ratio lysate:methanol:chloroform = 4:4:1, vol/vol/vol and centrifuge at 14000 x g for 15 min. Protein will be between the 2 solvent layers. Both layers are aspirated and precipitation was repeated by adding H<sub>2</sub>O:MeOH:CHCl<sub>3</sub> 4:4:1 and

centrifuged at 14000 x g for 15 min. Both layers were aspirated again, and pellet obtained was washed once with cold MeOH and left to dry for 10 min.

- Resuspend the pellets in PBS (or 100 mM Hepes pH7.4) supplemented with 2% SDS.
- Once the proteins are fully dissolved, the following **click reagents (CuAAC)** are added respectively to the sample (the reagents are added in ratio equivalent to DYn-2) :
  - Biotin azide : **1 equivalent** (0.5 mM)
  - Copper(II)-TBTA complex : **2 equivalents** (1 mM)
  - Ascorbate (prepared *in situ*) : **4 equivalents** (2 mM)
- The samples are then incubated for 1 h at RT on a wheel preferably and **protected from light**.
- Quench the CuAAC reaction by adding 1mM EDTA for 10min.
- The samples are then precipitated using cold methanol and chloroform using the following ratio lysate:methanol:chloroform = 4:4:1, vol/vol/vol and centrifuge at 14000 x g for 15 min. Protein will be between 2 solvent layers. Both layers are aspirated and precipitation was repeated by adding H<sub>2</sub>O:MeOH:CHCl<sub>3</sub> 4:4:1 and centrifuged at 14000 x g for 15 min. Both layers were aspirated again, and pellet obtained was washed once with cold MeOH and left to dry for 10 min (protected from light).
- Protein pellet are resuspended in 100 µL of 100 mM Hepes buffer pH7.4, supplemented with 2 % SDS.
- **Streptavidin pull-down:** Add pre-washed (100 mM Hepes buffer pH7.4) streptavidin beads to each samples (need to add with precision, the same amount of beads to each samples) and incubate for 2h at room temperature. Wash the beads with 1% SDS (x2) then with 4M urea (x2), 1M NaCl (x1), and H<sub>2</sub>O (x2).
- Resuspend the beads in 5X Laemmli buffer and boil for 5 min at 95 °C.
- Samples are resolved by SDS-PAGE for immunoblotting.





# Paper I



# Caffeine stabilizes Cdc25 independently of Rad3 in *Schizosaccharomyces pombe* contributing to checkpoint override

John P. Alao, Johanna J. Sjölander, Juliane Baar, Nejla Özbaki-Yagan, Bianca Kakoschky and Per Sunnerhagen\*

Department of Chemistry and Molecular Biology, Lundberg Laboratory, University of Gothenburg, Box 462, SE-405 30 Göteborg, Sweden.

## Summary

**Cdc25 is required for Cdc2 dephosphorylation and is thus essential for cell cycle progression. Checkpoint activation requires dual inhibition of Cdc25 and Cdc2 in a Rad3-dependent manner. Caffeine is believed to override activation of the replication and DNA damage checkpoints by inhibiting Rad3-related proteins in both *Schizosaccharomyces pombe* and mammalian cells. In this study, we have investigated the impact of caffeine on Cdc25 stability, cell cycle progression and checkpoint override. Caffeine induced Cdc25 accumulation in *S. pombe* independently of Rad3. Caffeine delayed cell cycle progression under normal conditions but advanced mitosis in cells treated with replication inhibitors and DNA-damaging agents. In the absence of Cdc25, caffeine inhibited cell cycle progression even in the presence of hydroxyurea or phleomycin. Caffeine induces Cdc25 accumulation in *S. pombe* by suppressing its degradation independently of Rad3. The induction of Cdc25 accumulation was not associated with accelerated progression through mitosis, but rather with delayed progression through cytokinesis. Caffeine-induced Cdc25 accumulation appears to underlie its ability to override cell cycle checkpoints. The impact of Cdc25 accumulation on cell cycle progression is attenuated by *Srk1* and *Mad2*. Together our findings suggest that caffeine overrides checkpoint enforcement by inducing the inappropriate nuclear localization of Cdc25.**

Accepted 24 March, 2014. \*For correspondence.  
E-mail Per.Sunnerhagen@cmb.gu.se; Tel. (+46) 31 786 3830;  
Fax (+46) 31 786 3801.

© 2014 The Authors. *Molecular Microbiology* published by John Wiley & Sons Ltd.

This is an open access article under the terms of the Creative Commons Attribution License, which permits use, distribution and reproduction in any medium, provided the original work is properly cited.

## Introduction

The ability to rapidly delay cell cycle progression in response to environmental and genotoxic insults, is essential for the maintenance of genomic integrity and/or cell viability. Cells have thus evolved molecular signalling pathways that sense DNA damage or environmental stress and activate cell cycle checkpoints. Understanding the interplay between the cellular environment, genome maintenance and cell cycle progression is important for understanding and/or improving the prevention, progression, and treatment of many diseases (Schumacher *et al.*, 2008; Hoeijmakers, 2009).

Cell cycle progression in *Schizosaccharomyces pombe* is regulated by the activity of the cyclin-dependent kinase (CDK) Cdc2 and its regulatory cyclin Cdc13 (Lu *et al.*, 2012). Negative regulation of Cdc2, and thus cell cycle progression, is enforced by the Mik1 and Wee1 kinases which phosphorylate Tyr15 to inhibit its activity. Conversely, the Cdc25 phosphatase positively regulates Cdc2 activity by dephosphorylating Tyr15 and is essential for G2/M cell cycle progression in *S. pombe* (Lu *et al.*, 2012). Cdc25 levels increase throughout G2 but its activity is highly regulated by a combination of translational and post-translational mechanisms. The effective inhibition of Cdc25 and Cdc2 activity is thus essential for full activation of the DNA damage and stress activated cell cycle checkpoints (Alao and Sunnerhagen, 2008).

The central activator of the DNA damage response (DDR) pathway in *S. pombe* is the ataxia telangiectasia mutated (ATM) and ataxia – and rad related (ATR) kinase homologue Rad3, a member of the phosphatidylinositol 3 kinase-like kinase (PIKK) family (Humphrey, 2000; Lovejoy and Cortez, 2009). In response to stalled replication, *S. pombe* activates the replication or S-M checkpoint. Following its activation by stalled replication forks, Rad3 phosphorylates and activates the Cds1 kinase, a functional homologue of the mammalian Chk1 kinase (Boddy *et al.*, 1998; Lindsay *et al.*, 1998; Brondello *et al.*, 1999). Additionally, Rad3 phosphorylates the Chk2 kinase (Chk2 in mammalian cells) in response to DNA damage occurring during the G2 phase of the cell cycle to enforce the DNA damage checkpoint. Cds1 and Chk1 phosphorylate

multiple serine and threonine residues on Cdc25, thereby inactivating it (Alao and Sunnerhagen, 2008). Cds1 also induces the synthesis of Mik1, which is required for the degradation of Cdc25 remaining in the nucleus (Alao and Sunnerhagen, 2008). Rad3-induced activation of Cds1 and Chk1 requires the adaptor molecules Mrc1 and Crb2 respectively. This differential requirement for adaptor molecules ensures the cell cycle phase-specific activation of Cds1 and Chk1. Mik1 and Wee1 ensure full checkpoint activation and cell cycle arrest by phosphorylating Cdc2 on Tyr15. Mutants unable to effectively activate cell cycle checkpoints in response to DNA damage are highly sensitive to genotoxins (Alao and Sunnerhagen, 2008).

The mitogen-activated protein kinase (MAPK) pathway which regulates the environmental stress response (ESR) pathway, has also been shown to influence cell cycle progression in *S. pombe* by regulating Cdc25 activity. The p38 MAPK homologue Sty1 promotes G2/M progression in *S. pombe* by stabilizing Cdc25 (Shiozaki and Russell, 1995; Kishimoto and Yamashita, 2000). Simultaneously, exposure to environmental stress also induces the Sty1-mediated expression, phosphorylation and nuclear localization of Srk1 (Smith *et al.*, 2002; Asp and Sunnerhagen, 2003). Srk1 phosphorylates the same residues as do Cds1 and Chk1 on Cdc25, resulting in its nuclear export and transient cell cycle arrest (Lopez-Aviles *et al.*, 2005). Srk1 is not required for DNA damage-induced cell cycle arrest but regulates mitotic onset during the normal cell cycle by inhibiting Cdc25. Sty1 thus positively regulates Cdc25 by enhancing its stability and negatively by inhibiting its activity via Srk1.

The nuclear exclusion of Cdc25 plays a key role in regulating its ability. During the normal cell cycle, Cdc25 localizes predominantly in the nucleus from late G2 until the onset of mitosis. Phosphorylation of the nine regulatory serine and threonine residues within the N-terminal domain of Cdc25 creates binding sites for the 14-3-3 protein Rad24. Phosphorylation of these residues by Cds1, Chk1, or Srk1 thus results in the Rad24-mediated nuclear export of Cdc25 (Lopez-Girona *et al.*, 1999; Frazer and Young, 2011; 2012). The nuclear export of Cdc25 is not, however, required for the activation of the DNA damage and replication checkpoints since *S. pombe* mutants expressing constitutively nuclear Cdc25 arrest normally (Frazer and Young, 2011; 2012). In contrast, cell cycle arrest in response to environmental stress is dependent on Srk1-mediated Cdc25 phosphorylation and nuclear export (Smith *et al.*, 2002; Lopez-Aviles *et al.*, 2005). The stockpiling of Cdc25 following activation of the DDR or ESR has been frequently observed and is dependent on Sty1 (Kovelman and Russell, 1996; Kishimoto and Yamashita, 2000; Alao *et al.*, 2010). Sty1 thus modulates Cdc25 activity both positively through stabilization and negatively through Srk1. Recent studies have demon-

strated that Cdc25 levels are not rate-limiting for cell size in *S. pombe* (Frazer and Young, 2011; 2012). Constitutively nuclear mutants are less stable than wild-type (wt) Cdc25 and are degraded in a Mik1-dependent manner during DNA damage or replication stress-induced checkpoint activation (Frazer and Young, 2011; 2012). These findings suggest that nuclear export is required for the stockpiling of Cdc25 observed in response to DDR and ESR activation (Kovelman and Russell, 1996; Kishimoto and Yamashita, 2000; Lopez-Aviles *et al.*, 2005; Alao *et al.*, 2010). Normal turnover of Cdc25 requires the activity of the Pub1 ubiquitin ligase (Nefsky and Beach, 1996). The Clp1 (Flp1) phosphatase negatively regulates Cdc25 activity and stability at the end of mitosis. Clp1-mediated inhibition of Cdc25 activity is required for mitotic exit, activation of the septation initiation network (SIN), and progression through cytokinesis (Trautmann *et al.*, 2001; Esteban *et al.*, 2004; 2008; Mikhailov *et al.*, 2004). Consequently, the elevated Cdc25 activity in *clp1Δ* and *pub1Δ* mutants slows progression through cytokinesis (Esteban *et al.*, 2004; 2008; Wolfe and Gould, 2004).

The production of radical oxygen species (ROS) can result in DNA damage and activation of the DDR pathway. Similarly, DNA damage is associated with the production of ROS. Co-activation of the DDR and ESR pathways is thus a common event. It remains unclear, however, how the DDR and ESR pathways are integrated in terms of Cdc25 activity and cell cycle progression (Alao and Sunnerhagen, 2008). Activation of Sty1 enforces Cdc25 activity and mitotic progression (Shiozaki and Russell, 1995; Kishimoto and Yamashita, 2000; Alao *et al.*, 2010). Mutants unable to activate the DDR pathway are driven into mitosis in a Sty1-dependent manner when exposed to ultraviolet radiation which induces both ROS production and DNA damage (Degols and Russell, 1997; Alao *et al.*, 2010). Conversely, strong activation of the ESR induces Sty1-dependent Srk1 activation, Cdc25 inhibition, and cell cycle arrest (Lopez-Aviles *et al.*, 2005). The activation of Sty1/Srk1 signalling by osmotic stress can thus partially compensate for the absence of DNA damage cell cycle checkpoints (Alao *et al.*, 2010). In the absence of DNA damage, exposure to various stresses induces the rapid but temporary accumulation of mitotic and septated cells. This effect is dependent on both Sty1 and Cdc25 suggesting that these stresses advance progression through G2. Srk1 thus suppresses the positive effects of Sty1 on cell cycle progression. The elevated septation index may also reflect delayed progression through cytokinesis as a consequence of deregulated Cdc25 activity (Trautmann *et al.*, 2001; Esteban *et al.*, 2004; 2008; Mishra *et al.*, 2004; Wolfe and Gould, 2004).

Caffeine is a methylxanthine commonly found in beverages such as tea and coffee, making it one of the most widely consumed neuroactive stimulants globally (Bode

and Dong, 2007; Butt and Sultan, 2011). Caffeine exerts pleiotropic effects on cellular physiology and has generated much interest due to its ability to override DNA damage-induced cell cycle checkpoints (Moser *et al.*, 2000; Bode and Dong, 2007). Caffeine has been shown to inhibit the activity of several PIKKs including ATM, ATR and Rad3 *in vitro* (Bode and Dong, 2007). These findings lead to the proposal that caffeine inhibits cell cycle checkpoint activation mediated by Rad3 and related PIKKs *in vivo* (Bode and Dong, 2007). This view remains controversial however, as caffeine has been shown to override DDR-activated checkpoint signalling without inhibiting ATM or ATR (Cortez, 2003). Furthermore, a direct inhibition of Rad3-induced phosphorylation of Cds1 or Chk1 in *S. pombe* cells exposed to genotoxins has not been demonstrated (Moser *et al.*, 2000). Exposure to caffeine activates the Sty1-regulated ESR pathway in *S. pombe*. Furthermore, the ESR pathway is required for tolerance to caffeine in *S. pombe* (Calvo *et al.*, 2009). Consequently, caffeine is likely to exert both positive and negative influences on cell cycle progression in a Cdc25-dependent manner (Alao and Sunnerhagen, 2008). Co-inhibition of p38 MAPK downstream signalling has been shown to enhance the drug-mediated inhibition of DNA damage checkpoint signalling in mammalian cells (Manke *et al.*, 2005; Reinhardt *et al.*, 2007). It remains unclear, however, how co-activation of Sty1 signalling influences the ability of caffeine to override DNA damage-induced checkpoints and sensitivity to genotoxic agents in *S. pombe* (Moser *et al.*, 2000; Alao and Sunnerhagen, 2008; Calvo *et al.*, 2009). Exposure to caffeine has been shown induce the accumulation of Cdc25A in mammalian cells. Similarly, the inhibition of ATR-Chk1 (functional homologues of Rad3 and Cds1 in mammalian cells) signalling also induces the accumulation of Cdc25A (Sørensen *et al.*, 2003; 2004). Cdc25A degradation is required for activation of the S-phase checkpoint in mammalian cell lines. Hence, caffeine-induced stabilization of Cdc25A, rather than inhibition of ATM/ATR signalling, may underlie its ability to override DNA damage checkpoints (Cortez, 2003; Sørensen *et al.*, 2003; 2004; 2005; Mochida and Yanagida, 2006). In addition, caffeine has also been shown to induce Cdc25B accumulation in mammalian cells (Varmeh and Manfredi, 2009). The effect of exposure to caffeine or *rad3* $\Delta$ *cds1* deletion on Cdc25 stability in *S. pombe* has not been previously reported. Furthermore, the impact of caffeine-mediated Sty1 activation on its ability to override DNA damage checkpoint activation has not been investigated.

In this study, we have investigated the effect of caffeine on Cdc25 stability, cell cycle progression and DNA damage/replication checkpoint activation in *S. pombe*. We also investigated the impact of Sty1 co-activation on the ability of caffeine to override DNA damage/replication

checkpoints in this organism. Our findings demonstrate that caffeine induces Cdc25 accumulation independently of Rad3. Caffeine-induced Cdc25 accumulation was associated with delayed progression through cytokinesis. Interestingly, the ability of caffeine to override checkpoint signalling was not associated with the inhibition of Rad3. The ability of caffeine to override checkpoint signalling was dependent on Cdc25 expression. Lastly, our findings indicate that co-activation of Sty1 attenuates the ability of caffeine to override DNA damage checkpoint signalling.

## Results

### *Caffeine induces Cdc25 accumulation independently of Rad3 and Cds1*

Exposure to 10 mM caffeine resulted in rapid accumulation of HA-tagged Cdc25 under control of the endogenous promoter in log phase *S. pombe* cells (Fig. 1A). We obtained similar results by exposing cells expressing GFP-tagged Cdc25 under control of the endogenous promoter (Cdc25-GFP<sup>int</sup>) (Frazer and Young, 2011; 2012), or Myc-tagged Cdc25 under control of the endogenous promoter, to caffeine (Fig. 1B and Supplementary Fig. S1A). Caffeine also induced accumulation of Cdc25<sup>(9A)</sup>-GFP<sup>int</sup> (Frazer and Young, 2011; 2012), in which the nine N-terminal serine/threonine residues phosphorylated by Cds1, Chk1 and Srk1 are mutated to alanine (Fig. 1C). Interestingly, Cdc25 levels were also constitutively elevated in *rad3* $\Delta$  and *cds1* $\Delta$  mutants (Fig. 1D). Rad3 and Cds1 thus appear to regulate Cdc25 stability in *S. pombe* as reported for the functional homologues, ATR, Chk1 and Cdc25A in mammalian cells (Sørensen *et al.*, 2004). Caffeine also induced further accumulation of Cdc25 in *rad3* $\Delta$  mutants (Fig. 1E). The ability of caffeine to induce Cdc25 accumulation is therefore independent of Rad3 inhibition. The accumulation of Cdc25 observed in caffeine-treated cells and in *rad3* $\Delta$  and *cds1* $\Delta$  mutants was not due to enhanced transcription. In fact, *cdc25*<sup>+</sup> mRNA expression was suppressed under these conditions (Fig. 1F and Supplementary Fig. S1C). The stability of Cdc25 was increased in both *rad3* $\Delta$  and *cds1* $\Delta$  mutants (Fig. 1G and H, Supplementary Fig. S1D). Thus, caffeine or deletion of the *rad3*<sup>+</sup> or *cds1*<sup>+</sup> genes stabilizes Cdc25 by post-translational mechanisms. Caffeine suppressed Cdc2 Tyr15 phosphorylation in untreated log phase cultures, as well as in cultures exposed to hydroxyurea (HU) (Fig. 1I). These findings suggest that caffeine partly suppresses Cdc2 Tyr15 phosphorylation by stabilizing Cdc25.

### *Effect of caffeine on cell cycle progression in S. pombe*

The effect of caffeine-mediated Cdc25 accumulation and Cdc2 phosphorylation on the cell cycle kinetics of

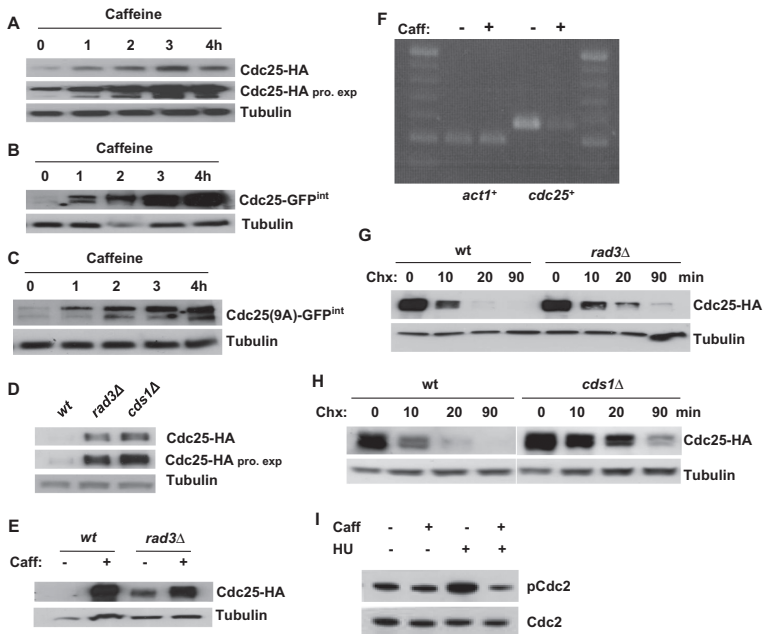


**Fig. 1.** Caffeine induces Cdc25 accumulation in *S. pombe*.

A. Strains expressing Cdc25-HA were incubated with 10 mM caffeine and harvested at the indicated time points. Total protein lysates were resolved by SDS-PAGE and Cdc25 detected using antibodies directed against HA. Tubulin was used to monitor gel loading. Pro exp. = prolonged exposure.

B and C. Strains expressing Cdc25-GFP<sup>int</sup> or Cdc25<sup>(9A)</sup>-GFP<sup>int</sup> were treated as in A.

D. Total protein lysates from log phase wt, *rad3Δ* and *cds1Δ* cultures were resolved by SDS-PAGE and probed using antibodies directed against HA. Tubulin was used to monitor gel loading. Pro exp. = prolonged exposure.

E. Wt and *rad3Δ* strains were grown with or without 10 mM caffeine for 24 h and analysed as in D.

F. Total RNA was extracted from wt cells exposed to 10 mM caffeine for 2 h. The expression levels of *cdc25+* were analysed by RT-PCR.

G. Wt and *rad3Δ* cells expressing Cdc25-HA were grown to log phase, exposed to 100  $\mu\text{g ml}^{-1}$  Chx and harvested at the indicated time points. Cell lysates were treated as in A.

H. Wt and *cds1Δ* cells expressing Cdc25-HA were grown to log phase and treated as in G.

I. Cells expressing HA-tagged Chk1 were exposed to 20 mM HU with or without 10 mM caffeine. Cells were pre-treated with HU for 2 h and then cultured with or without caffeine for a further 2 h. Total lysates were probed with antibodies directed against phosphorylated and total Cdc2.

*S. pombe* was investigated. Exposure of wt log phase cultures to 10 mM caffeine did not significantly affect cell division kinetics (Fig. 2A). However, exposure of *cds1Δ* mutants to caffeine did induce a significant increase in the percentage of septating cells within 1 h of exposure, followed by a transient decline in the septation index between 3 and 4 h after exposure (Fig. 2A). A similar increase in the septation index was observed when *rad3Δ* mutants were exposed to caffeine. In contrast to *cds1Δ* mutants however, the caffeine-induced increase in the septation index was sustained (Fig. 2A). Caffeine induces the accumulation of Cdc25 independently of Rad3 (Fig. 1). The suppression of Cdc2 activity is required for exiting mitosis and progression through cytokinesis. Modest increases in Cdc25 activity

will thus drive cells through mitosis and cytokinesis. In contrast, high levels of Cdc25 activity will advance entry into mitosis but delay progression through cytokinesis (Trautmann *et al.*, 2001; Esteban *et al.*, 2004; 2008; Mishra *et al.*, 2004; Wolfe and Gould, 2004). To test this possibility, FACS analysis was used to monitor the progression through cytokinesis of cells exposed simultaneously to caffeine and HU. As the cells pass through cytokinesis, they accumulate as a 1C population due to HU-induced nucleotide depletion (Fig. 2B). When *rad3Δ* mutants were exposed to caffeine, their progression through cytokinesis was clearly delayed relative to the wt strain (Fig. 2A and B). Consistent with the results in Fig. 2A, *cds1Δ* mutants were advanced through both mitosis and cytokinesis (Fig. 2B).

We also observed that caffeine influenced cell cycle progression to a similar degree in strains expressing Cdc25–GFP<sup>int</sup> or Cdc25<sup>(9A)</sup>–GFP<sup>int</sup> (Supplementary Fig. S3A). Further analyses demonstrated a simultaneous increase in both the number of binucleates and the septation index (Supplementary Fig. S2C). These observations suggest a general decrease in the progression from mitosis and cytokinesis in these strains following exposure to caffeine.

To further examine the effect of caffeine on cell cycle progression, we monitored its effects on the kinetics of cell division in *wee1Δ* mutants. The absence of Wee1 results in constitutively high Cdc2 activity that advances the entry of shortened cells into mitosis (Russell and Nurse, 1987). The effect of caffeine on the septation index of *wee1Δ* mutants was similar to that observed in *rad3Δ* mutants (Fig. 2A and C). The short length at division of *wee1Δ* mutants imposes a size constraint that delays progression into S phase (Nurse, 1990). Unlike wt cells in log phase, *wee1Δ* mutants spend a significantly longer amount of time in G1 and can be monitored by FACS analysis (Fig. 2D). Hence, although a G1 population is not detectable in wt cells under normal growth conditions, *wee1Δ* mutants can be used to monitor G1- to S-phase progression. Exposure to caffeine induced a rapid decline in the G1 population of *wee1Δ* mutants 1–2 h after exposure following by a gradual increase at 3–4 h (Fig. 2D). Caffeine thus induces cell cycle progression in *S. pombe wee1Δ* mutants.

To determine if caffeine delays progression through cytokinesis, its effect on cell division in *nda3-KM311<sup>CS</sup>* mutants was examined. The *S. pombe nda3<sup>+</sup>* gene encodes β-tubulin, which is unable to polymerize into microtubules at the restrictive temperature (18–20°C) in *nda3-KM311<sup>CS</sup>* mutants. The failure to form mitotic spindles at the restrictive temperature prevents ‘satisfaction’ of the spindle checkpoint and results in metaphase arrest (Hiraoka *et al.*, 1984). Mutants lacking *mad2<sup>+</sup>* are unable to activate the spindle checkpoint and attempt mitosis without mitotic spindles, resulting in chromosome missegregation and loss of viability (Fig. 2E–G; He *et al.*, 1997). Caffeine (10 mM) prevented chromosome missegregation and loss of viability in *mad2Δ* mutants grown at the restrictive temperature. Caffeine similarly suppressed the sensitivity of *mad2Δ* mutants to the microtubule depolymerizing agent methylbenzimidazol-2-yl carbamate (carbendazim/MBC) (Fig. 2E). As a culture of *nda3-KM311<sup>CS</sup>* mutants arrests in metaphase at the restrictive temperature, a corresponding decrease in the septation index can be observed. This decline in the septation index was not observed in *nda3-KM311<sup>CS</sup> mad2Δ* double mutants, which continue to progress through mitosis (Fig. 2G) (Hiraoka *et al.*, 1984; He *et al.*, 1997). Caffeine abolished this decline in the septation index in the *nda3-KM311<sup>CS</sup>* mutant, suggesting it either overrides the

spindle checkpoint or delays the progression of septating cells through cytokinesis (Fig. 2G). Our finding that caffeine prevents chromosome missegregation and loss of viability in *mad2Δ* mutants clearly supports the latter explanation (Fig. 2E–G). A similar delay in the progression through cytokinesis was observed in *nda3-KM311<sup>CS</sup> clp1Δ* and *nda3-KM311<sup>CS</sup> pub1Δ* mutants, which harbour elevated Cdc25 levels, when grown at the restrictive temperature (Supplementary Fig. S2D and E). Caffeine thus exerts both positive and negative effects on cell cycle progression in *S. pombe*.

#### *Mad2 delays caffeine-induced cell cycle progression in S. pombe*

Exposure to caffeine activates the ESR pathway regulated through the MAPK Sty1 (Calvo *et al.*, 2009). We previously demonstrated that exposure to osmotic stress, which similarly activates Sty1, partially delays progression through mitosis in a Mad2-dependent manner (Alao *et al.*, 2010). The effect of Mad2 on caffeine-induced cell cycle progression was thus investigated. *S. pombe* cells partially delay progression through mitosis following exposure to the microtubule depolymerizing agent MBC (50 μg ml<sup>-1</sup>) in a Mad2-dependent manner (He *et al.*, 1997; Castagnetti *et al.*, 2010) (Fig. 3A and B). Caffeine (10 mM) suppressed MBC-induced chromosome missegregation. *mad2<sup>+</sup>* cells exposed to MBC and caffeine had a 4C DNA content, indicating that caffeine delays progression through cytokinesis (Fig. 3A). The rate and magnitude of MBC-induced chromosome missegregation was greater in *mad2Δ* mutants relative to *mad2<sup>+</sup>* cells (Fig. 3A and B). Caffeine suppressed chromosome missegregation less efficiently in *mad2Δ* mutants although DNA replication was not delayed (Fig. 3A and B). Cell cycle progression, as indicated by the increased 4C DNA content, was also advanced in *mad2Δ* mutants relative to *mad2<sup>+</sup>* cells exposed to caffeine alone (Fig. 3A and B).

We next compared the rate of cell cycle progression in wt and *mad2Δ* mutants arrested with 20 mM HU for 2 h and subsequently exposed to 10 mM caffeine. The rate and degree of chromosome missegregation was slightly higher in *mad2Δ* mutants relative to wt cells (Fig. 3C). Furthermore, caffeine was more effective at enhancing sensitivity to HU in *mad2Δ* mutants (Fig. 3D). The ability of caffeine to override the HU induced replication (S-M) checkpoint is thus enhanced by the *mad2* deletion. Together, these observations suggest that Mad2 attenuates the ability of caffeine to advance cell cycle progression. They also provide further evidence that caffeine can advance entry into mitosis but slows progression through cytokinesis. Concurrently, caffeine partly compensates for the lack of a spindle checkpoint by delaying progression through cytokinesis (Figs 2E–G and 3A–D).

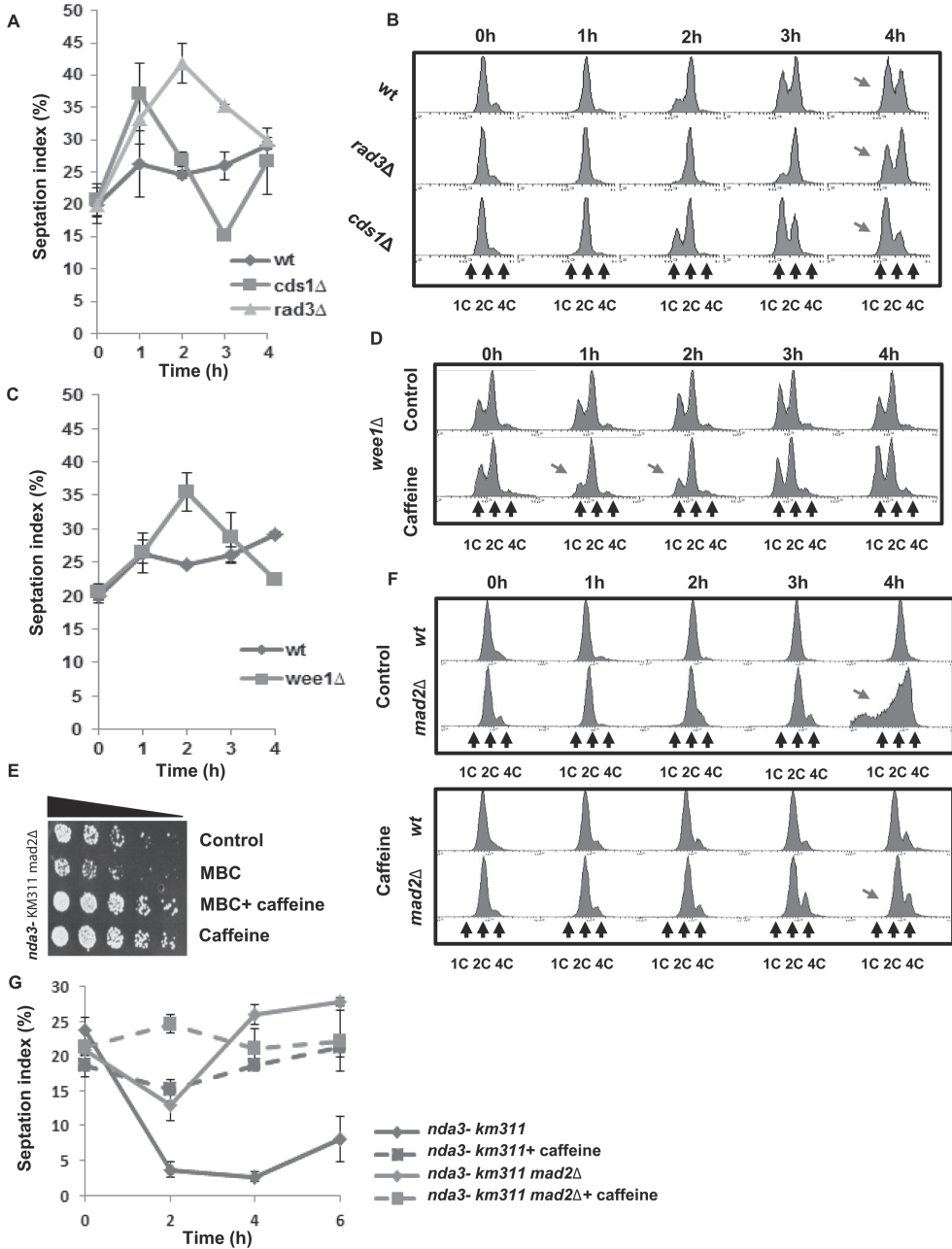




**Fig. 2.** Caffeine modulates cell progression in *S. pombe*.

A. Wt, *rad3Δ*, and *cds1Δ* strains were exposed to 10 mM caffeine. Samples were harvested at the indicated time points and fixed in 70% ethanol. Cells were stained with aniline blue and the septation index determined by fluorescence microscopy. At least 200 cells were counted for each time point. Error bars represent the mean of at least three independent experiments  $\pm$  S.E.

B. Wt, *rad3Δ*, and *cds1Δ* strains were simultaneously exposed to 20 mM HU and 10 mM caffeine. Samples were harvested at the indicated time points, fixed in 70% ethanol and analysed by FACS. Arrows indicate differential rates of cell cycle progression.

C and D. *wee1Δ* mutants were treated as in A and B. Arrows indicate differential rates of cell cycle progression. Wt septation index from A was included for clarity.

E. *nda3-KM311 mad2Δ* mutants were incubated at 18°C untreated (Control), treated with 50  $\mu\text{g ml}^{-1}$  MBC, 50  $\mu\text{g ml}^{-1}$  MBC and 10 mM caffeine, or 10 mM caffeine for 4 h. Equal cell numbers were spotted onto YES agar plates and incubated for 3 days.

F. *nda3-KM311* and *nda3-KM311 mad2Δ* mutants were incubated at 18°C in the absence (top panel) or presence (bottom panel) of 10 mM caffeine. Samples were harvested at the indicated time points and analysed by FACS.

G. *nda3-KM311* and *nda3-KM311 mad2Δ* were treated as in F. Samples were harvested at the indicated time points and fixed in 70% ethanol. Cells were stained with aniline blue and the septation index determined by fluorescence microscopy. At least 200 cells were counted for each time point. Error bars represent the mean of at least three independent experiments  $\pm$  S.E.

### Caffeine advances cell cycle progression through Cdc25

The *cdc2-3w* allele abolishes the requirement for Cdc25-mediated entry into mitosis and activation of the replication checkpoint. Mutants carrying the *cdc2-3w* allele remain under the control of Wee1 phosphorylation and deletion of Cdc25 results in increased cell length (Enoch *et al.*, 1992; Basi and Enoch, 1996) (Fig. 4A). To further investigate the role of Cdc25 in mediating the effects of caffeine, we compared its impact on cell cycle progression in *cdc2-3w* and *cdc2-3w cdc25Δ* mutants. Exposure of *cdc2-3w* mutants to 10 mM caffeine induced the sustained accumulation of septated cells with a 4C DNA content. In contrast, caffeine exerted only minor effects on cell cycle progression in *cdc2-3w cdc25Δ* mutants (Fig. 4B and C). A simultaneous increase in both the number of binucleates and the septation index was observed (Supplementary Fig. S4B). It remains unclear if the slight increase in the > 4C DNA peak reflects a delay in the cell cycle progression of the *cdc2-3w cdc25Δ* mutant. Exposure of *cdc2-3w* mutants to caffeine in the presence of latrunculin B (Lat B) (in order to inhibit cytokinesis), demonstrated that progression through mitosis and the subsequent S phase was only moderately delayed (Supplementary Fig. S4C). Caffeine thus delays progression through cytokinesis in *cdc2-3w* mutants. In contrast, caffeine did inhibit mitotic progression in *cdc2-3w cdc25Δ* mutants under similar conditions (Supplementary Fig. S4C). We next compared the ability of caffeine to enhance sensitivity to phleomycin in *cdc2-3w* and *cdc2-3w cdc25Δ* mutants. Caffeine overrode the partial checkpoint arrest in *cdc2-3w* mutants exposed to 10  $\mu\text{g ml}^{-1}$  phleomycin, resulting in the accumulation of cells with missegregated chromosomes (Fig. 4D). In *cdc2-3w cdc25Δ* mutants, caffeine blocked the phleomycin-induced increase of the septation index (Fig. 4E). Interestingly, *cdc2-3w cdc25Δ* but not *cdc2-3w* mutants became elongated following exposure to caffeine (Fig. 4A and Supplementary Fig. S4A). These observations suggested that caffeine inhibits cell cycle progression in the absence of Cdc25. To test this possibility, we compared the effect of caffeine on HU sensitivity in *cdc2-3w*

and *cdc2-3w cdc25Δ* mutants. Co-exposure to 10 mM caffeine did not further enhance the sensitivity of *cdc2-3w* mutants to 20 mM HU (Fig. 4F). In marked contrast, caffeine significantly suppressed the sensitivity of *cdc2-3w cdc25Δ* mutants to HU (Fig. 4F). Furthermore, exposure to 10 mM caffeine induced Cdc2 Tyr15 dephosphorylation in *cdc2-3w* but not *cdc2-3w cdc25Δ* mutants (Fig. 4G). These findings indicate that Cdc25 mediates the ability of caffeine to promote cell cycle progression. Our findings demonstrate that caffeine exerts positive and negative effects on cell cycle progression. In the absence of Cdc25, the negative effects predominate and thus slow progression through the cell cycle. Consequently, caffeine exerts opposing effects on cell cycle progression in *cdc2-3w* and *cdc2-3w cdc25Δ* mutants.

### Srk1 counteracts the ability of caffeine to override the replication checkpoint

The ability of caffeine to override cell cycle checkpoints is dependent on Cdc25. However, exposure to caffeine also activates Sty1 which delays cell cycle progression by inducing and stabilizing the Srk1 kinase (Calvo *et al.*, 2009) (Supplementary Fig. S5A and B). Srk1 regulates entry into mitosis by negatively regulating Cdc25 activity during the normal cell cycle and following activation of the ESR (Smith *et al.*, 2002; Lopez-Aviles *et al.*, 2005; Alao *et al.*, 2010). Co-activation of Srk1 may thus inhibit the ability of caffeine to override cell cycle checkpoints. Hence, we investigated the ability of Srk1 to attenuate the ability of caffeine to override the replication and DNA damage checkpoints. As previously reported, caffeine overrides the HU-induced replication checkpoint in *S. pombe* (Wang *et al.*, 1999; Moser *et al.*, 2000) (Fig. 5A). Wt cells and *srk1Δ* mutants were exposed to 20 mM HU for 2 h and then incubated for a further 4 h in the absence or presence of 10 mM caffeine. Under these conditions, wt cells attempt mitosis with incompletely replicated DNA resulting in chromosome missegregation and a loss of viability (Wang *et al.*, 1999; Moser *et al.*, 2000) (Fig. 5A–C). Remarkably,

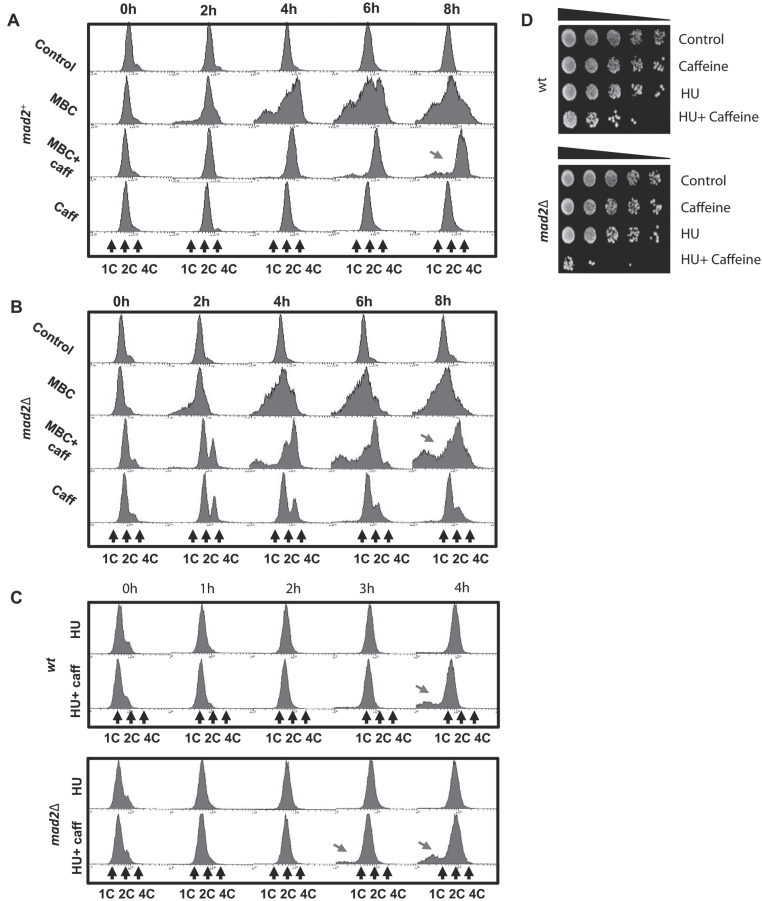


**Fig. 3.** Mad2 attenuates the effect of caffeine on the cell cycle progression.

A and B. *nda3-KM311* and *nda3-KM311 mad2Δ* strains were incubated at 30°C in the presence of 50  $\mu\text{g ml}^{-1}$  MBC or 10 mM caffeine alone or in combination. Samples were harvested at the indicated time points and analysed by FACS. Arrows indicate differential rates of cell cycle progression.

C. Wt and *mad2Δ* mutants were incubated for 2 h with 20 mM HU (0–2 h) and then incubated for a further 2 h (2–4 h) in the presence or absence of 10 mM caffeine. Samples were treated as in A. Arrows indicate differential rates of cell cycle progression.

D. Wt and *mad2Δ* strains were incubated with 20 mM HU alone or in combination with 10 mM caffeine at 30°C for 8 h. Equal cell numbers were spotted onto YES agar plates and incubated at 30°C for 3 days.

the ability of caffeine to override the replication checkpoint was greatly enhanced in *srk1Δ* mutants (Fig. 5A–C). Caffeine also induced *Srk1* accumulation in the presence of HU (Supplementary Fig. S2B). The percentage of septated cells was higher in *srk1Δ* mutants relative to wt cells, suggesting an increased rate of progression through mitosis (Fig. 5A). The rate and degree of chromosome missegregation was also higher in *srk1Δ* mutants. The ability of caffeine to enhance sensitivity to HU was also elevated in *srk1Δ* mutants relative to wt cells (Fig. 5B and

C). We cannot rule out, however, that elevated Cdc25 activity in the *srk1Δ* mutants also delays progression through cytokinesis and thus an increase in the septation index (Supplementary Fig. S5C).

Interestingly, the cell length at division in *srk1Δ* mutants exposed to HU and caffeine was longer than that of wt cells, as opposed to the situation in unexposed cells when *srk1Δ* mutants are slightly shorter (Fig. 5D and E). In *S. pombe*, the timing of mitosis is determined by cell length (Nurse, 1975; Russell and Nurse, 1987). Given the

faster rate of cell cycle progression observed in *srk1Δ* mutants, this seemed counterintuitive. Previous studies have demonstrated that *Srk1* stabilizes Cdc25 levels in *S. pombe* (Lopez-Aviles *et al.*, 2005). Mutants lacking *Srk1* may thus proceed initially from G2 into mitosis more slowly than wt cells when exposed to caffeine in the presence of HU as Cdc25 accumulates.

#### Caffeine mediates checkpoint override by stabilizing Cdc25

Our findings on the differential impact of caffeine on cell cycle progression in *cdc2-3w* and *cdc2-3w cdc25Δ* mutants suggested a central role for Cdc25 in mediating these effects. The theory that caffeine overrides cell cycle checkpoints by inhibiting the ATM/Rad3-mediated phosphorylation of downstream targets remains controversial (Cortez, 2003). Furthermore, a direct inhibition of the Rad3-mediated phosphorylation of Cds1 or Chk1 in *S. pombe* has not been demonstrated (Wang *et al.*, 1999; Moser *et al.*, 2000). We thus re-examined the effect of caffeine on Rad3-mediated signalling following exposure to HU or phleomycin. Interestingly, 10 mM caffeine did not abolish Chk1 phosphorylation in *S. pombe* cells exposed to 10 μg ml<sup>-1</sup> phleomycin, whereas *rad3Δ* deletion completely abolished phleomycin-induced Chk1 phosphorylation, as expected (Fig. 6A). Similarly, 10 mM caffeine did not inhibit Cds1 phosphorylation following exposure to 20 mM HU (Fig. 6B). Phosphatase treatment of immunoprecipitated HA-tagged Cds1 demonstrated that the kinase is constitutively phosphorylated in log-phase cells (Fig. 6C and Supplementary Fig. S6A). This phosphorylation was not abolished in *rad3Δ* mutants although an increase in the levels of hypo-phosphorylated Cds1 was clearly detectable (Fig. 6C). Prolonged exposure (24 h) to 10 mM caffeine resulted in a pronounced increase of both Cds1 isoforms in both wt and *rad3Δ* mutants (Fig. 6C). Hence, caffeine does not inhibit Cds1 phosphorylation and induces its accumulation independently of Rad3. Similar results were observed with Chk1 in wt and *rad3Δ* cells (Supplementary Fig. S6B).

Caffeine stabilizes Cdc25 in *S. pombe* (Fig. 1). Since caffeine appeared not to inhibit Rad3 signalling (Fig. 6A–C), we hypothesized that caffeine might induce Cdc25 levels above the threshold required to maintain checkpoint activation. The levels of Cdc25 in cells co-exposed to 20 mM HU and 10 mM caffeine were higher than in cultures exposed to either agent alone (Fig. 6D and Supplementary Fig. S6C). We next compared the effect of caffeine on replication checkpoint activation in strains expressing Cdc25–GFP<sup>int</sup> and Cdc25<sup>(9A)</sup>–GFP<sup>int</sup> (Frazer and Young, 2011; 2012) (Supplementary Fig. S6D) expressing strains. Both strains were incubated with 20 mM HU for 2 h, exposed to 10 mM caffeine and the

kinetics of cell cycle progression investigated. The ability of caffeine to override the replication checkpoint in Cdc25<sup>(9A)</sup>–GFP<sup>int</sup> cultures was modestly enhanced relative to Cdc25–GFP<sup>int</sup> as measured by cell cycle progression (Fig. 6H), but barely as measured by cell survival (Fig. 6E). The rate of mitotic progression and septation index were also higher in Cdc25<sup>(9A)</sup>–GFP<sup>int</sup> cells exposed to HU and caffeine (Fig. 6F). These results were similar to those observed in experiments using *srk1Δ* mutants (Fig. 5A–C). The sensitivity to HU and degree of chromosome missegregation in Cdc25<sup>(9A)</sup>–GFP<sup>int</sup> mutants in the presence of caffeine was also greater than observed in Cdc25–GFP<sup>int</sup> cells (Fig. 6E and H). In contrast, when Cdc25–GFP<sup>int</sup> and Cdc25<sup>(9A)</sup>–GFP<sup>int</sup> cells were grown in 20 mM HU for 4 h and then transferred into fresh rich media, no difference in the kinetics of cell cycle re-entry was observed (Fig. 6G).

On exposure to 20 mM HU, Cdc25–GFP<sup>int</sup> becomes phosphorylated, is exported from the nucleus and accumulates (stockpiles) in the cytoplasm. In contrast, Cdc25<sup>(9A)</sup>–GFP<sup>int</sup> cannot be phosphorylated and is degraded within the nucleus (Frazer and Young, 2011; 2012) (Fig. 7A and B). Co-exposure to 10 mM caffeine suppressed the accumulation of Cdc25–GFP<sup>int</sup> (Fig. 7A). In contrast, co-exposure to caffeine clearly induced the accumulation of Cdc25<sup>(9A)</sup>–GFP<sup>int</sup>. Caffeine similarly suppressed the degradation of Cdc25<sup>(9A)</sup>–GFP<sup>int</sup> in cells exposed to 10 μg ml<sup>-1</sup> phleomycin (Fig. 7C). Microscopic analyses of Cdc25–GFP<sup>int</sup> and Cdc25<sup>(9A)</sup>–GFP<sup>int</sup> expressing strains, demonstrated increased nuclear levels of Cdc25–GFP in cells co-exposed to HU and caffeine relative to cells exposed to HU alone (Fig. 7E and F). The ability of caffeine to override checkpoint signalling was cAMP independent, as *pka1Δ* mutants, which lack the catalytic subunit of protein kinase A, are sensitized to HU by caffeine (Supplementary Fig. S6E). Similarly, Mik1 was not required for the effect of caffeine on DNA damage checkpoints (Supplementary Fig. S6E). Caffeine thus appears to stabilize Cdc25 by suppressing the rate of its degradation within the nucleus. Indeed, the Cdc25–GFP in cells exposed to HU alone appeared to be more stable than Cdc25–GFP co-exposed to HU and caffeine (Fig. 7A). These observations suggest that caffeine interferes with both the nuclear export and degradation of Cdc25. This may explain the failure of caffeine to induce Cdc25–GFP<sup>int</sup> accumulation in the presence of HU (Fig. 7A). Together these findings provide further evidence that caffeine overrides cell cycle checkpoints by inducing the nuclear accumulation of Cdc25.

## Discussion

In the current study, we have investigated the effect of caffeine on Cdc25 stability and its impact on the cell cycle

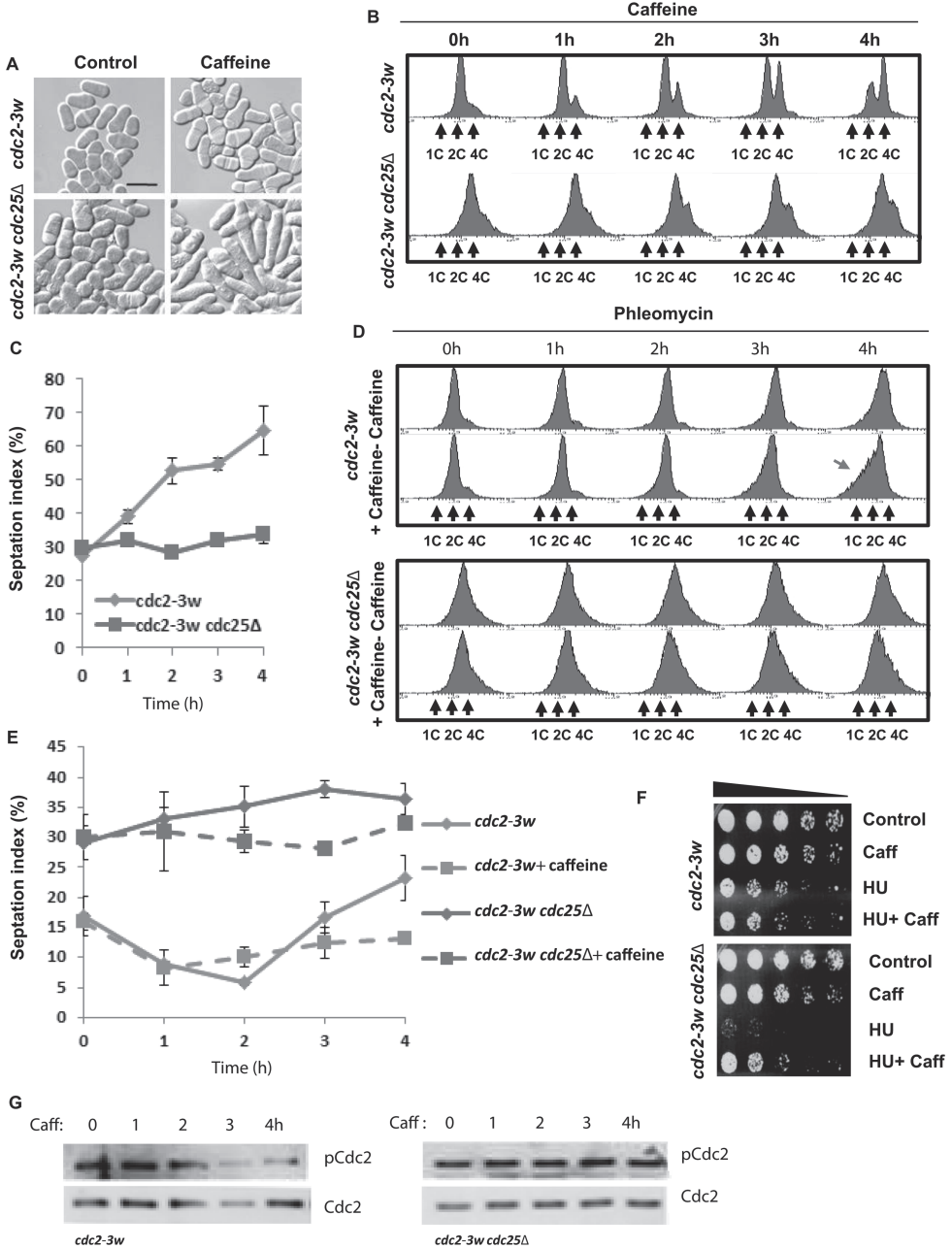


**Fig. 4.** Caffeine promotes cell cycle progression in a Cdc25-dependent manner.

- A. *cdc2-3w* and *cdc2-3w cdc25Δ* strains were incubated with 10 mM caffeine for 4 h, fixed in 70% ethanol. Scale bar, 20 μM.  
 B. *cdc2-3w* and *cdc2-3w cdc25Δ* strains were incubated with 10 mM caffeine. Samples were harvested at the indicated time points and analysed by FACS.  
 C. Strains in B were stained with aniline blue and the septation index determined by fluorescence microscopy. At least 200 cells were counted for each time point. Error bars represent the mean of at least three independent experiments ± S.E.  
 D. *cdc2-3w* and *cdc2-3w cdc25Δ* strains were incubated with 10 μg ml<sup>-1</sup> phleomycin alone or in combination with 10 mM caffeine. Samples were harvested at the indicated time points and analysed by FACS. Red arrow indicates chromosome missegregation.  
 E. *cdc2-3w* and *cdc2-3w cdc25Δ* strains were incubated with 10 μg ml<sup>-1</sup> phleomycin alone or in combination with 10 mM caffeine. Samples harvested at the indicated time points were stained with aniline blue and the septation index determined by fluorescence microscopy. Error bars represent the mean of at least three independent experiments ± S.E.  
 F. *cdc2-3w* and *cdc2-3w cdc25Δ* strains were incubated for 3 h with 20 mM HU and then incubated for a further 3 h in the presence or absence of 10 mM caffeine. Equal cell numbers were spotted onto YES agar plates and incubated at 30°C for 3 days.  
 G. *cdc2-3w* and *cdc2-3w cdc25Δ* strains were incubated with 10 mM caffeine and harvested at the indicated time points. Total lysates were probed with antibodies directed against phosphorylated and total Cdc2.

kinetics of *S. pombe*. Caffeine has generated much interest due to its ability to override checkpoint signalling in both yeast and mammalian cells (Bode and Dong, 2007). Previous studies in *S. pombe* and mammalian cells have proposed that caffeine overrides checkpoint signalling by inhibiting Rad3 and its mammalian homologues ATM and ATR (Wang *et al.*, 1999; Moser *et al.*, 2000; Zhou *et al.*, 2000). The assertion that caffeine overrides checkpoint signalling by inhibiting Rad3 or ATM and ATR remains controversial. Caffeine has been shown to override checkpoint signalling without inhibiting ATM or ATR in mammalian cells (Cortez, 2003). Caffeine has previously been reported to stabilize Cdc25A in mammalian cells. This study also demonstrated the constitutive regulation of Cdc25A by ATR and Chk1 (Sørensen *et al.*, 2004). Herein, we have demonstrated for the first time that caffeine stabilizes Cdc25 in *S. pombe* independently of Rad3 and Cds1 (a functional homologue of mammalian Chk1). A recent study reported that caffeine induces Sty1 activation in *S. pombe* (Calvo *et al.*, 2009). Sty1 regulates Cdc25 stability and activity (Shiozaki and Russell, 1995; Kishimoto and Yamashita, 2000; Lopez-Aviles *et al.*, 2005) but the impact of this activity on caffeine-induced checkpoint override has not been previously reported. Herein we have demonstrated that Sty1 and Mad2 attenuate the ability of caffeine to override checkpoint signalling. The current model of caffeine-induced checkpoint override thus needs to be modified to include its effects on Cdc25 stability and activity.

#### Effect of caffeine on Cdc25 stability

Exposure to caffeine resulted in rapid accumulation of Cdc25 in *S. pombe*. In mammalian cells, caffeine or the inhibition of ATR-Chk1 signalling has similarly been shown to induce the stabilization of Cdc25A. Caffeine has similarly been shown to stabilize Cdc25B in mammalian cells (Varmeh and Manfredi, 2009). Furthermore, Chk1 has been shown to regulate Cdc25A activity and mitotic entry even during the normal cell cycle (Shiromizu *et al.*, 2006;

Enomoto *et al.*, 2009; Matsuyama *et al.*, 2011). Our findings demonstrate that *rad3* or *cds1* deletion similarly stabilizes Cdc25 in *S. pombe*. Interestingly, caffeine stabilized Cdc25 in both *rad3* and *cds1* mutants, demonstrating that this stabilization is not due to the inhibition of Rad3 signalling. The levels of *cdc25<sup>+</sup>* mRNA were suppressed in caffeine treated wt cells as well as in *rad3* and *cds1* mutants. Exposure to caffeine or the deletion of *rad3<sup>+</sup>* (or *cds1<sup>+</sup>*) thus stabilizes Cdc25 at the post-translational level, albeit by different mechanisms. In *S. pombe*, Cdc25 degradation is mediated by Pub1 and the anaphase-promoting complex/cyclosome (APC/C). Furthermore, the Clp1-mediated dephosphorylation of Cdc25 is required for its rapid degradation as cells exit mitosis (Wolfe and Gould, 2004; Esteban *et al.*, 2008). Caffeine may thus interfere with any of these pathways. Recent studies have demonstrated that the accumulation of Cdc25 does not affect cell size in *S. pombe* (Frazer and Young, 2011; 2012). In our studies, the accumulation of Cdc25 in response to caffeine exposure or deletion of *rad3<sup>+</sup>* (or *cds1<sup>+</sup>*) was likewise not associated with reduced cell size. Mutant isoforms of Cdc25 (Cdc25<sup>(9A)</sup>-GFP<sup>int</sup>) that cannot be phosphorylated are unstable and degraded in a Mik1-dependent manner following activation of the replication or G2 checkpoints (Frazer and Young, 2011; 2012). Caffeine induced Cdc25<sup>(9A)</sup>-GFP<sup>int</sup> accumulation both in untreated cells and in cells exposed to HU or phleomycin. Our findings suggest that caffeine attenuates the nuclear degradation of Cdc25 in *S. pombe*. Previous findings have shown that Pub1 does not mediate the ubiquitin-dependent degradation of nuclear Cdc25-GFP (Frazer and Young, 2012). The effect of caffeine on Cdc25 stability is thus unlikely to result from the inhibition of Pub1 activity. The APC/C is also believed to mediate the degradation of Cdc25 as cells exit mitosis, and its Clp1-mediated dephosphorylation during exit from mitosis is required for its rapid degradation. The levels of Cdc25 remain elevated in actively growing *S. pombe* cultures exposed to caffeine. Furthermore, Cdc25 is detectable in stationary-phase cells previously exposed to caffeine but not in untreated cultures. These observations

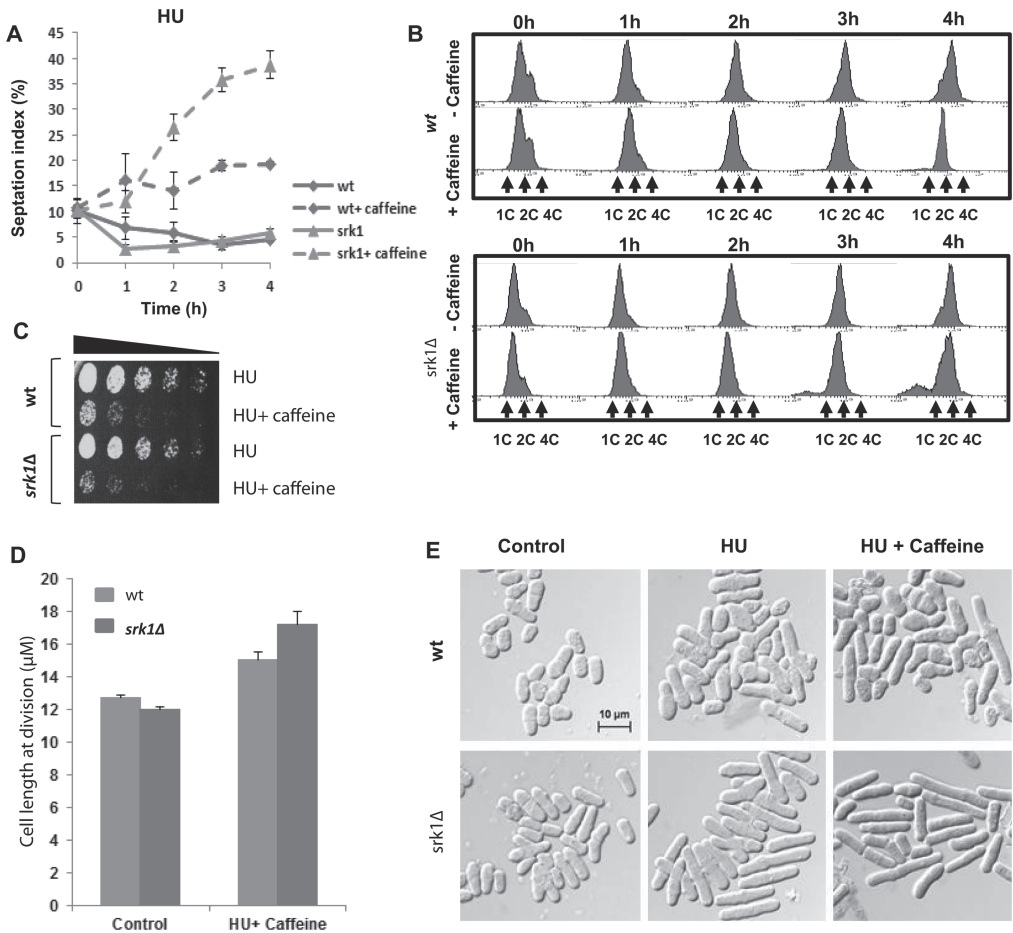


**Fig. 5.** Srk1 suppresses caffeine-induced checkpoint override.

A. Wt and *srk1Δ* strains were incubated with 20 mM HU for 2 h and then for a further 4 h in the presence or absence of 10 mM caffeine. Samples harvested at the indicated time points were stained with aniline blue and the septation index determined by fluorescence microscopy. Error bars represent the mean of at least three independent experiments  $\pm$  S.E.

B. Samples from A were analysed by FACS.

C. Wt and *srk1Δ* strains were incubated with 20 mM HU for 4 h in the presence or absence of 10 mM caffeine. Equal cell numbers were spotted onto YES agar plates and incubated at 30°C for 3 days.

D. Wt and *srk1Δ* strains were incubated with 20 mM HU for 2 h and then for a further 2 h in the presence of 10 mM caffeine. Cell length at division was determined by microscopy. At least 30 cells were counted for each sample.

E. Wt and *srk1Δ* strains were incubated with 20 mM HU for 2 h and then for a further 2 h in the presence or absence of 10 mM caffeine. Cells were fixed in 70% ethanol and examined by microscopy. Scale bar, 10  $\mu$ m.

suggest that caffeine interferes with the degradation of Cdc25 during mitosis. Caffeine may thus interfere with APC/C-mediated Cdc25 degradation. Alternatively, caffeine may stabilize Cdc25 by inhibiting its dephosphorylation. Future studies will address the roles of Rad3 and Cds1 in regulating Cdc25 stability in normally cycling cells.

#### Effect of caffeine on cell cycle kinetics

We have noted with interest that the precise effect of caffeine on the cell cycle kinetics of *S. pombe* is strongly influenced by mutations that positively affect Cdc2 activity. On entry into mitosis, the suppression of Cdc25 and Cdc2



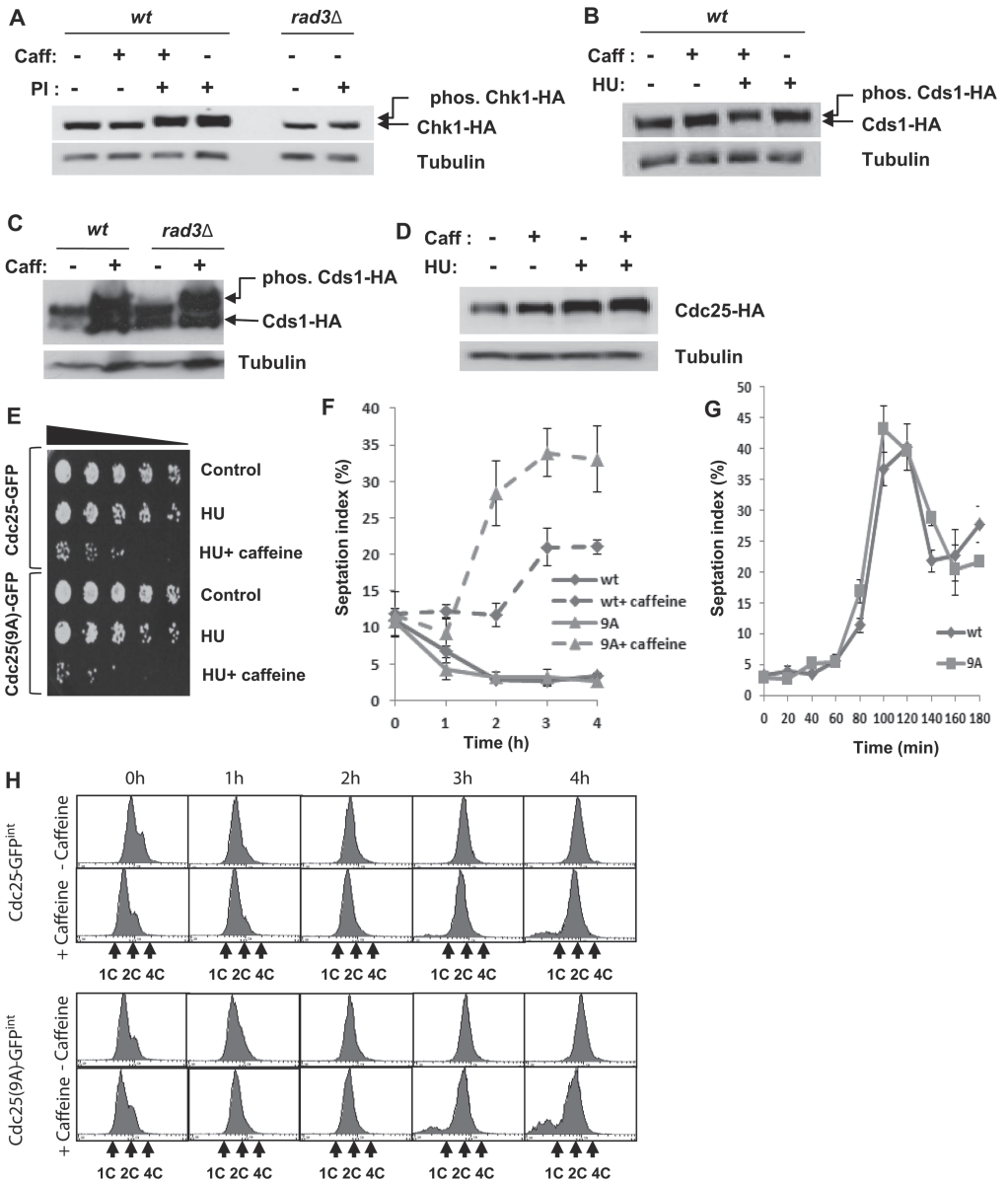
activity is required for mitotic exit and progression through cytokinesis (Wolfe and Gould, 2004; Esteban *et al.*, 2008). Exposure to caffeine induced Cdc25 accumulation and a significant reduction in the level of Cdc2 Tyr15 phosphorylation even in normally cycling cells (Fig. 11). The minimal effect of caffeine on the cell cycle kinetics of wt cells was likely due to the cells' ability to counteract the increase in Cdc25 activity. Our findings demonstrate for instance that Rad3 and Cds1 negatively regulate Cdc25 stability during the normal cell cycle. Furthermore, the positive effects of caffeine-induced Sty1 activation on Cdc25 activity and cell cycle progression are countered by the simultaneous activation of Srk1 (reviewed in Alao and Sunnerhagen, 2008). Accordingly, exposure to caffeine substantially influenced the rate of cell cycle progression in *cdc2-3w*, *cds1Δ*, *rad3Δ*, *srk1Δ* and *wee1Δ* mutants (Figs 2, 4 and 5). These mutants are unable to effectively negatively regulate Cdc2 activity. Exposure of *wee1Δ* mutants to caffeine clearly promoted progression through S phase, indicating that caffeine can positively influence cell cycle progression. Exposure of *cdc2-3w*, *cds1Δ* and *rad3Δ* mutants to caffeine was also associated with a rapid increase in the population of septating cells. Recent studies have demonstrated that the activity and localization, rather than its expression level, determine the ability of Cdc25 to promote entry into mitosis (Frazer and Young, 2011; 2012). The precise impact of caffeine-induced Cdc25 accumulation on cell cycle progression is thus influenced by the genetic background of the exposed strain. Caffeine-induced Cdc25 accumulation likely advances entry into mitosis but delays progression through cytokinesis as a consequence (Wolfe and Gould, 2004; Esteban *et al.*, 2008). Careful analyses of the effects of caffeine on cell cycle progression in these mutants demonstrated that caffeine indeed delays progression through mitosis and cytokinesis. Crucially, Cdc25 expression was required for cell cycle progression in the presence of caffeine. Activation of the *cdc2-3w* allele occurs independently of Cdc25 but is still subject to negative regulation by Wee1. Cdc25 thus continues to influence cell cycle progression in *cdc2-3w* mutants (Enoch *et al.*, 1992; Basi and Enoch, 1996). Exposure of *cdc2-3w* mutants to caffeine was associated with a decreased rate of progression through mitosis. In contrast, cell cycle progression was inhibited when *cdc2-3w cdc25Δ* mutants were exposed to caffeine. We also observed that exposure to caffeine suppressed Tyr15 phosphorylation on Cdc2 in *cdc2-3w* but not *cdc2-3w cdc25Δ* mutants. Our study demonstrates that caffeine positively modulates cell cycle progression by inducing Cdc25 accumulation. Consequently, caffeine delays cell cycle progression and enhances resistance to HU in *cdc2-3w cdc25Δ* mutants. This effect on cell cycle progression is however strongly attenuated in wt cells exposed to caffeine under normal conditions.

#### *Caffeine modulates spindle checkpoint activation*

Exposure to caffeine suppressed the requirement for the spindle checkpoint in wt and *mad2Δ* mutants following microtubule depolymerization. Cell cycle analyses demonstrated that caffeine delays progression through cytokinesis thus delaying the chromosome missegregation that would otherwise occur. Following exposure to MBC at 30°C, the spindle checkpoint is only partially able to prevent progression through mitosis (Castagnetti *et al.*, 2010). Interestingly, caffeine was more effective at suppressing MBC-induced chromosome missegregation in wt cells than in *mad2Δ* mutants. Furthermore, *mad2Δ* mutants were clearly advanced through mitosis and S phase relative to wt cells following exposure to caffeine alone. Caffeine was also more effective at suppressing resistance to HU in *mad2Δ* mutants than in wt cells. Our studies clearly demonstrate that caffeine exerts both positive and negative effects on cell cycle progression in *S. pombe*. They also suggest that Mad2 and the spindle checkpoint suppress the ability of caffeine to promote cell cycle progression. We and others have previously demonstrated that activation of the stress response pathway interferes with spindle dynamics and partially delays cell cycle progression in a Mad2-dependent manner (Tatebe *et al.*, 2005; Kawasaki *et al.*, 2006; Robertson and Hagan, 2008; Alao *et al.*, 2010). It is thus likely that caffeine interferes with satisfaction of the spindle checkpoint, resulting in sustained Mad2 activation and delayed progression through mitosis. Sustained inhibition of the APC/C following exposure to caffeine may also account in part for the accumulation of Cdc25. Paradoxically, caffeine can also compensate for the loss of the spindle checkpoint in *mad2Δ* mutants by delaying progression through cytokinesis.

#### *Sty1 modulates caffeine activity*

Sty1 is a key regulator of the ESR and has been shown to enhance Cdc25 activity (Shiozaki and Russell, 1995; Kishimoto and Yamashita, 2000). However, Sty1 can also negatively regulate Cdc25 activity via activation of Srk1. It has been previously demonstrated that exposure to osmotic stress induces Cdc25 accumulation and delays cell cycle progression in part through activation of Srk1 (Tatebe *et al.*, 2005; Kawasaki *et al.*, 2006; Robertson and Hagan, 2008; Alao *et al.*, 2010). Following exposure to osmotic stress, Srk1 phosphorylates Cdc25 targeting it for nuclear export (Lopez-Aviles *et al.*, 2005). The accumulation or 'stockpiling' of Cdc25 has been observed under various conditions and is dependent on Sty1-induced Srk1 activation (Kovelman and Russell, 1996; Kishimoto and Yamashita, 2000; Lopez-Aviles *et al.*, 2005; Alao *et al.*, 2010; Frazer and Young, 2011; 2012).



The stockpiling of Cdc25 may facilitate rapid resumption of cell cycle progression following adaptation to stress or DNA damage repair (Kovelman and Russell, 1996; Degols and Russell, 1997). *Srk1* thus facilitates the stock-

pling of Cdc25 while simultaneously inhibiting its ability to promote cell cycle progression. *Srk1* also negatively regulates Cdc25 activity during the normal cell cycle (Lopez-Aviles *et al.*, 2005). Exposure to caffeine induces



**Fig. 6.** Caffeine modulates checkpoint responses independently of Rad3.

- A. Cells expressing HA-tagged Chk1 were pre-treated with 10 mM caffeine for 30 min and incubated further for another 2.5 h in the presence of  $10 \mu\text{g ml}^{-1}$  phleomycin. Total protein lysates were probed with monoclonal antibodies directed against HA. Tubulin was used to monitor gel loading. Alternatively, *rad3Δ* mutants expressing HA-tagged Chk1 were incubated for 2.5 h in the presence of  $10 \mu\text{g ml}^{-1}$  phleomycin.
- B. Cells expressing HA-tagged Cds1 were exposed to 20 mM HU and for a further 2 h with or without 10 mM caffeine. Total protein lysates were treated as in A.
- C. Wt and *rad3Δ* mutants expressing HA-tagged Cds1 were exposed to 10 mM caffeine for 24 h. Total protein lysates were treated as in A.
- D. Cells expressing HA-tagged Cdc25 were exposed to 20 mM HU and for a further 2 h with or without 10 mM caffeine. Total protein lysates were treated as in A.
- E. Cdc25-GFP<sup>int</sup> and Cdc25<sup>(9A)</sup>-GFP<sup>int</sup> expressing strains were incubated for 3 h with 20 mM HU and then incubated for a further 3 h in the presence or absence of 10 mM caffeine. Equal cell numbers were spotted onto YES agar plates and incubated at 30°C for 3 days.
- F. Strains in E were incubated with 20 mM HU for 2 h and then for a further 4 h in the presence or absence of 10 mM caffeine. Samples harvested at the indicated time points were stained with aniline blue and the septation index determined by fluorescence microscopy. Error bars represent the mean of at least three independent experiments  $\pm$  S.E.
- G. Cdc25-GFP<sup>int</sup> and Cdc25<sup>(9A)</sup>-GFP<sup>int</sup> expressing strains were incubated for 3 h with 20 mM HU, washed with sterile distilled water and resuspended in fresh YES media. Samples harvested at the indicated time points were stained with aniline blue and the septation index determined by fluorescence microscopy. Error bars represent the mean of at least three independent experiments  $\pm$  S.E.
- H. Strains in F were analysed by FACS.

activation of Sty1 (Calvo *et al.*, 2009). We predicted that the simultaneous induction of Cdc25 accumulation and activation of Sty1–Srk1 signalling by caffeine would inhibit its ability to positively mediate entry into mitosis. In our studies, deletion of *srk1<sup>+</sup>* only modestly influenced the effect of caffeine on cell cycle progression relative to wt cells (Supplementary Fig. S2A and B). In contrast, the ability of caffeine to override the replication checkpoint was greatly enhanced in *srk1Δ* mutants. Consequently, *srk1Δ* mutants showed increased chromosome missegregation and sensitivity when exposed to HU and subsequently caffeine. Srk1 thus attenuates the ability of caffeine to override checkpoints, presumably by inhibiting Cdc25 activity. We have previously shown that exposure to osmotic stress delays cell cycle progression in an Srk1-dependent manner (Alao *et al.*, 2010). Exposure to potassium chloride or caffeine induces Cdc25 accumulation in *S. pombe*. Srk1 thus appears to play a crucial role in counteracting Cdc25 activity under these conditions.

#### Effect of caffeine on checkpoint signalling

Previous studies have proposed that caffeine overrides checkpoint signalling in *S. pombe* by inhibiting Rad3 (Wang *et al.*, 1999; Moser *et al.*, 2000). These studies have provided biochemical evidence that caffeine does indeed override checkpoint signalling in this organism. Caffeine inhibits HU-induced Chk1 phosphorylation in *cds1Δ* mutants (Moser *et al.*, 2000). The direct inhibition of Cds1 or Chk1 phosphorylation in S phase and G2 respectively has however not been demonstrated. Interestingly, caffeine did not inhibit Rad3-induced Cds1 or Chk1 phosphorylation in our studies. Caffeine has similarly been shown to override checkpoint signalling independently of ATR inhibition in mammalian cells (Cortez, 2003). We have demonstrated here that caffeine induces Cdc25 accumulation in *S. pombe*. The inhibition of Cdc25 activity is essential for full activation of the replication and

DNA damage checkpoints (Furnari *et al.*, 1997; 1999; Boddy *et al.*, 1998; Zeng *et al.*, 1998). Intriguingly, caffeine did not inhibit Rad3 induced Cds1 or Chk1 phosphorylation following exposure to HU or phleomycin. Since caffeine suppresses Cdc2 phosphorylation under these conditions, its positive effect on Cdc25 stability may underlie its ability to override checkpoints. Cdc25A degradation is required for S phase arrest in mammalian cells (Mailand *et al.*, 2000; Jin *et al.*, 2003). Our findings clearly demonstrate that caffeine induces the nuclear accumulation of Cdc25. Cdc2 and Cdc13 are highly enriched in the nucleus of S phase arrested and late G2 phase cells (Decottignies *et al.*, 2001). Caffeine may thus lead to inappropriate Cdc2 activation during cell cycle arrest. The deletion of *srk1<sup>+</sup>* or expression of Cdc25<sup>(9A)</sup>-GFP<sup>int</sup> had little effect on the rate of cell cycle progression in cells exposed to caffeine. In contrast, the ability of caffeine to override checkpoint signalling was greatly enhanced in these mutants. Furthermore, Cdc25-GFP<sup>int</sup> and Cdc25<sup>(9A)</sup>-GFP<sup>int</sup> re-entered the cell cycle with similar kinetics when released from a HU block. We have also observed that Cdc25 expression is necessary for the positive effects of caffeine on cell cycle progression. These findings provide further evidence that Cdc25 accumulation and not Rad3 inhibition underlies the caffeine-induced checkpoint override.

#### Conclusions

We have demonstrated for the first time that caffeine induces Cdc25 stabilization independently of Rad3 in *S. pombe*. Similarly, *rad3* or *cds1* deletion stabilized Cdc25, suggesting a constitutive role in regulating its stability. Cdc25 expression is required for mitotic progression in *S. pombe* cells exposed to caffeine. Srk1 and Mad2 attenuate the ability of caffeine to drive cells through mitosis. Furthermore, caffeine-induced Cdc25 accumulation delays progression through cytokinesis. Caffeine did

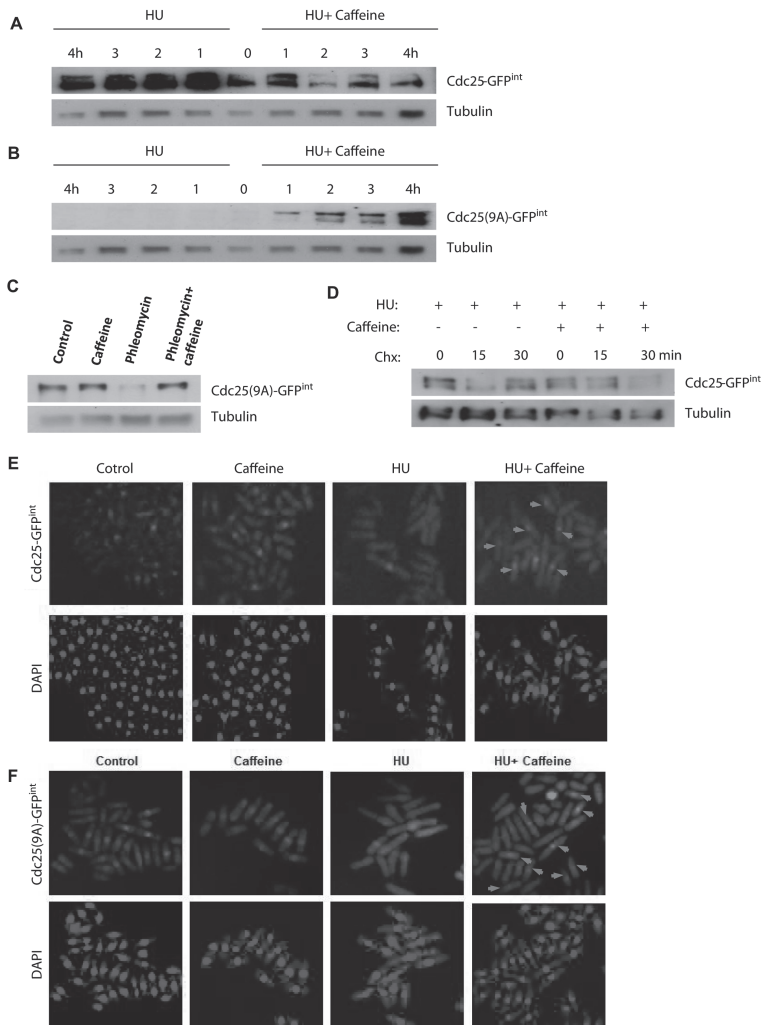


**Fig. 7.** Caffeine stabilizes Cdc25 in the presence of HU.

A and B. Cdc25-GFP<sup>int</sup> and Cdc25<sup>(9A)</sup>-GFP<sup>int</sup> expressing strains were incubated with 20 mM HU with or without 10 mM caffeine and harvested at the indicated time points. Total protein lysates were probed with monoclonal antibodies directed against GFP. Tubulin was used to monitor gel loading.

C. Cdc25<sup>(9A)</sup>-GFP<sup>int</sup>-expressing cells were pre-treated with 10 mM caffeine and then incubated for a further 1.5 h in the presence of 10 µg ml<sup>-1</sup> phleomycin. Total protein lysates were treated as in A.

D. Cdc25-GFP<sup>int</sup>-expressing cells were cultured for 2 h in the presence of 20 mM HU and then for 1 h in the presence or absence of 10 mM caffeine. Cells were then exposed to 100 µg ml<sup>-1</sup> of Chx and harvested at the indicated time points. Total protein lysates were probed with monoclonal antibodies directed against GFP. Tubulin was used to monitor gel loading.

E and F. Cdc25-GFP<sup>int</sup> and Cdc25<sup>(9A)</sup>-GFP<sup>int</sup> expressing strains were incubated for 3 h with 20 mM HU and then incubated for a further 1 h in the presence or absence of 10 mM caffeine. Cells were fixed, stained with antibodies against tubulin and examined by fluorescence microscopy. Nuclei were stained using DAPI. Red arrows indicate cells with predominantly nuclear Cdc25 localization.

**Table 1.** *S. pombe* strains.

<i>h<sup>-</sup></i> L972	Lab stock
<i>h<sup>-</sup></i> <i>cds1::ura4<sup>+</sup></i>	H. Okayama
<i>h<sup>-</sup></i> <i>chk1::KanMX6</i>	This study
<i>h<sup>-</sup></i> <i>leu1 ura4 his3 srk1::ura4<sup>+</sup></i>	Lab stock
<i>h<sup>-</sup></i> <i>wee1::ura4<sup>+</sup> leu1-32 ura4-D18 (FY7283)</i>	YGRC
<i>h<sup>-</sup></i> <i>cdc2-3w (FY8156)</i>	YGRC
<i>h<sup>-</sup></i> <i>cdc2-3w cdc25::ura4<sup>+</sup> leu1-32 ura4-D18</i>	YGRC
<i>h<sup>-</sup></i> <i>Chk1:ep leu1-32 ade6-216</i>	N. Walworth
<i>h<sup>-</sup></i> <i>Chk1:ep leu1-32 ade6-216 rad3::KanMX6</i>	This study
<i>h<sup>-</sup></i> <i>leu1 ura4 cds1-2HA6His[ura4<sup>+</sup>] (FY11064)</i>	YGRC
<i>h<sup>-</sup></i> <i>leu1 ura4 cds1-2HA6His[ura4<sup>+</sup>] rad3::KanMX6</i>	This study
<i>h<sup>-</sup></i> <i>cdc25-6HA [ura4<sup>+</sup>] leu1-32 ura4-D18 (FY7031)</i>	YGRC
<i>h<sup>-</sup></i> <i>cdc25-6HA [ura4<sup>+</sup>] leu1-32 ura4-D18 rad3::KanMX6</i>	This study
<i>h<sup>-</sup></i> <i>cdc25-6HA [ura4<sup>+</sup>] leu1-32 ura4-D18 rad24::KanMX6</i>	This study
<i>h<sup>-</sup></i> <i>cdc25-6HA [ura4<sup>+</sup>] leu1-32 ura4-D18 cds1::KanMX6</i>	This study
<i>h<sup>-</sup></i> <i>ura4-D18 leu1-32 cdc25-12myc::ura4<sup>+</sup></i>	P. Russell
<i>h<sup>-</sup></i> <i>leu1 ura4-D18 pka1::ura4<sup>+</sup> his2 (FY10302)</i>	YGRC
<i>h<sup>-</sup></i> <i>leu1 cut2-364 (FY11545)</i>	YGRC
<i>h<sup>-</sup></i> <i>leu1 nda3-KM311</i>	A. Bueno
<i>h<sup>-</sup></i> <i>nda3-KM311 mad2::ura4 leu1-32 ura4-D18</i>	S. Sazer
<i>h<sup>-</sup></i> <i>leu1 nda3-KM311 cdc25-myc::ura4<sup>+</sup> ura4D18 ade6M21X leu1-32</i>	K. Gould
<i>h<sup>-</sup></i> <i>leu1 nda3-KM311 cdc25-myc::ura4<sup>+</sup> clp1Δ ura4-D18 ade6-M21X leu1-32</i>	K. Gould
<i>h<sup>-</sup></i> <i>cdc25-GFP<sup>mt</sup> cdc25::ura4<sup>+</sup> ura4-D18 leu1-32</i>	P. Young
<i>h<sup>-</sup></i> <i>cdc25<sup>(9A)</sup>-GFP<sup>mt</sup> cdc25::ura4<sup>+</sup> ura4-D18 leu1-32</i>	P. Young
<i>h<sup>-</sup></i> <i>srk1-HA ::Kan<sup>r</sup> ura4-D18 leu1-32</i>	R. Alique
<i>h<sup>-</sup></i> <i>mik1::ura4 leu1 ura4 (FY8317)</i>	YGRC

YGRC, Yeast Genetic Resource Center, Osaka, Japan.

not inhibit Rad3 signalling in cells exposed to HU or phleomycin. Our findings suggest strongly that caffeine at least partially overrides checkpoint signalling by stabilizing Cdc25.

## Experimental procedures

### Strains, media and reagents

Strains are listed in Table 1. Cells were grown in yeast extract plus supplements medium (YES). Stock solutions of caffeine (Sigma Aldrich AB, Stockholm, Sweden) (100 mM) were prepared in water stored at  $-20^{\circ}\text{C}$ . HU (Sigma Aldrich AB) was dissolved in water at a concentration of 1 M and stored at  $-20^{\circ}\text{C}$ . Phleomycin (Sigma Aldrich AB) was dissolved in water and stock solutions ( $10\ \mu\text{g ml}^{-1}$ ) stored at  $-20^{\circ}\text{C}$ . MBC (Carbendazim/methylbenzimidazol-2-yl carbamate) and latrunculin B (Lat B) (Sigma Aldrich AB) were stored at  $-20^{\circ}\text{C}$  as  $10\ \text{mg ml}^{-1}$  stock solutions in DMSO.

### Molecular genetics

Deletion of open reading frames was done by PCR-based genomic targeting using a *KanMX6* construct (Bähler *et al.*, 1998). Disruptions were verified by screening for UV or HU sensitivity (where appropriate) followed by PCR using genomic DNA extracted from mutants with the expected UV- or HU-sensitive phenotype.

### Microscopy

Aniline blue staining and septation index assays were carried out as previously described (Kippert and Lloyd, 1995;

Dunaway and Walworth, 2004; Forsburg and Rhind, 2006). Images were obtained with a Zeiss AxioCam on a Zeiss Axioplan 2 microscope with a  $100\times$  objective using a 4,6-diamidino-2-phenylindole (DAPI) filter set. Strains expressing recombinant GFP constructs were fixed in methanol at  $-20^{\circ}\text{C}$ . Fixed cells were mounted in VECTASHIELD<sup>®</sup> mounting medium and visualized using differential interference contrast (DIC) or a GFP filter set.

### Fluorescence-activated cell sorting (FACS)

Approximately  $10^7$  cells were harvested at the desired time points, resuspended in 70% ethanol and stored at  $4^{\circ}\text{C}$  until use. FACS analyses were performed according to the protocol of Sazer and Sherwood (1990), using propidium iodide ( $32\ \mu\text{g ml}^{-1}$ ) as outlined on the Forsburg lab page (<http://www-bcf.usc.edu/~forsburg/yeast-flow-cytometry.html>). Flow cytometry was performed with a BD FACSAria<sup>™</sup> cell sorting system (Becton Dickinson AB, Stockholm, Sweden).

### Immunoblotting

Monoclonal antibodies directed against GFP, HA, and Myc were from Santa Cruz Biotechnology (Heidelberg, Germany). Polyclonal antibodies directed against phospho-(Ser317) Chk1 and mouse monoclonal antibodies directed against phospho-(Thr180/Tyr182) p38 were from Cell Signaling Technology [Bionordika (Sweden) AB, Stockholm, Sweden]. Monoclonal antibodies directed against  $\alpha$ -tubulin and phospho-(Tyr15) Cdc2 (Cdk1) were from Sigma-Aldrich (Sigma Aldrich AB). Monoclonal antibodies against Cdc2 were from Abcam (Cambridge, UK). For immunoblotting,

protein extracts were prepared as previously described (Asp and Sunnerhagen, 2003) with the addition of 1× PhosStop phosphatase inhibitor cocktail (Roche Diagnostics Scandinavia AB, Bromma, Sweden). Proteins were separated by SDS-PAGE. Epitope-tagged proteins were detected with the appropriate monoclonal antibodies.

#### Immunoprecipitation and phosphatase assays

For immunoprecipitation of HA-tagged Cds1, protein extractions were performed as previously described (Asp and Sunnerhagen, 2003). Lysates were incubated with 2 µg of anti-HA (F-7) antibody overnight at 4°C, followed by further incubation with 50 µl of Protein A/G agarose (Santa Cruz Biotechnology) for 1 h. Immunoprecipitated HA-tagged Cds1 was treated with λ protein phosphatase as previously described with the exception that 1× PhosStop phosphatase inhibitor cocktail was added as appropriate (Asp and Sunnerhagen, 2003).

#### RT-PCR

Early- to mid-log-phase cells were harvested by centrifugation, washed once in water and snap-frozen. Total RNA was extracted using the RiboPure™-Yeast kit (Ambion) according to the instructions. DNase I-treated total RNA was subsequently used in semi-quantitative and quantitative RT-PCR reactions. A One-Step RT-PCR Kit (Qiagen AB, Sollentuna, Sweden) was used for semi-quantitative RT-PCR reactions according to the manufacturer's instructions. cDNA was synthesized using a SuperScript™ III kit (Invitrogen AB, Lidingö, Sweden) according to the manufacturer's instructions. Quantitative Real-Time PCR was performed by the Core Genomics Facility (University of Gothenburg), using the Power SYBR® Green PCR Master Mix. One hundred nanograms of each cDNA and 0.5 mM of the primers were used in reaction volumes of 10 µl. The same primer pairs and annealing temperatures as in the One-Step PCR was used, and PCR for each cDNA sample was performed in triplicate. The specificity of the PCR was checked by comparing the  $T_m$  of the PCR-product to a sample without template.

The Comparative CT Method was used to analyse the results. The mean threshold cycle obtained for each sample was used to calculate initial *cdc25*<sup>+</sup> mRNA levels normalized against *act1*<sup>+</sup> mRNA, assuming the efficiencies of the PCR reactions were equal. Thereafter the *cdc25*<sup>+</sup> mRNA levels in the *cds1* and *rad3* deletion mutants were compared to wt by the ratio (*cdc25*<sup>+</sup> mRNA level)<sub>sample</sub> / (*cdc25*<sup>+</sup> mRNA level)<sub>control</sub>, where the untreated wt sample served as the control.

#### Competing interests

The authors declare that they have no competing interests.

#### Authors' contributions

J.P.A. and P.S. conceived and designed the study. J.P.A. performed experiments, analysed data and wrote the manuscript. J.J.S. performed experiments on Cdc25 expression

and stability. J.B. performed experiments on Cdc25 stability, cell cycle kinetics and spindle checkpoint regulation. N.Ö.-Y. performed experiments on Cdc25 stability and the effect of caffeine on the DDR. B.K. performed studies on the regulation of the spindle checkpoint.

#### Acknowledgements

We are grateful to Paul Young for supplying the Cdc25–GFP<sup>int</sup> and Cdc25<sup>(9A)</sup>–GFP<sup>int</sup> expressing strains, Kathy Gould for the *nda3-km311 cdc25-myc* strains, Avelino Bueno for the *nda3-KM311* deletion mutants, Nancy Walworth for the Chk1 epitope-tagged strains, and Rosa Aligue for the *srk1-HA* strain. This work was financially supported by grants from the Swedish Research Council (2010-4645) and the Swedish Cancer Fund (10-0633).

#### References

- Alao, J.P., and Sunnerhagen, P. (2008) Rad3 and Sty1 function in *Schizosaccharomyces pombe*: an integrated response to DNA damage and environmental stress? *Mol Microbiol* **68**: 246–254.
- Alao, J.P., Huis in't Veld, P.J., Buhse, F., and Sunnerhagen, P. (2010) Hyperosmosis enhances radiation and hydroxyurea resistance of *S. pombe* checkpoint mutants through the spindle checkpoint and delayed cytokinesis. *Mol Microbiol* **77**: 143–157.
- Asp, E., and Sunnerhagen, P. (2003) Mkp1 and Mkp2, two MAPKAP-kinase homologues in *Schizosaccharomyces pombe*, interact with the MAP kinase Sty1. *Mol Genet Genomics* **268**: 585–597.
- Basi, G., and Enoch, T. (1996) Identification of residues in fission yeast and human p34cdc2 required for S-M checkpoint control. *Genetics* **144**: 1413–1424.
- Bähler, J., Wu, J.Q., Longtine, M.S., Shah, N.G., McKenzie, A., 3rd, Steever, A.B., et al. (1998) Heterologous modules for efficient and versatile PCR-based gene targeting in *Schizosaccharomyces pombe*. *Yeast* **14**: 943–951.
- Boddy, M.N., Furnari, B., Mondesert, O., and Russell, P. (1998) Replication checkpoint enforced by kinases Cds1 and Chk1. *Science* **280**: 909–912.
- Bode, A.M., and Dong, Z. (2007) The enigmatic effects of caffeine in cell cycle and cancer. *Cancer Lett* **247**: 26–39.
- Brondello, J.M., Boddy, M.N., Furnari, B., and Russell, P. (1999) Basis for the checkpoint signal specificity that regulates Chk1 and Cds1 protein kinases. *Mol Cell Biol* **19**: 4262–4269.
- Butt, M.S., and Sultan, M.T. (2011) Coffee and its consumption: benefits and risks. *Crit Rev Food Sci Nutr* **51**: 363–373.
- Calvo, I.A., Gabrielli, N., Iglesias-Baena, I., Garcia-Santamarina, S., Hoe, K.L., Kim, D.U., et al. (2009) Genome-wide screen of genes required for caffeine tolerance in fission yeast. *PLoS ONE* **4**: e6619.
- Castagnetti, S., Olfierenko, S., and Nurse, P. (2010) Fission yeast cells undergo nuclear division in the absence of spindle microtubules. *PLoS Biol* **8**: e1000512.
- Cortez, D. (2003) Caffeine inhibits checkpoint responses without inhibiting the ataxia-telangiectasia-mutated (ATM)

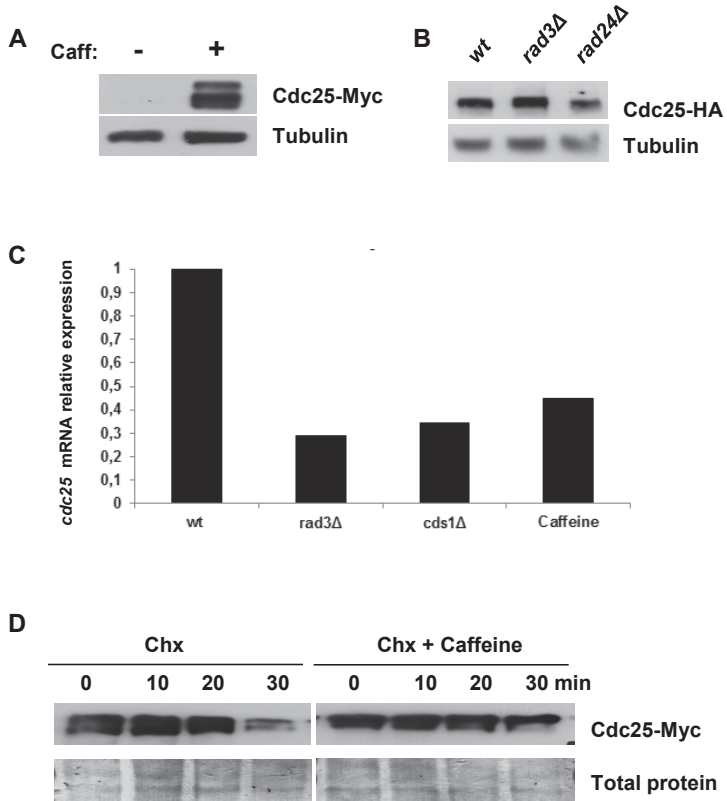
- and ATM- and Rad3-related (ATR) protein kinases. *J Biol Chem* **278**: 37139–37145.
- Decottignies, A., Zarzov, P., and Nurse, P. (2001) *In vivo* localisation of fission yeast cyclin-dependent kinase cdc2p and cyclin B cdc13p during mitosis and meiosis. *J Cell Sci* **114**: 2627–2640.
- Degols, G., and Russell, P. (1997) Discrete roles of the Spc1 kinase and the Atf1 transcription factor in the UV response of *Schizosaccharomyces pombe*. *Mol Cell Biol* **17**: 3356–3363.
- Dunaway, S., and Walworth, N.C. (2004) Assaying the DNA damage checkpoint in fission yeast. *Methods* **33**: 260–263.
- Enoch, T., Carr, A.M., and Nurse, P. (1992) Fission yeast genes involved in coupling mitosis to completion of DNA replication. *Genes Dev* **6**: 2035–2046.
- Enomoto, M., Goto, H., Tomono, Y., Kasahara, K., Tsujimura, K., Kiyono, T., et al. (2009) Novel positive feedback loop between Cdk1 and Chk1 in the nucleus during G2/M transition. *J Biol Chem* **284**: 34223–34230.
- Esteban, V., Blanco, M., Cueille, N., Simanis, V., Moreno, S., and Bueno, A. (2004) A role for the Cdc14-family phosphatase Flp1p at the end of the cell cycle in controlling the rapid degradation of the mitotic inducer Cdc25p in fission yeast. *J Cell Sci* **117**: 2461–2468.
- Esteban, V., Sacristan, M., Andres, S., and Bueno, A. (2008) The Flp1/Clp1 phosphatase cooperates with HECT-type Ubr1/2 protein-ubiquitin ligases in *Schizosaccharomyces pombe*. *Cell Cycle* **7**: 1269–1276.
- Forsburg, S.L., and Rhind, N. (2006) Basic methods for fission yeast. *Yeast* **23**: 173–183.
- Frazer, C., and Young, P.G. (2011) Redundant mechanisms prevent mitotic entry following replication arrest in the absence of Cdc25 hyper-phosphorylation in fission yeast. *PLoS ONE* **6**: e21348.
- Frazer, C., and Young, P.G. (2012) Carboxy-terminal phosphorylation sites in Cdc25 contribute to enforcement of the DNA damage and replication checkpoints in fission yeast. *Curr Genet* **58**: 217–234.
- Furnari, B., Rhind, N., and Russell, P. (1997) Cdc25 mitotic inducer targeted by Chk1 DNA damage checkpoint kinase. *Science* **277**: 1495–1497.
- Furnari, B., Blasina, A., Boddy, M.N., McGowan, C.H., and Russell, P. (1999) Cdc25 inhibited *in vivo* and *in vitro* by checkpoint kinases Cds1 and Chk1. *Mol Biol Cell* **10**: 833–845.
- He, X., Patterson, T.E., and Sazer, S. (1997) The *Schizosaccharomyces pombe* spindle checkpoint protein mad2p blocks anaphase and genetically interacts with the anaphase-promoting complex. *Proc Natl Acad Sci USA* **94**: 7965–7970.
- Hiraoka, Y., Toda, T., and Yanagida, M. (1984) The *NDA3* gene of fission yeast encodes beta-tubulin: a cold-sensitive *nda3* mutation reversibly blocks spindle formation and chromosome movement in mitosis. *Cell* **39**: 349–358.
- Hoeijmakers, J.H. (2009) DNA damage, aging, and cancer. *N Engl J Med* **361**: 1475–1485.
- Humphrey, T. (2000) DNA damage and cell cycle control in *Schizosaccharomyces pombe*. *Mutat Res* **451**: 211–226.
- Jin, J., Shirogane, T., Xu, L., Nalepa, G., Qin, J., Elledge, S.J., et al. (2003) SCFbeta-TRCP links Chk1 signaling to degradation of the Cdc25A protein phosphatase. *Genes Dev* **17**: 3062–3074.
- Kawasaki, Y., Nagao, K., Nakamura, T., and Yanagida, M. (2006) Fission yeast MAP kinase is required for the increased securin–separase interaction that rescues separate mutants under stresses. *Cell Cycle* **5**: 1831–1839.
- Kippert, F., and Lloyd, D. (1995) The aniline blue fluorochrome specifically stains the septum of both live and fixed *Schizosaccharomyces pombe* cells. *FEMS Microbiol Lett* **132**: 215–219.
- Kishimoto, N., and Yamashita, I. (2000) Multiple pathways regulating fission yeast mitosis upon environmental stresses. *Yeast* **16**: 597–609.
- Kovelman, R., and Russell, P. (1996) Stockpiling of cdc25 during a DNA replication checkpoint arrest in *Schizosaccharomyces pombe*. *Mol Cell Biol* **16**: 86–93.
- Lindsay, H.D., Griffiths, D.J., Edwards, R.J., Christensen, P.U., Murray, J.M., Osman, F., et al. (1998) S-phase-specific activation of Cds1 kinase defines a subpathway of the checkpoint response in *Schizosaccharomyces pombe*. *Genes Dev* **12**: 382–395.
- Lopez-Aviles, S., Grande, M., Gonzalez, M., Helgesen, A.L., Alemany, V., Sanchez-Piris, M., et al. (2005) Inactivation of the Cdc25 phosphatase by the stress-activated Srk1 kinase in fission yeast. *Mol Cell* **17**: 49–59.
- Lopez-Girona, A., Furnari, B., Mondesert, O., and Russell, P. (1999) Nuclear localization of Cdc25 is regulated by DNA damage and a 14-3-3 protein. *Nature* **397**: 172–175.
- Lovejoy, C.A., and Cortez, D. (2009) Common mechanisms of PIKK regulation. *DNA Repair (Amst)* **8**: 1004–1008.
- Lu, L.X., Domingo-Sananes, M.R., Huzarska, M., Novak, B., and Gould, K.L. (2012) Multisite phosphoregulation of Cdc25 activity refines the mitotic entrance and exit switches. *Proc Natl Acad Sci USA* **109**: 9899–9904.
- Mailand, N., Falck, J., Lukas, C., Syljuasen, R.G., Welcker, M., Bartek, J., et al. (2000) Rapid destruction of human Cdc25A in response to DNA damage. *Science* **288**: 1425–1429.
- Manke, I.A., Nguyen, A., Lim, D., Stewart, M.Q., Elia, A.E., and Yaffe, M.B. (2005) MAPKAP Kinase-2 is a cell cycle checkpoint kinase that regulates the G(2)/M transition and S phase progression in response to UV irradiation. *Mol Cell* **17**: 37–48.
- Matsuyama, M., Goto, H., Kasahara, K., Kawakami, Y., Nakanishi, M., Kiyono, T., et al. (2011) Nuclear Chk1 prevents premature mitotic entry. *J Cell Sci* **124**: 2113–2119.
- Mikhailov, A., Shinohara, M., and Rieder, C.L. (2004) Topoisomerase II and histone deacetylase inhibitors delay the G2/M transition by triggering the p38 MAPK checkpoint pathway. *J Cell Biol* **166**: 517–526.
- Mishra, M., Karagiannis, J., Trautmann, S., Wang, H., McCollum, D., and Balasubramanian, M.K. (2004) The Clp1p/Flp1p phosphatase ensures completion of cytokinesis in response to minor perturbation of the cell division machinery in *Schizosaccharomyces pombe*. *J Cell Sci* **117**: 3897–3910.
- Mochida, S., and Yanagida, M. (2006) Distinct modes of DNA damage response in *S. pombe* G0 and vegetative cells. *Genes Cells* **11**: 13–27.
- Moser, B.A., Brondello, J.M., Baber-Furnari, B., and Russell, P. (2000) Mechanism of caffeine-induced checkpoint override in fission yeast. *Mol Cell Biol* **20**: 4288–4294.

- Nefsky, B., and Beach, D. (1996) Pub1 acts as an E6-AP-like protein ubiquitin ligase in the degradation of *cdc25*. *EMBO J* **15**: 1301–1312.
- Nurse, P. (1975) Genetic control of cell size at cell division in yeast. *Nature* **256**: 547–551.
- Nurse, P. (1990) Universal control mechanism regulating onset of M-phase. *Nature* **344**: 503–508.
- Reinhardt, H.C., Aslanian, A.S., Lees, J.A., and Yaffe, M.B. (2007) p53-deficient cells rely on ATM- and ATR-mediated checkpoint signaling through the p38MAPK/MK2 pathway for survival after DNA damage. *Cancer Cell* **11**: 175–189.
- Robertson, A.M., and Hagan, I.M. (2008) Stress-regulated kinase pathways in the recovery of tip growth and microtubule dynamics following osmotic stress in *S. pombe*. *J Cell Sci* **121**: 4055–4068.
- Russell, P., and Nurse, P. (1987) Negative regulation of mitosis by *wee1<sup>+</sup>*, a gene encoding a protein kinase homolog. *Cell* **49**: 559–567.
- Sazer, S., and Sherwood, S.W. (1990) Mitochondrial growth and DNA synthesis occur in the absence of nuclear DNA replication in fission yeast. *J Cell Sci* **97**: 509–516.
- Schumacher, B., Garinis, G.A., and Hoeijmakers, J.H. (2008) Age to survive: DNA damage and aging. *Trends Genet* **24**: 77–85.
- Shiozaki, K., and Russell, P. (1995) Cell-cycle control linked to extracellular environment by MAP kinase pathway in fission yeast. *Nature* **378**: 739–743.
- Shiromizu, T., Goto, H., Tomono, Y., Bartek, J., Totsukawa, G., Inoko, A., et al. (2006) Regulation of mitotic function of Chk1 through phosphorylation at novel sites by cyclin-dependent kinase 1 (Cdk1). *Genes Cells* **11**: 477–485.
- Smith, D.A., Toone, W.M., Chen, D., Bähler, J., Jones, N., Morgan, B.A., et al. (2002) The *Srk1* protein kinase is a target for the *Sty1* stress-activated MAPK in fission yeast. *J Biol Chem* **277**: 33411–33421.
- Sørensen, C.S., Syljuåsen, R.G., Falck, J., Schroeder, T., Rönstrand, L., Khanna, K.K., et al. (2003) Chk1 regulates the S phase checkpoint by coupling the physiological turnover and ionizing radiation-induced accelerated proteolysis of Cdc25A. *Cancer Cell* **3**: 247–258.
- Sørensen, C.S., Syljuåsen, R.G., Lukas, J., and Bartek, J. (2004) ATR, Claspin and the Rad9–Rad1–Hus1 complex regulate Chk1 and Cdc25A in the absence of DNA damage. *Cell Cycle* **3**: 941–945.
- Sørensen, C.S., Hansen, L.T., Dziegielewska, J., Syljuåsen, R.G., Lundin, C., Bartek, J., et al. (2005) The cell-cycle checkpoint kinase Chk1 is required for mammalian homologous recombination repair. *Nat Cell Biol* **7**: 195–201.
- Tatebe, H., Shimada, K., Uzawa, S., Morigasaki, S., and Shiozaki, K. (2005) *Wsh3/Tea4* is a novel cell-end factor essential for bipolar distribution of *Tea1* and protects cell polarity under environmental stress in *S. pombe*. *Curr Biol* **15**: 1006–1015.
- Trautmann, S., Wolfe, B.A., Jorgensen, P., Tyers, M., Gould, K.L., and McCollum, D. (2001) Fission yeast Clp1p phosphatase regulates G2/M transition and coordination of cytokinesis with cell cycle progression. *Curr Biol* **11**: 931–940.
- Varmeh, S., and Manfredi, J.J. (2009) Inappropriate activation of cyclin-dependent kinases by the phosphatase Cdc25b results in premature mitotic entry and triggers a p53-dependent checkpoint. *J Biol Chem* **284**: 9475–9488.
- Wang, S.W., Norbury, C., Harris, A.L., and Toda, T. (1999) Caffeine can override the S-M checkpoint in fission yeast. *J Cell Sci* **112** (Part 6): 927–937.
- Wolfe, B.A., and Gould, K.L. (2004) Fission yeast Clp1p phosphatase affects G2/M transition and mitotic exit through Cdc25p inactivation. *EMBO J* **23**: 919–929.
- Zeng, Y., Forbes, K.C., Wu, Z., Moreno, S., Piwnicka-Worms, H., and Enoch, T. (1998) Replication checkpoint requires phosphorylation of the phosphatase Cdc25 by Cds1 or Chk1. *Nature* **395**: 507–510.
- Zhou, B.B., Chaturvedi, P., Spring, K., Scott, S.P., Johanson, R.A., Mishra, R., et al. (2000) Caffeine abolishes the mammalian G(2)/M DNA damage checkpoint by inhibiting ataxia-telangiectasia-mutated kinase activity. *J Biol Chem* **275**: 10342–10348.

### Supporting information

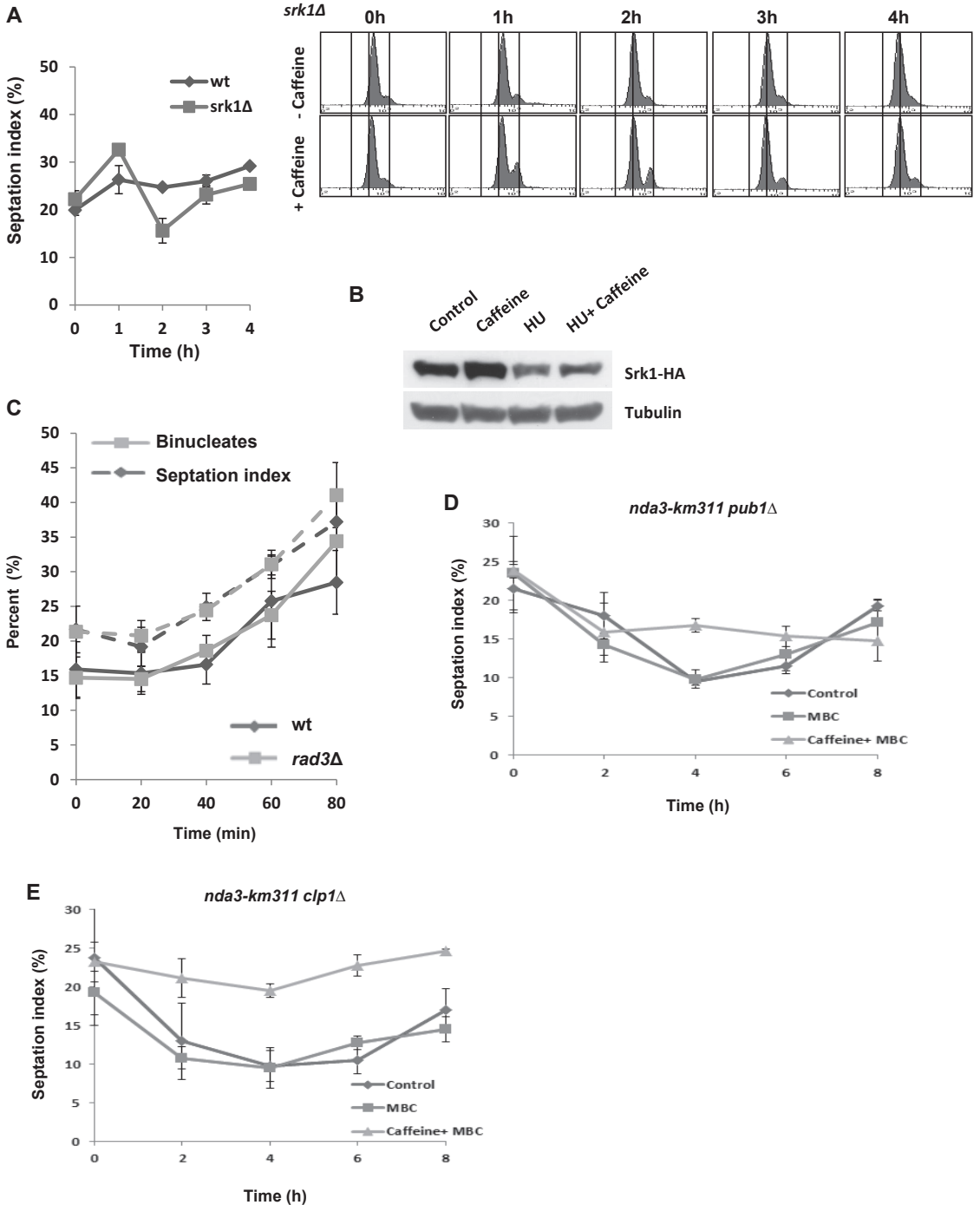
Additional supporting information may be found in the online version of this article at the publisher's web-site.

## Supplementary Figure 1



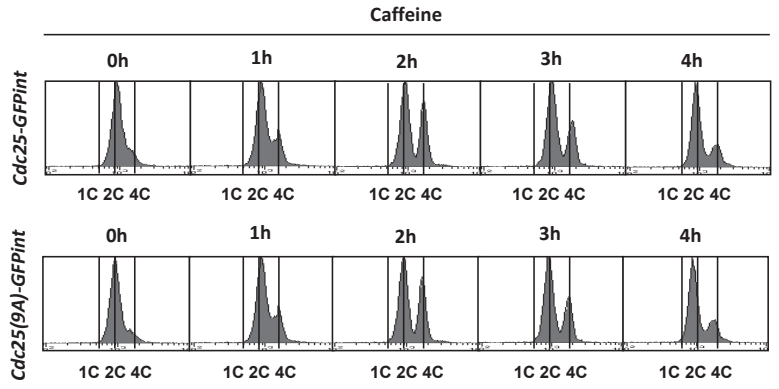
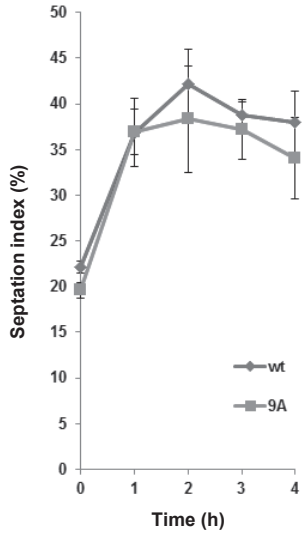


## Supplementary Figure 2

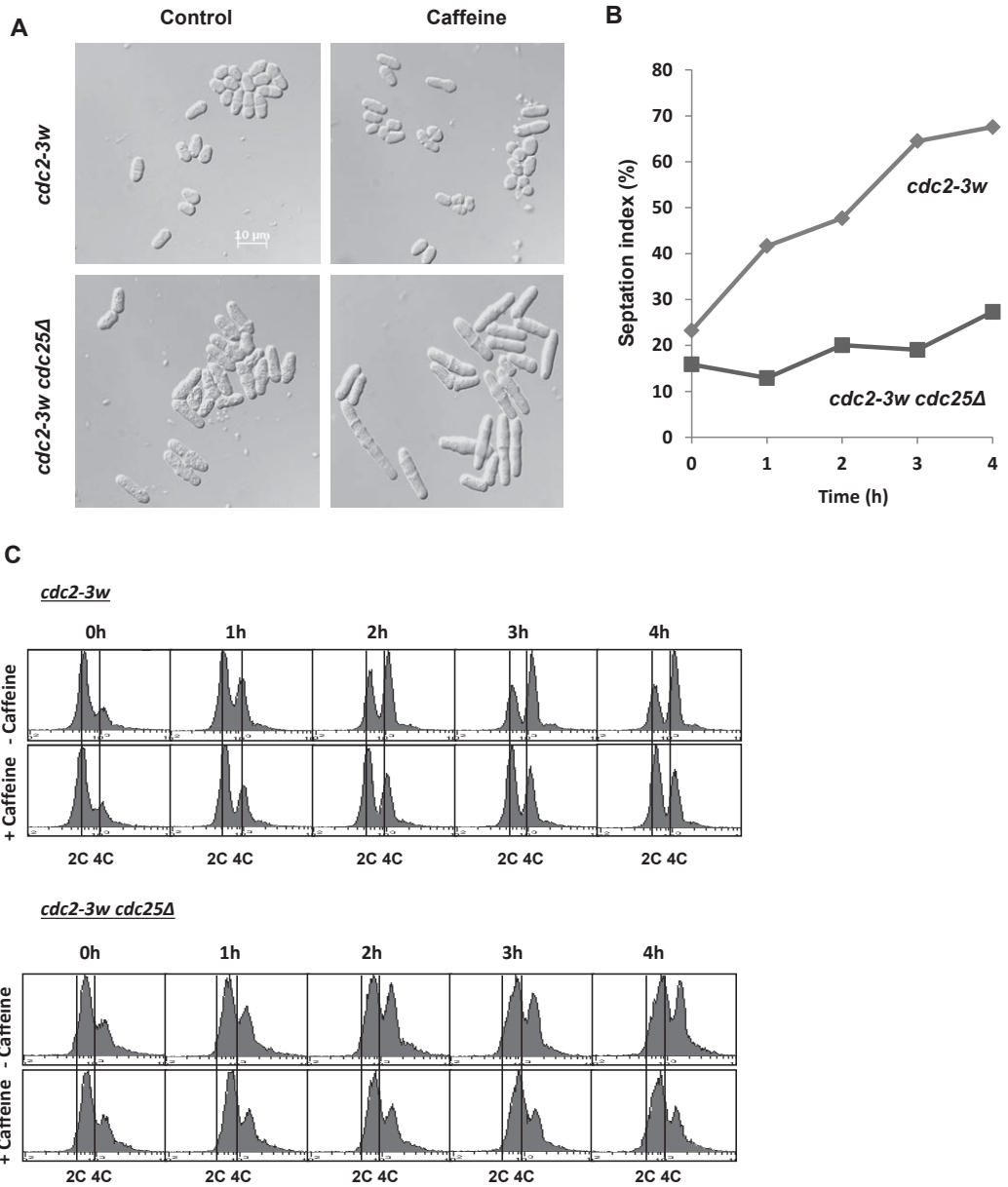




Supplementary  
Figure 3

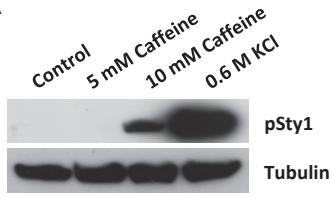


**Supplementary  
Figure 4**

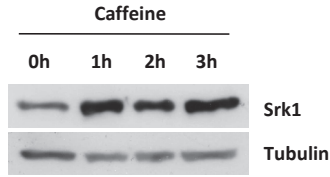


# Supplementary Figure 5

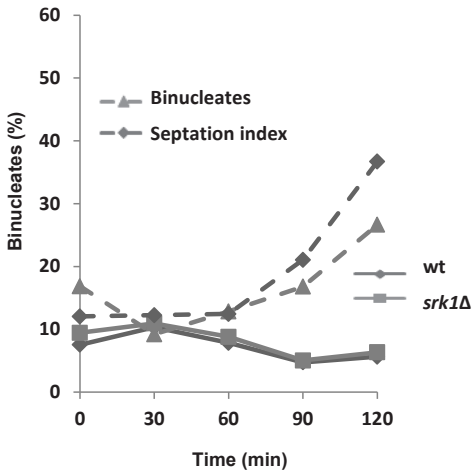
**A**



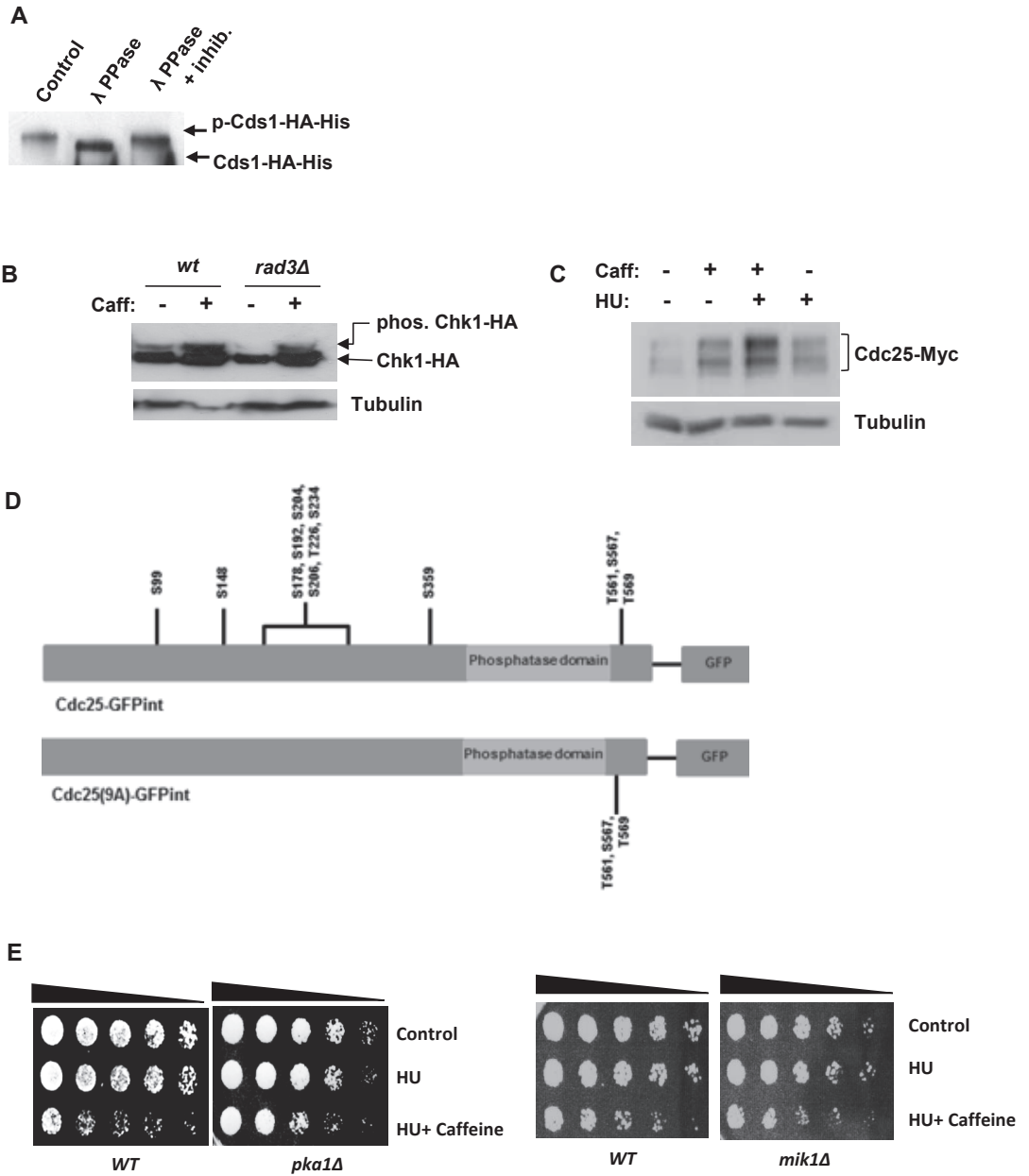
**B**



**C**



Supplementary  
Figure 6



## Paper II



# **Caffeine stabilises fission yeast Wee1 in a Rad24-dependent manner but attenuates its expression in response to DNA damage contributing to checkpoint override**

John P. Alao<sup>1,2</sup>, Johanna Johansson-Sjölander<sup>1</sup>, Charalampos Rallis<sup>2</sup> and Per Sunnerhagen<sup>1</sup>

<sup>1</sup> Department of Chemistry and Molecular Biology, University of Gothenburg, Box 462, SE-405 30, Gothenburg, Sweden

<sup>2</sup> School of Health, Sports and Bioscience, University of East London, Stratford campus, London, E15 4LZ, United Kingdom

Keywords: caffeine, fission yeast, DNA damage, Cdc25, Wee1, checkpoint signalling

Running title: Caffeine and Wee1 in checkpoint override

## **Abstract**

The ability to delay cell cycle progression in response to DNA damage or environmental stress is crucial for maintaining cellular viability. The widely consumed neuroactive compound caffeine has generated much interest due to its ability to override the DNA damage and replication checkpoints. Previously the inhibition of Ataxia Telangiectasia Mutated (ATM) and its homologues was thought to be the target of caffeine's inhibitory activity. Later findings indicate that the Target of Rapamycin Complex 1 (TORC1) is the preferred target of caffeine. Effective Cdc2 inhibition requires both the activation of the Wee1 kinase and inhibition of the Cdc25 phosphatase. The TORC1, DNA damage and environmental stress response pathways all converge on Cdc25 and Wee1. We previously demonstrated that caffeine overrides DNA damage checkpoints by modulating Cdc25 stability. The effect of caffeine on cell cycle progression under normal growth conditions resembles that of TORC1 inhibition. Furthermore, caffeine activates the Sty1 regulated environmental stress response. Caffeine may thus modulate cell cycle progression and checkpoints, by affecting multiple signalling pathways that regulate Cdc25 and Wee1 levels, localisation and activity. Here we show that the activity of caffeine stabilises both Cdc25 and Wee1. The stabilising effect of caffeine and genotoxic agents on Wee1 was dependent on the Rad24 chaperone that binds both Cdc25 and Wee1. Interestingly, caffeine inhibited the accumulation of Wee1 in response to DNA damage. Caffeine therefore, modulates cell cycle progression contextually through increased Cdc25 activity and Wee1 repression following DNA damage by the co-activation and inhibition of multiple signalling pathways.



## Introduction

Cell cycle progression through mitosis is under the opposing control of the Cdc25 phosphatase and the Wee1 kinase. Cdc25 removes inhibitory phosphorylation moieties on Cdc2, which in turn enhances Cdc25 activity in a positive feedback loop. In contrast, Wee1 phosphorylates Cdc2 on tyrosine residue 15 to inhibit its activity. Cdc2 in turn negatively regulates Wee1 by phosphorylation leading to its nuclear exclusion or degradation (1-3). Cells must delay progress through S-phase and mitosis in response to stalled replication, DNA double strand breaks and other forms of damage, in order to effect DNA repair and maintain viability (4, 5). Effective activation and maintenance of DNA damage checkpoints thus involves the dual regulation of both Cdc25 and Wee1 via a “double lock” mechanism (6). Activation of the DNA damage response pathway induces inhibitory Cdc25 phosphorylation, Rad24 binding, nuclear export and stockpiling within the cytoplasm. In contrast, increased Wee1 activation occurs via phosphorylation and this kinase accumulates within the nucleus (4, 5). Caffeine has generated much controversy by its ability to override checkpoint signalling but the underlying mechanisms remain unclear. Caffeine inhibits members of the members of the phosphatidylinositol 3 kinase-like kinase (PIKK) family including ataxia telangiectasia mutated (ATM) and ataxia – and rad related (ATR) kinase homologue Rad3 and Target of Rapamycin Complex 1 (TORC1) *in vitro* (7-10). Initial reports suggested that caffeine overrides DNA damage checkpoint signalling by inhibiting *Schizosaccharomyces pombe* Rad3 and its orthologues but this view remains controversial (11-13). Studies that are more recent indicate that TORC1 appears to be the major cellular target of caffeine *in vivo* (12, 14-16). TORC1 is a major regulator of cell cycle progression acting on both Cdc25 and Wee1. The inhibition of TORC1 activity suppresses Wee1 expression, results in increased Cdc25 activation and drives cells into mitosis. In addition, the effect of caffeine on cell cycle progression resembles that of TORC1 inhibition (17-19). We previously demonstrated that caffeine overrides checkpoint signalling in part, by stabilising Cdc25 expression. Interestingly, deletion of *rad3Δ* and its downstream target *cds1Δ* similarly resulted in Cdc25 stabilisation. These findings suggested a role of Rad3 signalling in regulating Cdc25 stability during the normal cell cycle. Similarly, the Sty1 regulated Environmental Stress Response (ESR) pathway also plays a role in regulating both Cdc25 and Wee1 expression levels and is activated by caffeine (5, 20). The integration of Cdc25 and Wee1 phosphorylation, localisation, stability and activity thus play a key role in modulating the timing of mitosis. TORC1, Rad3 and Sty1 regulate the major signalling pathways that converge on the Cdc25 and Wee1 axis (3, 5, 17). Herein we further explored the mechanism(s) by which caffeine stabilises Cdc25 and overrides checkpoint signalling and have investigated the impact of subcellular localisation under these conditions. Here we report that in addition to modulating Cdc25 activity, caffeine also suppressed the DNA damage induced stabilisation of Wee1 *S. pombe*. In contrast, caffeine stabilised Wee1 in a Rad24 dependent manner under normal cell cycle conditions. These findings demonstrate that caffeine overrides the DNA damage checkpoints by positively regulating Cdc25 and negatively regulating Wee1. These findings provide further evidence for the assertion that caffeine modulates TORC1 (and other pathways) and not Rad3 signalling to overcome the DNA damage checkpoint “double lock” mechanism.

## Results

### *Caffeine stabilises Cdc25 by inhibiting its nuclear degradation*

We previously demonstrated that caffeine stabilises both wild type (wt) Cdc25-GFP<sub>int</sub> and the Cdc25<sub>(9A)</sub>-GFP<sub>int</sub> mutant that lacks 9 major inhibitory phosphorylation sites and is normally degraded following exposure to genotoxic agents (18, 21, 22). In this study, exposure to 10 mM caffeine also stabilised the Cdc25<sub>(12A)</sub> mutant protein that lacks all 12 inhibitory phosphorylation sites (Fig. 1 A). Caffeine also stabilised Cdc25 in *mik1*Δ mutants. Mik1 is required for maintenance of the replication damage checkpoint signalling in *S. pombe* mutants expressing Cdc25<sub>(12A)</sub>-GFP<sub>int</sub> (21, 22). As observed for *rad3*Δ and *cds1*Δ mutants (18), Cdc25 appeared to be more stable in a *mik1*Δ genetic background (Fig. 1 A). Caffeine also suppressed the 20 mM hydroxyurea (HU)-induced degradation of the Cdc25<sub>(12A)</sub>-GFP<sub>int</sub> mutant (Fig. 1 B). The stabilising effect of caffeine was not due to stress-induced Sty1 activation, as exposure to 0.6 M KCl induced Cdc25<sub>(9A)</sub>-GFP<sub>int</sub> degradation (Fig. 1 C). Inhibition of Crm1-dependent nuclear export with 100 ng/ml leptomycin B (LMB) slightly suppressed Cdc25 expression in both wt and Cdc25<sub>(12A)</sub>-GFP<sub>int</sub> expressing mutants (Fig. 1 D). LMB also inhibited the stockpiling of Cdc25-GFP<sub>int</sub> following exposure to HU but failed to stabilise Cdc25<sub>(12A)</sub>-GFP<sub>int</sub> under these conditions (Fig. 1 D). Similarly, HU-induced stockpiling of Cdc25 was dependent on Rad24 (Fig. 1 E). As previously reported, caffeine is more effective at overriding DNA damage checkpoints in strains expressing Cdc25 mutant protein that cannot be negatively phosphorylated (Fig. 1 F,G).

### *Caffeine stabilises Wee1 in a Rad24 dependent manner*

TORC1 inhibition activates Cdc25 and suppressed Wee1 activity (19). As Cdc25 and Wee1 are both partially regulated by ubiquitin-dependent degradation, we next investigated the effect of caffeine on Wee1 expression. Exposure to caffeine induced a rapid and time-dependent increase in Wee1 levels. Wee1 levels increased with 30 min of exposure to caffeine and continued to rise over the course of the 4 h incubation periods (Fig. 2 A,B). The caffeine-induced accumulation of Wee1 was dependent on Rad24 expression (Fig. 2 C). The deletion of *rad24*<sup>+</sup> resulted in a partial reduction of Wee1 expression and induced a “wee” phenotype (Fig. 2 D,E). Additionally, inhibition of nuclear export with 100 ng/ml LMB stabilised Wee1 independently of Rad24 (Fig. 2 F). Caffeine also stabilised Mik1 under normal cell cycle conditions (Fig. 2 G). Caffeine thus interferes with the coordinated regulation of Cdc25 and Wee1, possibly via inhibition of TORC1 activity.

### *Caffeine suppresses DNA damage-induced Wee1 accumulation*

Exposure to DNA damaging agents has previously been shown to induce the accumulation of Wee1 (6). We thus studied the effect of caffeine on Wee1 expression under these conditions. Incubation with 10 mM caffeine alone induced the accumulation of Wee1 but had no impact on the slight suppressive effect of 20 mM HU on the protein (Fig. 3 A). Exposure to 10 μg/ml phleomycin induced Wee1 accumulation in a manner akin to that of caffeine. Interestingly, caffeine strongly inhibited phleomycin-induced Wee1 accumulation such that the levels were below those observed in untreated cells (Fig. 3 A). Caffeine-induced Wee1 accumulation was dependent on Rad24 expression (Fig. 3 B). Interestingly, exposure to HU did not induce Wee1 accumulation and co-exposure to caffeine abolished expression of this kinase. Wee1 accumulation in response to phleomycin exposure was not observed in

*rad24Δ* mutants. In marked contrast to wt cells, caffeine had no effect on Wee1 expression in *rad24Δ* mutants exposed to phleomycin (Fig. 3 C). We next compared the effect of phleomycin exposure on Cdc2 phosphorylation in wt and *rad24Δ* mutants. Exposure to 10 μg/ml phleomycin increased the basal level of Cdc2 phosphorylation (Fig. 3 D). In *rad24Δ* mutants, basal Cdc2 phosphorylation was not detected and exposure to phleomycin resulted in levels of Cdc2 phosphorylation below those of untreated wt cells (Fig. 3 D). Caffeine thus both stabilises Cdc25 (18) and suppresses Wee1 expression under genotoxic conditions. This activity would effectively lead to the abolition of the “double lock” DNA damage checkpoint mechanism.

### ***Caffeine mediates checkpoint override by suppressing Wee1 under genotoxic conditions***

We previously observed that the effect of caffeine on cell cycle progression in *S. pombe* is enhanced in *wee1Δ* and other checkpoint mutants (18). Caffeine (10 mM) overrode checkpoint signalling in *wee1Δ* mutants but to a lesser extent than in wt cells (Fig. 4 A). FACS analyses demonstrated that caffeine only slightly increases the sensitivity of *wee1Δ* mutants to 20 mM HU relative to wt cells (Fig. 4 B - D). We did not detect a differential level of sensitivity to HU in *rad24Δ* and *wee1Δ* mutants relative to wt cells (Fig. 4 E). Unlike wt cells and *wee1Δ* mutants however, *rad24Δ* mutants did not become elongated following exposure to HU (Fig. 4 F). Interestingly, caffeine was far more effective at overriding checkpoint signalling in response to HU in *rad24Δ* mutants (Fig. 4 G,I). We also observed that in contrast to HU, *rad24Δ* and *wee1Δ* mutants are highly sensitive to phleomycin (Fig. 4 H).

### ***Inhibition of TORC1 signalling overrides checkpoint signalling***

The TORC1 complex regulates the timing of mitosis and its inhibition by rapamycin or torin1 leads to an advanced entry into mitosis (19, 23). As caffeine inhibits TORC1 and advanced entry into mitosis (16, 18), we investigated if TORC1 inhibition similarly overrides checkpoint signalling. Exposure to 20 mM HU or 7.5 μM torin1 for 4 h did not affect the viability of wt *S. pombe* cells (Fig. 5 A). Unlike caffeine, co-exposure with torin1 did not affect the sensitivity of wt cells to HU (Figs. 4 G and 5 A). Cells co-exposed HU and torin1 were shorter than cells exposed to HU alone but no chromosome mis-segregation was observed. In contrast, cells exposed to torin1 alone, displayed a “wee” phenotype (Fig. 5 B).

In contrast to its effects on HU sensitivity, torin1 was far more effective at sensitising wild type cells to phleomycin than caffeine (Fig. 5 C-E, H,I). Similar results were obtained with *gaf1Δ* mutants, a transcription factor that partially mediates the effect of torin1 (24, 25), (Fig. 5 E). In addition, *gaf1Δ* mutants exposed to phleomycin and torin1 were shorter than cell exposed to phleomycin alone (Fig. 5 J). Torin1 thus overrides DNA damage checkpoint signalling independently of Gaf1. Rapamycin failed to override checkpoint signalling concentrations as high as 600 ng/ml in wt *S. pombe* cells (Fig. 5 G). Tco89 is a subunit of the TORC1 complex and *tco89Δ* mutants are hypersensitive to caffeine and rapamycin (15, 26). Rapamycin sensitised *tco89Δ* mutants to phleomycin in a manner similar to caffeine (Fig. 5 G). Together with previous findings (12, 15, 18), our study strongly suggests that caffeine overrides DNA damage checkpoint signalling by targeting Tor2 and the TORC1 complex.

## Discussion

The precise mechanisms whereby caffeine overrides DNA damage checkpoint signalling remain unclear. In the present study, we investigated further how caffeine modulates cell cycle progression through Cdc25 and Wee1. Initial studies suggested that caffeine inhibits Rad3 and its related homologues (11, 27). Caffeine however, exerts inhibitory activity on several members of the phosphatidylinositol 3 kinase-like kinase (PIKK) family (7-10). More recent studies suggest that the Tor2 containing TORC1 complex is the major target of caffeine *in vivo* (12, 14-16). TORC1 regulates the timing of mitosis by modulating Cdc25 and Wee1 activity. Inhibition of TORC1 activity thus advances cells into mitosis, an effect like that observed with caffeine (18, 19). DNA damage checkpoint activation and enforcement require the dual inhibition of Cdc25 activity and activation of Wee1 (6). We previously demonstrated that caffeine induces Cdc25 accumulation independently of Rad3 inhibition (18). As TORC1 regulates Cdc25 and Wee1 activity and is inhibited by caffeine, this inhibition may in fact underlie the effects of the compound on cell cycle progression.

### *Effect of caffeine on Cdc25 stability*

Cdc25 undergoes Cdc2-dependent activating phosphorylation as well as inhibitory phosphorylation via the Rad3 and Sty1 regulated signalling pathways (28). Caffeine stabilises wt and Cdc25 mutant proteins that cannot be phosphorylated in response to DNA damage. Caffeine thus clearly stabilises Cdc25 independently of its negative phosphorylation. Furthermore, caffeine is more effective at stabilising the Cdc25<sub>(9A)</sub>-GFP<sub>int</sub> and Cdc25<sub>(12A)</sub>-GFP<sub>int</sub> isoforms and hence checkpoint override in these genetic backgrounds. The stabilising effect of caffeine on Cdc25 is also independent of Sty1 signalling, as exposure to osmotic stress induced the degradation of Cdc25<sub>(9A)</sub>-GFP<sub>int</sub>. The Cdc25<sub>(9A)</sub>-GFP<sub>int</sub> and Cdc25<sub>(12A)</sub>-GFP<sub>int</sub> mutants are also rapidly degraded following exposure to genotoxic agents (18, 21, 22). These conditions must thus cause cellular changes that result in the targeting of these mutants for ubiquitin-dependent degradation. Inhibition of nuclear export with LMB resulted in a decrease in Cdc25 levels and prevented its stockpiling following exposure to HU. LMB also failed to prevent the HU-induced degradation of the Cdc25<sub>(12A)</sub>-GFP<sub>int</sub> mutant protein. As expected, caffeine-induced Cdc25 stabilisation was independent of Rad24. Caffeine thus appears to partially inhibit the nuclear degradation of Cdc25 in *S. pombe*. Accordingly, Cdc25<sub>(12A)</sub>-GFP<sub>int</sub> mutants are more susceptible to caffeine-mediated checkpoint override than wt cells. It remains unclear if caffeine-induced Cdc25 accumulation results from TORC1 inhibition.

### *Effect of caffeine on Wee1 stability*

Our previous studies suggested that Wee1 attenuates the effect of caffeine on cell cycle progression in *S. pombe* (18). Furthermore, Cdc25 and Wee1 are co-regulated during the cell cycle and thus determine the timing of mitosis (19, 29). We thus investigated the effect of caffeine on Wee1 expression. Interestingly, caffeine induced rapid Wee1 accumulation under normal growth conditions. This accumulation was dependent on Rad24 expression which was also induced by exposure to caffeine (Fig. 2 A - C). Sty1 was recently shown to modulate the ratio of Cdc25 to Wee1 in a Rad24-dependent manner (20). Deletion of *rad24*<sup>+</sup> resulted in reduced Wee1 expression indicating that unlike Cdc25, Wee1 stability

is dependent on Rad24 under normal cell cycle conditions (Figs. 1 E, 2 D and refs. (18, 21, 22)). Deletion of *rad24*<sup>+</sup> resulted in a “semi-wee” phenotype. These findings suggest that it is the lack of Wee1 expression rather than constitutively nuclear Cdc25 expression, that is responsible for the shorter length at division observed in *rad24Δ* mutants (Fig. 2 D and ref. (30)). Inhibiting nuclear export with LMB also stabilised Wee1 independently of Rad24. Caffeine also stabilised the Mik1 kinase, an S-phase specific inhibitor of Cdc2 (31). Caffeine thus appears to stabilise Cdc25, Mik1 and Wee1 under normal cell cycle conditions. We previously demonstrated that the effect of caffeine on cell cycle progression is dampened by *Srk1* and Wee1 activity (18). It remains unclear if Rad24 stabilises Mik1 and how caffeine affects this interaction in the presence of stalled replication forks or DNA damage. Remarkably, the effect of caffeine on Cdc25 and Wee1 is reversed under genotoxic conditions. Under these conditions Cdc25 is normally inactivated and sequestered in the cytoplasm or degraded in the nucleus, while Wee1 becomes activated and accumulates in the nucleus (21, 22). Exposure to caffeine under these conditions results in the stabilisation of Cdc25 within the nucleus (18) and degradation of Wee1 (Fig. 3 A,B). Exposure to phleomycin but not HU induced Wee1 accumulation in a Rad24-dependent manner. In contrast to caffeine or phleomycin exposure alone, Wee1 did not accumulate when the cells were co-exposed to both compounds. Interestingly, caffeine also abolished Wee1 expression in *rad24Δ* mutants exposed to HU. Total phospho-Cdc2 levels are also suppressed in *rad24Δ* mutants, consistent with a loss of Wee1 expression and a “semi-wee” phenotype. The TORC1 complex also regulates the activity of Cdc25 and Wee1 under normal cell cycle conditions to regulate the timing of mitosis (19). Furthermore, *Sty1* can modulate the relative expression levels of Cdc25 and Wee1 in a Rad24-dependent manner (20). Crosstalk between TORC1, *Sty1* and the replication checkpoint pathway has also been reported (32, 33). As caffeine inhibits TORC1 and activates *Sty1*, its effect on cell cycle progression may be context dependent and result from fundamental changes to physiological co-regulation of Cdc25 and Wee1. Caffeine-mediated TORC1 inhibition may also influence autophagy and 26S proteasomal degradation (34-36). In any case, caffeine clearly abolishes Cdc25 inhibition and degradation under genotoxic conditions independently of Rad24. In contrast, Wee1 degradation may result from changes to its phosphorylation and ability to interact with Rad24. Caffeine thus overrides the DNA damage “double lock” mechanism independently of Rad3 inhibition ((18) and this study).

### ***Differential effects of caffeine on DNA damage resistance***

The sensitivity of *rad24Δ* and *wee1Δ* mutants following a 4-hour exposure to HU was not enhanced relative to wt cells. Caffeine was however no more effective at driving checkpoint override in *wee1Δ* mutants exposed to HU than in wt cells. This may reflect the differential cell cycle kinetics of *wee1Δ* mutants which delay progression through G1, because of size constraints and the more important role of Mik1 under these conditions (21, 22). Future studies will investigate the effect of caffeine on Mik1 expression in cells exposed to HU. Alternatively, the increase in Cdc25 activity induced by caffeine in a *wee1Δ* background may delay progression through cytokinesis due to high Cdc2 activity. Caffeine was more effective at overriding the replication checkpoint in *rad24Δ* mutants compared to wt cells. Rad24 binding and nuclear export are not required for the inhibition of Cdc25 activity. Caffeine overrides checkpoints more efficiently in mutants expressing Cdc25 isoforms that cannot be phosphorylated (18). It remains unclear if Rad24 stabilises Mik1 in a

manner like Wee1. Increased nuclear levels of Cdc25 following exposure to HU combined with decreased Mik1 expression, might account for the greater effect of caffeine on *rad24Δ* mutants. Caffeine may also suppress Mik1 expression similarly to Wee1 (unpublished results). The sensitivity of *rad24Δ* and *wee1Δ* mutants to phleomycin was identical, probably reflecting the lack of Wee1 expression in these genetic backgrounds.

### ***TORC1 inhibition overrides DNA damage checkpoint signalling***

Recent studies have suggested that TORC1 and not Rad3 and its homologues is the preferred target of caffeine in vitro (12, 15, 18). TORC1 regulates the timing of mitosis by regulating the activity of the PP2A phosphatase, which in turn regulates the activity of Cdc25 and Wee1 (19, 37). Exposure of *S. pombe* cells to rapamycin or torin1, activates Cdc25 and suppresses the expression of Wee1, resulting in advanced entry into mitosis. Furthermore, the effect of caffeine on cell cycle progression mimics that of rapamycin and torin1 and is dependent of Cdc25 (18, 19). We thus hypothesised that TORC1 inhibition by rapamycin or torin1 should override DNA damage checkpoint signalling in a manner akin to caffeine. In wt, caffeine, rapamycin and torin1 all advance the timing of mitosis under normal cell cycle conditions in *S. pombe* (18, 19). In this study, caffeine and torin1 but not rapamycin overrode phleomycin-induced DNA damage checkpoint activation. Interestingly torin1 did not enhance sensitivity to HU in this context. This may be due to differential effects of caffeine on additional signalling pathways (e.g. Mik1 expression and global 26S proteasome-mediated protein degradation (Alao et al., unpublished results)). The TORC1 downstream transcription factor Gaf1 has recently been shown to mediate the effects of Tor2 inhibition on chronological lifespan in *S. pombe* (24, 25). Caffeine and torin1 clearly increased sensitivity to phleomycin in *gaf1Δ* mutants, suggesting this effect occurs independently of Gaf1.

Effective G2 checkpoint activation requires the dual inhibition of Cdc25 and activation of Wee1 (6). Mutants that fail to express *wee1* and *rad24* are especially sensitive to DNA damage as these genes regulate the G2 checkpoint. Both rapamycin and torin1 suppress Wee1 expression in *S. pombe*, although rapamycin is less effective in this regard (19). We have demonstrated that caffeine induces Wee1 expression under normal cell cycle conditions in a Rad24-dependent manner. Curiously, this effect is reversed under genotoxic conditions, where co-exposure to caffeine prevents Wee1 accumulation. The failure of rapamycin to override checkpoint signalling, may thus result from its less effective inhibition of TORC1 and Wee1 suppression relative to torin1 and caffeine. Indeed, rapamycin effectively overrode DNA damage checkpoint signalling in *tc089Δ* mutants that display hypersensitivity to the inhibitor (15, 26). Taken together our finding and those of others, strongly suggest that caffeine overrides DNA damage signalling independently of Rad3 by inhibiting TORC1 activity.

## **Experimental procedures**

### ***Strains, media and reagents***

Strains are listed in Table 1. Cells were grown in yeast extract plus supplements medium (YES) Stock solutions of caffeine (Sigma Aldrich AB, Stockholm, Sweden) (100 mM) were prepared in water stored at -20°C. HU (Sigma Aldrich AB) was dissolved in water at a concentration of 1 M and stored at -20°C. Phleomycin (Sigma Aldrich AB) was dissolved in water and stock solutions (10 µg/ml) stored at -20°C.



### ***Molecular genetics***

Deletion of the open reading frames was done by PCR-based genomic targeting using a *KanMX6* construct (38). Disruptions were verified by PCR using genomic DNA extracted from mutants.

### ***Microscopy***

Calcofluor white (Sigma-Aldrich) staining and septation index assays were carried out as previously described (18). (39, 40) Images were obtained with a Zeiss AxioCam on a Zeiss Axioplan 2 microscope with a 100 × objective using a 4,6-diamidino-2-phenylindole (DAPI) filter set.

### ***Fluorescence-activated cell sorting (FACS)***

Cells were harvested at the desired time points, resuspended in 70 % ethanol and stored at 4°C until use. FACS analyses were performed according to the previously described protocol (18), using propidium iodide (32 µg/ml) as outlined on the Forsburg lab page (<http://www-rcf.usc.edu/~forsburg/yeast-flow-protocol.html>). Flow cytometry was performed with a BD FACSAria™ cell sorting system (Becton Dickinson AB, Stockholm, Sweden).

### ***Immunoblotting***

Monoclonal antibodies directed against HA (F-7), Myc (9E10) and pan 14-3-3 (K-19) proteins were from Santa Cruz Biotechnology (Heidelberg, Germany). Monoclonal antibodies directed against GFP (11814460001) and  $\alpha$ -tubulin were from Sigma-Aldrich (Sigma Aldrich AB). Polyclonal antibodies directed against phospho-(Tyr15) Cdc2 were from Cell Signaling Technology (BioNordika, Stockholm, Sweden). Monoclonal antibodies against Cdc2 were from Abcam (Cambridge, UK). For immunoblotting, protein extracts were prepared as previously described (Alao et al., 2014) with addition of 1 × PhosStop phosphatase inhibitor cocktail (Roche Diagnostics Scandinavia AB, Bromma, Sweden). Proteins were separated by SDS-PAGE. Epitope-tagged proteins were detected with the appropriate monoclonal antibodies.

## **Competing interests**

The authors declare that they have no competing interests.

## **Acknowledgements**

We are grateful to J. Bähler, S. Ali, R. Lucena and D. R. Kellogg for technical support. This work was financially supported by Carl Trygger's Foundation (CTS 15:13) and the Swedish Cancer Fund (13-0438 and 16-0708).



## References

1. **Caspari T, Hilditch V.** 2015. Two distinct Cdc2 pools regulate cell cycle progression and the DNA damage response in the fission yeast *S. pombe*. *PLoS One* **10**:e0130748.
2. **Moseley JB.** 2017. Wee1 and Cdc25: Tools, pathways, mechanisms, questions. *Cell Cycle* **16**:599-600.
3. **de Gooijer MC, van den Top A, Bockaj I, Beijnen JH, Wurdinger T, van Tellingen O.** 2017. The G2 checkpoint-a node-based molecular switch. *FEBS Open Bio* **7**:439-455.
4. **Karlsson-Rosenthal C, Millar JB.** 2006. Cdc25: mechanisms of checkpoint inhibition and recovery. *Trends Cell Biol* **16**:285-292.
5. **Alao JP, Sunnerhagen P.** 2008. Rad3 and Sty1 function in *Schizosaccharomyces pombe*: an integrated response to DNA damage and environmental stress? *Mol Microbiol* **68**:246-254.
6. **Raleigh JM, O'Connell MJ.** 2000. The G(2) DNA damage checkpoint targets both Wee1 and Cdc25. *J Cell Sci* **113**:1727-1736.
7. **Humphrey T.** 2000. DNA damage and cell cycle control in *Schizosaccharomyces pombe*. *Mutat Res* **451**:211-226.
8. **Bode AM, Dong Z.** 2007. The enigmatic effects of caffeine in cell cycle and cancer. *Cancer Lett* **247**:26-39.
9. **Lovejoy CA, Cortez D.** 2009. Common mechanisms of PIKK regulation. *DNA Repair* **8**:1004-1008.
10. **Gibbs BF, Goncalves Silva I, Prokhorov A, Abooli M, Yasinska IM, Casely-Hayford MA, Berger SM, Fasler-Kan E, Sumbayev VV.** 2015. Caffeine affects the biological responses of human hematopoietic cells of myeloid lineage via downregulation of the mTOR pathway and xanthine oxidase activity. *Oncotarget* **6**:28678-28692.
11. **Moser BA, Brondello JM, Baber-Furnari B, Russell P.** 2000. Mechanism of caffeine-induced checkpoint override in fission yeast. *Mol Cell Biol* **20**:4288-4294.
12. **Wanke V, Cameroni E, Uotila A, Piccolis M, Urban J, Loewith R, De Virgilio C.** 2008. Caffeine extends yeast lifespan by targeting TORC1. *Mol Microbiol* **69**:277-285.
13. **Cortez D.** 2003. Caffeine inhibits checkpoint responses without inhibiting the ataxia-telangiectasia-mutated (ATM) and ATM- and Rad3-related (ATR) protein kinases. *J Biol Chem* **278**:37139-37145.
14. **Kuranda K, Leberre V, Sokol S, Palamarczyk G, Francois J.** 2006. Investigating the caffeine effects in the yeast *Saccharomyces cerevisiae* brings new insights into the connection between TOR, PKC and Ras/cAMP signalling pathways. *Mol Microbiol* **61**:1147-1166.

15. **Reinke A, Chen JC, Aronova S, Powers T.** 2006. Caffeine targets TOR complex I and provides evidence for a regulatory link between the FRB and kinase domains of Tor1p. *J Biol Chem* **281**:31616-31626.
16. **Rallis C, Codlin S, Bähler J.** 2013. TORC1 signaling inhibition by rapamycin and caffeine affect lifespan, global gene expression, and cell proliferation of fission yeast. *Aging Cell* **12**:563-573.
17. **Petersen J.** 2009. TOR signalling regulates mitotic commitment through stress-activated MAPK and Polo kinase in response to nutrient stress. *Biochem Soc Trans* **37**:273-277.
18. **Alao JP, Johansson-Sjölander J, Baar J, Özbaki-Yagan N, Kakoschky B, Sunnerhagen P.** 2014. Caffeine stabilizes Cdc25 independently of Rad3 in *Schizosaccharomyces pombe* contributing to checkpoint override. *Mol Microbiol* **92**:777-796.
19. **Atkin J, Halova L, Ferguson J, Hitchin JR, Lichawska-Cieslar A, Jordan AM, Pines J, Wellbrock C, Petersen J.** 2014. Torin1-mediated TOR kinase inhibition reduces Wee1 levels and advances mitotic commitment in fission yeast and HeLa cells. *J Cell Sci* **127**:1346-1356.
20. **Paul M, Ghosal A, Bandyopadhyay S, G P, Selvam U, Rai N, Sundaram G.** 2018. The fission yeast MAPK Spc1 senses perturbations in Cdc25 and Wee1 activities and targets Rad24 to restore this balance. *Yeast* **35**:261-271.
21. **Frazer C, Young PG.** 2011. Redundant mechanisms prevent mitotic entry following replication arrest in the absence of Cdc25 hyper-phosphorylation in fission yeast. *PLoS One* **6**:e21348.
22. **Frazer C, Young PG.** 2012. Carboxy-terminal phosphorylation sites in Cdc25 contribute to enforcement of the DNA damage and replication checkpoints in fission yeast. *Curr Genet* **58**:217-234.
23. **Petersen J, Nurse P.** 2007. TOR signalling regulates mitotic commitment through the stress MAP kinase pathway and the Polo and Cdc2 kinases. *Nat Cell Biol* **9**:1263-1272.
24. **Laor D, Cohen A, Kupiec M, Weisman R.** 2015. TORC1 regulates developmental responses to nitrogen stress via regulation of the GATA transcription factor Gaf1. *MBio* **6**:e00959.
25. **Rodríguez-López M, Gonzalez S, Hillson O, Tunnacliffe E, Codlin S, Tallada VA, Bähler J, Rallis C.** 2019. The GATA transcription factor Gaf1 represses tRNA genes, inhibits growth, and extends chronological lifespan downstream of fission yeast TORC1. *BioRxiv* 700286 doi:<https://doi.org/10.1101/700286>
26. **Hayashi T, Hatanaka M, Nagao K, Nakaseko Y, Kanoh J, Kokubu A, Ebe M, Yanagida M.** 2007. Rapamycin sensitivity of the *Schizosaccharomyces pombe tor2* mutant and organization of two highly phosphorylated TOR complexes by specific and common subunits. *Genes Cells* **12**:1357-1370.
27. **Jimenez G, Yucel J, Rowley R, Subramani S.** 1992. The *rad3<sup>+</sup>* gene of *Schizosaccharomyces pombe* is involved in multiple checkpoint functions and in DNA repair. *Proc Natl Acad Sci USA* **89**:4952-4956.

28. **Perry JA, Kornbluth S.** 2007. Cdc25 and Wee1: analogous opposites? *Cell Div* **2**:12.
29. **Lucena R, Alcaide-Gavilan M, Anastasia SD, Kellogg DR.** 2017. Wee1 and Cdc25 are controlled by conserved PP2A-dependent mechanisms in fission yeast. *Cell Cycle* **16**:428-435.
30. **Ford JC, Al-Khodairy F, Fotou E, Sheldrick KS, Griffiths DJF, Carr AM.** 1994. 14-3-3 protein homologs required for the DNA damage checkpoint in fission yeast. *Science* **265**:533-535.
31. **Lundgren K, Walworth N, Booher R, Dembski M, Kirschner M, Beach D.** 1991. Mik1 and Wee1 cooperate in the inhibitory tyrosine phosphorylation of Cdc2. *Cell* **64**:1111-1122.
32. **Hartmuth S, Petersen J.** 2009. Fission yeast Tor1 functions as part of TORC1 to control mitotic entry through the stress MAPK pathway following nutrient stress. *J Cell Sci* **122**:1737-1746.
33. **Fletcher J, Griffiths L, Caspari T.** 2018. Nutrient limitation inactivates Mrc1-to-Cds1 checkpoint signalling in *Schizosaccharomyces pombe*. *Cells* **7**.
34. **Gressner OA.** 2009. About coffee, cappuccino and connective tissue growth factor- Or how to protect your liver!? *Environ Toxicol Pharmacol* **28**:1-10.
35. **Marshall RS, Vierstra RD.** 2015. Eat or be eaten: The autophagic plight of inactive 26S proteasomes. *Autophagy* **11**:1927-1928.
36. **Zhao J, Zhai B, Gygi SP, Goldberg AL.** 2015. mTOR inhibition activates overall protein degradation by the ubiquitin proteasome system as well as by autophagy. *Proc Natl Acad Sci U S A* **112**:15790-15797.
37. **Martin R, Lopez-Aviles S.** 2018. Express yourself: how PP2A-B55(Pab1) helps TORC1 talk to TORC2. *Curr Genet* **64**:43-51.
38. **Bähler J, Wu JQ, Longtine MS, Shah NG, McKenzie A, 3rd, Steever AB, Wach A, Philippsen P, Pringle JR.** 1998. Heterologous modules for efficient and versatile PCR-based gene targeting in *Schizosaccharomyces pombe*. *Yeast* **14**:943-951.
39. **Dunaway S, Walworth NC.** 2004. Assaying the DNA damage checkpoint in fission yeast. *Methods* **33**:260-263.
40. **Forsburg SL, Rhind N.** 2006. Basic methods for fission yeast. *Yeast* **23**:173-183.

**Table 1. *S. pombe* strains**

---

<i>h<sup>-</sup></i> L972	Lab stock
<i>h<sup>+</sup></i> <i>cdc25-6HA [ura4<sup>+</sup>] leu1-32 ura4-D18</i> (FY7031)	YGRC
<i>h<sup>+</sup></i> <i>cdc25-6HA [ura4<sup>+</sup>] leu1-32 ura4-D18 rad24::KanMX6</i>	This study
<i>h<sup>-</sup></i> <i>cdc25-12myc::ura4<sup>+</sup> ura4-D18 leu1-32</i>	P. Russell
<i>h<sup>-</sup></i> <i>Cdc25-GFP<sub>int</sub> cdc25::ura4<sup>+</sup> ura4-D18 leu1-32</i>	P. Young
<i>h<sup>+</sup></i> <i>Cdc25<sub>(9A)</sub>-GFP<sub>int</sub> cdc25::ura4<sup>+</sup> ura4-D18 leu1-32</i>	P. Young
<i>h<sup>-</sup></i> <i>Cdc25<sub>(12A)</sub>-GFP<sub>int</sub> cdc25::ura4<sup>+</sup> ura4-D18 leu1-32</i>	P. Young
<i>h<sup>-</sup></i> <i>Cdc25<sub>(12A)</sub>-GFP<sub>int</sub> cdc25::ura4<sup>+</sup> ura4-D18 leu1-32 mik1::ura4<sup>+</sup></i>	P. Young
<i>h<sup>+</sup></i> <i>cut8::ura4</i> (FY9535)	YGRC
<i>h<sup>+</sup></i> <i>leu1 his2 ura4 cut8-8xMyc ura4<sup>+</sup></i>	YGRC
<i>h<sup>-</sup></i> <i>wee1::ura4<sup>+</sup> leu1-32 ura4-D18</i> (FY7283)	YGRC
<i>h<sup>-</sup></i> <i>wee1-3HA:6His leu1-32 ura4-D18</i> (FY16241)	YGRC
<i>h<sup>-</sup></i> <i>wee1-3HA:6His leu1-32 ura4-D18 rad24::KanMX6</i>	This study
<i>h<sup>-</sup></i> <i>rad24::ura4<sup>+</sup> leu1 ura4-D18 ade6-M210</i> (FY13517)	YGRC
<i>h<sup>-</sup></i> <i>mik1::ura4 leu1 ura4</i> (FY8317)	YGRC
<i>h<sup>+</sup></i> <i>ade6-M210 ura4-D18 leu1-32 gaf1::KanMX6</i>	Bioneer
<i>h<sup>+</sup></i> <i>ade6-M210 ura4-D18 leu1-32 tco89::KanMX6</i>	Bioneer

---

YGRC, Yeast Genetic Resource Center, Osaka, Japan

## Figure legends

### Figure 1. Caffeine induces the nuclear accumulation of Cdc25 in *S. pombe*

**A.** Strains expressing wt Cdc25-GFP, Cdc25<sub>(12A)</sub>-GFP or Cdc25-GFP from a *mik1Δ* genetic background, were incubated with 10 mM caffeine and harvested at the indicated time points. Total protein lysates were resolved by SDS-PAGE and Cdc25 detected using antibodies directed against GFP. Gel loading was monitored using antibodies directed against tubulin.

**B.** Strains expressing Cdc25<sub>(12A)</sub>-GFP<sub>int</sub> were pre-treated with 20 mM HU for two hours, followed by the addition of 10 mM caffeine. Cultures were incubated for a further 2 hours and total protein lysates were resolved by SDS-PAGE. Cdc25, phospho-Cdc2 and Cdc2 were detected using antibodies directed against GFP. Gel loading was monitored as in **A**.

**C.** Strains expressing wt Cdc25-GFP or Cdc25<sub>(9A)</sub>-GFP were cultured in YES containing 0.6 M KCl and harvested at the indicated time points. Samples were analysed as in **A**.

**D.** Strains expressing wt Cdc25-GFP or Cdc25<sub>(12A)</sub>-GFP<sub>int</sub> were incubated with 100 ng/ml LMB and 20 mM HU alone or in combination. Cells were pre-treated with HU for 2 h and then incubated with LMB for another 2 h as indicated. Samples were processed as in **A**.

**E.** The Cdc25-HA *rad24Δ* strain was exposed to 20 mM HU alone or in combination with 10 mM caffeine. Cells were pre-treated with HU for 2 h and then incubated with caffeine for another 2 h as indicated. Cdc25 was detected using antibodies directed against the HA epitope. Gel loading was monitored using antibodies directed against tubulin.

**F.** Strains expressing wt Cdc25-GFP and Cdc25<sub>(12A)</sub>-GFP<sub>int</sub> exposed to 20 mM HU alone or in combination with 10 mM caffeine as in **E**. Samples were adjusted for relative cell numbers, serially diluted, plated on YES agar and incubated for 2 - 3 days.

**G.** Cdc25<sub>(12A)</sub>-GFP<sub>int</sub> and Cdc25-GFP expressing strains from a *mik1Δ* genetic background were treated as in **F**.

**Figure 2. Caffeine induces Wee1 accumulation in a Rad24-dependent manner in *S. pombe*.**

**A.** A Wee1-HA expressing strain was incubated with 10 mM caffeine and harvested at the indicated time points. Total protein lysates were resolved by SDS-PAGE. Wee1 was detected using antibodies directed against the HA epitope. Rad24 was detected using a pan 14-3-3 antibody. A *rad24* $\Delta$  mutant was used to monitor antibody specificity. Gel loading was monitored using antibodies directed against tubulin.

**B.** Cells expressing Wee1-HA were treated as in **A**.

**C.** Wt and *rad24* $\Delta$  mutant cells expressing Wee1-HA were treated as in **A**.

**D.** Wt and *rad24* $\Delta$  cells expressing Wee1-HA were grown to log phase and treated as in **A**.

**E.** Log phase cultures of wt and *rad24* $\Delta$  cells were fixed in ethanol and examined by differential contrast microscopy.

**F.** Wt and *rad24* $\Delta$  strains expressing Wee1-HA were incubated with 100 ng/ml LMB for 1 h. Total protein lysates were resolved by SDS-PAGE and membranes probed with the indicated antibodies.

**G.** Cells expressing Mik1-HA were exposed to 10 mM caffeine and harvested at the indicated time points. Samples were treated as in **A**.

**Figure 3. Caffeine suppresses genotoxin-induced Wee1 accumulation in *S. pombe*.**

A. Cells expressing Wee1-HA were cultured with 10 mM caffeine alone or in combination with 20 mM HU or 10  $\mu$ g/ml phleomycin as indicated. Cultures were pre-treated with HU or phleomycin for 2 h and then for a further 2 h in the presence or absence of caffeine.

B. Wee1-HA *rad24* $\Delta$  cells were treated as in A.

C. Wt cells expressing Wee1-HA and Wee1-HA *rad24* $\Delta$  cells were exposed to 10  $\mu$ g/ml phleomycin for 1 h. Total protein lysates were resolved by SDS-PAGE and membranes probed with antibodies against phospho- and total Cdc2.

**Figure 4. Differential effects of caffeine on cell cycle progression in *S. pombe wee1* $\Delta$  and *rad24* $\Delta$  mutants.**

A. Duplicate cultures of wt and *wee1* $\Delta$  cells were incubated with 10  $\mu$ g/ml phleomycin for 2 h. The cultures were then incubated for a further 4 h with or without 10 mM caffeine and samples harvested at the indicated time points. Cells were fixed in 70 % ethanol, stained with aniline blue and the septation index determined by fluorescent microscopy.

B. Samples from A were stained with propidium iodide and analysed by FACS. Arrows indicate cell with mis-segregated chromosomes.

C. Wt and *wee1* $\Delta$  cells were incubated with 20 mM HU for 2 h. The cultures were then incubated for a further 2 h in the presence of 10 mM caffeine as indicated. Cultures were adjusted for relative cell numbers, serially diluted and plated onto YES agar plates. Plates were incubated at 30°C for 2 - 3 days.

D. Wt and *wee1* $\Delta$  cells were treated as in A. Cells were fixed in 70 % ethanol and examined by differential contrast microscopy.

E. Wt and *rad24* $\Delta$  *wee1* $\Delta$  cells were exposed to 20 mM HU for 4 h. Cells were fixed in 70 % ethanol and examined by differential contrast microscopy.

F,G. Wt and *rad24* $\Delta$  *wee1* $\Delta$  cells were treated as in A.

H. Wt and *rad24* $\Delta$  *wee1* $\Delta$  cells were exposed to 10  $\mu$ g/ml phleomycin for 2 h. Cultures were adjusted for relative cell numbers, serially diluted and plated onto YES agar plates. Plates were incubated at 30° C for 2 - 3 days.

**Figure 5. Inhibition of TORC1 overrides checkpoint signalling similarly to caffeine**

**A.** Wt cells were incubated with 20 mM HU for 2 h. The cultures were then incubated for a further 2 h in the presence of 10 mM caffeine as indicated. Cultures were adjusted for relative cell numbers, serially diluted and plated onto YES agar plates. Plates were incubated at 30° C for 2 - 3 days.

**B.** Cells in A were fixed in 70 % ethanol, stained with DAPI and examined by differential contrast microscopy.

**C.** Wt cells were incubated with 10 µg/ml phleomycin for 2 h. The cultures were then incubated for a further 2 h in the presence of 10 mM caffeine or 7.5 µM torin1 as indicated. Cultures were adjusted for relative cell numbers, serially diluted and plated on YES agar plates. Plates were incubated at 30° C for 2- 3 days.

**D.** Wt cells expressing Wee1-HA, were incubated with 5 µg/ml of phleomycin for 2 h. The cultures were then incubated for a further 2 h in the presence of 10 mM caffeine, 200 ng/ml rapamycin or 5 µM torin1 as indicated. Cultures were adjusted for relative cell numbers, serially diluted and plated on YES agar plates. Plates were incubated at 30° C for 2 - 3 days.

**E.** *gaf1Δ* mutant cells were incubated with 5 µg/ml of phleomycin for 2 h. The cultures were then incubated for a further 2 h in the presence of 10 mM caffeine, 200 ng/ml rapamycin or 5 µM torin1 as indicated. Cultures were adjusted for relative cell numbers, serially diluted and plated on YES agar plates. Plates were incubated at 30°C for 2 - 3 days.

**F.** *tc089Δ* mutant cells were incubated with 5 µg/ml of phleomycin for 2 h. The cultures were then incubated for a further 2 h in the presence of 10 mM caffeine, 200 ng/ml rapamycin or 5 µM torin1 as indicated. Cultures were adjusted for relative cell numbers, serially diluted and plated onto YES agar plates. Plates were incubated at 30°C for 2- 3 days.

**G.** Wt cells were exposed to 5 µg/ml of phleomycin for 2 h. The cultures were then incubated for a further 2 h in the presence of 200 ng/ml or 600 ng/ml rapamycin as indicated. Cells exposed to 600 ng/ml rapamycin served as a control. Cultures were adjusted for relative cell numbers, serially diluted and plated on YES agar plates. Plates were incubated at 30° C for 2 - 3 days.

**H.** Wt cells were incubated with 5 µg/ml of phleomycin for 2 h. The cultures were then incubated for a further 2 h in the presence of 200 ng/ml rapamycin or 5 µM torin1. Samples were harvested at the indicated time points. Cells were fixed in 70 % ethanol, stained with calcofluor white and the septation index determined by fluorescent microscopy.

**I.** *gaf1Δ* mutants were incubated with 5 µg/ml of phleomycin for 2 h. The cultures were then incubated for a further 2 h in the presence of 10 mM caffeine or 5 µM torin1. Cells were fixed in 70 % ethanol, stained with aniline blue or calcofluor white and the septation index determined by fluorescent microscopy.

**J.** *gaf1Δ* mutants were incubated with 5 µg/ml of phleomycin for 2 h. The cultures were then incubated for a further 2 h in the presence of 10 mM caffeine or 5 µM torin1. Cells were fixed in 70 % ethanol, stained with DAPI and examined by differential contrast microscopy.



### **Supplementary Figure S1**

Wt cells were incubated with 20 mM HU for 2 h. The cultures were then incubated for a further 2 h in the presence of 200 ng/ml rapamycin or 5  $\mu$ M torin1. Samples were harvested at the indicated time points. Cells were fixed in 70 % ethanol, stained with DAPI and examined by differential contrast microscopy.

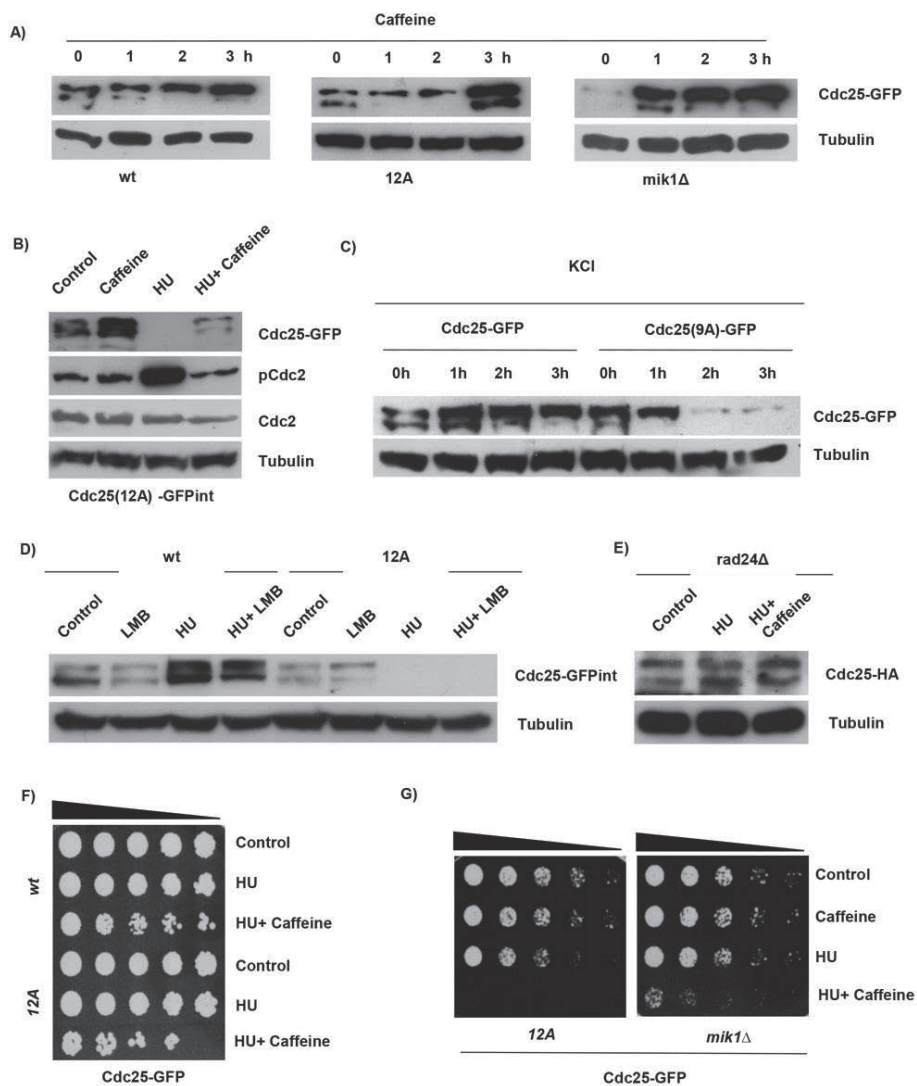


**Fig. 1**

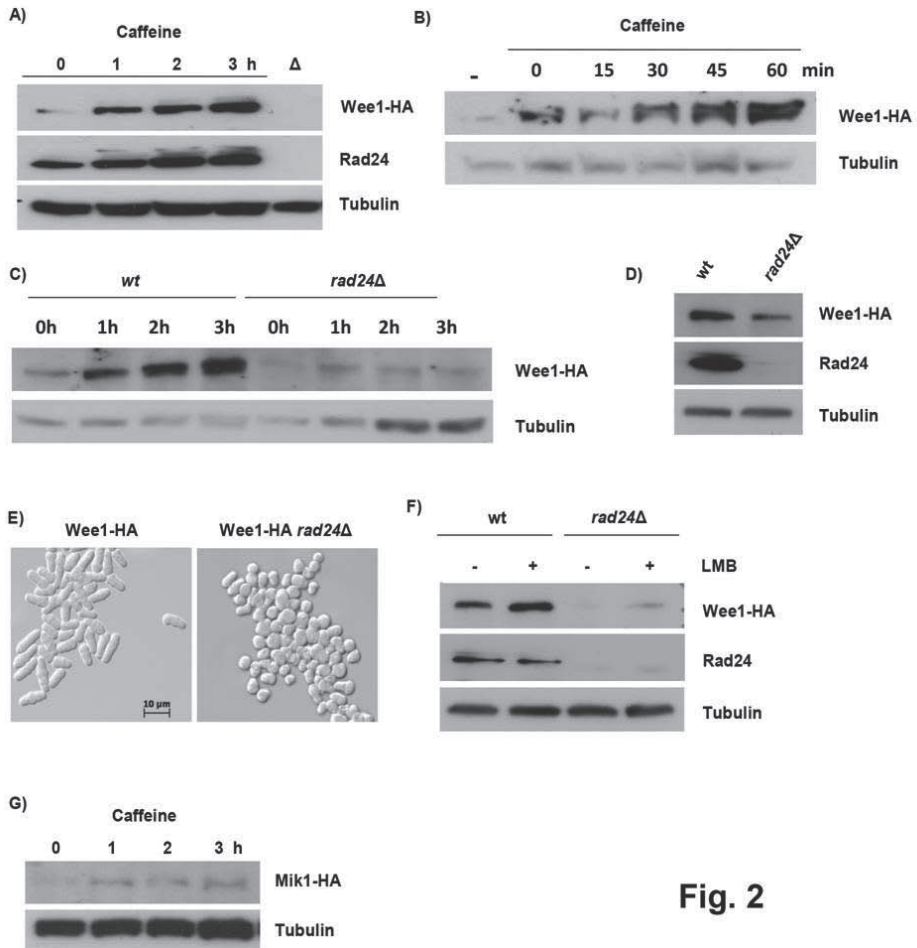


**Fig. 2**

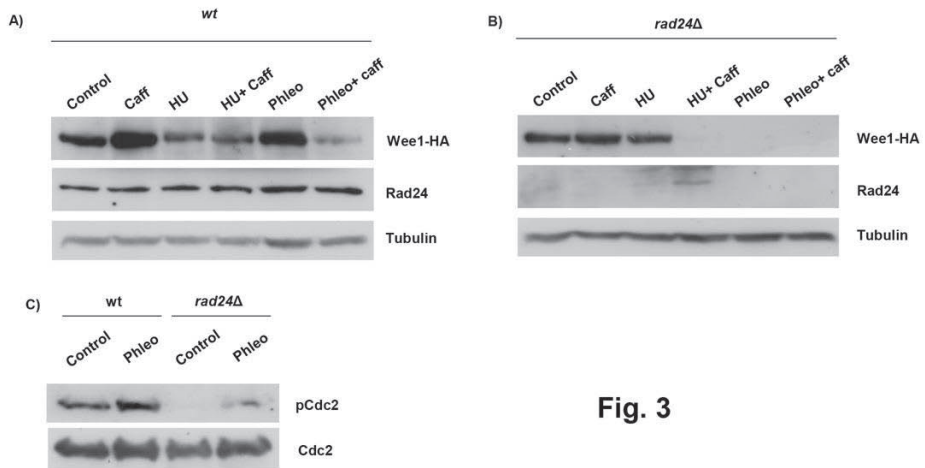


**Fig. 3**

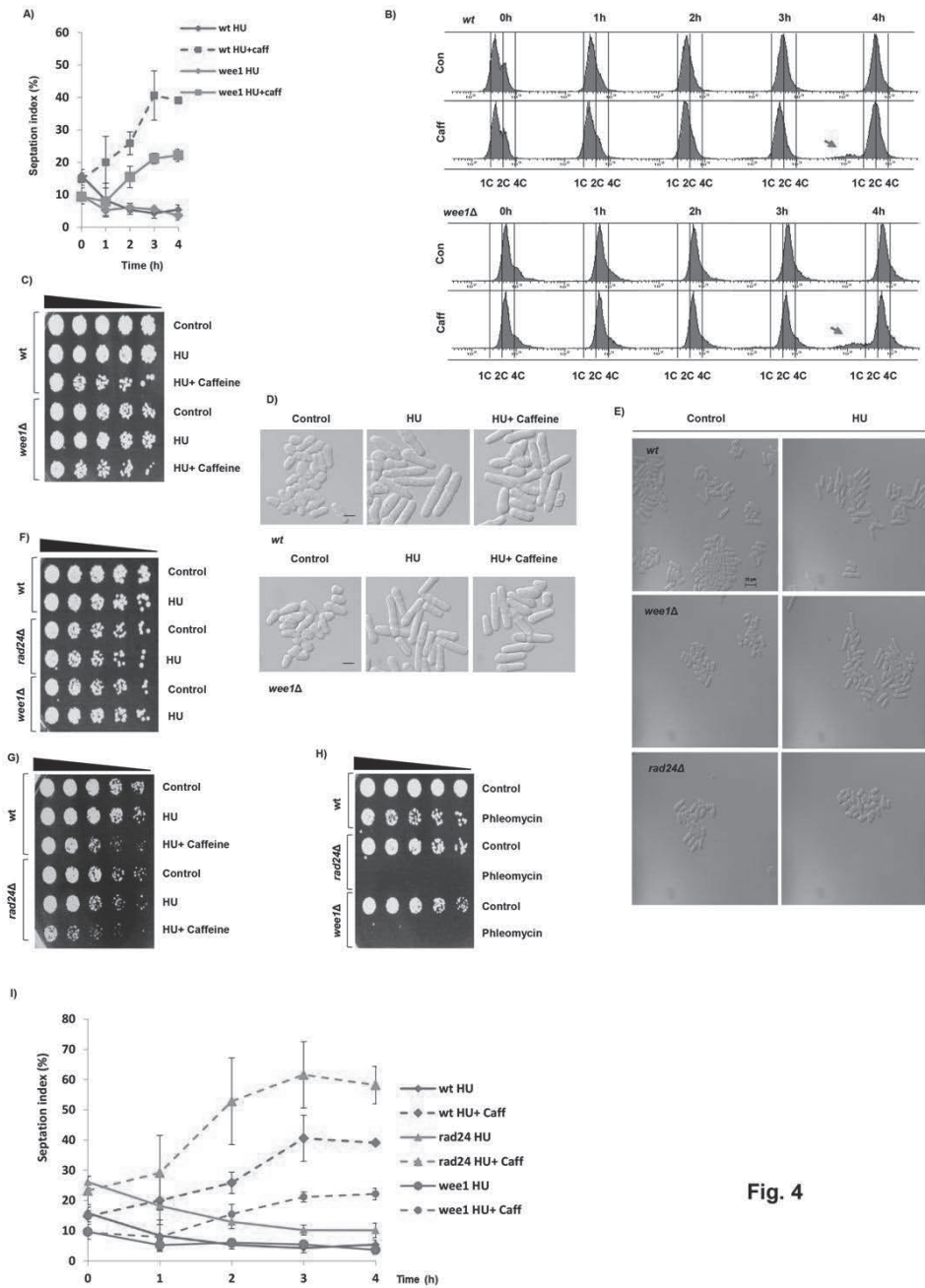


**Fig. 4**

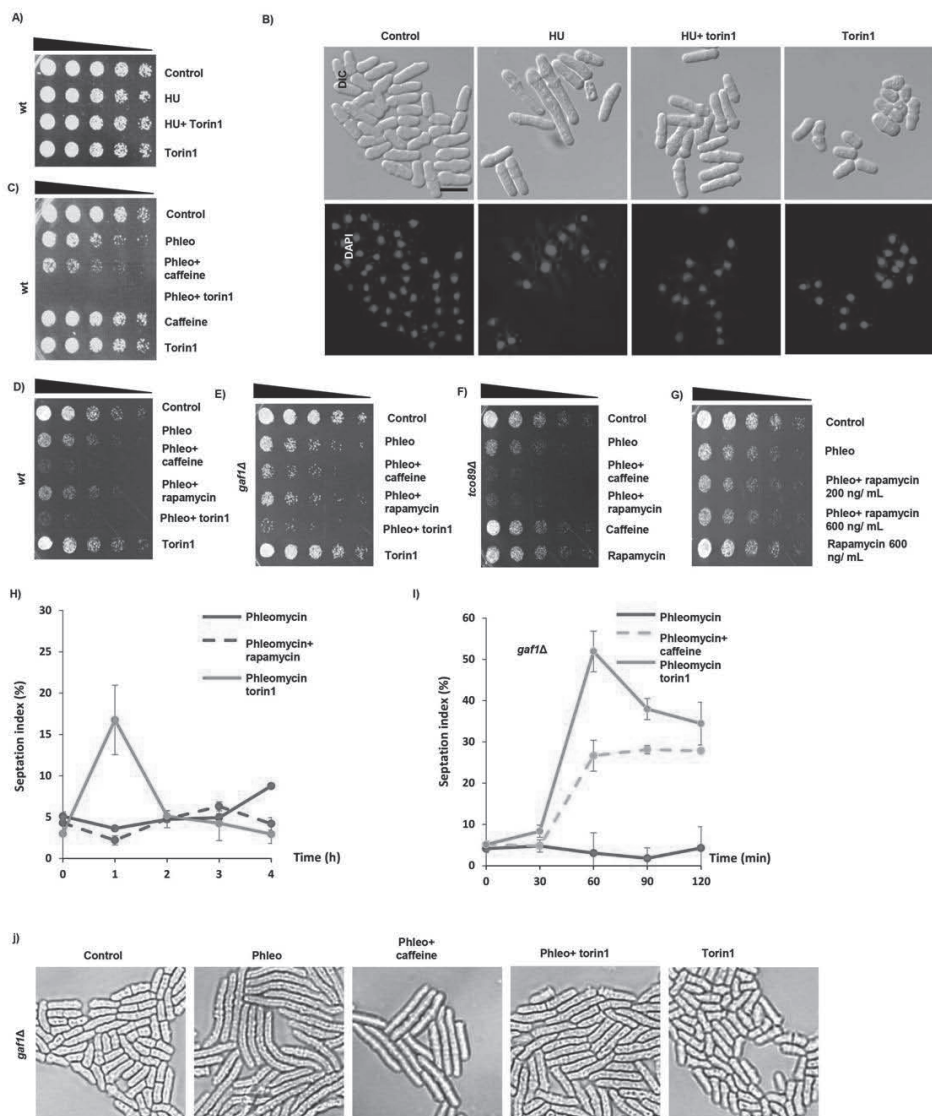
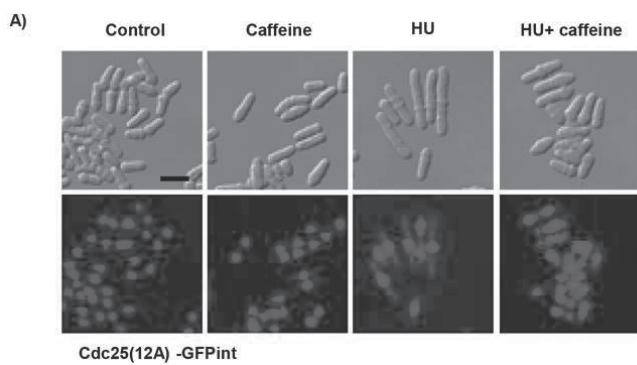


Fig. 5



**Supplementary Fig. S1**






# Paper III



RESEARCH ARTICLE

# The fission yeast FHIT homolog affects checkpoint control of proliferation and is regulated by mitochondrial electron transport

Johanna J. Sjölander and Per Sunnerhagen \*

Department of Chemistry and Molecular Biology, Lundberg Laboratory, University of Gothenburg, P.O. Box 462, Göteborg, SE-405 30, Sweden

## Abstract

Genetic analysis has strongly implicated human *FHIT* (Fragile Histidine Triad) as a tumor suppressor gene, being mutated in a large proportion of early-stage cancers. The functions of the FHIT protein have, however, remained elusive. Here, we investigated *aph1<sup>+</sup>*, the fission yeast homolog of *FHIT*, for functions related to checkpoint control and oxidative metabolism. In sublethal concentrations of DNA damaging agents, *aph1Δ* mutants grew with a substantially shorter lag phase. In *aph1Δ* mutants carrying a hypomorphic allele of *cds1* (the fission yeast homolog of Chk2), in addition, increased chromosome fragmentation and missegregation were found. We also found that under hypoxia or impaired electron transport function, the Aph1 protein level was strongly depressed. Previously, FHIT has been linked to regulation of the human 9-1-1 checkpoint complex constituted by Hus1, Rad1, and Rad9. In *Schizosaccharomyces pombe*, the levels of all three 9-1-1 proteins are all downregulated by hypoxia in similarity with Aph1. Moreover, deletion of the *aph1<sup>+</sup>* gene reduced the Rad1 protein level, indicating a direct relationship between these two proteins. We conclude that the fission yeast FHIT homolog has a role in modulating DNA damage checkpoint function, possibly through an effect on the 9-1-1 complex, and that this effect may be critical under conditions of limiting oxidative metabolism and reoxygenation.

**Keywords:** 9-1-1 complex; Aph1; checkpoint proteins; hypoxia; *Schizosaccharomyces pombe*

## Introduction

Inactivation of *FHIT*, through deletion, point mutation, or DNA methylation, is a very common event in cancer. It occurs in over half of human cancers, in particular in epithelial tumors, of which 70% suffer this impairment (Huebner and Croce, 2001; Saldivar et al., 2011). The first line of arguments for FHIT as a tumor suppressor protein was essentially based on this type of evidence. *FHIT* is located in the *FRA3B* locus, the most inducible fragile region in the human genome, revealing a cytologically distinguishable gap at chromosome 3p14.2 under certain experimental conditions (Durkin et al., 2008). Because of the location at a fragile site, it was initially questioned if FHIT was a true tumor suppressor or just frequently altered. *FHIT<sup>+/-</sup>* mice are, however, much more prone to develop tumors in response to carcinogen treatment (Fong et al., 2000; Zanasi et al., 2001), and both *FHIT<sup>+/-</sup>* and *FHIT<sup>-/-</sup>* mice have a higher frequency of spontaneous

tumor development (Zanasi et al., 2001). The tumor development of FHIT deficient mice can also be partially repressed by *FHIT* gene therapy (Dumon et al., 2001) and re-expression of FHIT in *fhit* deficient cells is able to induce apoptosis (Roz et al., 2002). The *FHIT* gene, or its expression, is commonly lost early in cancer development, and inactivation of *FHIT* is therefore proposed to result in a “mutator” phenotype (reviewed by Waters et al., 2014). Thus, the current view is that *FHIT*, due to its location on a fragile site, is prone to break in replication stress, and that its loss leads to more replication stress as well as to incompetence in appropriately handling new damage (Saldivar et al., 2012). This, in turn, leads to further progression of cancer development.

Though *FHIT* is now fully established as an important tumor suppressor, much less is understood about the actual cellular roles of the FHIT protein, in part because of the low abundance of the FHIT protein. FHIT was first described as a diadenosine 5',5''-P<sub>1</sub>,P<sub>3</sub>-triphosphate

\*Corresponding author: e-mail: per.sunnerhagen@cmb.gu.se

**Abbreviations:** Ap<sub>3</sub>A, diadenosine 5',5''-P<sub>1</sub>,P<sub>3</sub>-triphosphate; Ap<sub>4</sub>A, diadenosine 5',5''-P<sub>1</sub>,P<sub>3</sub>-tetraphosphate; DAPI, 4,6-diamidino-2-phenylindole; DIC, differential interference contrast; Dox, doxorubicin; FHIT, fragile histidine triad; HU, hydroxyurea; PL, phleomycin; ROS, reactive oxygen species; YES, yeast extract with supplement

(Ap<sub>3</sub>A) hydrolase (Murphy et al., 2000). Expression of wt FHIT or a FHIT<sup>H96N</sup> mutant protein, lacking the Ap<sub>3</sub>A hydrolase activity, were however equally effective in abrogating tumor progression (Siprashvili et al., 1997), indicating that it is rather the substrate binding, not cleavage, that is important for the anti-tumor activities. More recently, *in vitro* and *in vivo* studies in *Saccharomyces cerevisiae*, showed that the budding yeast homolog of FHIT, Hnt2 as well as human FHIT catabolize m<sup>7</sup>GpppG dinucleotides generated from the 5'-cap structures from degraded messenger RNAs (mRNAs) (Taverniti and Séraphin, 2015). Inefficient degradation of m<sup>7</sup>GpppG results in elevated concentrations of this intermediate, which has been reported to inhibit mRNA splicing (Izaurrealde et al., 1994) and export to the cytoplasm of nuclear RNAs (Hamm and Mattaj, 1990) as well as to promote mRNA deadenylation (Wu et al., 2009).

The FHIT protein is located in the cytoplasm and nucleus (Zhao et al., 2006) as well as in mitochondria (Druck et al., 2019). In mitochondria, FHIT physically interacts with ferredoxin reductase, and this interaction is important for induction of apoptosis through elevated production of reactive oxygen species (ROS) (Druck et al., 2019). FHIT has also been implicated in regulation of checkpoint responses. In *fhit*<sup>-/-</sup> cells, Chk1 is constitutively hyperactive, resulting in enhanced S and G2 checkpoint responses (Hu et al., 2005). Loss of FHIT also confers lower levels of hHus1 (Ishii et al., 2006), a protein in the 9-1-1 DNA sliding clamp complex involved in DNA damage sensing, DNA repair, and induction of checkpoint control (reviewed by Parrilla-Castellar et al., 2004).

Both fission and budding yeast FHIT orthologs exist. *Schizosaccharomyces pombe* Aph1 has 43% amino acid sequence identity and 55% similarity with human FHIT (Huang et al., 1995), and 41% identity and 57% similarity with Hnt2 of the budding yeast *S. cerevisiae* (Chen et al., 1998). Only limited functional studies have been performed with the yeast orthologs, mostly inspired by the dinucleotide hydrolase activity of the enzymes. For both yeast orthologs, gene disruption leads to strong accumulation of intracellular diadenosine oligophosphate (Ingram and Barnes, 2000; Rubio-Teixeira et al., 2002), and overexpression of *aph1*<sup>+</sup> lowers these concentrations, as expected (Ingram and Barnes, 2000). Studies of *S. cerevisiae* Hnt2 have already shed some light on FHIT function, with the binding and cleavage of the m<sup>7</sup>GpppG cap structures (Taverniti and Séraphin, 2015). In a previous genetic interaction screen (Ryan et al., 2012), Aph1 was found to interact positively with the mitochondrial TOM complex (translocase of the outer membrane) as well as Hus1 in the 9-1-1 checkpoint complex. Studying the FHIT orthologs in budding and fission yeast is a promising starting point for elucidating its molecular functions.

In this study, we wanted to address the function of FHIT through its ortholog Aph1 in the genetically amenable fission yeast. We started by investigating effects on cellular proliferation by a deletion of *aph1*<sup>+</sup>, and found that loss of Aph1 leads to unregulated proliferation of cells exposed to a number of DNA-damaging agents. Furthermore, the combination of *aph1Δ* and a partial defect in the checkpoint protein Cds1 (ortholog of human Chk2) results in elevated chromosome fragmentation and missegregation in doxorubicin (Dox).

The human FHIT interaction with the electron transport chain (Druck et al., 2019) and the Aph1 interaction with the TOM complex (Ryan et al., 2012) inspired us to also investigate a possible dependence of Aph1 levels on oxidative phosphorylation. We found that Aph1 protein levels were strongly downregulated in hypoxia or low glucose levels as well as by blocking mitochondrial electron transport.

As FHIT has been shown to modulate hHus1 expression (Ishii et al., 2006), we investigated a possible link between Aph1 and the 9-1-1 proteins. Aph1 loss additionally resulted in a strong reduction of the Rad1 protein level, indicating a positive regulation of the 9-1-1 complex. Interestingly all three 9-1-1 proteins; Rad1, Hus1, and Rad9, were similarly downregulated in hypoxia.

Altogether it seems that some features are conserved between human FHIT and fission yeast Aph1. Mutation of those genes resulted in unregulated proliferation and DNA damage. That Aph1, in contrast to FHIT (Murphy et al., 2000), prefers to cleave Ap<sub>4</sub>A over Ap<sub>3</sub>A (Ingram and Barnes, 2000), is apparently not important for these conserved functions. Therefore, *S. pombe* should be an attractive model for studies on the anti-proliferative functions of Aph1/FHIT at the cellular level.

## Materials and methods

### *S. pombe* strains and growth conditions

All strains are listed in Table 1. Growth was at 30°C in YES medium, unless indicated otherwise.

### Quantification of growth rate and lag phase

Pre-cultures were grown to saturation density by inoculation in 10 mL YES and growth for 48 h. Stationary phase cultures were thereafter transferred to microtiter plates containing YES with the indicated additions to a final OD<sub>600nm</sub> of 0.125 in 200 μL total volume per well containing either 9 mM hydroxyurea (HU), 0.2 μM phleomycin (PL), or 19 μg/mL Dox. YES alone was used for controls.

**Table 1** *S. pombe* strains used in this study.

Strain	Genotype	Source or reference
972h <sup>-</sup>	h <sup>-</sup>	Lab stock
JJS30	h <sup>-</sup> aph1::KanMX	This work
JJS31	h <sup>-</sup> aph1 <sup>+</sup> ::(HA) <sub>3</sub> :HphMX	This work
JJS32	h <sup>-</sup> rad1 <sup>+</sup> ::(HA) <sub>3</sub> :HphMX	This work
JJS33	h <sup>-</sup> rad1 <sup>+</sup> ::(HA) <sub>3</sub> :HphMX aph1::KanMX	This work
JJS34	h <sup>-</sup> rad1 <sup>+</sup> ::(HA) <sub>3</sub> :HphMX hus1::NatMX	This work
JJS35	h <sup>-</sup> rad1 <sup>+</sup> ::(HA) <sub>3</sub> :HphMX rad9::NatMX	This work
JJS36	h <sup>-</sup> hus1 <sup>+</sup> ::(HA) <sub>3</sub> :HphMX	This work
JJS46	h <sup>-</sup> hus1 <sup>+</sup> ::(HA) <sub>3</sub> :HphMX aph1::KanMX	This work
JJS37	h <sup>-</sup> hus1 <sup>+</sup> ::(HA) <sub>3</sub> :HphMX rad1::NatMX	This work
JJS38	h <sup>-</sup> hus1 <sup>+</sup> ::(HA) <sub>3</sub> :HphMX rad9::NatMX	This work
JJS39	h <sup>-</sup> rad9 <sup>+</sup> ::(HA) <sub>3</sub> :HphMX	This work
JJS40	h <sup>-</sup> rad9 <sup>+</sup> ::(HA) <sub>3</sub> :HphMX aph1::KanMX	This work
JJS41	h <sup>-</sup> rad9 <sup>+</sup> ::(HA) <sub>3</sub> :HphMX rad1::NatMX	This work
JJS42	h <sup>-</sup> rad9 <sup>+</sup> ::(HA) <sub>3</sub> :HphMX hus1::NatMX	This work
NW222	h <sup>-</sup> ade6-216 leu1-32 chk1 <sup>+</sup> ::(HA) <sub>3</sub>	N. Walworth
JJS43	h <sup>-</sup> ade6-216 leu1-32 chk1 <sup>+</sup> ::(HA) <sub>3</sub> cds1Δ::KanMX	This work
JJS44	h <sup>-</sup> ade6-216 leu1-32 chk1 <sup>+</sup> ::(HA) <sub>3</sub> cds1::(myc) <sub>9</sub> :HphMX	This work
JJS45	h <sup>-</sup> ade6-216 leu1-32 chk1 <sup>+</sup> ::(HA) <sub>3</sub> cds1::(myc) <sub>9</sub> :HphMX aph1::KanMX	This work

Air-permeable film (Breathe-Easy, Diversified Biotech, Boston, USA) was used instead of a lid, as differential oxygenation depending on the position of the plate affected results in the growth experiments. Cell growth with high-intensity shaking was monitored every 20 min. in a Bioscreen Analyzer C (Growth Curves USA) for 72 h as described (Warringer and Blomberg, 2003). Raw data were processed with the PRECOG tool (Fernandez-Ricaud et al., 2016).

#### HU and UV survival tests

Logarithmically growing cells (OD<sub>600nm</sub> ≈ 0.5) were diluted to OD<sub>600nm</sub> = 0.3, and serially diluted 1:3 in a 96 well plate. From each well, 5 μL was plated onto YES agar with or without 5 mM HU. Irradiation with UV at 254 nm was 200 μJ/cm<sup>2</sup>.

#### Microscopy

Evaluation of chromosome fragmentation/misseggregation: cells were fixed with ethanol and stained with 4',6-diamidino-2-phenylindole (DAPI) essentially, as described (Alao et al., 2014). Images were obtained with a Zeiss AxioCam on a Zeiss Axioplan 2 microscope with a ×100 objective, using the appropriate filter (DAPI or DIC). For quantifications at least 200 cells/replicate was counted. Three independent experiments were quantified.

Survival assay with propidium iodide (PI): Live cells were, at the indicated time point, stained with 10 μg/mL PI and subjected for analysis by microscopy. Images were obtained with a Zeiss AxioCam on a Zeiss Axioplan 2

microscope with a ×100 objective, using the appropriate filter (red fluorescence or DIC). For quantifications, at least 200 cells/replicate were counted. Three independent experiments were quantified.

#### Growth in hypoxia

Hypoxic conditions were generated by continuously leading nitrogen gas into the liquid medium. Nitrogen gas was first led through a tube down into distilled water, to moisten the gas, and then further into a closed chamber with multiple tubing, equally distributing the gas into each culture, with the same total volume, within the same experiment.

#### Western blot

Cell pellets were collected by centrifugation and snap-frozen on dry ice. Cells were thawed on ice and lysed by shaking with acid-washed glass beads in a FastPrep FP120 device (Savant) at speed 5 for 30 s. Lysis was performed in lysis buffer A (50 mM NaCl, 50 mM Tris pH 7.6, 0.2% Triton X-100, 0.25% NP40) containing phosphatase inhibitor cocktail 04906837001 and protease inhibitor cocktail 04693159001 (Roche). Protein concentration was determined using the BCA assay. Equal protein concentrations of each sample were loaded and proteins were separated on a sodium dodecyl sulfate-polyacrylamide gel electrophoresis (SDS-PAGE) and blotted onto nitrocellulose membranes.

HA epitope-tagged versions of Aph1, Rad1, Hus1-, and Rad9 as well as Chk1 were detected by mouse anti-HA

Sc7392 (Santa Cruz Biotechnology) or mouse anti-HA 2367 S from Cell Signaling Technology (Bionordika AB, Stockholm, Sweden). Cds1 was detected using Mouse anti-c-myc Sc40 (Santa Cruz Biotechnology). To be able to detect the low-abundance Aph1 protein, incubation with the primary antibody was for 72 h. The loading control was  $\alpha$ -tubulin detected by mouse anti- $\alpha$ -tubulin T5168 (Sigma), or staining of total protein with Ponceau S Solution (Sigma). The secondary antibody was horseradish peroxidase-coupled  $\alpha$ -mouse A4416 (Sigma).

## Results

### Deletion of *aph1*<sup>+</sup> leads to proliferation in sublethal concentrations of genotoxins

The starting point in this assay was a stationary phase culture (48 h from inoculation), diluted into fresh YES media for reinitiating of growth. We used a Bioscreen C analyzer (Growth curves USA) to generate multiple

independent growth curves simultaneously. *aph1* $\Delta$  cells always re-entered growth slightly earlier than wt in control conditions (Figure 1A). In the presence of the genotoxic compounds PL (Figure 1B), Dox (Figure 1C) or HU (Figure 1D), *aph1* $\Delta$  cells displayed a much shorter lag, and also reached a higher cell density compared to wt *972h*<sup>-</sup> cells in PL and HU (Figures 1B and 1D). Thus, *aph1* $\Delta$  mutants are clearly more prone to restart growth under genotoxic conditions, showing that proliferation control is deregulated in this mutant.

### Aph1 is needed for adaptation to stationary phase

We investigated survival in a density saturated culture. We inoculated cells in liquid YES media to an OD<sub>600</sub> of 0.3, and thereafter evaluated survival by a propidium iodide (PI) permeability/exclusion assay, where intact cells exclude PI (Moreno et al., 1991). After 24 h, where wt and *aph1* $\Delta$  were approximately reaching maximum density, survival was indistinguishable between wt and *aph1* $\Delta$ , whereas after 72 h, more *aph1* $\Delta$  cells were PI

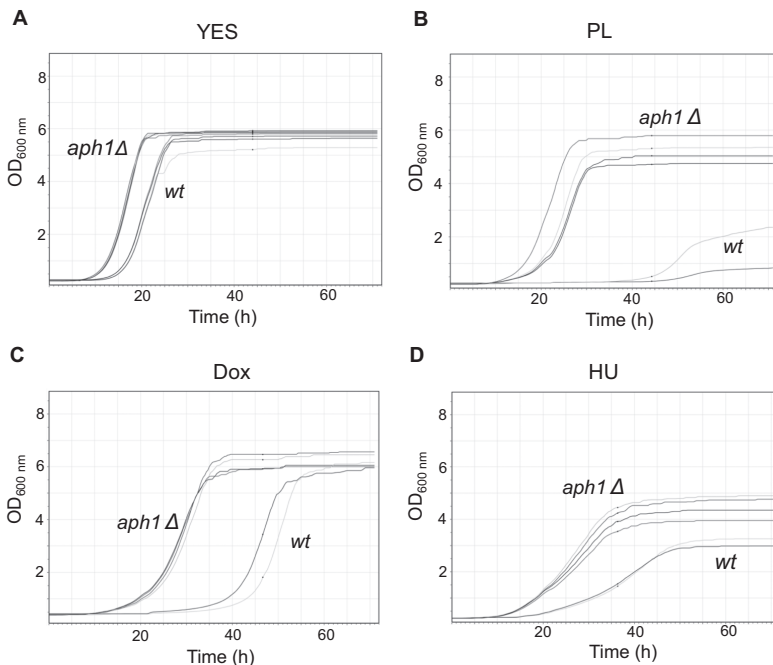


**Figure 1** Loss of Aph1 leads to unregulated proliferation in sublethal concentrations of genotoxic agents. Stationary phase cultures of wt (*972h*<sup>-</sup>) and *aph1* $\Delta$  (JJS30), 48 h from inoculation, were re-diluted in fresh media containing YES with or without genotoxins for re-entry of growth for 72 h. Multiple individual curves from independent precultures are shown from the Bioscreen C analyzer. Treatments were (A) YES alone; (B) YES containing 0.2  $\mu$ M PL; (C) YES with 19  $\mu$ g/mL Dox; (D) YES with 9.5 mM HU.

permeable (Figure S1A), indicating lower survival in the prolonged stationary phase in cells lacking Aph1. This implies that *aph1Δ* has a problem adapting to a non-proliferation mode, which may explain why *aph1Δ* mutants reinitiate growth earlier also in the control conditions in the Bioscreen (Figure 1A).

We also followed the expression of Aph1 protein during growth from the early logarithmic phase to the stationary phase. The Aph1 protein level was rising throughout the course (up to  $OD_{600nm} = 2.5$ ), but in the stationary phase ( $OD_{600nm} = 9.9$ ), Aph1 protein was undetectable (Figure S1B). Thus, Aph1 levels build up during proliferation and sharply decline when cells cease growth. One interpretation of the above findings is that a graded expression during proliferation and non-proliferation aids to appropriately adapt between growth and non-growth.

### Aph1 influences checkpoint control

As FHT function has been shown to modulate Chk1 and Chk2 activation (Ishii et al., 2006; Yutori et al., 2008), two important kinases involved in checkpoint control, we introduced a (Myc)<sub>9</sub> epitope tag to the C-terminal of Cds1. This was done with the purpose of following the Cds1 protein band shift upon activation through phosphorylation by Rad3 (Lindsay et al., 1998) in a genetic background that already had a HA tag on Chk1, for following Chk1 activation that also results in a band shift (Walworth and Bernards, 1996). Although we did observe the expected band shift upon Cds1 activation (Figure S2A), unexpectedly, the introduction of the Myc<sub>(9)</sub> tag partially interfered with Cds1 function (Figure S2B). Activation of Chk1 by HU was seen in the double-tagged strain, indicating that DNA damage activated Chk1 to compensate for the loss of Cds1. Chk1 is normally not activated by HU, but is known to be activated by HU in *cds1Δ* (Lindsay et al., 1998). This was paralleled by the survival on 5 mM HU plates, where the sensitivity of this *chk1-HA cds1-(myc)<sub>9</sub>* strain was intermediate between the *chk1-HA* strain and the *chk1-HA cds1Δ* strain (Figure S2B). Deletion of *aph1<sup>+</sup>* in a *chk1-HA cds1-(myc)<sub>9</sub>* background did suppress a growth delay in HU (Figure S2D) and Dox (Figure 2A). However, *aph1Δ* in this background gave no clear additional phenotype on survival in HU (Figure S2D). When inspecting cells in the microscope after 72 h growth in 19 μg/mL Dox, the frequency of cells with cut and/or fragmented chromosomes was clearly higher in *aph1Δ* than in wt cells (Figure 2B). Among cells with cut/fragmented chromosomes, the defect was more pronounced in *aph1Δ* with some cells having no nuclei staining but only punctuate cytoplasmic staining with DAPI (Figure 2B, see white arrows in DAPI picture of *chk1-HA cds1-(myc)<sub>9</sub> aph1Δ*).

Even though the *aph1Δ* knockout in the strain carrying the partially defective *cds1-(myc)<sub>9</sub>* allele resulted in an increased frequency of fragmented/cut chromosomes in the presence of genotoxins, proliferation thus continued unabated, indicating loss of cell cycle checkpoint control. It is therefore plausible that the Aph1 is involved in checkpoint control of proliferation.

### Aph1 protein expression is suppressed by hypoxia

Knowing that FHT is partially localized in mitochondria (Druck et al., 2019), and that the FHT-controlled microRNA miR-30c is suppressed under hypoxic conditions (Huang et al., 2013), we speculated that Aph1/FHT expression may be influenced by the oxygenation status of the cells. We investigated Aph1 levels in cells growing in hypoxia, as described in the Materials and Methods section. As seen in Figure 3A, after 2 h in hypoxic conditions, the Aph1 protein level is strongly reduced, and after 3 h, Aph1 is virtually absent. This process is reversible, as restoring normoxia brings Aph1 back to near-normal levels within 2 h (Figure 3A). To ascertain whether this effect was due to the oxygenation status, we used a different method to produce hypoxia, the reducing agent sodium dithionite. At higher concentrations, upwards of 1 mM, exposure to dithionite for 2 h had the same effect on Aph1 as displacing air with nitrogen gas (Figure 3B). To examine whether these effects on Aph1 were due to decreased respiratory activity, we used the electron transport chain poison azide. As seen in Figure 3C, treating cells for 2 h with sodium azide also caused Aph1 protein to decrease. Importantly, even at the highest azide concentration (0.5 mM), the optical density of the culture was increasing, demonstrating that the cells were still alive. This indicates that it is not the redox state of the environment *per se* that causes the reduction of Aph1, but rather the activity of the mitochondrial electron transport chain. To further investigate the relationship between the Aph1 level and energy metabolism rate, we reduced the glucose concentration in the medium for exponentially growing cells. As seen in Figure 3D, a reduction of glucose concentration from 3% to 0.3% caused a marked reduction of Aph1 within 1 h, and after 2 h the Aph1 level was even lower. Reducing glucose to 0.1% or eliminating it altogether results in further drops of Aph1 protein levels. Together, these observations establish a strong correlation between electron transport chain activity and the level of Aph1 protein.

### Expression of Rad1 is dependent on Aph1

In logarithmically growing unstressed *aph1Δ* cells, the Rad1 level was strongly reduced compared to wt. The expression of Rad9 and Hus1 was virtually unaltered in *aph1Δ* mutants, however (Figure 4A).

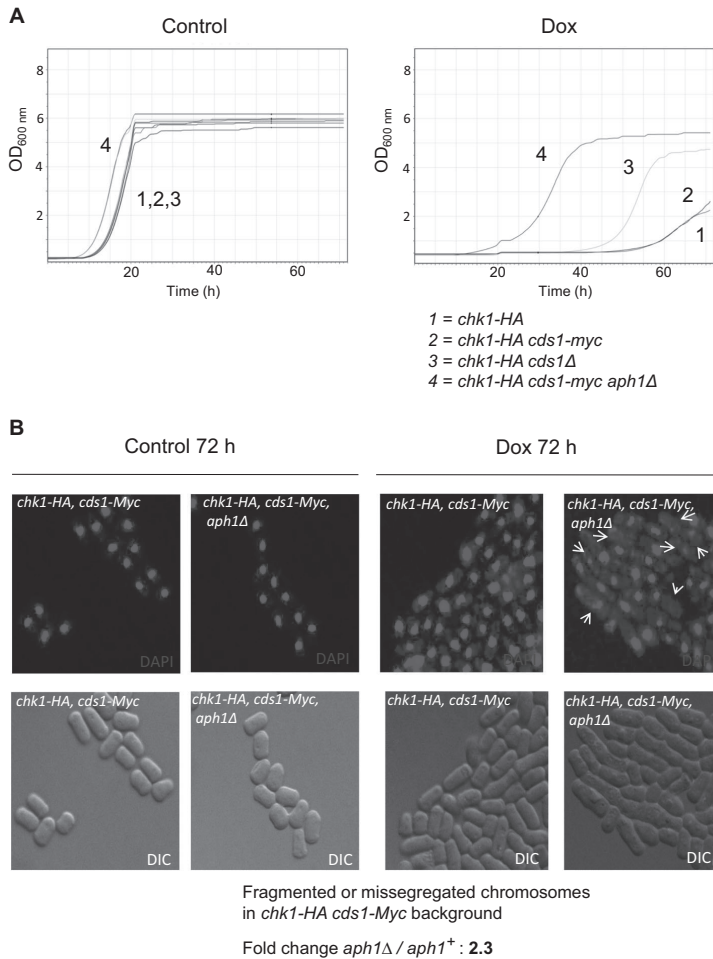


**Figure 2** Loss of Aph1 leads to checkpoint control override in cells carrying a *cds1* hypomorphic allele leading to elevated chromosome fragmentation in doxorubicin. The *aph1Δ* allele in a *chk1-HA cds1-(myc)<sub>9</sub>* background leads to a shorter lag phase and growth to higher densities. Stationary phase cultures of *chk1-HA* (NW222), *chk1-HA cds1-(myc)<sub>9</sub>* (JJS44), *chk1-HA cds1Δ* (JJS43), and *chk1-HA cds1-(myc)<sub>9</sub> aph1Δ* (JJS45), 48 h from inoculation, were re-diluted in fresh media containing YES with or without Dox for re-entry of growth 72 h in a Bioscreen C analyzer. (A) Representative growth curves. Treatments were YES only or 19 μM Dox. (B) The higher proliferation in *chk1-HA cds1-(myc)<sub>9</sub> aph1Δ* (JJS45) was accompanied by elevated chromosome fragmentation and/or missegregation. Cells from *chk1-HA cds1-(myc)<sub>9</sub> aph1Δ* (JJS45) were fixed in ethanol after 72 h of growth, stained with 4',6-diamidino-2-phenylindole (DAPI) and evaluated by microscopy for fragmentation and missegregation. Cells from three independent Bioscreen experiments were collected by centrifugation, cleared of growth media and vortexed in 70% ethanol for 30 s. This was done directly at the end of the 72 h Bioscreen run. Representative pictures of DAPI-stained cells are shown. Note that although there is some missegregation present in Dox-treated *chk1-HA cds1-(myc)<sub>9</sub> wt* (JJS44), this phenotype is much stronger in *cds1-(myc)<sub>9</sub> aph1Δ* (JJS45) where some cells (white arrows) appear to lack nuclei entirely. For quantification of cells with fragmented and/or cut chromosomes, at least 200 cells were counted for each of the three replicates.



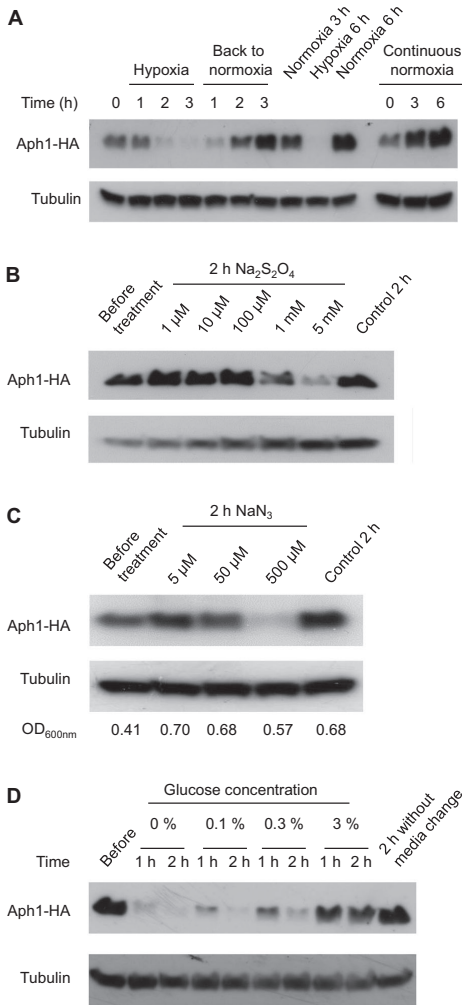


**Figure 3** Aph1 is downregulated in conditions of low mitochondrial electron transport. Logarithmically growing *aph1-HA* (JJS31) cells were subjected to different treatments and analyzed by western blotting. (A and B) Hypoxia results in a reversible decrease in the Aph1 protein level. (A) Cells were subjected to either hypoxia induced by leading N<sub>2</sub> into the culture or normoxia. (B) Cells were subjected to hypoxia introduced by dithionite of the indicated concentration for 2 h. (C) Blocking of mitochondrial electron transport by addition of sodium azide leads to a reduction in Aph1 protein level. Cells were treated with NaN<sub>3</sub> of the indicated concentration for 2 h. (D) Reducing the glucose level in media also lowers the Aph1 protein level. Cells were subjected to a media change where the new medium contained different glucose concentrations.

In *rad1Δ* and *rad9Δ* mutants, the level of Hus1 is markedly suppressed; likewise, Rad9 levels are suppressed in *rad1Δ* and *hus1Δ* mutants (Figure 4B). By contrast, deletion of *rad9<sup>+</sup>* or *hus1<sup>+</sup>* does not appreciably affect the expression of Rad1. Thus, Rad1 influences expression of the other two 9-1-1 proteins, but not vice versa; this pattern is analogous to what has been observed for the human 9-1-1 orthologs (Bao et al., 2004).

Considering these findings in combination with our data showing lower levels of Rad9 and Hus1 in *rad1Δ* mutants (Figure 4A), it appears that Aph1 has a more direct influence on Rad1 levels than on the other 9-1-1 proteins (Figure 4C). Furthermore, while eliminating Rad1 altogether (as in *rad1Δ* mutants, Figure 4B) does suppress Rad9 and Hus1 levels, reducing Rad1 partially (as in *aph1Δ* mutants, Figure 4A) is not enough to achieve this effect.

**The 9-1-1 proteins are, like Aph1, downregulated in hypoxia**

Given the effects on the Rad1 level of deleting *aph1<sup>+</sup>*, the effect of deleting *rad1<sup>+</sup>* on the levels of other 9-1-1 proteins, and our finding that hypoxia causes depletion of Aph1 protein; it is natural to ask whether hypoxia also affects the levels of the 9-1-1 proteins. As shown in Figure 4D, there was indeed a clear drop in the levels of all three 9-1-1 proteins within 2–3 h after purging oxygen from the medium.

**Discussion**

We have shown that *aph1Δ* mutants restart growth from the stationary phase at a much earlier point when exposed to various genotoxic agents (PL, HU, and Dox) than wt (Figures 1B–D), indicating that elimination of Aph1 results in unresponsiveness to checkpoint control. The *aph1Δ* mutants also reentered growth slightly earlier even in normal conditions (Figure 1A), indicating that deleting *aph1<sup>+</sup>* results in a phenotype also generally more prone to restart growth from a non-proliferating state. We further noted that *aph1Δ* cells are defective in adapting to the stationary phase, as seen by the defective survival in the prolonged stationary phase (Figure S1). Thus, the rapid re-entry into proliferation from the stationary phase may represent the fact that mutant cells are still partially set for proliferation, from the previous logarithmic phase.

In the case of combining a partially defective *cds1-Myc* allele with *aph1Δ* (Figure S2), the shorter lag and higher yield seen in Dox (Figure 2A) was also accompanied by a higher fraction of fragmented and/or cut chromosomes in Dox compared to that in the partially defective *cds1-Myc* allele alone (Figure 2B). These observations, together, point

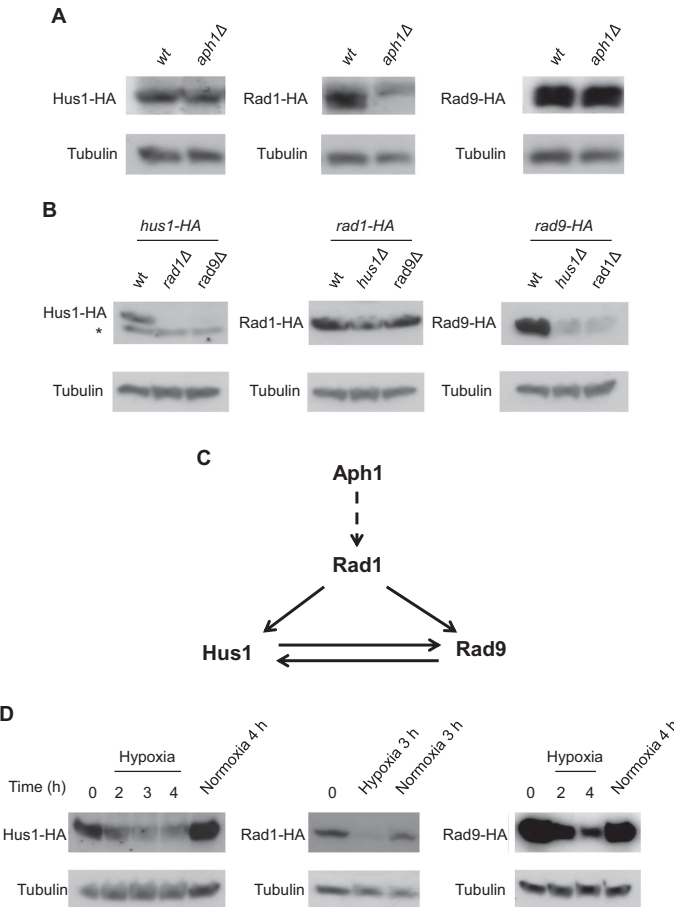


**Figure 4** Aph1 regulates the level of Rad1, and all 9-1-1 proteins are downregulated in hypoxia. Logarithmic growing cells expressing C-terminally (HA)<sub>3</sub> tagged versions of Hus1, Rad1, and Rad9 from their endogenous promoters were subjected to different treatments or investigated in different genetic backgrounds, and analyzed by western blotting. (A) Rad1, but not Hus1 or Rad9 protein levels, is reduced by deleting *aph1*<sup>+</sup>. Strains used were *hus1-HA* (JJS36), *hus1-HA aph1Δ* (JJS46), *rad1-HA* (JJS32), *rad1-HA aph1Δ* (JJS33), *rad9-HA* (JJS39), *rad9-HA aph1Δ* (JJS40). (B) Hus1 and Rad9, but not Rad1 protein levels are reduced by the absence of one other 9-1-1 complex member. Strains used were *hus1-HA* (JJS36), *hus1-HA rad1Δ* (JJS37), *hus1-HA rad9Δ* (JJS38), *rad1-HA* (JJS32), *rad1-HA hus1Δ* (JJS34), *rad1-HA rad9Δ* (JJS35), *rad9-HA* (JJS39), *rad9-HA hus1Δ* (JJS42), *rad9-HA rad1Δ* (JJS41). (C) Model based on the results from A and B, showing Aph1 regulation of the 9-1-1 complex through the Rad1 protein level. (D) The protein levels of Hus1, Rad1, and Rad9 are all down-regulated in hypoxia. Hypoxia was induced by leading N<sub>2</sub> gas into cultures of cells from strains *hus1-HA* (JJS36), *rad1-HA* (JJS32) and *rad9-HA* (JJS39). \*marks a non-specific background band detected by the anti-HA antibody.

towards a role for Aph1 in cell cycle checkpoint control under genotoxic conditions.

Human FHIT has been shown to be located in the cytosol, nucleus (Zhao et al., 2006) and mitochondria (Druck et al., 2019). Aph1 is located in the cytosol and nucleus (Matsuyama et al., 2006), and is predicted by its similarity to the budding yeast Hnt2, but not actually

shown, to also be present in mitochondria. We have not investigated the localization of Aph1 in fission yeast, however, its strong dependence on oxygenation (Figures 3A and 3B), and on a functioning mitochondrial electron transport chain (Figure 3C) are indications of an Aph1 pool within the mitochondria. The human FHIT mitochondrial pool physically interacts with ferredoxin

reductase, and this interaction has been proposed to confer a higher ROS production leading to induction of apoptosis (Druck et al., 2019). In the unicellular organism *S. pombe*, there are indications of programmed cell death with characteristics reminiscent of apoptosis (Su et al., 2017). We have not investigated if there is a link between Aph1 and programmed cell death in *S. pombe*; however, our observations with the dysregulated restart of proliferation in sublethal concentrations of DNA-damaging agents (Figures 1 and 2, Figure S2C), and failure of efficient adaptation to non-growth upon nutrient limitation (Figure S1), rather point towards a role for Aph1 in control of proliferation. We, therefore, propose that Aph1 links aerobic respiration in mitochondria with proliferation control under genotoxic conditions as well as in nutrient limitation. The earlier observation that overexpression of Aph1 leads to longer generation time (Ingram and Barnes, 2000) is in line with the anti-proliferative functions for *S. pombe* Aph1.

Human FHIT preferentially hydrolyzes Ap<sub>3</sub>A over Ap<sub>4</sub>A (Murphy et al., 2000). As a FHIT<sup>H96N</sup> mutant protein binds Ap<sub>3</sub>A efficiently, but has a strong catalytic defect, and nevertheless maintains the anti-tumor capabilities of FHIT (Siprashvili et al., 1997), the leading hypothesis has been that FHIT bound to its substrate constitutes the active tumor suppressor signaling unit. In contrast to human FHIT, *S. pombe* Aph1 prefers to hydrolyze Ap<sub>4</sub>A over Ap<sub>3</sub>A (Ingram and Barnes, 2000). Despite this difference, *aph1Δ* mutants display unrestrained restart of growth in genotoxic conditions (Figures 1 and 2), indicating that this difference is not important for the anti-proliferative functions of Aph1.

FHIT has been shown to regulate both the levels (Kiss et al., 2018) and the translation of mRNAs important in cancer development (Kiss et al., 2017a). Thus, it is plausible that some of the biochemical basis for the tumor suppressor functions of FHIT is through its actions on mRNAs (Kiss et al., 2017b). As the binding rather than hydrolysis of the substrate seems to be important for the anti-tumor functions of FHIT, one can also not exclude the fact that other substrates similar in structures to Ap<sub>3</sub>A and m<sup>7</sup>GpppG may be important for FHIT cellular functions. In human cells, it was recently shown that FHIT positively regulates TK1 (Thymidine kinase 1) by stimulation of translation of *TK1* transcripts (Kiss, Waters et al., 2017b) as well as a number of other important tumor suppressor transcripts (Kiss et al., 2017a). The reduction of TK1 leads to replication stress and the DNA strand breaks because of a reduction in the dTTP pool (Saldivar et al., 2012). The stimulation of TK1 translation is interestingly linked to the binding of FHIT to m<sup>7</sup>GpppN cap structures (Kiss et al., 2017b) rather than to the substrate Ap<sub>3</sub>A. Importantly the FHIT<sup>H96N</sup> mutant protein, which has no catalytic activity against Ap<sub>3</sub>A nor to m<sup>7</sup>GpppG (Taverniti and Séraphin,

2015), is as effective in stimulation of translation as the wt version. Similarly wt FHIT and the FHIT<sup>H96N</sup> mutant proteins are equally effective in preventing DNA damage, whereas another mutant allele, FHIT<sup>Y114F</sup>, defective in m<sup>7</sup>GpppG binding, was defective in this function (Kiss et al., 2017b). Therefore, the translational impact on *TK1* may be through binding to 5' cap structures either generated by 3'-5' mRNA decay, that may otherwise compete for eIF4E binding as proposed (Kiss et al., 2017b), or to the 5' cap while still on intact mRNA. As we have shown that Aph1 positively regulates Rad1 in the 9-1-1 complex (Figure 4A), it would be interesting to see if this occurs through binding to 5' cap structures, as for FHIT in the regulation of *TK1*.

Deleting *aph1*<sup>+</sup> resulted in a strong reduction of the Rad1 protein level (Figure 4A), confirming a link between Aph1 and the 9-1-1 complex. As the 9-1-1 complex is a heterotrimer (Dore et al., 2009), this should result in a lower pool of this important complex. This parallels the finding that suppression of human FHIT levels leads to downregulation of the 9-1-1 protein hHus1 (Ishii et al., 2006). Deletion of Rad1 resulted in downregulation of both Rad9 and Hus1 protein levels, whereas deletion of Rad9 and Hus1 did not significantly affect the Rad1 level (Figure 4B). The link between Aph1 and the 9-1-1 complex seems to be through Rad1, as *aph1Δ* mutants showed a reduced Rad1 protein level, however, not those of the other two 9-1-1 constituents (Figure 4B). Thus, the reduction in Rad1 protein level seen in *aph1Δ* did not reduce Hus1 or Rad9 levels, indicating that the low Rad1 level still present in *aph1Δ* is enough to sustain Hus1 and Rad9 levels. Interestingly all three 9-1-1 proteins were downregulated in hypoxia (Figure 4D) similar to Aph1 (Figures 3A and 3B), indicating that cells reentering to normal oxygenation from hypoxia may have to face the higher oxygen level with a lagging 9-1-1 complex level, potentially resulting in DNA damage.

We have characterized some aspects of the regulation of Aph1 protein level in fission yeast with respect to growth conditions such as the growth phase, oxygenation, and glucose availability (Figure 3 and Figure S1B). The downregulation of the *S. pombe* Aph1 protein level in hypoxia is reversed when regaining normoxia (Figure 3A). It is unknown if human FHIT is also regulated by oxygen availability and activity of electron transport. FHIT is however downregulated in human pulmonary arterial hypertension (PAH), and FHIT positively regulates BMPR2 (bone morphogenetic protein receptor type 2), also downregulated in PAH, and important for the development of PAH (Dannewitz Prosseda et al., 2019). Pulmonary hypertension (PH) can be caused by hypoxia (Weitzenblum and Chaouat, 2001) or conditions mimicking hypoxia by high NO production leading to

inhibition of mitochondrial electron transport and induction of Hif1 $\alpha$  (hypoxia-inducible factor  $\alpha$ ) (Fijalkowska et al., 2010). An emerging “metabolic theory of PAH” states that also PAH may be caused by mitochondria-based metabolic abnormalities resulting in reduced oxidative phosphorylation (Paulin and Michelakis, 2014). This indicates that FHIT may also be downregulated in hypoxia, or in other conditions leading to blockage of mitochondrial electron transport. We, therefore, speculate that FHIT/Aph1 downregulation in lower oxygen and upregulation when oxygen returns may both be important in hypoxia and reoxygenation. In agreement with this, FHIT<sup>-/-</sup> mice had more severe pulmonary hypertension and this was not reversed in normoxia, as opposed to in FHIT<sup>+/+</sup> mice (Dannewitz Prosseda et al., 2019). If FHIT is important for the appropriate cellular responses to hypoxia/reoxygenation, loss of these functions would be important also in cancer development, where hypoxia is a common feature even in small tumors (Li and O’Donoghue, 2008), and where reoxygenation of hypoxic cancer cells from tumors results in a high colonization ability (Young and Hill, 1990). Mammalian FHIT also positively regulates the miR-30c microRNA. Through this action on miR-30c, FHIT counteracts the epithelial–mesenchymal transition (EMT) in human lung cancer cells (Suh et al., 2014). Hypoxia induces downregulation of miR-30c (Huang et al., 2013), and this downregulation promotes EMT in human carcinoma cells. It is thus a credible notion that the suppression of Aph1 expression in hypoxia that we have observed similarly affects the expression of other gene products, as the Aph1 reduction in hypoxia (Figure 3A) is correlated with strongly reduced protein levels of all three 9-1-1 proteins (Figure 4D).

## Conclusions

Historically, fission yeast has been an important starting point for elucidating basic cell cycle and checkpoint mechanisms. Altogether, it seems that some aspects are conserved between fission yeast Aph1 and human FHIT, including anti-proliferative functions, regulation of the 9-1-1 complex, and a likely association with the mitochondrial electron transport chain. Aph1 in fission yeast, with its extensive possibilities for genetic analysis, should, therefore, be an excellent model to elucidate the biological role of the human FHIT protein.

## Acknowledgments and funding

This work was supported by grants from the Royal Society of Arts and Sciences, Sigurd and Elsa Goljes Minne and the Lennander’s Foundations to J.J.S., and from the Swedish Cancer Fund (2013-512 and 2016-378) to P.S.

## References

- Alao JP, Sjölander JJ, Baar J, Özbaki-Yagan N, Kakoschky B, Sunnerhagen P (2014) Caffeine stabilizes Cdc25 independently of Rad3 in *Schizosaccharomyces pombe* contributing to checkpoint override. *Mol Microbiol* 92: 777–96, <https://doi.org/10.1111/mmi.12592>
- Bao S, Lu T, Wang X, Zheng H, Wang LE, Wei Q, Hittelman WN, Li L (2004) Disruption of the Rad9/Rad1/Hus1 (9-1-1) complex leads to checkpoint signaling and replication defects. *Oncogene* 23: 5586–93, <https://doi.org/10.1038/sj.onc.1207753>
- Chen J, Brevet A, Blanquet S, Plateau P (1998) Control of 5',5'-dinucleoside triphosphate catabolism by APH1, a *Saccharomyces cerevisiae* analog of human FHIT. *J Bacteriol* 180: 2345–9.
- Dannewitz Prosseda S, Tian X, Kuramoto K, Boehm M, Sudheendra D, Miyagawa K, Zhang F, Solow-Cordero D, Saldívar JC, Austin ED, Loyd JE, Wheeler L, Andruska A, Donato M, Wang L, Huebner K, Metzger RJ, Khatri P, Spiekerkoetter E (2019) FHIT, a novel modifier gene in pulmonary arterial hypertension. *Am J Respir Crit Care Med* 199: 83–98, <https://doi.org/10.1164/rccm.201712-2553OC>
- Doré AS, Kilkenny ML, Rzechorzek NJ, Pearl LH (2009) Crystal structure of the Rad9-Rad1-Hus1 DNA damage checkpoint complex- implications for clamp loading and regulation. *Mol Cell* 34: 735–45, <https://doi.org/10.1016/j.molcel.2009.04.027>
- Druck T, Cheung DG, Park D, Trapasso F, Pichiorri F, Gaspari M, Palumbo T, Aqeilan RI, Gaudio E, Okumura H, Juliano R, Raso C, Green K, Huebner K, Croce CM (2019) Fhit-Fdxr interaction in the mitochondria: modulation of reactive oxygen species generation and apoptosis in cancer cells. *Cell Death Dis* 10: 147, <https://doi.org/10.1038/s41419-019-1414-7>
- Dumon KR, Ishii H, Fong LY, Zanesi N, Fidanza V, Mancini R, Vecchione A, Baffa R, Trapasso F, Durning MJ, Huebner K, Croce CM (2001) FHIT gene therapy prevents tumor development in Fhit-deficient mice. *Proc Natl Acad Sci USA* 98: 3346–51, <https://doi.org/10.1073/pnas.061020098>
- Durkin SG, Ragland RL, Arlt MF, Mülle JG, Warren ST, Glover TW (2008) Replication stress induces tumor-like microdeletions in FHIT/FRA3B. *Proc Natl Acad Sci USA* 105: 246–51, <https://doi.org/10.1073/pnas.0708097105>
- Fernandez-Ricaud L, Kourtchenko O, Zackrisson M, Warringer J, Blomberg A (2016) PRECOG: a tool for automated extraction and visualization of fitness components in microbial growth phenomics. *BMC Bioinformatics* 17: 249, <https://doi.org/10.1186/s12859-016-1134-2>
- Fijalkowska I, Xu W, Comhair SA, Janocha AJ, Mavrakis LA, Krishnamachary B, Zhen L, Mao T, Richter A, Erzurum SC, Tudor RM (2010) Hypoxia inducible-factor1 $\alpha$  regulates the metabolic shift of pulmonary hypertensive endothelial cells. *Am J Pathol* 176: 1130–8, <https://doi.org/10.2353/ajpath.2010.090832>
- Fong LY, Fidanza V, Zanesi N, Lock LF, Siracusa LD, Mancini R, Siprashvili Z, Ottey M, Martin SE, Druck T, McCue PA, Croce CM, Huebner K (2000) Muir-Torre-like syndrome in Fhit-deficient mice. *Proc Natl Acad Sci USA* 97: 4742–7, <https://doi.org/10.1073/pnas.080063497>

- Hamm J, Mattaj IW (1990) Monomethylated cap structures facilitate RNA export from the nucleus. *Cell* 63: 109–18, [https://doi.org/10.1016/0092-8674\(90\)90292-M](https://doi.org/10.1016/0092-8674(90)90292-M)
- Hu B, Han SY, Wang X, Ottey M, Potoczek MB, Dicker A, Huebner K, Wang Y (2005) Involvement of the Fhit gene in the ionizing radiation-activated ATR/CHK1 pathway. *J Cell Physiol* 202: 518–23, <https://doi.org/10.1002/jcp.20139>
- Huang J, Yao X, Zhang J, Dong B, Chen Q, Xue W, Liu D, Huang Y (2013) Hypoxia-induced downregulation of miR-30c promotes epithelial-mesenchymal transition in human renal cell carcinoma. *Cancer Sci* 104: 1609–17, <https://doi.org/10.1111/cas.12291>
- Huang Y, Garrison PN, Barnes LD (1995) Cloning of the *Schizosaccharomyces pombe* gene encoding diadenosine 5',5''-P<sub>1</sub>,P<sub>4</sub>-tetrphosphate (Ap4A) asymmetrical hydrolase: sequence similarity with the histidine triad (HIT) protein family. *Biochem J* 312: 925–32, <https://doi.org/10.1042/bj3120925>
- Huebner K, Croce CM (2001) FRA3B and other common fragile sites: the weakest links. *Nat Rev Cancer* 1: 214–21, <https://doi.org/10.1038/35106058>
- Ingram SW, Barnes LD (2000) Disruption and overexpression of the *Schizosaccharomyces pombe* aph1 gene and the effects on intracellular diadenosine 5',5''-P<sub>1</sub>,P<sub>4</sub>-tetrphosphate (Ap4A), ATP and ADP concentrations. *Biochem J* 350 Pt 3: 663–9, <https://doi.org/10.1042/bj3500663>
- Ishii H, Mimori K, Inoue H, Inageta T, Ishikawa K, Semba S, Druck T, Trapasso F, Tani K, Vecchione A, Croce CM, Mori M, Huebner K (2006) Fhit modulates the DNA damage checkpoint response. *Cancer Res* 66: 11287–92, <https://doi.org/10.1158/0008-5472.CAN-06-2503>
- Izaurralde E, Lewis J, McGuigan C, Jankowska M, Darzynkiewicz E, Mattaj IW (1994) A nuclear cap binding protein complex involved in pre-mRNA splicing. *Cell* 78: 657–68, [https://doi.org/10.1016/0092-8674\(94\)90530-4](https://doi.org/10.1016/0092-8674(94)90530-4)
- Kiss DL, Baez W, Huebner K, Bundschuh R, Schoenberg DR (2017a) Impact of Fhit loss on the translation of cancer-associated mRNAs. *Mol Cancer* 16: 179, <https://doi.org/10.1186/s12943-017-0749-x>
- Kiss DL, Baez WD, Huebner K, Bundschuh R, Schoenberg DR (2018) Loss of fragile histidine triad (Fhit) protein expression alters the translation of cancer-associated mRNAs. *BMC Res Notes* 11: 178, <https://doi.org/10.1186/s13104-018-3278-9>
- Kiss DL, Waters CE, Ouda IM, Saldivar JC, Karras JR, Amin ZA, Mahrous S, Druck T, Bundschuh RA, Schoenberg DR, Huebner K (2017b) Identification of Fhit as a post-transcriptional effector of Thymidine Kinase 1 expression. *Biochim Biophys Acta* 1860: 374–82, <https://doi.org/10.1016/j.bbaggm.2017.01.005>
- Li XF, O'Donoghue JA (2008) Hypoxia in microscopic tumors. *Cancer Lett* 264: 172–80, <https://doi.org/10.1016/j.canlet.2008.02.037>
- Lindsay HD, Griffiths DJF, Edwards RJ, Christensen PU, Murray JM, Osman F, Walworth N, Carr AM (1998) S-phase-specific activation of Cds1 kinase defines a subpathway of the checkpoint response in *Schizosaccharomyces pombe*. *Genes Dev* 12: 382–95, <https://doi.org/10.1101/gad.12.3.382>
- Matsuyama A, Arai R, Yashiroda Y, Shirai A, Kamata A, Sekido S, Kobayashi Y, Hashimoto A, Hamamoto M, Hiraoka Y, Horinouchi S, Yoshida M (2006) ORFeome cloning and global analysis of protein localization in the fission yeast *Schizosaccharomyces pombe*. *Nat Biotechnol* 24: 841–7, <https://doi.org/10.1038/nbt1222>
- Moreno S, Klar A, Nurse P (1991) Molecular genetic analysis of the fission yeast *Schizosaccharomyces pombe*. *Methods Enzymol* 194: 795–823, [https://doi.org/10.1016/0076-6879\(91\)94059-L](https://doi.org/10.1016/0076-6879(91)94059-L)
- Murphy GA, Halliday D, McLennan AG (2000) The Fhit tumor suppressor protein regulates the intracellular concentration of diadenosine triphosphate but not diadenosine tetraphosphate. *Cancer Res* 60: 2342–4.
- Parrilla-Castellar ER, Arlander SJ, Karnitz L (2004) Dial 9-1-1 for DNA damage: the Rad9-Hus1-Rad1 (9-1-1) clamp complex. *DNA Repair* 3: 1009–14, <https://doi.org/10.1016/j.dnarep.2004.03.032>
- Paulin R, Michelakis ED (2014) The metabolic theory of pulmonary arterial hypertension. *Circ Res* 115: 148–64, <https://doi.org/10.1161/CIRCRESAHA.115.301130>
- Roz L, Gramegna M, Ishii H, Croce CM, Sozzi G (2002) Restoration of fragile histidine triad (FHIT) expression induces apoptosis and suppresses tumorigenicity in lung and cervical cancer cell lines. *Proc Natl Acad Sci USA* 99: 3615–20, <https://doi.org/10.1073/pnas.062030799>
- Rubio-Teixeira M, Varnum JM, Bieganowski P, Brenner C (2002) Control of dinucleoside polyphosphates by the FHIT-homologous HNT2 gene, adenine biosynthesis and heat shock in *Saccharomyces cerevisiae*. *BMC Mol Biol* 3: 7, <https://doi.org/10.1186/1471-2199-3-7>
- Ryan CJ, Roguev A, Patrick K, Xu J, Jahari H, Tong Z, Beltrao P, Shales M, Qu H, Collins SR, Kliegman JI, Jiang L, Kuo D, Tosti E, Kim HS, Edelmann W, Keogh MC, Greene D, Tang C, Cunningham P, Shokat KM, Cagney G, Svensson JP, Guthrie C, Espenshade PJ, Ideker T, Krogan NJ (2012) Hierarchical modularity and the evolution of genetic interactomes across species. *Mol Cell* 46: 691–704, <https://doi.org/10.1016/j.molcel.2012.05.028>
- Saldivar JC, Miura S, Bene J, Hosseini SA, Shibata H, Sun J, Wheeler LJ, Mathews CK, Huebner K (2012) Initiation of genome instability and preneoplastic processes through loss of Fhit expression. *PLoS Genet* 8: e1003077, <https://doi.org/10.1371/journal.pgen.1003077>
- Saldivar JC, Shibata H, Huebner K (2011) Pathology and biology associated with the fragile FHIT gene and gene product. *J Cell Biochem* 109: 858–65, <https://doi.org/10.1002/jcb.22481>
- Siprashvili Z, Sozzi G, Barnes LD, McCue P, Robinson AK, Eryomin V, Sard L, Tagliabue E, Greco A, Fusetti L, Schwartz G, Pierotti MA, Croce CM, Huebner K (1997) Replacement of Fhit in cancer cells suppresses tumorigenicity. *Proc Natl Acad Sci USA* 94: 13771–6, <https://doi.org/10.1073/pnas.94.25.13771>

- Su Y, Yang Y, Huang Y (2017) Loss of ppr3, ppr4, ppr6, or ppr10 perturbs iron homeostasis and leads to apoptotic cell death in *Schizosaccharomyces pombe*. *FEBS J* 284: 324–37, <https://doi.org/10.1111/febs.13978>
- Suh SS, Yoo JY, Cui R, Kaur B, Huebner K, Lee TK, Aqeilan RI, Croce CM (2014) FHIT suppresses epithelial-mesenchymal transition (EMT) and metastasis in lung cancer through modulation of microRNAs. *PLoS Genet* 10: e1004652, <https://doi.org/10.1371/journal.pgen.1004652>
- Taverniti V, Séraphin B (2015) Elimination of cap structures generated by mRNA decay involves the new scavenger mRNA decapping enzyme Aph1/FHIT together with DcpS. *Nucleic Acids Res* 43: 482–92, <https://doi.org/10.1093/nar/gku1251>
- Walworth NC, Bernards R (1996) Rad-dependent response of the chk1-encoded protein kinase at the DNA damage checkpoint. *Science* 271: 353–6, <https://doi.org/10.1126/science.271.5247.353>
- Warringer J, Blomberg A (2003) Automated screening in environmental arrays allows analysis of quantitative phenotypic profiles in *Saccharomyces cerevisiae*. *Yeast* 20: 53–67, <https://doi.org/10.1002/yea.931>
- Waters CE, Saldivar JC, Hosseini SA, Huebner K (2014) The FHIT gene product: tumor suppressor and genome “caretaker”. *Cell Mol Life Sci* 71: 4577–87, <https://doi.org/10.1007/s00018-014-1722-0>
- Weitzenblum E, Chaouat A (2001) Hypoxic pulmonary hypertension in man: what minimum daily duration of hypoxaemia is required? *Eur Respir J* 18: 251–3, <https://doi.org/10.1183/09031936.01.00242501>
- Wu M, Nilsson P, Henriksson N, Niedzwiecka A, Lim MK, Cheng Z, Kokkoris K, Virtanen A, Song H (2009) Structural basis of m7GpppG binding to Poly(A)-specific ribonuclease. *Structure* 17: 276–86, <https://doi.org/10.1016/j.str.2008.11.012>
- Young SD, Hill RP (1990) Effects of reoxygenation on cells from hypoxic regions of solid tumors: analysis of transplanted murine tumors for evidence of DNA overreplication. *Cancer Res* 50: 5031–8.
- Yutori H, Semba S, Komori T, Yokozaki H (2008) Restoration of fragile histidine triad expression restores Chk2 activity in response to ionizing radiation in oral squamous cell carcinoma cells. *Cancer Sci* 99: 524–30, <https://doi.org/10.1111/j.1349-7006.2007.00707.x>
- Zanesi N, Fidanza V, Fong LY, Mancini R, Druck T, Valtieri M, Rudiger T, McCue PA, Croce CM, Huebner K (2001) The tumor spectrum in FHIT-deficient mice. *Proc Natl Acad Sci USA* 98: 10250–5, <https://doi.org/10.1073/pnas.191345898>
- Zhao P, Hou N, Lu Y (2006) Fhit protein is preferentially expressed in the nucleus of monocyte-derived cells and its possible biological significance. *Histol Histopathol* 21: 915–23, <https://doi.org/10.14670/HH-21.915>

### Supporting Information

Additional supporting information may be found online in the Supporting Information section at the end of the article.

Received 18 June 2019; accepted 15 September 2019.  
Final version published online 00 Month 2019.

Supplementary Fig. S1. Aph1 is needed for adaptation to stationary phase.

A,B) *aph1Δ* mutants are sensitive to prolonged stationary phase.

A)  $OD_{600\text{ nm}}$  was measured at 24 and 72 h from inoculation. The growth curves show that both wt (972 h') and *aph1Δ* (JJS30) reach the same maximal density at 24 h.

B) At 24 h, wt (972 h') and *aph1Δ* (JJS30) cells are equally effective at excluding PI, whereas at 72 h *aph1Δ* mutants have more PI permeable cells, indicating that these cells are no longer viable.

C) The Aph1 protein level was followed by Western blotting in a strain, JJS31, which expresses a (HA)<sub>3</sub>-tag in the C-terminal of Aph1. The Aph1 level was rising during logarithmic growth, but was absent when reaching maximum density,

Supplementary Figure S2. *cds1-(myc)<sub>9</sub>* is a hypomorphic allele, and *aph1Δ* in this background results in more proliferation than wt under exposure to DNA damaging agents.

A) When activated by HU, Cds1 C-terminally tagged with (Myc)<sub>9</sub> migrates slower as expected, and the *aph1Δ* allele does not change this. *chk1-HA* (NW222), *chk1-HA cds1-(myc)<sub>9</sub>* (JJS44) and *chk1-HA cds1-(myc)<sub>9</sub> aph1Δ* (JJS45) were treated for 2 h with 20 mM HU, and activation of Cds1 was investigated through Western blotting by presence of a band shift to a slower migrating band.

B) The compromised Cds1 function caused by the (Myc)<sub>9</sub> tag results in Chk1 activation in HU, indicating DNA damage. Strains *chk1-HA* (NW222), *chk1-HA cds1Δ* (JJS43), *chk1-HA cds1-(myc)<sub>9</sub>* (JJS44), and *chk1-HA cds1-(myc)<sub>9</sub> aph1Δ* (JJS45) were either treated for 2 h with 20 mM HU or 1 h with 10 μM/ml PL as a positive control. Chk1 activation was visualized by Western blotting showing the band shift of Chk1 to a slower migration form upon activation.

C) The *aph1Δ* allele in cells containing the partially defective (Myc)<sub>9</sub>-tagged Cds1 results in higher proliferation in HU (12 mM). Strains *chk1-HA* (NW222), *chk1-HA cds1Δ* (JJS43), *chk1-HA cds1-(myc)<sub>9</sub>*

(JJS44), and *chk1-HA cds1-(myc)<sub>9</sub> aph1Δ* (JJS45) were monitored by growth in a Bioscreen C analyzer. Two independent cultures from the same Bioscreen run are shown per strain and treatment. The curves are representatives of three independent Bioscreen runs.

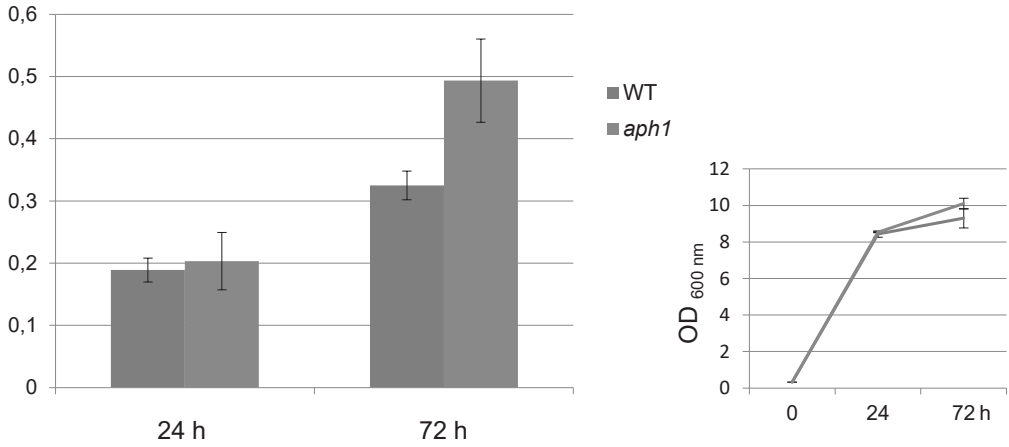
D) The (Myc)<sub>9</sub> tag on Cds1 leads to a compromised function of Cds1 as seen by higher sensitivity against HU but not UV. Logarithmic growing cells of *chk1-HA* (NW222), *chk1-HA cds1Δ* (JJS43) *chk1-HA cds1-(myc)<sub>9</sub>* (JJS44) and *chk1-HA cds1-(myc)<sub>9</sub> aph1Δ* (JJS45), were serial diluted and spotted on a YES plates as control, a YES plate containing 5 mM HU, or a YES plate placed under UV (200 μJ/cm<sup>2</sup>).



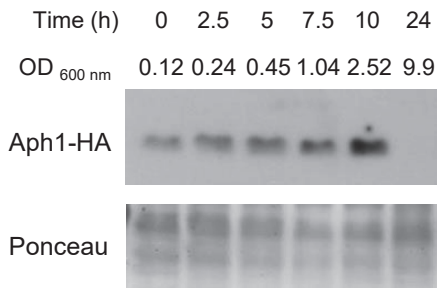
# Supplementary Figure S1

## A

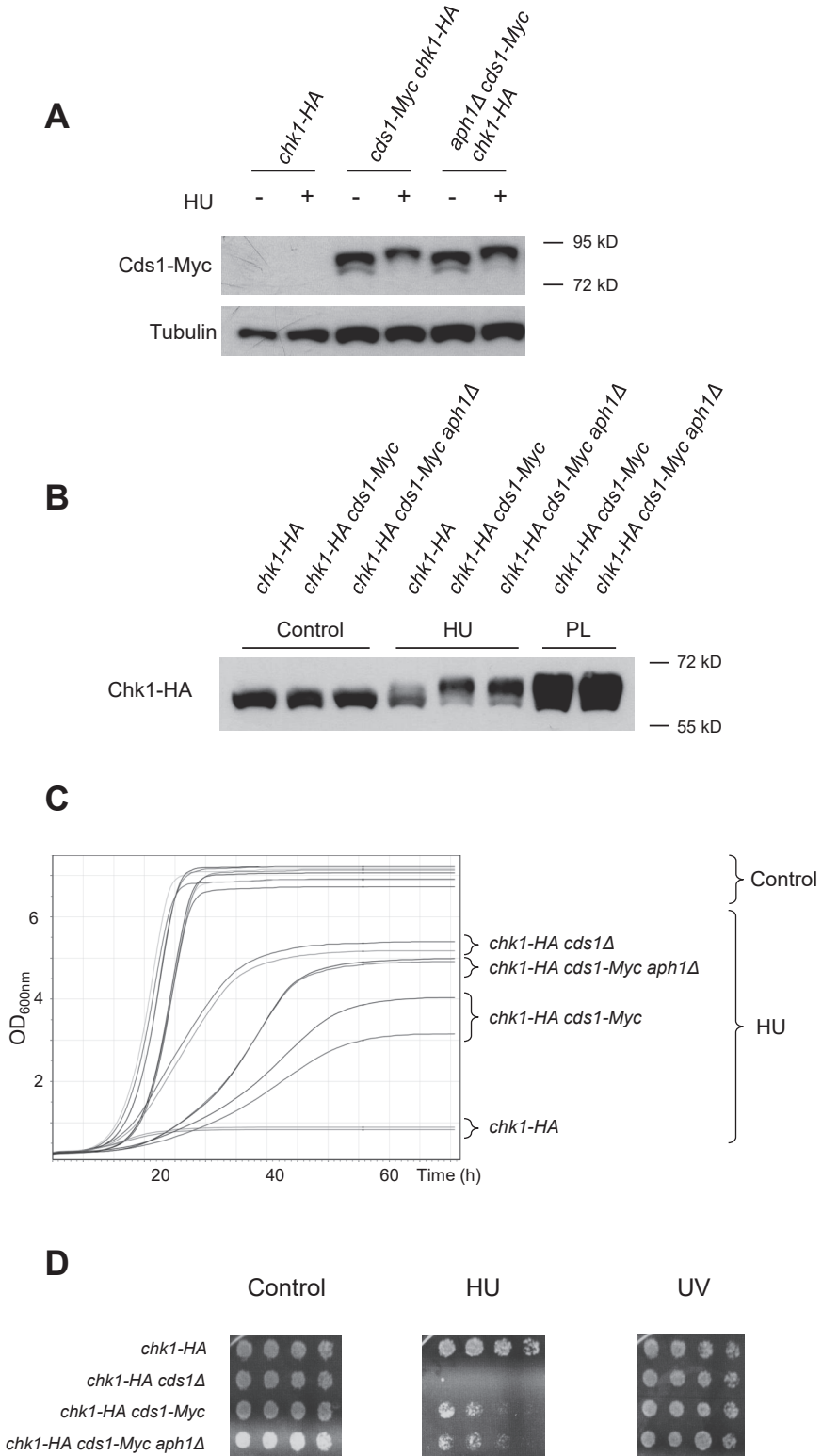
### Fraction PI-stained cells



## B



# Supplementary Figure S2



## Paper IV



# A redox-sensitive thiol in Wis1 modulates the fission yeast MAPK response to H<sub>2</sub>O<sub>2</sub> and is the target of a small molecule

Johanna J. Sjölander<sup>1</sup>, Agata Tarczykowska<sup>1</sup>, Cecilia Picazo<sup>1,2</sup>, Itziar Cossio<sup>1#</sup>, Itedale Namro Redwan<sup>1†</sup>, Chunxia Gao<sup>1</sup>, Carlos Solano<sup>1¶</sup>, Michel B. Toledano<sup>3</sup>, Morten Grøtli<sup>1</sup>, Mikael Molin<sup>1,2\*</sup> and Per Sunnerhagen<sup>1\*</sup>

<sup>1</sup>Department of Chemistry and Molecular Biology, Lundberg Laboratory, University of Gothenburg, P.O. Box 462, Göteborg, SE-405 30, Sweden

<sup>2</sup>Department of Biology and Biological Engineering, Chalmers, Kemigården 10, 412 96 Göteborg, Sweden

<sup>3</sup>Oxidative Stress and Cancer Laboratory, Integrative Biology and Molecular Genetics Unit (SBIGEM), CEA Saclay, FRANCE

<sup>#</sup>Present address: Fundación CNIC Carlos III - Centro Nacional de Investigaciones Cardiovasculares Melchor Fernández Almagro 3 28029, Madrid, Spain.

<sup>†</sup> Present address: Cellink Arvid Wallgrens Backe 20, 413 46 Gothenburg, Sweden

<sup>¶</sup> Present address: Nexam Chemicals, Molekylvägen 1B, 223 63 Lund, Sweden

\* *Corresponding authors:* Mikael Molin

Phone : +46 31 772 8175

E-mail : [mikael.molin@chalmers.se](mailto:mikael.molin@chalmers.se)

Per Sunnerhagen

Phone: +46 31 7863830

E-mail: [per.sunnerhagen@cmb.gu.se](mailto:per.sunnerhagen@cmb.gu.se)

*Keywords:* Sty1, cysteine oxidation, stress signaling, *Schizosaccharomyces pombe*

*Running title:* Redox regulation of Wis1 blocked by small molecule

## Abstract

Oxidation of a highly-conserved cysteine (Cys) residue located in the kinase-activation loop of mitogen-activated protein kinase kinases (MAPKK) inactivates mammalian MKK6. This residue is conserved in the fission yeast MAPKK Wis1, which belongs to the H<sub>2</sub>O<sub>2</sub>-responsive MAPK Sty1 pathway. Here, we show that H<sub>2</sub>O<sub>2</sub> reversibly inactivates Wis1 through this residue (C458) *in vitro*. We found that C458 is constitutively oxidized *in vivo* and that serine substitution of this residue significantly enhances Wis1 activation upon the addition of H<sub>2</sub>O<sub>2</sub>. The allosteric MAPKK inhibitor, INR119, which binds into a pocket next to the activation loop and to C458 prevented the inhibition of Wis1 by H<sub>2</sub>O<sub>2</sub> *in vitro*, and significantly increased Wis1 activity *in vivo*. We propose that the constitutive oxidation of C458 inhibits Wis1 and that INR119 cancels out this inhibitory effect by binding close to this residue. The inhibitory effect of the oxidation of this conserved Cys residue in MKK6 (C196) is thus conserved in the *S. pombe* MAPKK Wis1.

## Introduction

MAPKs are evolutionarily conserved kinases that operate in a three-tier kinase cascade module that comprises the MAPK, which is activated by phosphorylation on juxtaposed Tyr and Ser residues by a dual-specificity MAPK kinase (MAPKK), itself activated by phosphorylation by a MAPKK kinase (MAPKKK). MAPKs regulate cellular responses by phosphorylating transcription factors and other kinases (1).

The *Schizosaccharomyces pombe* Sty1 kinase is the homolog of the mammalian stress-activated MAPK p38. Like p38, Sty1 responds to external stress stimuli including heat, osmotic and acidic stresses, metals, UV-induced DNA damage, and hydrogen peroxide ( $H_2O_2$ ) (2). In the Sty1 pathway, the  $H_2O_2$  signal is integrated at the level of a membrane-bound two-component phosphorelay system including the histidine kinases Mak2 and Mak3 (3). Mak2/3 relay the  $H_2O_2$  signal to the MAPKKKs (4) Win1 (5) and Wis4/Wik1/Wak1 (6) by phosphate transfer on an aspartic residue of the Mcs4 response regulator *via* the phosphorelay protein Mpr1. MAPKKKs, in turn, activate the MAPKK Wis1 by phosphorylation on S469 and T473. Wis1, the homolog of the mammalian MAPKK MEK1, activates the MAPK Sty1 (7), by dual phosphorylation on T171 and Y173 (8). Sty1 is the only known target of Wis1. When active, Sty1 phosphorylates the Aft1 transcription factor, which regulates a transcriptional response to stress. Similar to the Sty1 pathway, the human p38 MAPK pathway is activated by  $H_2O_2$  stress (9).

Surprisingly, one of the MAPKKs of p38, MKK6, is inactivated by cell exposure to low doses of  $H_2O_2$  through the formation of a disulfide bond between a Cys residue, evolutionarily conserved among MAPKKs at position -1 of the DFG motif in the kinase activation loop (C196) and another conserved residue (C109) (Fig. 1 A, Supplementary Fig S1 A), and this disulfide inhibits ATP binding (10). The aspartate residue of the highly conserved DFG motif coordinates  $Mg^{2+}$ , which contributes to the phosphotransfer reaction from ATP (11). The MKK6 C196 residue is conserved in all MAPKKs, including in Wis1 and in the *S. cerevisiae* Wis1 homologue Pbs2, but not in other S/T kinase families, and may have a conserved redox function.

Here we have examined the possible role in signaling of the residue corresponding to MKK6 C196 in *S. pombe* Wis1, which in this enzyme is situated at position C458. We found that similar to human MKK6, Wis1 is inactivated by  $H_2O_2$  through reversible oxidation, both *in vitro* and *in vivo*, and in a manner dependent on the presence of

the C458 residue. We used the kinase inhibitor INR119 that behaves as a non-ATP competitive allosteric MEK1 inhibitor (12). INR119 binds MEK1 in a pocket also conserved in Wis1 and close to C458. We found that INR119 activates Wis1 kinase activity by preventing C458 oxidation. Lastly, we observed that Wis1 C458 is crucial for cells to resist to H<sub>2</sub>O<sub>2</sub>, but not to KCl, consistent with the need of appropriate, dose-dependent Sty1 pathway activation upon stress.

## Results

### H<sub>2</sub>O<sub>2</sub> inhibits Wis1 kinase activity by oxidation of C458

In mammals, H<sub>2</sub>O<sub>2</sub> reversibly inhibits the p38 MAPK MKK6 by causing the formation of a disulfide bond between C109 and C196 (10). C196 is located in the kinase-activating loop, directly upstream (-1) of the highly conserved DFG kinase motif, which binds Mg<sup>2+</sup> and thereby contributes to catalysis. C196 is conserved in the other mammalian MAPKKs, in the *S. pombe* and *S. cerevisiae* MAPKKs Wis1 and Pbs2, respectively (Fig. 1 A), and in several MAPKs (Supplementary Fig. S1 A) (11). The *S. pombe* MAPKK Wis1 carries the residue corresponding to C196 in MKK6 at position 458, but lacks the MKK6 C109 residue. We examined whether Wis1 C458 is a site of redox regulation.

We first inquired whether Wis1 kinase activity is modulated by H<sub>2</sub>O<sub>2</sub> *in vitro*, using Wis1 and Sty1 purified from two different *S. pombe* strains (see Materials and Methods). When purified in the absence of EDTA, Wis1 phosphorylated Sty1 even without the addition of ATP (Supplementary Fig. S1 B) suggesting that ATP co-purified with Wis1. However, we achieved reproducible Wis1, ATP and Mg<sup>2+</sup>-dependent Sty1 phosphorylation when Wis1 was purified in the presence of EDTA and under non-reducing conditions (Fig. 1 C, Supplementary Fig. S1 C). Notably, Wis1 purified under these conditions lost its ability to phosphorylate Sty1 when incubated with H<sub>2</sub>O<sub>2</sub> during 5 min. The effect of H<sub>2</sub>O<sub>2</sub> was dose-dependent, visible at 50 μM, increased at 100 and 500 μM, and was reversed by the thiol reductant tris(2-carboxyethyl)phosphine (TCEP) in samples exposed to H<sub>2</sub>O<sub>2</sub> at 50 and 100 μM, but not at 500 μM (Fig. 1 C, left panel, Supplementary Fig. S1 D).

We next tested whether C458 is required for the inhibition of Wis1 by H<sub>2</sub>O<sub>2</sub> using a Wis1 mutant with substitution of C458 to serine (C458S) (Fig. 1 C, right panel). Wis1<sup>C458S</sup> retained full kinase activity *in vitro*. H<sub>2</sub>O<sub>2</sub> only decreased this activity by about



half, but did not completely inhibit it, as seen with WT protein, and this partial inhibition was not reversed by TCEP.

We conclude that H<sub>2</sub>O<sub>2</sub> reversibly inhibits Wis1 kinase activity by oxidation of C458 to either the sulfenic (-SOH) or disulfide bond forms. However, one or more additional atomic targets of H<sub>2</sub>O<sub>2</sub> in Wis1 are necessary to account for the partial and irreversible inhibition of Wis1<sup>C458S</sup>.

### **Wis1 C458 is oxidized *in vivo***

We inquired whether Wis1 becomes oxidized *in vivo* upon cell exposure to H<sub>2</sub>O<sub>2</sub> by differentially labelling reduced *vs* oxidized Cys residues with N-ethyl maleimide (NEM) and methoxy polyethylene glycol (mPEG) 5000, respectively (see Materials and Methods). mPEG adds 5 kDa per modified Cys residue, thereby decreasing protein electrophoretic mobility in proportion to the number of residues modified. We first used lysates from cells not exposed to H<sub>2</sub>O<sub>2</sub>. Migration of HA-tagged Wis1 was partially shifted by mPEG to a doublet band of slower migration (Fig. 2 A), thus indicating that in exponentially growing cells, one or more Wis1 Cys residues are partially oxidized into a form sensitive to reduction by DTT. The Wis1<sup>C458S</sup> mutant protein was also shifted, but its band shift lacked the upper band of the doublet, therefore indicating that this residue contributes to the constitutive oxidation seen in wt protein (Fig. 2 D). As a control, a *wis1* mutant lacking all 6 Cys residues (*wis1-6CS*) did not display any electrophoretic mobility shift after mPEG derivatization, therefore confirming that the mPEG-induced gel shift seen with wt Wis1 protein is caused by mPEG derivatization at Cys residues (Supplementary Fig. S2). For unclear reasons, the Wis1<sup>6CS</sup> mutant protein migrated as a double band, in a manner independent of mPEG derivatization. We next monitored the effect of cell exposure to H<sub>2</sub>O<sub>2</sub>. Surprisingly, H<sub>2</sub>O<sub>2</sub> did not change the pattern of migration of mPEG-derivatized Wis1, as monitored by a time course analysis at 500 μM, or in a dose range from very low (50 μM) to very high (10 mM) doses (Fig. 2 B,C). We conclude that C458 is constitutively oxidized *in vivo*.

We then tested the importance of C458 for Wis1 function *in vivo*, first by comparing the H<sub>2</sub>O<sub>2</sub>-induced phosphorylation of Sty1 (Fig. 2 E). *wis1-C458S* mutants sustained potent Sty1 oxidation, but surprisingly phosphorylation was detected already at 100 μM H<sub>2</sub>O<sub>2</sub>, a dose that did not trigger wild-type Wis1 kinase activity (Fig. 2 E). Wis1<sup>C458S</sup>-induced Sty1 phosphorylation was also higher at 200 and 500 μM H<sub>2</sub>O<sub>2</sub>, but at

1 mM plateaued at the same intensity as the wt. We then tested the effect of the *wisI-C458S* substitution on the cellular resistance to H<sub>2</sub>O<sub>2</sub> (Fig. 2 F). Interestingly, this mutant was as sensitive to H<sub>2</sub>O<sub>2</sub> as the *wisIΔ* null mutant, whereas it retained wt tolerance to KCl. The *wisI-6CS* mutant was similarly sensitive to H<sub>2</sub>O<sub>2</sub>, whereas Ser substitution of any of three other of the remaining Cys residues only caused a mild loss of H<sub>2</sub>O<sub>2</sub> resistance.

We conclude that C458 is constitutively oxidized *in vivo*, and thus imparts an inhibitory effect on Wis1 kinase activity, in keeping with the negative effect of the oxidation of C458 by low levels H<sub>2</sub>O<sub>2</sub> seen *in vitro* (Fig. 1). This negative effect of C458 is overcome in the wt enzyme by H<sub>2</sub>O<sub>2</sub> ≥ 500 μM through upstream signaling. The increased H<sub>2</sub>O<sub>2</sub> sensitivity endowed indicates that activation of Sty1 is deleterious if not prevented at very low concentrations of H<sub>2</sub>O<sub>2</sub>.

### **The allosteric MEK1 modulator INR119 binds Wis1 close to C458 *in silico***

The MAPKK MEK1 is the closest structural homolog of Wis1 in the mammalian kinome, with 47 % amino acid (aa) sequence identity. Several allosteric MEK1/MEK2 inhibitors have been reported (13). In general, they bind in a unique active pocket adjacent to the Mg-ATP binding site and acts by inducing unusual conformations in unphosphorylated MEK1/2, trapping them in a closed but catalytically inactive conformation. A human MEK1 homology-based structural model of Wis1 (PDBID:1S9J) (14) indicates that this pocket is present in Wis1, close to C458 (Fig. 3 A). We thus inquired whether allosteric modulators that bind this pocket could modulate the Wis1 H<sub>2</sub>O<sub>2</sub> response. We tested INR119 among several other allosteric modulators of MEK1 we had previously constructed (12). INR119 was designed as a modification of PD98059 (Fig. 3 B), a non-ATP-competitive inhibitor of MEK1 (Supplementary Fig. S3 A) (15). INR119 docked into the allosteric site of Wis1 in the homology-based structural model (Fig. 3 A, Supplementary Fig. S3 B,C) by forming two hydrogen bonds to the backbone of the protein (Supplementary Fig. S3 C), between the chromone carbonyl oxygen and the NH group of S483, and between the NH<sub>2</sub>-group of the aniline and the carbonyl oxygen of F460, the phenylalanine in the DFG motif. INR119 is thus predicted to bind in the close vicinity of C458 (12), at -1 of the DFG motif (16).

To test whether INR119 binds Wis1, we employed a thermal shift assay (17) that measures stabilization of the target protein at elevated temperatures through binding of a ligand. We initially tested binding in live cells, showing that INR119 stabilizes soluble Wis1

at all temperatures tested (Supplementary Fig. S3 D). The elevated temperature itself resulted in massive stabilization of soluble Wis1, precluding calculation of a thermal shift. We therefore tested INR119 binding to Wis1 in crude lysates (Fig. 3 C) in which no Wis1 stabilization upon heat was seen, allowing us to calculate a thermal shift to +2°C at 3 μM INR119, in support of a direct interaction.

### **INR119 enhances Wis1 activity in response to H<sub>2</sub>O<sub>2</sub>**

We first tested the effect of INR119 on Wis1 kinase activity *in vitro* (Fig. 3 D). INR119 did not alter Wis1 activity at concentrations of 3 μM up to 50 μM. Surprisingly, however, at these doses INR119 prevented inactivation of Wis1 by H<sub>2</sub>O<sub>2</sub> (Fig. 3 D, lanes 6 - 9, compare *e.g.* lanes 2 vs 6). We next tested the effect of INR119 on the activity of Wis1 *in vivo* by incubating cells with the inhibitor prior to exposure to H<sub>2</sub>O<sub>2</sub> (500 μM). We observed a strong and Wis1-dependent enhanced Sty1 phosphorylation (Fig. 4 A, Supplementary Fig. S4 A). Enhancement was even more potent at low levels of H<sub>2</sub>O<sub>2</sub> (250 μM), but was lost at high levels of the oxidant (5 mM) (Fig. 4 C). However, the enhancing effect of INR119 was not seen in mutants expressing the Wis1<sup>C458S</sup> protein, which by itself increases kinase activity (Fig. 4 B). This was in contrast to Wis1<sup>C394S</sup> and Wis1<sup>C477S</sup>, on which the drug exerted the same effect as on the wt protein (Supplementary Fig. S4 B,C). According to our homology model C394 and C477 are too far away from C458 to enable formation of Cys-Cys bridges, and distant from the INR119 binding site (Supplementary Fig. S4 D).

As a control of the specificity for peroxide stress, we investigated the impact of INR119 on Wis1 activity under other stress conditions. INR119 neither affected the responses to osmotic (Supplementary Fig. S4 E) nor to heat stress (Supplementary Fig. S4 F). INR119 did not alter Wis1 activity in the absence of H<sub>2</sub>O<sub>2</sub> (Fig. 4 A – C), suggesting that its effect is dependent upon the activation of Wis1 by the upstream H<sub>2</sub>O<sub>2</sub> sensing two-component Mak1/2 system and the MAPKKKs Win1 and Wis4 (Fig. 5 A). Indeed, INR119 was not able to stimulate Wis1 activity in the *win1Δ wis4Δ* double mutant (Fig. 5 B), but in contrast enhanced the constitutive activity of the *wis1-S469D,T473D* (*wis1<sup>DD</sup>*) allele that carries Asp substitutions of the Ser and Thr residues phosphorylated by Win1/Wis4 (Supplementary Fig. S5) (18). To verify whether the effect of INR119 of enhancing activity of Wis1 translated into the expression of the target genes of Atf1, one of the transcription factor regulated by the Wis1-Sty1 pathway, we measured the expression of *srx1<sup>+</sup>* (19) by quantitative PCR (qPCR). INR119 increased *srx1<sup>+</sup>* expression about two-fold at 50 – 200 μM

H<sub>2</sub>O<sub>2</sub> (Fig. 4 D). The effect of INR119 on *srxI*<sup>+</sup> expression was Wis1-dependent, as it was not seen in a *wis1Δ* mutant (Supplementary Fig. S4 G). Thus, INR119 potently boosts Sty1 phosphorylation by Wis1 and Sty1-dependent *srxI*<sup>+</sup> expression in response to low doses of H<sub>2</sub>O<sub>2</sub>. INR119 may either prevent the reaction of C458 with H<sub>2</sub>O<sub>2</sub>, or alternatively, cancel out the inhibitory effect of oxidized C458 on Wis1 activity.

## Discussion

The human p38 pathway is activated by H<sub>2</sub>O<sub>2</sub> (9), but paradoxically MKK6, the MAPKK upstream of p38, is inactivated by a disulfide bond between C196 (equivalent of Wis1 C458) and C106, and formed in response to low doses of H<sub>2</sub>O<sub>2</sub> (10). C196 is evolutionarily conserved in mammalian and yeast MAPKKs (Fig. 1 A), as well as in several budding and fission yeast MAPKKs, but not in other mammalian kinases (Supplementary Fig. S1 A), which suggests that the redox regulation of C196 is specifically conserved in MAPK pathways (10).

We showed here that the *S pombe* MAPKK Wis1 carries the conserved MKK6 Cys residue C196 at position C458, but not MKK6 C106, and is also inactivated by low doses H<sub>2</sub>O<sub>2</sub> *in vitro* by oxidation of this residue (Fig. 1 C, Supplementary Fig. S1 D). This conclusion is based on both the reversion of kinase inactivation by thiol reduction, which indicates that inactivation is due to reversible oxidation of a Cys residue, presumably to the sulfenic acid form, rather than to a disulfide bond with another Cys residue, and on the effect of the Ser substitution of Wis1 C458, which prevented inactivation. Of note, the reversion of Wis1 inactivation by reduction and its prevention by Ser substitution of Wis1 C458 were both partial, pointing to the presence of other irreversibly modified atomic targets of H<sub>2</sub>O<sub>2</sub> in Wis1. We found that Wis1 oxidation *in vivo* is constitutive, and partially dependent upon C458, the substitution of which allowed Wis1 to be activated by H<sub>2</sub>O<sub>2</sub> at low levels that did not impact the WT enzyme (Fig. 2 E). Lastly, the MEK1 inhibitor INR119, which we show is expected to bind Wis1 close to C458 (Fig. 3 A, Supplementary Fig. S3 B,C), prevented inactivation of Wis1 by H<sub>2</sub>O<sub>2</sub> *in vitro*, and potently boosted the activity of Wis1, but not of Wis1<sup>C458S</sup> *in vivo*. Altogether, the *in vitro* and *in vivo* data and the effect of INR119 indicate a negative effect of the constitutively oxidized C458 on Wis1 kinase activity, imposing a threshold that limits undue activation of the pathway at low stress levels (Fig. 6 A) At elevated doses of H<sub>2</sub>O<sub>2</sub> this inhibitory effect is overcome by more potent activation of the

upstream pathway (Fig. 6 B), which explains observations of a graded Sty1 pathway response to H<sub>2</sub>O<sub>2</sub> (20) and identifies Wis1 C458 as an important regulatory mechanism underlying this property. By changing the conformation of the allosteric site INR119 may either cancel out the inhibitory effect of oxidized C458, or prevent this oxidation from occurring (Fig. 6 C). We also found that the Ser substitution of Wis1 C458 endowed cells with a marked sensitivity to H<sub>2</sub>O<sub>2</sub>, but not to KCl, clearly pointing to the deleterious effect of un-restrained Wis1 kinase activation, which is consistent with the toxicity of Wis1 overexpression and Sty1 hyperactivity, causing cell death (6, 21, 22).

The endoplasmic reticulum (ER) transmembrane kinase Ire-1 senses ER stress and activates the unfolded protein response (UPR). In worms and mammals, Ire1 is regulated by sulfenylation of another conserved Cys residue at position +2, relative to the DFG motif (23), which indicates that redox modification of conserved Cys residues located in the kinase activation loop constitutes a conserved mechanism for regulating kinases. Other protein kinases have also been reported to be modulated by thiol oxidation. Notably, oxidation of a conserved cysteine located at DFG +13 in the activation loop (24) of mouse and rat type II protein kinase A catalytic subunits by H<sub>2</sub>O<sub>2</sub> inhibits kinase activity *in vitro* (25-27). Conversely, protein kinase G and type I PKA are both activated *in vitro* through oxidation of the homologous activation loop cysteine upon H<sub>2</sub>O<sub>2</sub> addition (28, 29). Interestingly, we recently found that a significant proportion of DFG +13 cysteine residues in the catalytic subunit of the *S. cerevisiae* PKA are glutathionylated *in vivo* in a manner inhibiting PKA activity and increasing cellular H<sub>2</sub>O<sub>2</sub>-resistance (30). Thus, redox modulation of cysteine residues in the activating loop appears to be a conserved means of regulating protein kinases.

Ire1 was shown to be sulfenylated by ER and mitochondrial H<sub>2</sub>O<sub>2</sub>, as well as H<sub>2</sub>O<sub>2</sub> produced by a NADPH oxidase in response to arsenite stress, in a manner activating the p38-SKN1 (the worm homolog of NRF2) pathway by, in turn, sulfenylating NSY-1, the worm MAPKKK upstream of p38, brought in the vicinity of Ire1 by the scaffold protein TRAF. Interestingly, Ire1 C663 sulfenylation, or any of the downstream further modified oxidized states of Ire1 C663, totally impaired its ability to induce the UPR (23). The regulation of these two mutually exclusive functions of IRE-1 in the activation of the UPR and of SKN1 by cysteine oxidation of a unique Ire1 Cys residue indicates that in Wis1, the constitutively oxidized C458 may similarly afford a qualitatively altered function of this enzyme.

In summary, we showed here that the constitutive oxidation of the *S pombe* MAPKK Wis1, C458, inhibits kinase activity, and this inhibition is required for an appropriate pathway response to peroxide. We also showed that the allosteric MEK1 inhibitor, INR119, potentiated Wis1 activity by interfering with the inhibitory effect of this residue. In this regard, it is interesting to note that other allosteric MEK1/2 inhibitors, PD98059, UO126 and PD184352, when used at sub-inhibitory concentrations prolonged EGF and H<sub>2</sub>O<sub>2</sub>-induced MEK5 activation (31), a kinase also bearing the conserved DFG -1 Cys residue and a side target of allosteric MEK1/2 inhibitors (31, 32), which suggest the presence of a thiol-redox mechanism similar to the one of Wis1.

## Materials and methods

### Synthesis of INR119

INR119 was synthesized as previously described (12).

### Multiple sequence alignment

Conservation of MKK6 C109 and C196 was investigated through multiple alignment of human MKK6 against *S. pombe*, *S. cerevisiae*, and human MAPKKs, as well as a selection of MAPKs, MAPKKs and other serine/threonine kinases in these organisms. Alignment was performed through Clustal O with standard settings, and the result was edited in Jalview. Cysteine residues (C) are colored in red, to visualize their conservation.

### Fission yeast strains and growth conditions

Cells were grown at 30°C in YES (33), except for cells overexpressing protein, where instead Edinburgh minimal medium (EMM) was used. *S. pombe* strains are listed in Table 1.

### Genetic engineering of point mutations

We designed full or partial *wisI*<sup>+</sup> sequences containing the different substitutions. To engineer missense C-to-S point mutations, the second base in the codon for cysteine was changed from a G to a C giving TCC or TCT. The designed sequences for construction of all C to S substituted strains all contain a C-terminal His<sub>6</sub>-tag followed by the *hphMX6* hygromycin resistance cassette (34), as well as a 3' flanking *wisI*<sup>+</sup> sequence. The designed DNA molecules were synthesized and cloned into pMX plasmid vectors, by the Thermo Fisher GeneArt service. DNA fragments containing the *wisI* portion were excised from the plasmid vector with the appropriate restriction enzymes, and thereafter used to transform *S. pombe* 972 *h<sup>r</sup>* to hygromycin resistance and integrated into the endogenous chromosomal *wisI*<sup>+</sup> locus by homologous recombination. Correct integrated sequences and substitutions were confirmed by full gene sequencing.

For construction of JJS16, a strain expressing N-terminally HA-tagged and C-terminally (His)<sub>6</sub>-tagged Wis1<sup>6CS</sup> from the endogenous promoter, the following design was used. The sequence started with the sequence upstream of *wisI*<sup>+</sup>, the starting point being a generated *Sma* I cleavage site, where the original CTTGGG 384 bp upstream of *wisI*<sup>+</sup> had

been changed to CCCGGG. As *Sma* I generates blunt ends, the fragment will not change the original sequence upon integration by homologous recombination. After the start codon an (HA)<sub>3</sub>-epitope tag was added, followed by the full *wis1* sequence containing all 6 C-to-S substitutions, as well as the His<sub>6</sub>-tag before the stop codon. After the hygromycin resistance cassette, a sequence directly downstream of *wis1* followed, ending with a natural *Nde* I site located 144 bp from the stop codon. The same method was used to obtain a non-tagged version of the full *wis1* sequence containing all 6 C-to-S substitutions, except no (HA)<sub>3</sub>-epitope tag was added after the start codon. The fragments were cut out from the delivered vector and transformed into 972 *h*<sup>-</sup>, generating JJS16 and JJS22 respectively. Sequences designed to generate strains JJS17 (*wis1-C394S*), JJS18 (*wis1-C458S*) and JJS19 (*wis1-C477S*) expressing Wis1 C-terminally tagged with (His)<sub>6</sub> and with C-to-S substitutions from the endogenous promoter, instead started at a *wis1*<sup>+</sup> internal natural *Hind* III site. After the *hphMX6* cassette, a sequence downstream of *wis1*<sup>+</sup> ending with a *Bam* HI site was generated by changing GGTAGT 180 bp downstream of *wis1*<sup>+</sup> to GGATCC. Fragments were cut out from the plasmids with *Hind* III and *Bam* HI, and transformed into 972 *h*<sup>-</sup>. For construction of JJS9 (*wis1-C458S* overexpressed from the *nmt1* promoter) the same fragment used to construct JJS18 was instead transformed into strain JJS6.

### **Culture and stress exposure of fission yeast cells**

Unless otherwise stated in the figure legends, cultures growing in mid-log phase were concentrated 20 × by mild centrifugation and pre-treated with the indicated concentration of INR119 dissolved in DMSO for the time stated in the figure legend. Controls were pre-treated with the corresponding DMSO concentration. At the time of stress induction, pre-treated cultures were once again diluted to the original density. Samples representing different time points were harvested through centrifugation in 400 × g for 20 s, and were thereafter snap frozen in dry ice.

### **Cell lysis and western blot**

Unless otherwise stated cells were lysed by shaking with acid washed glass beads in a FastPrep FP120 device (Savant) with speed 5 for 30 sec. Lysis was performed in lysis buffer A (50 mM NaCl, 50 mM Tris pH 7.6, 0.2 % Triton X-100, 0.25 % NP40) containing phosphatase inhibitor cocktail 04906837001 and protease inhibitor cocktail 04693159001 (Roche). Protein concentration was determined using the BCA assay. Equal



protein concentrations of each sample were loaded and proteins were separated on a SDS-PAGE and thereafter blotted onto nitrocellulose membranes.

Phosphorylation of Sty1 was detected by mouse anti-phospho-(Thr180/Tyr182)-p38 antibodies from Cell Signaling Technology (Bionordika AB, Stockholm, Sweden). HA-tagged Wis1 was detected with mouse monoclonal anti-HA #2367 (Cell Signaling). Loading control was  $\alpha$ -tubulin detected by mouse anti- $\alpha$ -tubulin T5168 (Sigma). Total Sty1 was detected using polyclonal rabbit anti-Hog1 sc-9079 (Santa Cruz Biotechnology), or for MHNSTY1 with mouse monoclonal anti-c-Myc sc-40 (9E10), (Santa Cruz Biotechnology). The secondary antibodies were horseradish peroxidase-coupled anti-mouse A4416 and anti-rabbit A6154 (Sigma).

### **Preparation of semi-purified protein for *in vitro* kinase assays**

HA-Wis1-His<sub>6</sub> and MHNSTY1 were expressed separately. HAWis1His<sub>6</sub> has an N-terminal HA-tag and a C-terminal His<sub>6</sub>-tag and is expressed in strain JJS7. The substrate is MHNSTY1, a Sty1 version with N-terminal Myc- and His<sub>6</sub> tags (expressed from plasmid pREP41MHNSTY1 in strain KS1598). As a control, the *wis1Δ* strain JJS1 was used instead of JJS7. Cells were harvested 16 h after induction of the overexpression from the *nmt1* promoters by removing thiamine from the media. Harvest was done by centrifugation in RT in 850 × g, and thereafter cells were resuspended in ice cold lysis buffer H (50 mM NaCl, 50 mM Hepes, 100 mM KCl, 10 % glycerol, 0.2 % Triton X-100, 0.25 % NP-40, adjusted to pH 7.0, and supplemented with phosphatase inhibitor cocktail 04906837001, protease inhibitor cocktail 04693159001 (Roche) as well as 10 mM EDTA). All steps from the harvest point until the kinase assay started was carried out at 0 – 8°C. Cells were lysed in a FastPrep FP120 device (Savant) at speed 5 for 40 sec. Lysates were cleared of debris through centrifugation for 5 min at 13 000 rpm in a microcentrifuge, and supernatants was further centrifuged in 5 min 5000 × g. Lysates were thereafter incubated with cComplete His-Tag Purification Resin (#28555800, Roche) for 1 h. This resin is compatible with 10 mM EDTA. Beads with HA-Wis1-His<sub>6</sub> was washed three times with lysis buffer H, and carefully resuspended beads with now bound HA-Wis1-His<sub>6</sub> was thereafter aliquoted in equal volumes.

Beads with MHNSTY1 bound were loaded onto a 10 ml plastic column and washed by passing 3 ml 30 mM imidazole in lysis buffer H through the column. MHNSTY1 was thereafter eluted in lysis buffer H containing 300 mM imidazole, by passing 4 times

through the column. Eluted Sty1 was subsequently diluted to lower the imidazole concentration to 30 mM during the kinase assay.

### ***In vitro* kinase assays**

Assays were carried out at 30°C and 1000 rpm in a thermal mixer. Kinase reactions were stopped by addition of sample buffer and denaturing at 95°C for 7 min. The whole volume in each tube was loaded in a single well in a gel and the result was analyzed by western blot.

For kinase assays with H<sub>2</sub>O<sub>2</sub> and TCEP, resuspended and aliquoted beads with HA-Wis1-His<sub>6</sub> were treated first for 5 min in pairs with H<sub>2</sub>O<sub>2</sub> giving the indicated final concentration, and subsequently for one tube in each pair for 5 min with 1 mM TCEP. Thereafter MHNSTY1 was added and the kinase reaction was started by addition of MgCl<sub>2</sub>/ATP, giving a final concentration of 20 mM MgCl<sub>2</sub> (10 mM available for reaction) and 1 mM ATP. Kinase reactions were stopped after 20 min.

For kinase assays with INR119 and H<sub>2</sub>O<sub>2</sub>, resuspended and aliquoted beads with HA-Wis1-His<sub>6</sub> bound were first pre-treated for 15 min with the indicated concentration of INR119 at a final DMSO concentration of 2.5 %. As a control, beads treated with 2.5 % DMSO alone were used. Subsequently the beads with HA-Wis1-His<sub>6</sub> bound were incubated 5 min at the indicated H<sub>2</sub>O<sub>2</sub> concentration. Thereafter the Wis1 activity against the substrate was investigated by addition of MHNSTY1, as well as by addition of MgCl<sub>2</sub>/ATP, giving a final concentration of 20 mM MgCl<sub>2</sub> (10 mM available for reaction) and 1 mM ATP. Kinase reactions were stopped after 20 min.

### **mPEG assays**

HA-tagged Wis1 protein was expressed from its own promoter (wt strain JJS15 or *wis1-6CS* strain JJS16) or was overexpressed from the inducible *nmt1* promoter (strain JJS7 and *wis1-C458S*). Cells were harvested pure trichloroacetic acid (TCA) added at a final concentration of 20 %. Cells were disrupted in a FastPrep FP120 device (Savant) at speed 5 for 40 s, and everything except the beads was then transferred to new tubes. The samples were pelleted by centrifugation and washed three times with ice-cold acetone. Oxidized cysteine residues in the protein extracts were thereafter labeled through the mPEG (Sigma Aldrich #63187) method, which allows labelling of reversibly oxidized cysteine residues. We used a protocol adapted from Burgoyne et al. 2013 (35). Samples were first incubated with

50 mM NEM (Sigma Aldrich #04259) (in 1 % SDS, 100 mM Tris, 10 mM EDTA, pH 7.0) at 37 °C for 2 h with agitation (1400 rpm) to block reduced thiols. Samples were spun down and the supernatant was precipitated with 20 % ice-cold TCA, washed three times with acetone and dried in a SpeedVac to get rid of residual acetone. The dried samples were next incubated with 50 mM DTT (in 1 % SDS, 100 mM Tris, 10 mM EDTA, pH 7.0) to reduce the reversibly oxidized thiols, at 37°C for 2 h with agitation (1400 rpm). After this incubation step, each sample was divided into two tubes and precipitated and washed with acetone three times. Samples were subsequently incubated either in 2 mM mPEG (in 1 % SDS, 100 mM Tris, 10 mM EDTA, pH 7.0) at 37 °C for 2 h with agitation (1400 rpm), for reaction of reduced (initially oxidized) thiols, or again blocked by 50 mM NEM. Samples were then precipitated and washed with acetone. For the samples labeled NEM-NEM-mPEG, the reactions were in the following order: NEM – DTT – NEM – DTT – mPEG. Samples (4 - 20 µg protein) were separated by SDS-PAGE. Wis1 protein bands were detected by western blot using anti-HA.

### **Survival assays**

Logarithmically growing cells (972 *h*, JJS20, JJS17, JJS18, JJS19, JJS22 and JJS1) at OD<sub>600</sub> of 0.5 were used. Three-fold serial dilutions of each strain were spotted on normal YES plates or YES plates containing stress agents (0.5 mM H<sub>2</sub>O<sub>2</sub>, 1 M KCl). The experiment was performed in duplicates. The plates were then incubated at 30°C for 48 h and photographed.

### **Homology structural modeling of Wis1 and docking**

The structure of Wis1 was obtained by homology modeling. The protein sequences of Wis1 were obtained from Genbank (ID: NP\_595457). The crystal structure of human MEK1 (PDBID: 1S9J) (14) was used as the template. The sequence similarity between these two proteins is 47 %. The homology model was built using Structure Prediction Wizard (36) in Schrödinger Suite (Schrödinger, LLC, New York, NY). The energy-based model building method was used. The ClustalW method was used to align the target and template sequences in Prime.

For docking, compound INR119 was built in Maestro, and prepared by Ligprep in Schrödinger Suite (Schrödinger, LLC, New York, NY). On the basis of the obtained Wis1 structure from the homology model, the Receptor Grid Generation panel (Schrödinger, LLC, NY) was used to generate grids to specify the position and size of the active site, as well as

the allosteric site next to the ATP binding site. To grant full flexibility to the ligands, the XP (37) (extra precision) docking function of Glide (38) was used and the number of poses per ligand was set to 100. To select the best docked poses, a post-docking minimization was carried out on the output complexes and the number of docking poses per ligand for output saving was set to be 10.

### ***In vivo* MEK1 kinase assay**

MCF-7 breast cancer cells were cultured in DMEM supplemented with 10 % fetal calf serum, 0.5 % L-glutamine and 0.5 % PenStrep (Gibco, by Life Technologies). Cells were grown in 37°C in a humidified atmosphere containing 5 % CO<sub>2</sub>.

Non-starved cells were treated for 90 min with either DMSO alone or different concentrations (2 – 100 µM) of INR119 dissolved in DMSO. Cells were lysed by addition of HEPES lysis buffer (50 mM HEPES pH 7.5, 10 mM NaCl, 1 % Triton X-100, 10 % glycerol, 5 mM MgCl<sub>2</sub>, 1 mM EDTA) supplemented with phosphatase inhibitor cocktail P5726 and P0044 (Sigma Aldrich) and protease inhibitor cocktail 04693159001 (Roche), together with incubation at 4°C with gentle shaking for 30 min. Phosphorylation of Erk1/2 was analyzed by western blot as described previously (39).

### **Thermal shift assays**

*S. pombe* strain JJS6 expressing Wis1 with an N-terminal (HA)<sub>3</sub> tag from the inducible *nmtI*<sup>+</sup> promoter integrated in the chromosomal *wisI*<sup>+</sup> locus was grown for 24 h in EMM without thiamine for a final OD<sub>600</sub> of 2.0 to induce maximal expression of Wis1. For each sample, 6.4 × 10<sup>8</sup> cells were used. For thermal shift assays in live cells, cells was subjected to 15 min 25µM INR119 pre-treatment, and then heated to the indicated temperature for 3 min. Subsequently, the temperature was lowered to 25°C for 3 min before snap freezing on dry ice. Cells were thereafter thawed on ice and lysed by shaking with acid washed glass beads in a FastPrep FP120 device (Savant) at speed setting 5 for 30 sec. Lysis was performed in ice-cold lysis buffer A (50 mM NaCl, 50 mM Tris pH 7.6, 0.2 % Triton X-100, 0.25 % NP40) containing phosphatase inhibitor cocktail 04906837001 and protease inhibitor cocktail 04693159001 (both from Roche). Lysates was subjected to centrifugation at 20 000 × g for 20 min to separate between soluble and insoluble proteins. Finally, the supernatants containing soluble protein were analyzed by western blot.

For thermal shift assay on crude extracts, cells were instead first lysed as described above and then subjected to a 5 min centrifugation at 13 000 rpm in a microcentrifuge to get rid of foam. Protein lysates were thereafter preincubated with 3  $\mu$ M INR119 for 15 min, and then heated to the indicated temperature for 3 min. Subsequently, the temperature was lowered to 25°C for 3 min before snap freezing on dry ice. Frozen lysates were thawed on ice and subjected to centrifugation at 20 000  $\times$  g for 20 min to separate between soluble and insoluble proteins. Finally, the supernatants containing soluble protein were analysed by western blot.

### **Quantitative RT-PCR**

Lysates were prepared from exponentially growing cultures that were incubated under the conditions and times indicated. RNA was isolated and quantitative RT-PCR (qPCR) was performed as described (40) using primers *qsrx1F*, 5'-GCTCACGATGAA-GCAGGGCG-3' and *qsrx1R*, 5'-GGCGTAGAGTGTAGGGGAGCA-3'. A primer pair each were used for the reference genes *act1*<sup>+</sup> and *nda3*<sup>+</sup>: *qact1F*, 5'-CCGTGCCCTGAA-GCTCTTT-3'; *qact1R*, 5'-GCCTCATGAATACCGCGTTT-3'; *qnda3F*, 5'-AATAT-GATGGTCGCCGCTGA-3'; and *qnda3R*, 5'-ACGAAAAGAGCGGCAACTG-3'. Data and error bars represent the average and standard deviation of 4 independent biological samples.

### **Acknowledgements**

This work was financially supported by grants from Helge Axson Johnson's Foundation to JJS, ANR PrxAge from the French Agence Nationale de Recherche to MBT, from the Swedish Research Council to MG (2015-05642), and from the Swedish Cancer fund to MM (17-0778) and to PS (13-0438 and 16-0708).

## References

1. **Gordley RM, Bugaj LJ, Lim WA.** 2016. Modular engineering of cellular signaling proteins and networks. *Curr Opin Struct Biol* **39**:106-114.  
<https://doi.org/10.1016/j.sbi.2016.06.012>
2. **Degols G, Shiozaki K, Russell P.** 1996. Activation and regulation of the Spc1 stress-activated protein kinase in *Schizosaccharomyces pombe*. *Mol Cell Biol* **16**:2870-2877.  
<https://doi.org/10.1128/MCB.16.6.2870>
3. **Buck V, Quinn J, Soto Pino T, Martin H, Saldanha J, Makino K, Morgan BA, Millar JB.** 2001. Peroxide sensors for the fission yeast stress-activated mitogen-activated protein kinase pathway. *Mol Biol Cell* **12**:407-419.  
<https://doi.org/10.1091/mbc.12.2.407>
4. **Nguyen AN, Lee A, Place W, Shiozaki K.** 2000. Multistep phosphorelay proteins transmit oxidative stress signals to the fission yeast stress-activated protein kinase. *Mol Biol Cell* **11**:1169-1181.  
<https://doi.org/10.1091/mbc.11.4.1169>
5. **Samejima I, Mackie S, Warbrick E, Weisman R, Fantes PA.** 1998. The fission yeast mitotic regulator *win1*<sup>+</sup> encodes an MAP kinase kinase kinase that phosphorylates and activates Wis1 MAP kinase kinase in response to high osmolarity. *Mol Biol Cell* **9**:2325-2335.  
<https://doi.org/10.1091/mbc.9.8.2325>
6. **Shieh JC, Wilkinson MG, Buck V, Morgan BA, Makino K, Millar JB.** 1997. The Mcs4 response regulator coordinately controls the stress-activated Wak1-Wis1-Styl1 MAP kinase pathway and fission yeast cell cycle. *Genes Dev* **11**:1008-1022.  
<https://doi.org/10.1101/gad.11.8.1008>
7. **Wilkinson MG, Samuels M, Takeda T, Toone WM, Shieh JC, Toda T, Millar JB, Jones N.** 1996. The Atf1 transcription factor is a target for the Styl1 stress-activated MAP kinase pathway in fission yeast. *Genes Dev* **10**:2289-2301.  
<https://doi.org/10.1101/gad.10.18.2289>
8. **Millar JB, Buck V, Wilkinson MG.** 1995. Pyp1 and Pyp2 PTPases dephosphorylate an osmosensing MAP kinase controlling cell size at division in fission yeast. *Genes Dev* **9**:2117-2130.  
<https://doi.org/10.1101/gad.9.17.2117>
9. **McCubrey JA, Lahair MM, Franklin RA.** 2006. Reactive oxygen species-induced activation of the MAP kinase signaling pathways. *Antioxid Redox Signal* **8**:1775-1789.  
<https://doi.org/10.1089/ars.2006.8.1775>
10. **Diao Y, Liu W, Wong CC, Wang X, Lee K, Cheung PY, Pan L, Xu T, Han J, Yates JR, 3rd, Zhang M, Wu Z.** 2010. Oxidation-induced intramolecular disulfide bond inactivates mitogen-activated protein kinase kinase 6 by inhibiting ATP binding. *Proc Natl Acad Sci U S A* **107**:20974-20979.  
<https://doi.org/10.1073/pnas.1007225107>
11. **Möbitz H.** 2015. The ABC of protein kinase conformations. *Biochim Biophys Acta* **1854**:1555-1566.  
<https://doi.org/10.1016/j.bbapap.2015.03.009>
12. **Redwan IN, Dyrager C, Solano C, Fernandez de Troconiz G, Voisin L, Bliman D, Meloche S, Grötli M.** 2014. Towards the development of chromone-based MEK1/2 modulators. *Eur J Med Chem* **85**:127-138.  
<https://doi.org/10.1016/j.ejmech.2014.07.018>

13. **Shang J, Lu S, Jiang Y, Zhang J.** 2016. Allosteric modulators of MEK1: drug design and discovery. *Chem Biol Drug Des* **88**:485-497.  
<https://doi.org/10.1111/cbdd.12780>
14. **Ohren JF, Chen H, Pavlovsky A, Whitehead C, Zhang E, Kuffa P, Yan C, McConnell P, Spessard C, Banotai C, Mueller WT, Delaney A, Omer C, Sebolt-Leopold J, Dudley DT, Leung IK, Flamme C, Warmus J, Kaufman M, Barrett S, Teclé H, Hasemann CA.** 2004. Structures of human MAP kinase kinase 1 (MEK1) and MEK2 describe novel noncompetitive kinase inhibition. *Nat Struct Mol Biol* **11**:1192-1197.  
<https://doi.org/10.1038/nsmb859>
15. **Dudley DT, Pang L, Decker SJ, Bridges AJ, Saltiel AR.** 1995. A synthetic inhibitor of the mitogen-activated protein kinase cascade. *Proc Natl Acad Sci U S A* **92**:7686-7689.  
<https://doi.org/10.1073/pnas.92.17.7686>
16. **Treiber DK, Shah NP.** 2013. Ins and outs of kinase DFG motifs. *Chem Biol* **20**:745-746.  
<https://doi.org/10.1016/j.chembiol.2013.06.001>
17. **Jafari R, Almquist H, Axelsson H, Ignatushchenko M, Lundbäck T, Nordlund P, Martínez Molina D.** 2014. The cellular thermal shift assay for evaluating drug target interactions in cells. *Nat Protoc* **9**:2100-2122.  
<https://doi.org/10.1038/nprot.2014.138>
18. **Shiozaki K, Shiozaki M, Russell P.** 1998. Heat stress activates fission yeast Spc1/StyI MAPK by a MEKK-independent mechanism. *Mol Biol Cell* **9**:1339-1349.  
<https://doi.org/10.1091/mbc.9.6.1339>
19. **Vivancos AP, Castillo EA, Biteau B, Nicot C, Ayté J, Toledano MB, Hidalgo E.** 2005. A cysteine-sulfenic acid in peroxiredoxin regulates H<sub>2</sub>O<sub>2</sub>-sensing by the antioxidant Pap1 pathway. *Proc Natl Acad Sci U S A* **102**:8875-8880.  
<https://doi.org/10.1073/pnas.0503251102>
20. **Vivancos AP, Jara M, Zuin A, Sansó M, Hidalgo E.** 2006. Oxidative stress in *Schizosaccharomyces pombe*: different H<sub>2</sub>O<sub>2</sub> levels, different response pathways. *Mol Genet Genomics* **276**:495-502.  
<https://doi.org/10.1007/s00438-006-0175-z>
21. **Shiozaki K, Russell P.** 1995. Cell-cycle control linked to extracellular environment by MAP kinase pathway in fission yeast. *Nature* **378**:739-743.  
<https://doi.org/10.1038/378739a0>
22. **Smith DA, Toone WM, Chen D, Bähler J, Jones N, Morgan BA, Quinn J.** 2002. The Srk1 protein kinase is a target for the Sty1 stress-activated MAPK in fission yeast. *J Biol Chem* **277**:33411-33421.  
<https://doi.org/10.1074/jbc.M204593200>
23. **Hourihan JM, Moronetti Mazzeo LE, Fernandez-Cardenas LP, Blackwell TK.** 2016. Cysteine sulfenylation directs IRE-1 to activate the SKN-1/Nrf2 antioxidant response. *Mol Cell* **63**:553-566.  
<https://doi.org/10.1016/j.molcel.2016.07.019>
24. **Huse M, Kuriyan J.** 2002. The conformational plasticity of protein kinases. *Cell* **109**:275-282.  
[https://doi.org/10.1016/S0092-8674\(02\)00741-9](https://doi.org/10.1016/S0092-8674(02)00741-9)
25. **Humphries KM, Deal MS, Taylor SS.** 2005. Enhanced dephosphorylation of cAMP-dependent protein kinase by oxidation and thiol modification. *J Biol Chem* **280**:2750-2758.  
<https://doi.org/10.1074/jbc.M410242200>

26. **Humphries KM, Juliano C, Taylor SS.** 2002. Regulation of cAMP-dependent protein kinase activity by glutathionylation. *J Biol Chem* **277**:43505-43511.  
<https://doi.org/10.1074/jbc.M207088200>
27. **de Piña MZ, Vázquez-Meza H, Pardo JP, Rendón JL, Villalobos-Molina R, Riveros-Rosas H, Piña E.** 2008. Signaling the signal, cyclic AMP-dependent protein kinase inhibition by insulin-formed H<sub>2</sub>O<sub>2</sub> and reactivation by thioredoxin. *J Biol Chem* **283**:12373-12386.  
<https://doi.org/10.1074/jbc.M706832200>
28. **Burgoyne JR, Madhani M, Cuello F, Charles RL, Brennan JP, Schröder E, Browning DD, Eaton P.** 2007. Cysteine redox sensor in PKGI $\alpha$  enables oxidant-induced activation. *Science* **317**:1393-1397.  
<https://doi.org/10.1126/science.1144318>
29. **Burgoyne JR, Rudyk O, Cho HJ, Prsyazhna O, Hathaway N, Weeks A, Evans R, Ng T, Schroder K, Brandes RP, Shah AM, Eaton P.** 2015. Deficient angiogenesis in redox-dead Cys17Ser PKARI $\alpha$  knock-in mice. *Nat Commun* **6**:7920.  
<https://doi.org/10.1038/ncomms8920>
30. **Roger F, Picazo C, Asami C, Reiter W, Hanzén S, Gao C, Lagniel G, Welkenhuysen N, Labarre J, Nyström T, Grötl M, Hartl M, Molin M.** 2019. Peroxiredoxin promotes longevity and H<sub>2</sub>O<sub>2</sub>-resistance in yeast through redox-modification of PKA. *bioRxiv*:676270.  
<https://doi.org/10.1101/676270>
31. **Mody N, Leitch J, Armstrong C, Dixon J, Cohen P.** 2001. Effects of MAP kinase cascade inhibitors on the MKK5/ERK5 pathway. *FEBS Lett* **502**:21-24.  
[https://doi.org/10.1016/S0014-5793\(01\)02651-5](https://doi.org/10.1016/S0014-5793(01)02651-5)
32. **Kamakura S, Moriguchi T, Nishida E.** 1999. Activation of the protein kinase ERK5/BMK1 by receptor tyrosine kinases. Identification and characterization of a signaling pathway to the nucleus. *J Biol Chem* **274**:26563-26571.  
<https://doi.org/10.1074/jbc.274.37.26563>
33. **Moreno S, Klar A, Nurse P.** 1991. Molecular genetic analysis of the fission yeast *Schizosaccharomyces pombe*. *Meth Enzymol* **194**:795-823.  
[https://doi.org/10.1016/0076-6879\(91\)94059-L](https://doi.org/10.1016/0076-6879(91)94059-L)
34. **Hentges P, Van Driessche B, Tafforeau L, Vandenhoute J, Carr AM.** 2005. Three novel antibiotic marker cassettes for gene disruption and marker switching in *Schizosaccharomyces pombe*. *Yeast* **22**:1013-1019.  
<https://doi.org/10.1002/yea.1291>
35. **Burgoyne JR, Oviosu O, Eaton P.** 2013. The PEG-switch assay: a fast semi-quantitative method to determine protein reversible cysteine oxidation. *J Pharmacol Toxicol Methods* **68**:297-301.  
<https://doi.org/10.1016/j.vascn.2013.07.001>
36. **Jacobson MP, Friesner RA, Xiang Z, Honig B.** 2002. On the role of the crystal environment in determining protein side-chain conformations. *J Mol Biol* **320**:597-608.  
[https://doi.org/10.1016/S0022-2836\(02\)00470-9](https://doi.org/10.1016/S0022-2836(02)00470-9)
37. **Friesner RA, Murphy RB, Repasky MP, Frye LL, Greenwood JR, Halgren TA, Sanschagrin PC, Mainz DT.** 2006. Extra precision glide: docking and scoring incorporating a model of hydrophobic enclosure for protein-ligand complexes. *J Med Chem* **49**:6177-6196.  
<https://doi.org/10.1021/jm051256o>



38. **Halgren TA, Murphy RB, Friesner RA, Beard HS, Frye LL, Pollard WT, Banks JL.** 2004. Glide: a new approach for rapid, accurate docking and scoring. 2. Enrichment factors in database screening. *J Med Chem* **47**:1750-1759.  
<https://doi.org/10.1021/jm030644s>
39. **Dinér P, Alao JP, Söderlund J, Sunnerhagen P, Grotli M.** 2012. Preparation of 3-substituted-1-isopropyl-1H-pyrazolo[3,4-d]pyrimidin-4-amines as RET kinase inhibitors. *J Med Chem* **55**:4872–4876.  
<https://doi.org/10.1021/jm3003944>
40. **Alao JP, Johansson-Sjölander J, Baar J, Özbaki-Yagan N, Kakoschky B, Sunnerhagen P.** 2014. Caffeine stabilizes Cdc25 independently of Rad3 in *Schizosaccharomyces pombe* contributing to checkpoint override. *Mol Microbiol* **92**:777-796.  
<https://doi.org/10.1111/mmi.12592>
41. **Nguyen AN, Ikner AD, Shiozaki M, Warren SM, Shiozaki K.** 2002. Cytoplasmic localization of Wis1 MAPKK by nuclear export signal is important for nuclear targeting of Spc1/Sty1 MAPK in fission yeast. *Mol Biol Cell* **13**:2651-2663.  
<https://doi.org/10.1091/mbc.02-03-0043>
42. **Nguyen AN, Shiozaki K.** 1999. Heat-shock-induced activation of stress MAP kinase is regulated by threonine- and tyrosine-specific phosphatases. *Genes Dev* **13**:1653-1663.  
<https://doi.org/10.1101/gad.13.13.1653>
43. **Veal EA, Findlay VJ, Day AM, Bozonet SM, Evans JM, Quinn J, Morgan BA.** 2004. A 2-Cys peroxiredoxin regulates peroxide-induced oxidation and activation of a stress-activated MAP kinase. *Mol Cell* **15**:129-139.  
<https://doi.org/10.1016/j.molcel.2004.06.021>
44. **Morigasaki S, Shimada K, Ikner A, Yanagida M, Shiozaki K.** 2008. Glycolytic enzyme GAPDH promotes peroxide stress signaling through multistep phosphorelay to a MAPK cascade. *Mol Cell* **30**:108-113.  
<https://doi.org/10.1016/j.molcel.2008.01.017>
45. **Morigasaki S, Shiozaki K.** 2013. Phosphorelay-dependent and -independent regulation of MAPKKK by the Mcs4 response regulator in fission yeast. *Commun Integr Biol* **6**:e25020.  
<https://doi.org/10.4161/cib.25020>
46. **Di Y, Holmes EJ, Butt A, Dawson K, Mironov A, Kotiadis VN, Gourlay CW, Jones N, Wilkinson CR.** 2012. H<sub>2</sub>O<sub>2</sub> stress-specific regulation of *S. pombe* MAPK Sty1 by mitochondrial protein phosphatase Ptc4. *EMBO J* **31**:563-575.  
<https://doi.org/10.1038/emboj.2011.438>
47. **Nakagawa CW, Yamada K, Mutoh N.** 1998. Two distinct upstream regions are involved in expression of the catalase gene in *Schizosaccharomyces pombe* in response to oxidative stress. *J Biochem* **123**:1048-1054.  
<https://doi.org/10.1093/oxfordjournals.jbchem.a022042>
48. **Quinn J, Findlay VJ, Dawson K, Millar JB, Jones N, Morgan BA, Toone WM.** 2002. Distinct regulatory proteins control the graded transcriptional response to increasing H<sub>2</sub>O<sub>2</sub> levels in fission yeast *Schizosaccharomyces pombe*. *Mol Biol Cell* **13**:805-816.  
<https://doi.org/10.1091/mbc.01-06-0288>
49. **Zhou X, Ma Y, Sugiura R, Kobayashi D, Suzuki M, Deng L, Kuno T.** 2010. MAP kinase kinase kinase (MAPKKK)-dependent and -independent activation of Sty1 stress MAPK in fission yeast. *J Biol Chem* **285**:32818-32823.  
<https://doi.org/10.1074/jbc.M110.135764>

50. **Morigasaki S, Ikner A, Tatebe H, Shiozaki K.** 2013. Response regulator-mediated MAPKKK heteromer promotes stress signaling to the Spc1 MAPK in fission yeast. *Mol Biol Cell* **24**:1083-1092.

<https://doi.org/10.1091/mbc.e12-10-0727>

## Figure 1

### Wis1 is inhibited by oxidation of Cys458 *in vitro* despite lacking a cysteine homologous to MKK6C109

A) Multiple alignment of the human, fission yeast and budding yeast MAPKKs showing conservation of the cysteines involved in inhibition through disulfide formation in human MKK6. Cysteines are highlighted in red, The Wis1 sequence is marked with an asterisk, and the DFG motif by a green box. MKK6 Cys196/Wis1 Cys458 directly preceding the highly conserved DFG motif is conserved in all MAPKKs, whereas the position of MKK6 Cys106 is less conserved. Wis1 has no cysteine corresponding to MKK6 Cys106.

B) Schematic overview of the location of cysteines in Wis1 in relation to functional information within the Wis1 aa sequence. Five out of the total six cysteines are found within the kinase domain, and one within the nuclear export signal (NES). The locations of functional domains in this figure are based on Nguyen et al. (41).

C) Wis1 is inactivated by low levels of H<sub>2</sub>O<sub>2</sub> *in vitro* in a manner reversible by the reductant TCEP. In contrast, a Wis1<sup>C458S</sup> mutant enzyme is less inactivated and activity lost could not be rescued by reductant. Wis1 was treated for 5 min. with H<sub>2</sub>O<sub>2</sub> before starting the 20 min. kinase reaction through addition of MgCl<sub>2</sub>/ATP. This inactivation was in turn reversed by 5 min. incubation with the reductant TCEP at 1 mM before the kinase assay. Wt Wis1 was expressed from JJS7 and Wis1<sup>C458</sup> was expressed from JJS9.

## Figure 2

### Wis1 cysteines including C458 are oxidized *in vivo* and C458 is required for H<sub>2</sub>O<sub>2</sub> resistance

**A-D)** The mPEG assay shows that Wis1 C458 as well as other cysteines in Wis1 are constitutively oxidized *in vivo*. Cells analyzed were expressing HA-tagged wt Wis1 (JJS15) from the endogenous promoter (**A-C**), or wt Wis1 (JJS7) and *wis1-C458S* (JJS9) expressed from the *nmt1* promoter (**D**).

**A)** Slower migrating mPEG modified Wis1 bands appear in extracts of cells even without H<sub>2</sub>O<sub>2</sub> treatment. Formation of these slower migrating forms are blocked by an extra round of NEM before mPEG treatment.

**B)** Time-course of cells treated with 0.5 mM H<sub>2</sub>O<sub>2</sub>

**C)** Different H<sub>2</sub>O<sub>2</sub> concentrations at 20 min single time point

**D)** mPEG assay of wt and *wis1-C458S* cell extracts without H<sub>2</sub>O<sub>2</sub> added

**E)** Mutating C458 to S results in an elevated Sty1 phosphorylation upon adding low levels of H<sub>2</sub>O<sub>2</sub>. Samples from exponentially growing cells wt (972*h*<sup>-</sup>) and *wis1-C458S* (JJS18) were harvested before and at 20 min. of H<sub>2</sub>O<sub>2</sub> exposure and subjected to western blot.

**F)** Cells expressing *wis1<sup>C458S</sup>* are highly sensitive to H<sub>2</sub>O<sub>2</sub> but not to KCl. Exponentially growing cells of wt (972*h*<sup>-</sup>), *wis1<sup>C11S</sup>* (JJS20), *wis1<sup>C394S</sup>* (JJS17), *wis1<sup>C458S</sup>* (JJS18), *wis1<sup>C477S</sup>* (JJS19), *wis1<sup>6CS</sup>* (JJS22) and *wis1Δ* (JJS1) were serially diluted and spotted on YES plates with and without 0.5 mM H<sub>2</sub>O<sub>2</sub> or 1 M KCl.

### Figure 3

#### **The non-competitive MAPKK inhibitor INR119 binds Wis1 near C458 and protects Wis1 from inactivation by low H<sub>2</sub>O<sub>2</sub> *in vitro*.**

**A)** Homology model of Wis1 showing the predicted allosteric pocket with INR119 docked inside, and its close proximity to the location of C458 and bound ATP.

**B)** Structures of INR119 and PD98059.

**C)** Thermal shift assay of the INR119/Wis1 interaction. Cells (JJS6) expressing HA-tagged Wis1 from the *nmt1* promoter were lysed. Cellular extracts were pre-treated with 3  $\mu$ M INR119 for 15 min. and the extracts were heated to the indicated temperatures for 3 min. Soluble protein was separated by centrifugation and analyzed by western blot. Quantification of soluble Wis1 is shown, at temperatures from 30°C to 50°C. Values have been normalized relative to untreated extract at 30°C, and are the averages of four to seven independent experiments.

**D)** INR119 protects Wis1 from inactivation by low levels of H<sub>2</sub>O<sub>2</sub> *in vitro*. Semi-purified Wis1 (strain JJS7) was pre-treated for 15 min with the indicated concentration of INR119 and subsequently for an additional 5 min with 0.05 mM H<sub>2</sub>O<sub>2</sub>. Thereafter the substrate Sty1 was added, as well as MgCl<sub>2</sub>/ATP. Kinase reactions were stopped after 20 min, and results analyzed by western blot.

## Figure 4

### INR119 pretreatment strongly potentiates the Wis1 response to low H<sub>2</sub>O<sub>2</sub> *in vivo*

**A)** Western blot of Sty1 phosphorylation in cells pre-treated with 50 μM INR119 and at the indicated time-points following the addition 500 μM H<sub>2</sub>O<sub>2</sub>.

**B)** The ability of INR119 to enhance Sty1 activation is dependent on Wis1 C458. Strains wt (*972h*) and *wis1-C458S* (JJS18) were analyzed for Sty1 activation by immunoblot at the indicated time points following the addition of 0.5 mM H<sub>2</sub>O<sub>2</sub>.

**C)** The ability of INR119 to potentiate Wis1 signaling is more pronounced at low levels of H<sub>2</sub>O<sub>2</sub>. Western blot of cells (*972h*) pretreated with 50 μM INR119 and following the indicated time points after the addition of different amounts of H<sub>2</sub>O<sub>2</sub> (0.25 – 5 mM) as in **A**.

**D)** The Atf1-dependent transcript *srx1*<sup>+</sup> is enhanced by INR119. Wt (*972h*-) cells were mock-pretreated or pre-treated with INR119 for 20 min and thereafter treated with H<sub>2</sub>O<sub>2</sub> as in **A**. Samples were taken after 20 min of H<sub>2</sub>O<sub>2</sub> treatment and *srx1*<sup>+</sup> transcript levels were determined by qPCR.

## Figure 5

### **The INR119-induced enhancement of Sty1 pathway activation upon H<sub>2</sub>O<sub>2</sub> stress requires the upstream activation of Wis1 through the MAPKKKs.**

**A)** Schematic overview of the Sty1 pathway. This simplified schematic summarizes features of pathway architecture relevant for this paper. It is based on information from the literature on protein-protein interactions, modes of pathway activation, and downstream targets (2-8, 20, 21, 42-49). TF, transcription factor.

**B)** Western blot of the wt (*972h*) and *win1Δ wis4Δ* (JJS5) deletion mutant cells. Cells were pre-treated with INR119 at exposure to 500 μM H<sub>2</sub>O<sub>2</sub> as described in Fig. 4 A. The 0 min samples represent cells only pre-treated.

## Figure 6

### Proposed model of INR119 mechanism of action

**A, B)**  $H_2O_2$  induces pathway activation through MAPKKK activation, however at low  $H_2O_2$  concentrations **(A)** negative regulation targeting Wis1 C458 holds the activity of Wis1 back. At higher levels of  $H_2O_2$  Styl activation is independent of Wis1 C458 **(B)**. **C)** INR119 binds Wis1 in an allosteric site next to the active site very close to C458 and protects against negative regulation targeting C458 through stabilizing a conformation unresponsive to negative regulation through C458, resulting in higher Wis1 activity in low  $H_2O_2$  levels.



## Supplementary Figure S1

**Wis1 is inactivated by H<sub>2</sub>O<sub>2</sub> *in vitro* through a mechanism reversible by a reductant, and the active site cysteine of MKK6, involved in inactivation, is highly conserved in MAPKKs but not in serine/threonine kinases in general, indicating a conserved function in MAPK pathways.**

**A)** Multiple alignment showing the degree of conservation of MKK6 C196, corresponding to Wis1 C458. The active site cysteine MKK6 C196 is conserved in all MAPKKs of *S. pombe*, *S. cerevisiae* and humans as well as in multiple MAPKs, however not in MAPKKs or in serine/threonine kinases in general. MKK6 C109 is conserved in some but not all investigated MAPKKs. Cysteines are highlighted in red, the Wis1 sequence is marked with an asterisk, the DFG motif is boxed.

**B)** Kinase assay with Wis1 and Sty1 purified in the absence of EDTA indicates that ATP co-purifies with Wis1. Sty1 is not phosphorylated before (lane 1) or after (lane 2) assay incubation without Wis1 added. However, even without addition of ATP to the reaction buffer (lane 3), Wis1 phosphorylates Sty1 to the same degree as when ATP is included (lane 4).

**C)** The tagged Wis1 expressed from strain JJS7 is responsible for the phosphorylation of the tagged Sty1 in the *in vitro* kinase assay. Ni<sup>2+</sup>-beads with precipitates from strain JJS7 expressing HA-Wis1His<sub>6</sub> or *wis1Δ* (JJS1) was tested for activity against the substrate Sty1. No phosphorylation is seen when adding everything except HA-Wis1-His<sub>6</sub> from strain JJS7 (lane 2) or when exchanging the precipitates from strain JJS7 with precipitate from the *wis1Δ* strain JJS1 (lane 5). Note that no H<sub>2</sub>O<sub>2</sub> was included in this assay.

**D)** Inactivation of Wis1 by low levels of H<sub>2</sub>O<sub>2</sub> *in vitro* is caused by reversible thiol oxidation. Semi-purified Wis1 (strain JJS7) was first incubated 5 min in sample pairs with H<sub>2</sub>O<sub>2</sub> giving the indicated final concentration, and subsequently for one tube in each pair for 5 min with 1 mM TCEP. Thereafter the Wis1 substrate Sty1 (expressed from pREP41MHNSTY1 in strain KS1598), was added and the kinase reaction was started by addition of MgCl<sub>2</sub>/ATP. The kinase reaction was stopped after 20 min.

## Supplementary Figure S2

### **The constitutively mPEG-dependent altered migration of Wis1 is abolished in a cysteine-less mutant Wis1 protein (Wis1<sup>6CS</sup>).**

mPEG assay of strain JJS16 expressing cysteine-less Wis1<sup>6CS</sup> from the endogenous promoter. Samples were divided in two equal aliquots and subjected to either NEM-DTT-NEM treatment or NEM-DTT-mPEG.

## Supplementary Figure S3

### **The close structural PD98059 analog INR119 inhibits human MEK1 more efficiently than PD98059 *in vivo*, and a thermal shift assay indicates that it interacts directly with the *S. pombe* homolog Wis1 *in vivo*.**

**A)** INR119 inhibits the MAPKK MEK1 in human MCF-7 breast cancer cells. Western blot of protein extract from MCF-7 human breast cancer cells exposed for 90 min. to different concentrations of INR119 or PD98059. MEK1 activity was measured as the amount of phosphorylated Erk1/2.

**B, C)** INR119 is predicted to bind in an allosteric pocket in Wis1 and form a hydrogen bond with F460, the phenylalanine in the DFG-motif, as well as with S463.

**B)** Homology model of the Wis1 structure showing INR119 docked in the predicted allosteric site.

**C)** Predictions of interactions between INR119 and the amino acids forming the allosteric pocket.

**D)** Western blot of a thermal shift assay performed in live cells shows that INR119 stabilizes soluble Wis1 at elevated temperatures indicating a direct *in vivo* interaction, however also the heat itself strongly stabilizes soluble Wis1. Live *S. pombe* cells (JJS6) expressing tagged Wis1 was pre-incubated with 25  $\mu$ M INR119 for 15 min. and thereafter subjected to the indicated temperature for 3 min. The soluble fraction in lysates was thereafter obtained by centrifugation (see Materials and Methods).

## Supplementary Figure S4

### Potential by INR119 in oxidative stress is dependent on *wisI*<sup>+</sup>, but not on C394 or C477, the two cysteines in Wis1 closest to C458.

**A)** INR119 effects on Sty1 activation in response to H<sub>2</sub>O<sub>2</sub> are entirely dependent on Wis1. Western blot of Sty1 phosphorylation following H<sub>2</sub>O<sub>2</sub> addition to a wt and a *wis1Δ* (JJS1) isogenic deletion mutant. Cells were pre-treated with INR119 and exposed to 0.5 mM H<sub>2</sub>O<sub>2</sub> as described in Fig. 4 A. The 0 min samples represent pre-treated cells.

**B-D)** The enhancing effect of INR119 is neither dependent on C394 nor C477, the two cysteines closest to C458 in the Wis1 structure as the Sty1 phosphorylation is enhanced by INR119 in the *wis1-C394S* (**B**) and *wis1-C477S* (**C**) mutants. Strains used were wt (*972h*), *wis1-C394S*(JJS17), and *wis1-C477S* (JJS19).

**D)** Structural homology model of Wis1 with the distances between C398 and C477 and C458, as well as the INR119 binding site, indicated.

**E-F)** INR119 neither affects the response to KCl (**E**) nor heat (**F**). Wt (*972 h*) cells were mock-pretreated (“control”); or pre-treated with 50 μM INR119, for 20 min, and thereafter the culture was treated with KCl (0.6 M) or heat stressed (42°C).

**G)** The Atf1-dependent transcript *srxI*<sup>+</sup> is enhanced by INR119 in a Wis1-dependent manner. Cells were mock-pretreated or pre-treated with INR119 for 20 min as described in Fig. 4 D. Samples were taken after 20 min of H<sub>2</sub>O<sub>2</sub> treatment. *srxI*<sup>+</sup> transcript levels were determined by qPCR. Relative *srxI*<sup>+</sup> transcript levels in wt (*972 h*) and *wis1Δ* (JJS1), with or without exposure to 0.2 mM H<sub>2</sub>O<sub>2</sub>.

## Supplementary Figure S5

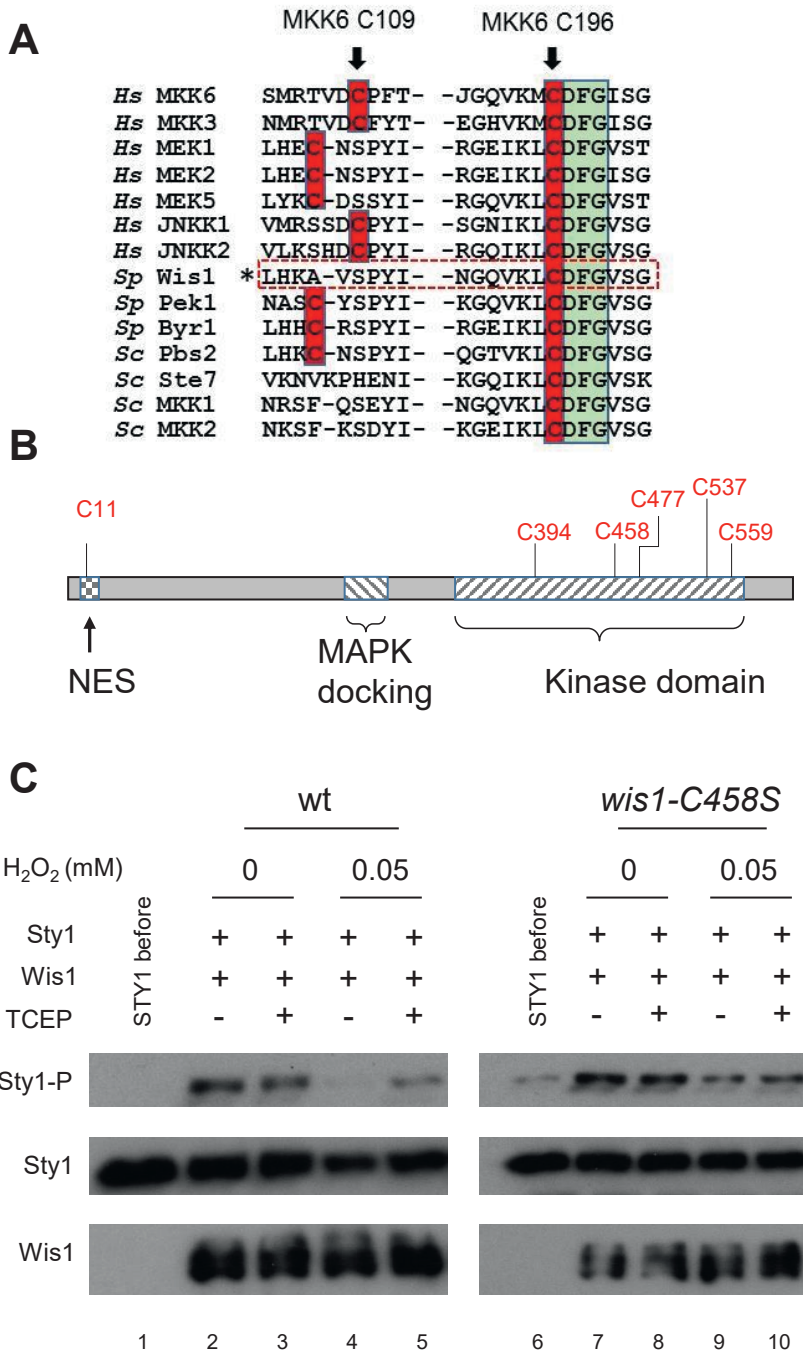
**INR119 induces enhanced Sty1 phosphorylation upon H<sub>2</sub>O<sub>2</sub> stress also in a *wis1<sup>DD</sup>* strain displaying constitutive Sty1 activation, suggesting it acts independently of Wis1 activation by the MAPKKKs.**

Immunoblot showing Sty1 phosphorylation in a control or INR119-treated *wis1-S469D,T473D* mutant (18).

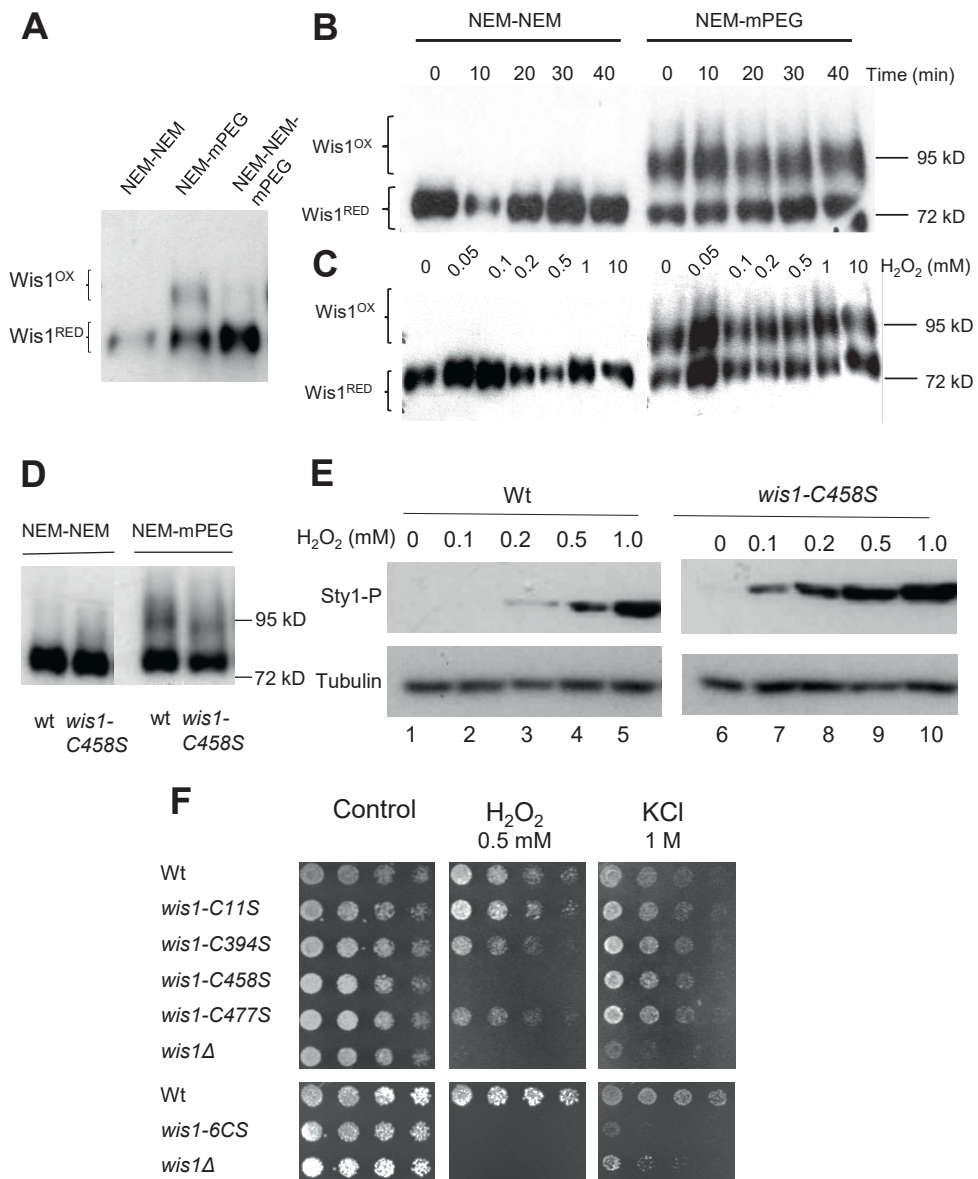
**Table 1.** *S. pombe* strains and plasmids used in this study.

Strain	Genotype	Source or reference
972	<i>h<sup>-</sup></i>	Lab stock
JJS1	<i>h<sup>-</sup> wisI::KanMX6</i>	This study
JJS5	<i>h<sup>-</sup> winI::nat wis4::KanMX6</i>	This study
JJS6	<i>h<sup>-</sup> KanMX6:nmtI<sup>+</sup>:(HA)<sub>3</sub>:wisI<sup>+</sup></i>	This study
JJS7	<i>h<sup>-</sup> KanMX6:nmtI<sup>+</sup>:(HA)<sub>3</sub>:wisI<sup>+</sup> His<sub>6</sub>:NatMX6</i>	This study
JJS9	<i>h<sup>-</sup> KanMX6:nmtI<sup>+</sup>:(HA)<sub>3</sub>:wisI<sup>C458S</sup> His<sub>6</sub>:HphMX6</i>	This study
JJS15	<i>h<sup>-</sup> wisI<sup>+</sup>-3HA:HphMX6</i>	This study
JJS16	<i>h<sup>-</sup> (HA)<sub>3</sub>:wisI<sup>C11S,C394S,C458S,C477S,C537S,C559S</sup>:His<sub>6</sub>:HphMX6</i>	This study
JJS20	<i>h<sup>-</sup> wisI<sup>C11S</sup> His<sub>6</sub>:HphMX6</i>	This study
JJS17	<i>h<sup>-</sup> wisI<sup>C394S</sup> His<sub>6</sub>:Hph MX6</i>	This study
JJS18	<i>h<sup>-</sup> wisI<sup>C458S</sup> His<sub>6</sub>:Hph MX6</i>	This study
JJS19	<i>h<sup>-</sup> wisI<sup>C477S</sup> His<sub>6</sub>:Hph MX6</i>	This study
JJS22	<i>h<sup>-</sup> wisI<sup>C11S,C394S,C458S,C477S,C537S,C559S</sup>:His<sub>6</sub>:HphMX6</i>	This study
KS1598	<i>h<sup>-</sup> leu1-32</i>	(50)
KS2081	<i>h<sup>-</sup> wisI- S469D,T473D:(Myc)<sub>12</sub>(ura4<sup>+</sup>)</i>	(18)
<b>Plasmids</b>		
	pREP41MHNSTY1	(43)



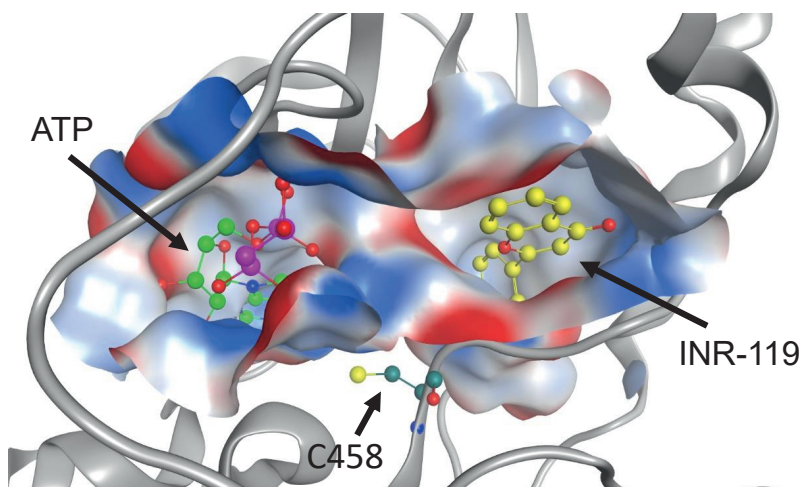
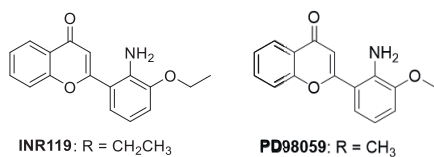
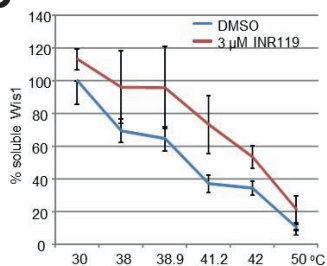
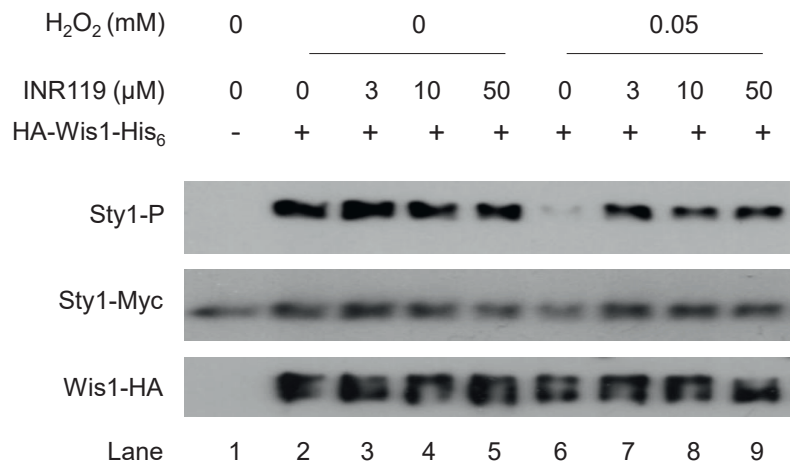


**Fig 1**



**Fig 2**



**A****B****C****D****Fig 3**

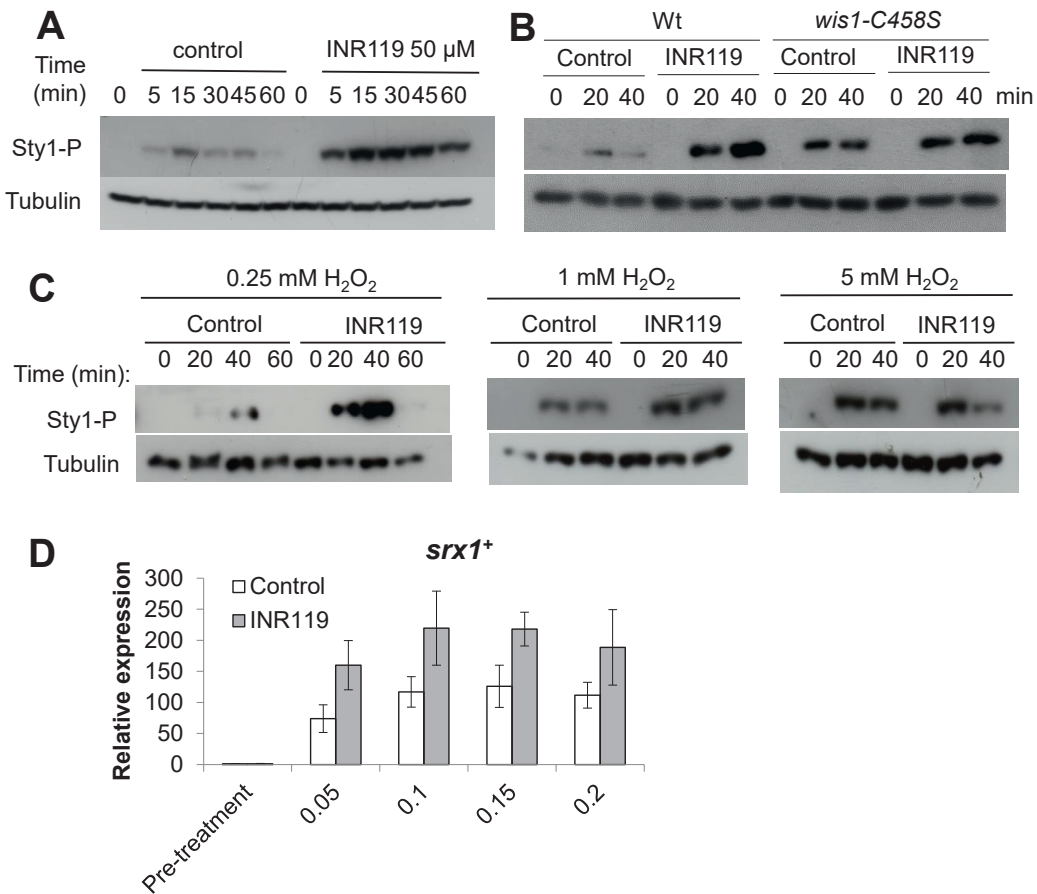


**Fig 4**

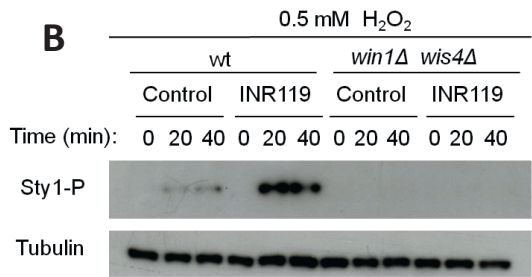
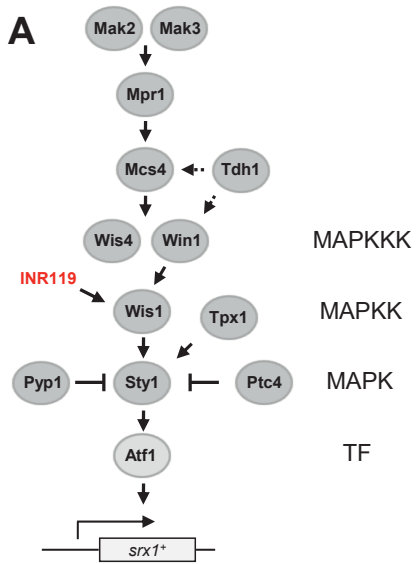
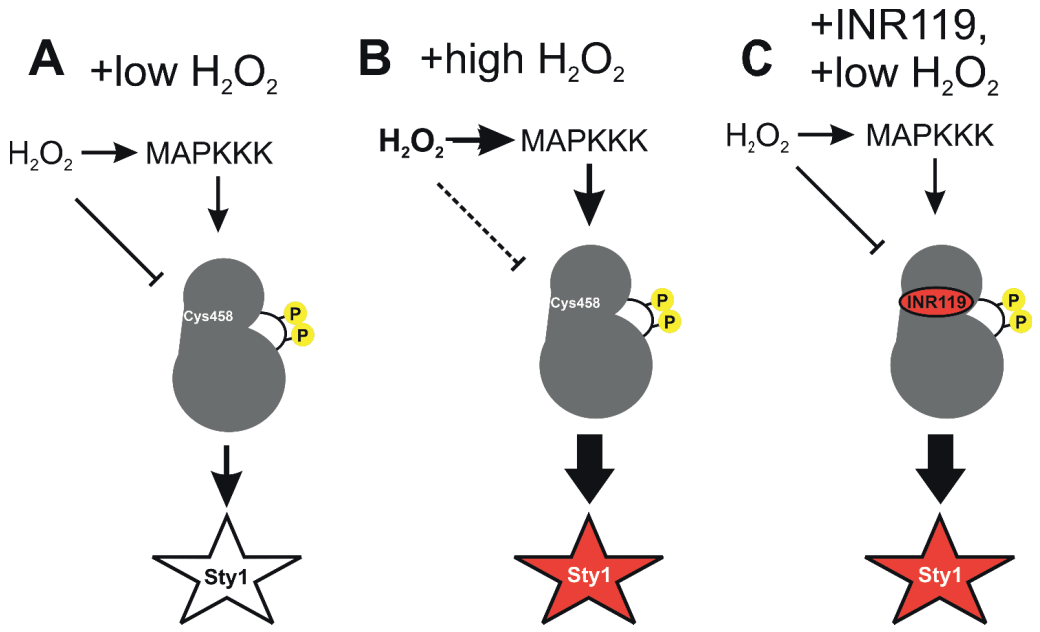


**Figure 5**



MKK6 C109

MKK6 C196

A

MAPKK_MKK6_[Homo_sapiens]/103-112	SMRTV-DGPF--T	MAPKK_MKK6_[Homo_sapiens]/190-202	LGQVKMDFGISG
MAPKK_MKK3_[Homo_sapiens]/114-123	NMRTV-DGIFY--T	MAPKK_MKK3_[Homo_sapiens]/201-213	EGHVKMDFGISG
MAPKK_MEK1_[Homo_sapiens]/48-56	LHEC--NSPY--I	MAPKK_MEK1_[Homo_sapiens]/181-193	RGEIKLDFGVSG
MAPKK_MEK2_[Homo_sapiens]/122-130	LHEC--NSPY--I	MAPKK_MEK2_[Homo_sapiens]/205-217	RGEIKLDFGVSG
MAPKK_MEK5_[Homo_sapiens]/216-224	LYKC--DSSY--I	MAPKK_MEK5_[Homo_sapiens]/294-306	RQVVKLDFGVST
MAPKK_JNKK1_[Homo_sapiens]/152-161	VMRSS-DGPI--I	MAPKK_JNKK1_[Homo_sapiens]/240-252	SGNIKLDFGISG
MAPKK_JNKK2_[Homo_sapiens]/170-179	VLKSH-DGPI--I	MAPKK_JNKK2_[Homo_sapiens]/254-266	RQVVKLDFGVSG
MAPKK_Wis1_[Schizosaccharomyces_pombe]/970-978	LHKA--VSPY--I	MAPKK_Wis1_[Schizosaccharomyces_pombe]/452-464	NGQVKLDFGVSG
MAPKK_Pek1_[Schizosaccharomyces_pombe]/129-137	NRSC--TSPY--I	MAPKK_Pek1_[Schizosaccharomyces_pombe]/217-229	KGQVKLDFGVSG
MAPKK_Byr1_[Schizosaccharomyces_pombe]/114-122	LHHC--RSPY--I	MAPKK_Byr1_[Schizosaccharomyces_pombe]/197-209	RGEIKLDFGVSG
MAPKK_PBS2_[Saccharomyces_cerevisiae]/410-418	LHKC--NSPY--I	MAPKK_PBS2_[Saccharomyces_cerevisiae]/497-509	QGTVKLDFGVSG
MAPKK_STE7_[Saccharomyces_cerevisiae]/242-251	VKNVK-PHEN--I	MAPKK_STE7_[Saccharomyces_cerevisiae]/342-354	KGQIKLDFGVSK
MAPKK_MKK1_[Saccharomyces_cerevisiae]/272-280	NRSF--QSEY--I	MAPKK_MKK1_[Saccharomyces_cerevisiae]/360-372	NGQVKLDFGVSG
MAPKK_MKK2_[Saccharomyces_cerevisiae]/265-273	NKSF--KSDY--I	MAPKK_MKK2_[Saccharomyces_cerevisiae]/359-365	KGQIKLDFGVSG
MAPK_p38_[Homo_sapiens]/75-83	LKHMK--HEN--V	MAPK_p38_[Homo_sapiens]/161-173	DDELKLDDFGLAR
MAPK_ERK1_[Homo_sapiens]/92-100	LLRFR--HEN--V	MAPK_ERK1_[Homo_sapiens]/177-189	TDELKLDDFGLAR
MAPK_ERK5_[Homo_sapiens]/105-113	LKHFK--HDN--I	MAPK_ERK5_[Homo_sapiens]/192-204	NGELKLDDFGLAR
MAPK_Sty1_[Schizosaccharomyces_pombe]/71-79	LKHLR--HEN--I	MAPK_Sty1_[Schizosaccharomyces_pombe]/152-164	NDELKLDDFGLAR
MAPK_Pmk1_[Schizosaccharomyces_pombe]/74-83	LHFR--NHRN--I	MAPK_Pmk1_[Schizosaccharomyces_pombe]/160-172	DDELKLDDFGLAR
MAPK_Spk1_[Schizosaccharomyces_pombe]/89-97	LRHFR--HEN--I	MAPK_Spk1_[Schizosaccharomyces_pombe]/174-186	NDLKVADDFGLAR
MAPK_HOG1_[Saccharomyces_cerevisiae]/74-82	LKHLR--HEN--L	MAPK_HOG1_[Saccharomyces_cerevisiae]/155-167	NDELKLDDFGLAR
MAPK_Kss1_[Saccharomyces_cerevisiae]/63-72	LRYPH--EEN--I	MAPK_Kss1_[Saccharomyces_cerevisiae]/154-166	NDELKLDDFGLAR
MAPKKK_RAF_1[isoform_a][Homo_sapiens]/417-425	LRKT--RRVN--I	MAPKKK_RAF_1[isoform_a][Homo_sapiens]/499-511	GLTVKLDGDFGLAT
MAPKKK_Win1_[Schizosaccharomyces_pombe]/1173-1181	LELF--DHPN--V	MAPKKK_Win1_[Schizosaccharomyces_pombe]/1255-1267	NGIMKFDGFSAK
MAPKKK_Wis4_[Schizosaccharomyces_pombe]/1090-1098	LERL--NHPN--V	MAPKKK_Wis4_[Schizosaccharomyces_pombe]/1172-1184	RGMIKYSDFGSAL
Cdc7_[Homo_sapiens]/108-117	LTVAG--GQDN--V	Cdc7_[Homo_sapiens]/189-201	LKKYALVDFGLAQ
Ark1_[Schizosaccharomyces_pombe]/141-149	QSNL--RHKN--I	Ark1_[Schizosaccharomyces_pombe]/228-235	DGEIKLSDFGWSV
Cdk1/Cdc2_[Schizosaccharomyces_pombe]/55-67	LKEVN--DENRNSNG	Cdk1/Cdc2_[Schizosaccharomyces_pombe]/145-157	EGNLKLDGDFGLAR
Klms1_[Saccharomyces_cerevisiae]/104-112	LKHLL--HPN--I	Klms1_[Saccharomyces_cerevisiae]/186-198	HENLVIDDFGFVN
Pek1_[Schizosaccharomyces_pombe]/649-657	ANKK--KHPF--L	Pek1_[Schizosaccharomyces_pombe]/730-742	DGHIRIADYGLK
Pto1_[Schizosaccharomyces_pombe]/253-261	LSRV--QHPF--I	Pto1_[Schizosaccharomyces_pombe]/335-347	FGLKLVDFGFPAK
Srk1_[Schizosaccharomyces_pombe]/185-193	MRRV--KHPN--I	Srk1_[Schizosaccharomyces_pombe]/301-313	IGRIRLADDFGLSK

B

Sty1	+	+	+	+
Wis1	-	-	+	+
ATP	-	+	-	+
Assay incubation	-	+	-	+
Sty1-P				
Sty1				
Lane	1	2	3	4

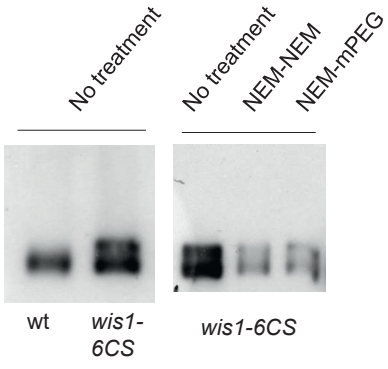
C

Sty1	+	+	+	+
Wis1	-	-	+	+
wis1Δ	-	-	-	+
Assay incubation	-	+	+	+
Sty1-P				
Sty1				
Wis1				
Lane	1	2	3	4

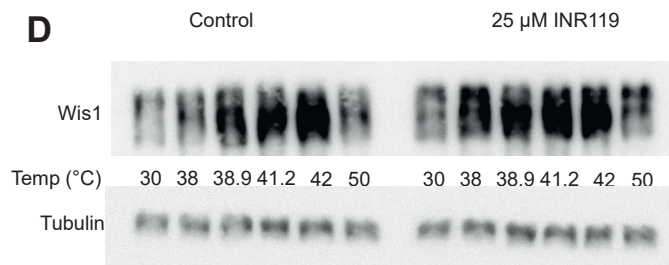
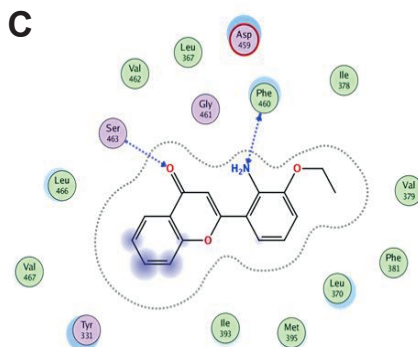
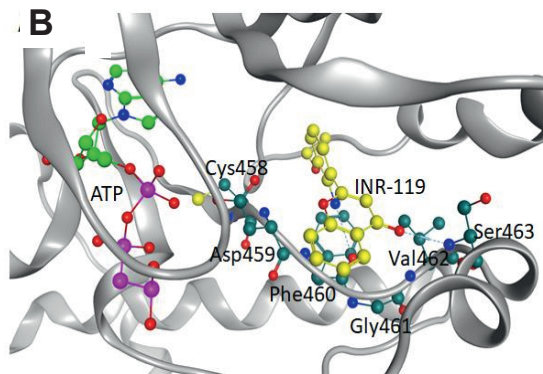
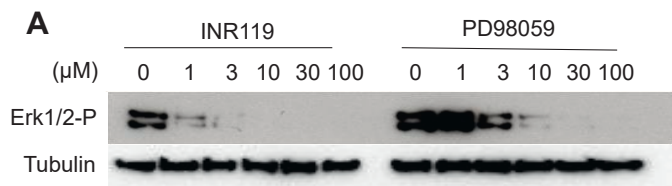
D

	H <sub>2</sub> O <sub>2</sub> (mM)		0		0.05		0.1		0.5	
TCEP	-	+	-	+	-	+	-	+	-	+
Wis1	+	+	+	+	+	+	+	+	+	+
Sty1										
Sty1-P										
Sty1										
Wis1										
Lane	1	2	3	4	5	6	7	8	9	10

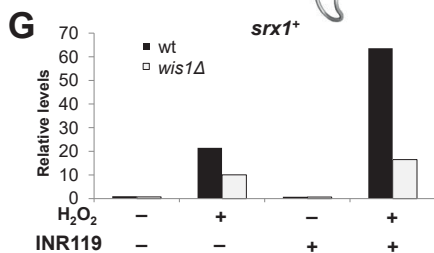
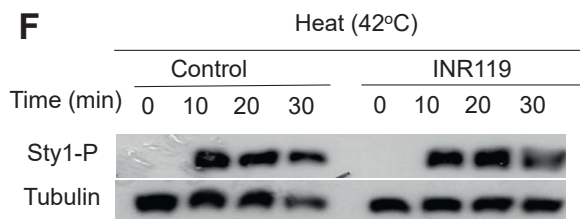
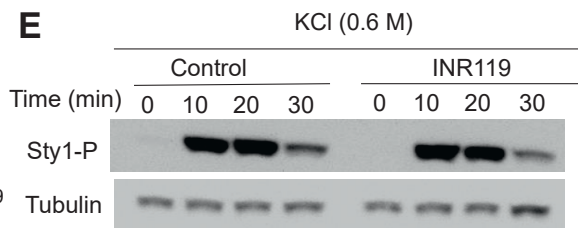
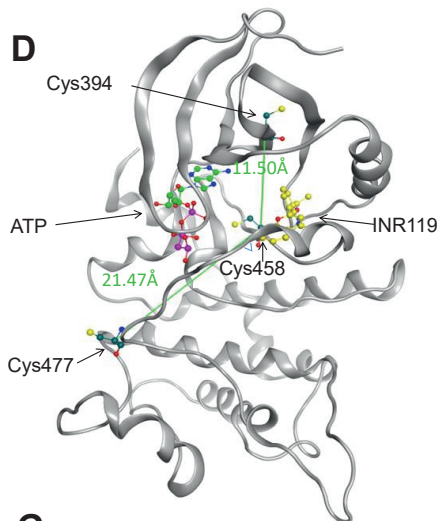
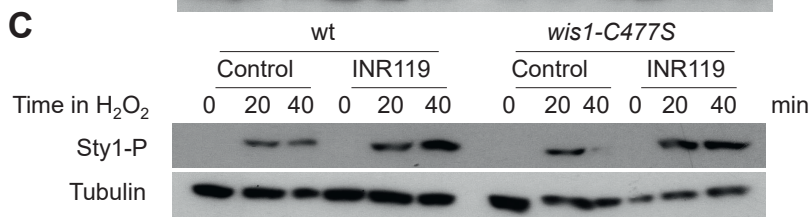
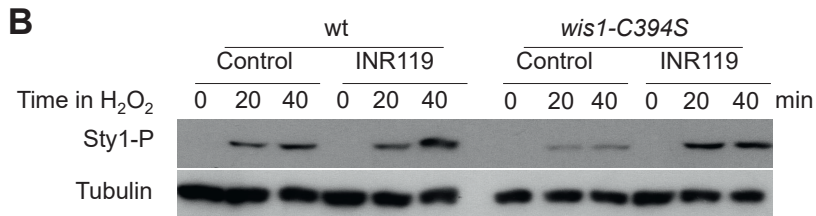
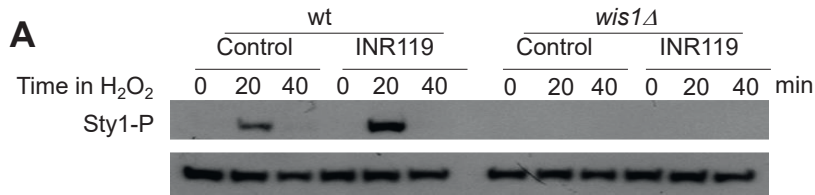
Supplementary Figure S1



Supplementary Figure S2

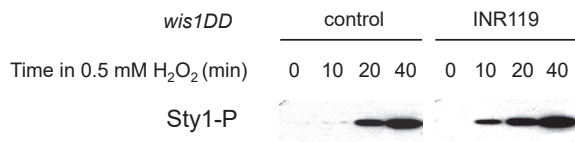


Supplementary Figure S3



Supplementary Figure S4





**Supplementary Figure S5**

